

**DEVELOPMENT OF A 1080 STEEL PLASMA SPRAYED COATING FOR
SLIDE/ROLL WEAR CONDITIONS**

Donald Mc Murchie

B.S., Oregon Institute of Technology, 1991

A thesis submitted to the faculty of the
Oregon Graduate Institute of Science & Technology
in partial fulfillment of the
requirements for the degree
Doctor of Philosophy
in
Materials Science and Engineering

July 1996

The thesis "Development of a 1080 Steel Plasma Sprayed Coating For Slide/Roll Wear Conditions" by Donald Mc Murchie has been examined and approved by the following Examination Committee:

Paul Clayton
Professor
Thesis Advisor

Milton Schell
Assistant Professor

David Atteridge
Professor

Roger Steele
Association of American Railroads

For:

My father, Donald Mc Murchie, Sr., in memoriam.

My Mother, Florence Gail Mc Murchie, with gratitude.

My wife, Xiaoyan Su, with love.

ACKNOWLEDGEMENTS

Paul Clayton

Milt Scholl

David Atteridge

Materials Science faculty and staff

Colleagues

Best Friend and Colleague, Xiaoyan Su

Thank you all!

TABLE OF CONTENTS

| | |
|--|------|
| List of Tables | x |
| List of Figures | xi |
| Abstract | xvii |
| Introduction | 1 |
| 1.0 Literature Review | 9 |
| 1.1 Introduction | 9 |
| 1.2 Introduction To Thermal Spray | 10 |
| 1.3 Thermal Systems | 10 |
| 1.3.1 General | 10 |
| 1.3.2 Flame Spray | 11 |
| 1.3.3 High Velocity Oxygen Fuel (HVOF) | 11 |
| 1.3.4 Twin Wire Arc | 12 |
| 1.3.5 D-Gun | 12 |
| 1.3.6 Plasma Spray | 13 |
| 1.3.7 Versions of Plasma Spray | 13 |
| 1.4 Plasma Spray System Components | 14 |
| 1.4.1 General | 14 |
| 1.4.2 The Plasma Gun | 15 |
| 1.4.3 The Arc | 19 |
| 1.4.4 Arc Stability | 19 |
| 1.5 Plasma Characteristics | 23 |
| 1.5.1 The Plasma | 23 |

| | | |
|-------|---|----|
| 1.5.2 | Plasma Gas | 24 |
| 1.5.3 | Plasma Thermal And Velocity Profiles .. | 27 |
| 1.6 | Behavior Of Individual Particles | 32 |
| 1.7 | Slide/Roll Ratio | 33 |
| 1.8 | Wear | 34 |
| 1.9 | Rolling Contact Fatigue | 36 |
| 1.10 | Lubrication | 37 |
| 2.0 | Single Splat Analysis | 39 |
| 2.1 | Introduction | 39 |
| 2.2 | Single Splat Analysis | 41 |
| 2.2.1 | Stereomicroscopic Examination Of Splats | 43 |
| 2.2.2 | Splat Morphology | 48 |
| 2.2.3 | Working Distance Effects | 51 |
| 2.3 | Practical Applications of SSA | 57 |
| 2.3.1 | Process Changes | 57 |
| 2.3.2 | Wire Selection | 57 |
| 3.0 | Experimental Procedures | 60 |
| 3.1 | Introduction | 60 |
| 3.2 | Plasma Spray Equipment | 63 |
| 3.3 | Plasma Spray Operation | 67 |
| 3.3.1 | Anode Calibration | 68 |
| 3.3.2 | Fixturing | 71 |
| 3.3.3 | Dwell And Traverse | 75 |
| 3.3.4 | Substrate Cooling | 75 |
| 3.4 | Materials | 78 |

| | | |
|--------|---|-----|
| 3.5 | Substrate Preparation | 78 |
| 3.5.1 | Surface Preparation Procedure | 79 |
| 3.5.2 | Substrate Surface Appearance | 80 |
| 3.5.3 | Knurling | 82 |
| 3.5.4 | Substrate Preheating | 83 |
| 3.5.5 | NiCr Intermediate Layer | 83 |
| 3.5.6 | Coating Froth & Interrupted Spray | 84 |
| 3.6 | Wear Test Equipment | 85 |
| 3.7 | Amsler Testing Equations | 87 |
| 3.8 | Dry Wear Testing | 88 |
| 3.9 | Lubricated Wear Testing | 90 |
| 3.10 | Lubricated Test Procedures | 91 |
| 3.10.1 | First Series (AMST46-51) | 91 |
| 3.10.2 | Series Two (AMST52-56) | 94 |
| 3.10.3 | Series Three (AMST175-183) | 95 |
| 3.11 | Water Lubrication | 96 |
| 3.12 | Layered Coatings | 96 |
| 3.13 | Parameter Envelope Study | 96 |
| 3.14 | Data Accumulation | 97 |
| 3.15 | Wear Curve Guidelines | 101 |
| 4.0 | Results | 104 |
| 4.1 | Introduction | 104 |
| 4.2 | Experimental Grouping | 106 |
| 4.3 | Early Work | 106 |
| 4.3.1 | Overview | 106 |

| | | |
|-------|---|-----|
| 4.3.2 | Wear Rates For Various Materials | 112 |
| 4.4 | Dry Wear Testing | 118 |
| 4.5 | Lubrication Tests | 118 |
| 4.5.1 | General Results | 118 |
| 4.5.2 | Coated vs Uncoated Lubrication Tests .. | 130 |
| 4.5.3 | Lubrication Test, Pure Rolling | 134 |
| 4.5.4 | Lubricated Testing Of Layered Coatings | 136 |
| 4.6 | Parameter Envelope | 139 |
| 4.6.1 | General | 139 |
| 4.6.2 | Microhardness | 149 |
| 4.7 | Debonding Results, Dry | 150 |
| 4.8 | Debonding Results, Lubricated | 163 |
| 4.9 | Intermediate Layers | 173 |
| 5.0 | Discussion | 175 |
| 5.1 | Debonding | 175 |
| 5.1.1 | Bonding And Surface Preparation | 175 |
| 5.1.2 | Debonding Mechanisms | 182 |
| 5.2 | Type I Debonding | 183 |
| 5.2.1 | General Description | 183 |
| 5.2.2 | Type I Debonding Characteristics | 189 |
| 5.3 | Edge Effects | 193 |
| 5.4 | Type II Debonding | 207 |
| 5.5 | Lamellar Structure and Formation of Wear Particles | 214 |
| 5.5.1 | Unlubricated | 214 |

| | |
|--|-----|
| 5.5.2 Lubricated Rollers | 219 |
| 5.6 Lubrication Reservoir Effect | 225 |
| 5.7 Repeatability | 227 |
| 6.0 Conclusions | 230 |
| 7.0 References | 232 |
| Appendix | 247 |

LIST OF TABLES

Table 2.1 Single Splat Analysis 54
Table 2.2 Particle Conditions 55
Table 2.3 Parameter Adjustments 56

LIST OF FIGURES

| | | |
|-----|--|----|
| 1.1 | Plasma jet at high gas pressure | 16 |
| 1.2 | Basic system requirements | 16 |
| 1.3 | A basic plasma gun | 17 |
| 1.4 | A modern plasma gun | 18 |
| 1.5 | Arc schematic showing basic arc regions | 21 |
| 1.6 | Eddy gas flow for arc stability | 22 |
| 1.7 | A neutral atom ionized | 26 |
| 1.8 | Plasma jet temperature and velocity profiles | 31 |
| 2.1 | Splat field with black/white backgrounds | 46 |
| 2.2 | Splat field with yellow/orange backgrounds | 46 |
| 2.3 | Working distance effects | 47 |
| 2.4 | Working distance effects | 47 |
| 2.5 | An idealized splat field | 50 |
| 2.6 | An idealized individual splat | 50 |
| 2.7 | Working distance of 195mm and 210mm | 53 |
| 2.8 | Working distance of 210mm and 230mm | 53 |
| 2.9 | Typical coating microstructure | 59 |
| 3.1 | Amsler roller | 62 |
| 3.2 | Plasma spray system schematic | 65 |
| 3.3 | Secondary shotblast layout | 66 |
| 3.4 | Schematic of shock diamonds in plasma jet | 70 |
| 3.5 | Five roller array, after spraying | 73 |
| 3.6 | Single splat specimen collection | 73 |

| | | |
|------|--|-----|
| 3.7 | Plasma gun with wire and powder feed tubes | 74 |
| 3.8 | Steel coupon being sprayed | 74 |
| 3.9 | Backside cooling | 77 |
| 3.10 | Specimen surface appearance, silica blasted | 81 |
| 3.11 | Specimen surface appearance, steel shot blasted .. | 81 |
| 3.12 | Knurled roller | 82 |
| 3.13 | Amsler wear test machine | 86 |
| 3.14 | Large edge effect on wear track | 89 |
| 3.15 | Application of grease with syringe | 93 |
| 3.16 | Removal of excess grease with a spatula | 93 |
| 3.17 | Raw data sheet | 99 |
| 3.18 | Spreadsheet | 100 |
| 3.19 | Data collection curves | 103 |
| 4.1 | Wear rates of uncoated rail steels | 105 |
| 4.2 | Early work, 1075 wire | 108 |
| 4.3 | Early work, 35% slide/roll | 109 |
| 4.4 | Early work, 5% slide/roll | 110 |
| 4.5 | Details of the early work testing | 111 |
| 4.6 | Wear rates, 1075 wire | 113 |
| 4.7 | Wear rates, 1080 3/32" dia wire | 114 |
| 4.8 | Wear rates, 1080 1/16" dia wire | 115 |
| 4.9 | A coating that did not wear out | 116 |
| 4.10 | 5% slide/roll, 1220 MPa, wear curves | 117 |
| 4.11 | Lubrication tests, revolutions per interval..... | 122 |

| | | |
|------|--|-----|
| 4.12 | Lubrication tests, retained lubricant per interval | 123 |
| 4.13 | Lubrication tests, effect of coating thickness ... | 124 |
| 4.14 | Lubrication tests, wear rates | 125 |
| 4.15 | Lubrication tests, revolutions per interval | 126 |
| 4.16 | Lubrication tests, retained lubricant per interval | 127 |
| 4.17 | Lubrication tests, effect of coating thickness ... | 128 |
| 4.18 | Lubrication tests, coating thickness vs wear rate | 129 |
| 4.19 | Comparison of coated vs uncoated, revs/interval .. | 131 |
| 4.20 | Coated vs uncoated, retained lubricant/interval .. | 132 |
| 4.21 | Coated vs uncoated, wear rates | 133 |
| 4.22 | Lubrication tests, pure rolling | 135 |
| 4.23 | Lubrication tests, layered coating | 137 |
| 4.24 | Layered coating cross-section | 138 |
| 4.25 | Wear rates vs contact pressure | 141 |
| 4.26 | Wear rates vs gas parameters | 142 |
| 4.27 | Parameter envelope test matrix | 143 |
| 4.28 | Parameter envelope, wear rates and test durations | 144 |
| 4.29 | Change in microstructure with gas parameters | 145 |
| 4.30 | Microhardness results of parameter envelope study | 149 |
| 4.31 | Early work, test duration of debonded coatings ... | 153 |
| 4.32 | Early work, test duration of no-debond coatings .. | 154 |
| 4.33 | Debonding incidence during parameter study | 155 |
| 4.34 | Debonding study test block | 156 |

| | | |
|------|---|-----|
| 4.35 | The effect of coating froth | 157 |
| 4.36 | Test duration, interrupted spray | 158 |
| 4.37 | Ten roller block, no type I debonding | 159 |
| 4.38 | Knurled substrate effect | 160 |
| 4.39 | Knurled substrate effect | 161 |
| 4.40 | Overview of AMST97-154 | 162 |
| 4.41 | Debonding incidence of lubricated coatings | 166 |
| 4.42 | Lubrication tests, short test duration | 167 |
| 4.43 | Lubrication tests, wear rates | 168 |
| 4.44 | Lubrication tests, 5% slide/roll | 169 |
| 4.45 | lubrication tests, 35% slide/roll | 170 |
| 4.46 | Dry test roller from lubricated test block | 171 |
| 4.47 | Water lubricated coating | 172 |
| 4.48 | NiCr intermediate layer test block | 174 |
| 5.1 | Coating tightly bonded to substrate | 179 |
| 5.2 | Knurled interface | 179 |
| 5.3 | Crack formed at coating/substrate interface | 180 |
| 5.4 | Porosity concentrated at the interface | 180 |
| 5.5 | Debonding damage at the interface | 181 |
| 5.6 | Damage zone in the debonded area | 181 |
| 5.7 | Type I debond | 186 |
| 5.8 | Type I debond | 186 |
| 5.9 | Delamination at lamellar interfaces | 187 |
| 5.10 | Delamination caused be a blister | 188 |
| 5.11 | Blister and delamination | 188 |

| | | |
|------|--|-----|
| 5.12 | Type I debond | 191 |
| 5.13 | Tensile force on substrate as splat cools | 192 |
| 5.14 | Edge effect at the edge of the wear track | 197 |
| 5.15 | Severe edge effect | 197 |
| 5.16 | Appearance of edge effect on weight loss curve ... | 198 |
| 5.17 | Schematic, wear track deepens as test progresses . | 199 |
| 5.18 | Weight loss and diameter reduction curves | 200 |
| 5.19 | Crowning and increased width during spraying | 201 |
| 5.20 | Shadow effect during spraying | 202 |
| 5.21 | Spraying into a corner | 203 |
| 5.22 | Defects in coating from shadow effects | 203 |
| 5.23 | Interlamellar crack on wear surface | 204 |
| 5.24 | Crack from edge effect growing toward substrate .. | 205 |
| 5.25 | Crack from edge effect to substrate | 205 |
| 5.26 | Edge effects induced during grinding operation ... | 206 |
| 5.27 | Edge effect crack leading to type II debonding ... | 210 |
| 5.28 | Type II debonding | 211 |
| 5.29 | Crack network on underside of coating | 212 |
| 5.30 | Edge effect particle, view from underside | 212 |
| 5.31 | More than one crack at fracture site | 213 |
| 5.32 | Angle of incidence effect during spraying | 216 |
| 5.33 | Undulation in microstructure has vertical section | 217 |
| 5.34 | Wear particles from dry testing | 218 |
| 5.35 | Higher magnification of wear particles | 218 |
| 5.36 | Wear crater in lubricated test roller | 221 |

| | | |
|------|--|-----|
| 5.37 | Wear surface of a lubricated roller | 222 |
| 5.38 | Wear surface of a dry roller | 222 |
| 5.39 | Wear surface of lubricated roller, higher mag. ... | 223 |
| 5.40 | Wear surface of a dry roller, higher mag. | 223 |
| 5.41 | Crack along lamellar interfaces | 224 |
| 5.42 | Another crack along lamellar interfaces | 224 |
| 5.43 | Wear rates showing repeatability | 228 |
| 5.44 | Wear rate comparison, coated vs uncoated | 229 |

ABSTRACT

The railroad industry has historically sought improvements in rail lubrication techniques. The Association of American Railroads (AAR) has sponsored research into novel solutions to this problem. Plasma sprayed coatings were thought to show promise as a lubricant reservoir or as a vehicle to produce a self-lubricating coating. A high carbon steel coating was to be developed that would withstand the high slide/roll ratios and loading conditions seen at the wheel/rail interface. A 1080 steel was selected because of its similarity to the composition of rail steel.

A literature review, concentrated on plasma generation and particle behavior in the plasma jet, was made. Substrate preparation techniques were researched and a protocol established that assured an acceptable bond, which is largely mechanical, between coating and substrate. Single splat analysis, a technique for predicting coating quality, was developed. Plasma spray parameters and techniques were optimized using the single splat analysis method. Backside cooling, a substrate cooling method, was initiated. N_2 and H_2 were used as primary and secondary gases.

Coatings were sprayed onto Amsler rollers and tested on an Amsler wear test machine. Up to 35% slide/roll and 1220 MPa contact pressures, dry and lubricated, were used to test coating performance. Wear rates for coatings were significantly lower than uncoated rollers. The spray parameter envelope was established by the likelihood of debonding rather

than by a fall off in wear performance. Two debonding mechanisms were identified and techniques implemented for their control. Reliability of the process in producing coatings that would consistently yield good wear performance was proven. The goal of developing a plasma sprayed 1080 steel coating that would withstand the rigors of laboratory test was met.

CHAPTER ONE

INTRODUCTION

Control of friction at the wheel/rail interface is the subject of ongoing research within the railroad industry. This research includes both friction reduction and friction enhancement. The delivery of the proper amount of grease to the correct location at the right time would prolong component life and generate significant savings in maintenance costs to the railroad companies. From the '70's to the '90's the standard axle load has increased significantly, to the general level of 33 tons, and with 39 tons being introduced.^(1,2,3) This has been in response to meeting the demands of a growing market.^(4,5) Rail costs are continuing to rise, as are installation costs, and maintenance cost is roughly three times the original cost over the life of a rail section⁽⁶⁾. Current technology, in the form of wheel and track oilers, is inadequate to provide a reliable lubricant delivery to the wheel/rail interface.

In areas where increased traction is desirable, the current method to increase the friction coefficient between wheel and rail is to apply sand to the track. Generally loss of traction is attributed to the accumulation of foreign matter, organic matter such as leaves and so forth mixed with other debris, that has adhered to the track. When the driver wheel is powered, slippage at the wheel/rail interface can

wheel is powered, slippage at the wheel/rail interface can occur. Sand application works to some degree, however significant improvement is desired.

Innovative technology is sought to address the problem of wheel/rail friction control. The use of surface engineering techniques was thought to be a promising approach to the problem. In its most essential form, surface engineering involves imbuing the surface of a material or component with qualities that are either not required or desired in the bulk of the material. Desirable implementation for the wheel/rail friction problem would be surface treatment in localized areas of track without affecting track performance in adjacent areas. Also the treatment used should be able to be retrofitted into existing track. It would be desirable for the same technology be used for friction reduction and for friction enhancement, thus allowing greater efficiency of application. The materials used would of necessity vary with the application, however the equipment and technique could be the same.

Thermal spray technology was the proposed surface engineering technique. Plasma spray was the thermal spray technique selected. The scope of the work in general includes both friction reduction and friction enhancement. A plasma sprayed coating could be applied onto specific areas of track where the coefficient of friction should be either reduced or enhanced in order for more efficient train movement operations. The research reported in this thesis is part of the greater work just described.

A 1080 steel coating was to be developed that would adhere to the track, maintain adherence under the severe

slide/roll wear conditions encountered in rail service, and display high wear resistance properties. In addition to the above qualities, the steel coating was to be assessed for possible use as a lubricant reservoir. In any event, the techniques developed for successful application of this coating could be transferred for use in any variation where similar results are desired. Even if the lubricant reservoir did not materialize, the coating could act as a base for polymers or other lubricating films. A solid lubricant, such as graphite or molybdenum disulfide, might be included as part of the coating. This would make a self-lubricating coating with more lubricant being exposed as part of the wear process. For friction enhancement, a coating could be made of a material known to have a high coefficient of friction, such Ni-Ti. The key to obtaining the benefits described is the development of the 1080 steel coating.

Plasma spray is an emerging technology. Coatings have been developed for wear purposes, however there has been no experience in the industry with testing coatings under anything even resembling the severe slide/roll wear conditions present in railroad applications. Very little help was obtained from research literature. Enough work has been done on coatings in general to promote confidence in the technology as a whole, however virtually no published work is available on the rolling/sliding behavior of coatings. Any work in this direction would be breaking new ground.

Once the concept of using plasma spray technology to produce a coating with desirable qualities was accepted and the goals of the research clear, work in earnest could begin. For clarity, the goals of the research are stated here:

Primary goals:

1. Develop a high-carbon plain steel coating that would withstand the extreme slide/roll wear conditions that are present at the wheel/rail interface.

- a. This coating could subsequently be used as a vehicle to anchor polymer or other lubricating coatings, or contain additives such as a soft metal, i.e. copper, a solid lubricant, i.e. graphite or molybdenum disulfide, that would make it a self-lubricating coating.

2. Investigate the possibility of the steel coating acting as a lubricant reservoir.

Secondary goals were designed to fall out of the primary goals if the primary aims were achieved.

Secondary goals:

1. Establishing protocols that would assure repeatable results.

2. Determine, at least conceptually, whether the technology could be used in the field.

3. Obtaining an understanding of the technology such that there could be a transfer of knowledge to address similar problems.

The extreme conditions seen in wheel/rail service are thought to be reproduced by a 35% slide/roll ratio at a contact pressure of 1220 MPa in small scale laboratory tests. As part of evaluating coating performance, wear tests were performed up to these extremes on the Amsler wear test machine. Some important issues were raised during wear testing that needed addressing in the research. Debonding failure at the coating/substrate interface immediately surfaced as a problem. The friction coefficient between a coated and an uncoated roller was lower than expected. Specimen geometry was identified as a major factor.

The major goals of the research were achieved, with the results offering a mixture of optimism and pessimism as far as use in the field is concerned. However, it is the growth of knowledge and understanding in coating performance that is the real value of this research. This is what is reported in the thesis.

Single splat analysis is a technique for predicting coating quality without destructive analysis. Behavior of the individual particles that make up a coating was studied in great detail. Individual splat size, morphology, spreading, flattening, and size distribution are looked at individually and collectively. Particle behavior in the plasma jet is also looked at. The condition of the plasma jet determines particle behavior in the jet, and in turn influences particle behavior at impact. The temperature and velocity of the plasma jet is determined by various spray parameters such as primary and secondary gas flows, electrical energy input, and gas selection.

Debonding was an issue of great importance during experimental work. Two debonding modes were identified, experiments made, and controls instituted that minimized incidence. Wear mechanisms that may be unique to coatings were identified. The lamellar structure of the coating caused not only a unique wear mechanism, but debonding and lubrication problems as well.

At the onset of the work, a survey of available literature was undertaken to determine what information was available. As previously stated, there was virtually no reported work on the wear performance of coatings under sliding/rolling load conditions. The absence of such research may be because of the substrate/coating bond quality issue, however this is only speculation.

Two basic areas of study were concentrated upon during preparatory work. First was a good background in plasma spray technology. It was necessary to understand the principles involved in producing a properly conditioned plasma jet. All materials, wire or powder, require a plasma jet at the proper temperature and velocity to melt and propel particles so that they will impact the substrate in the proper condition. The second area was individual particle behavior. Coatings, all types of coatings, whether they are used in wear, thermal barrier, free-standing, or any other application, are made up of individual particles. These two studies were synthesized and the principles tested in the laboratory. This study, from its beginnings in a literature survey to present, is a dynamic, growing body of knowledge, and is frozen here only for the purpose of reporting in this thesis.

Other necessary issues are dealt with in the literature review, such as rolling/sliding wear, friction, and wear in general, however the main emphasis is in the areas mentioned above.

This is applied research, with the requirement of answering the proposal of a new, innovative product idea with a go or no-go. Necessarily there is an enormous amount of cross-disciplinary elements present in the work. For example, a harnessed plasma is assumed, yet some understanding of plasma science is required for the generation, conditioning, and control of the plasma jet. To do an exhaustive review, conduct experimentation, and evaluate results from a plasma science point of view would require as much time as was available for the entire project. The study of plasma science is limited to the understanding of the production a specific plasma jet for use in producing a steel coating. This should not minimize the importance of this understanding, only emphasize the enormity of the problem in research performed when cross-discipline elements are required.

The study of plasma spray technology includes plasma science, gases, electric arc production and control, fluids, thermodynamics, and other issues. The application is a properly conditioned plasma jet for the material to be used. Individual particle study includes material-related issues, particle behavior in the plasma jet, and behavior upon impact through solidification. Understanding of these two areas allow the study of any coating.

The coating has been produced. It stays on the substrate under the severe service requirements set forth at the beginning of the research. Its wear performance compares very favorably with uncoated steel. The coefficient of friction is

lower than that of uncoated steel tested at the same extreme conditions. It does not act as a lubrication reservoir. The basic requirements of the research have been met in this product, with the only disappointment being failure as a lubricant reservoir.

1.0 LITERATURE REVIEW

1.1 Introduction.

This literature review concentrates on the relevant elements with which to accomplish the work. Required is a 1080 steel plasma sprayed coating that will provide improved wear performance under the severe slide/roll conditions of wheel/rail service. To make such a coating, a thorough understanding of plasma spray technology is required. Though plasma spray may be considered as a tool in the production of the coating, without in-depth understanding of the nuances of plasma generation and control the final product could not have been worked out.

The second area of concentration is particle behavior within the plasma jet and at impact, flattening, and solidification. Understanding of the basic constituent of a coating, the individual particle (splat), is imperative in making and evaluating a coating. This portion of the review is continued in Chapter 2 as part of the explanation of Single Splat Analysis, a key part of the work.

Other areas, those dealing with wear evaluation, test matrix, lubrication selection, and experimental procedures, are covered with less rigor. These elements of the research

were established in a previous work relating to lubrication testing of rail steel.⁽⁷⁾ This work required a significant cross-disciplinary integration of work, making it more than difficult to perform a comprehensive literature survey of all fields present in the research. For these reasons the bulk of the literature review is concentrated in the areas previously mentioned.

1.2 Introduction to Thermal Spray.

The main objective for a thermal spray system is to deposit a coating onto a substrate that provides surface attributes not required in the bulk material. A coating is made by presenting a molten stream of particles to the substrate which develops an overlay that has the desired properties.

There are many types of coatings, including metallic^{8,9} and intermetallic^{10,11}, ceramic^{12,13}, carbides^{14,15}, and composites^{16,17}. Applications include wear protection^{18,19}, corrosion protection^{20,21}, meeting special surface requirements such as a thermal barrier^{22,23}, or to attain specific electrical or thermal qualities²⁴. A near-net-shape²⁵ product can be manufactured without the intermediate steps of pouring and solidification.

1.3 Thermal Systems.

1.3.1 General.

A thermal spray coating is produced by the successive accumulation of molten particles that rapidly flatten and

solidify after impingement on the substrate surface²⁶. There are five main types of thermal spray systems:

1. Flame Spray.
2. High Velocity Oxygen Fuel (HVOF).
3. Twin-Wire Arc.
4. D-Gun.
5. Plasma Spray.

The coating material may be in a wire^{27,28} or powder^{29,30} form. Four of the five processes require a hot gas stream to melt and propel coating particles to the substrate. Twin-wire arc uses an arc to melt the wires and a hot gas jet moves the molten particles to the substrate. A brief description of each thermal spray system follows.

1.3.2 Flame Spray.³¹

The earliest of the thermal spray technologies. It is used when a low temperature and low velocity coating is required³². An oxy-acetylene style torch is used as a heat source, which melts a wire or powder. Compressed air is then used to break the wire down into particles and propel them to the substrate. The gas temperature limit is about 5625° F, 3100°C, because of the fuel-gas heat of combustion properties³³, which restricts the use of flame spray to non-refractory materials. Particle velocity ranges from 10-50 m/s for powder and 100-250 m/s for wire.

1.3.3 High Velocity Oxygen Fuel (HVOF).³⁴

An oxygen + fuel system that reaches sonic velocities³⁵ in the jet plume. Its chief feature is the high impact velocity of the spray particles with moderate heating of the spray

material.³⁶ It is used for a wide variety of industrial applications, ranging from wear surfaces to mirror-finished coatings³⁷. HVOF has the same temperature upper limit (determined by the fuel-gas properties) as flame spray, about 5625° F or 3100° C. Particle velocities range from 550-1000 m/s.

1.3.4 Twin-Wire Arc.

This system uses a dual wire feed, with the wires functioning as an anode and as a cathode. An arc is formed between them, and the resulting high temperature, from 12,000 to 20,000 K, melts the wire. The molten particles are propelled to the substrate by a carrier gas, such as air or Nitrogen.

1.3.5 D-Gun.³⁸

This is a proprietary system of the Union Carbide Co. The particles are melted and accelerated by the detonation of a gas mixture, similar to cannon fire. The D-Gun, or detonation gun, has a long barrel in which to propel the particles, and particle velocities reach 800-1000 m/s, which is the highest particle speed of all the thermal spray systems. Generally speaking, high particle speeds result in a very high quality, fine grained, low porosity coating. Gas temperatures are limited to about 5625°F, or 3100° C, for the same reason as listed for the HVOF and flame spray processes, and the system is used for non-refractory materials.

1.3.6 Plasma Spray.

Pressurized gas is directed through a nozzle that houses a high energy electric arc. Electrical energy is converted into thermal energy in the gas, the sudden increase in temperature provides sufficient energy to ionize the gas, converting it into a plasma. Plasma temperatures can reach up to 20,000 K. The plasma jet melts the powder or wire and propels the molten particles onto a substrate at high speeds. System temperatures are high enough to melt any material³⁹.

1.3.7 Versions of Plasma Spray.

There are several ways to implement plasma spray technology, depending on the desired results. Vacuum Plasma Spray (VPS) is used when atmospheric influences need to be eliminated completely⁴⁰. Low pressure plasma spray (LPPS) is carried out in a partial vacuum⁴¹. An inert environment can be achieved by spraying into a chamber that has been purged of the normal atmosphere by argon, or other inert or non-reactive gases, and the inert atmosphere maintained. All of these methods control the formation of undesirable oxides, in addition the velocity and thermal profiles are also enhanced. High pressure plasma spray (HPPS) is used to spray coatings under water⁴². Particle velocity is also reduced and the higher gas density yields an improvement in heat transfer from the plasma to the powder⁴³. Air plasma spray (APS) is the most versatile application, and can be used nearly anywhere.

1.4 Plasma Spray System Components.

1.4.1 General.

A basic plasma system requires a cathode, an anode, and a power supply to obtain a continuous plasma jet. Figure 1.1 schematically shows a controllable plasma jet. Figure 1.2 shows basic system requirements with the workpiece acting as the anode, an arrangement called plasma transferred arc (PTA)⁴⁴. The power supply is normally direct current⁴⁵, though radio frequency plasmas are used in some highly specialized applications^{46,47}. Alternating current power results in a higher contamination level and lower enthalpy when compared with dc plasma generators⁴⁸. The cathode and anode are non-consumable. The cathode is typically made from thoriated tungsten⁴⁵ and the anode is copper.

To obtain a plasma, a gas must be introduced into the system and forced through the arc. This brings up the consideration that the arc must now be confined so that the gas can be presented to the arc, a plasma formed, and the resulting energy directed in a controlled manner. A housing, the plasma gun, is constructed to accomplish this. The plasma gas, typically N_2 or N_2-H_2 , is fed under pressure into the arc chamber. There, the electrical energy is converted into thermal energy, and the gas, as it is ionized, is converted into a plasma. The gas expands rapidly, and exits the chamber through a passage, or nozzle. The anode is configured to act as a nozzle. Water cooling in the nozzle is required to protect the components from the high temperatures in the arc.

1.4.2 The Plasma Gun.

The arc needs to be confined, with the gas entering the arc chamber under pressure. Figure 1.3 shows an enclosed system. The plasma gun houses the cathode, the anode, which also serves as a nozzle, the arc chamber, and a gas intake. High pressure water circulating through the housing provides the needed cooling. Figure 1.4 shows the gun used in the OGI system. Note the extent of the water cooling employed, with water pressure about 200 psi and flow rate of 5-10 gpm, in this gun.

The components of a complete plasma spray system⁴⁹ are:

1. A plasma-generator (gun).
2. Power supplies, typically dc rectifiers.
3. A water-cooling/heat exchanger/pump circuit.
4. Powder or wire feeder.
5. A gas supply.
6. A control console with meters for power, gas, and water control.

Other components may be used, especially to control the environment, such as a vacuum or low pressure chamber, high pressure chamber, radiation (infrared and ultraviolet) protection, etc, however they are auxiliary to the basic system components.

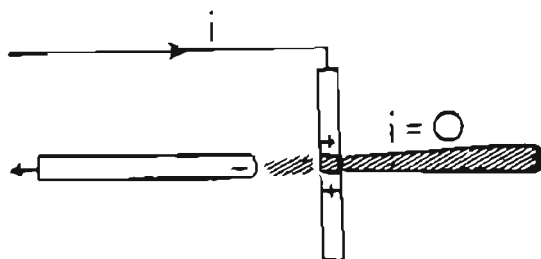


Figure 1.1. Continuous or discontinuous plasma jet at high gas pressure. Moderate but equal gas and electron temperatures. Zero net current in plasma jet⁵⁰.

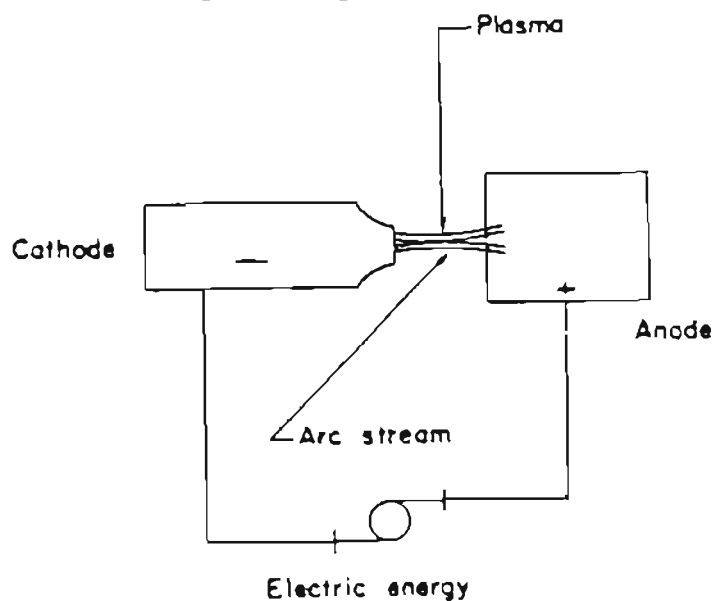


Figure 1.2. Basic system requirements: Cathode, anode, and power supply.

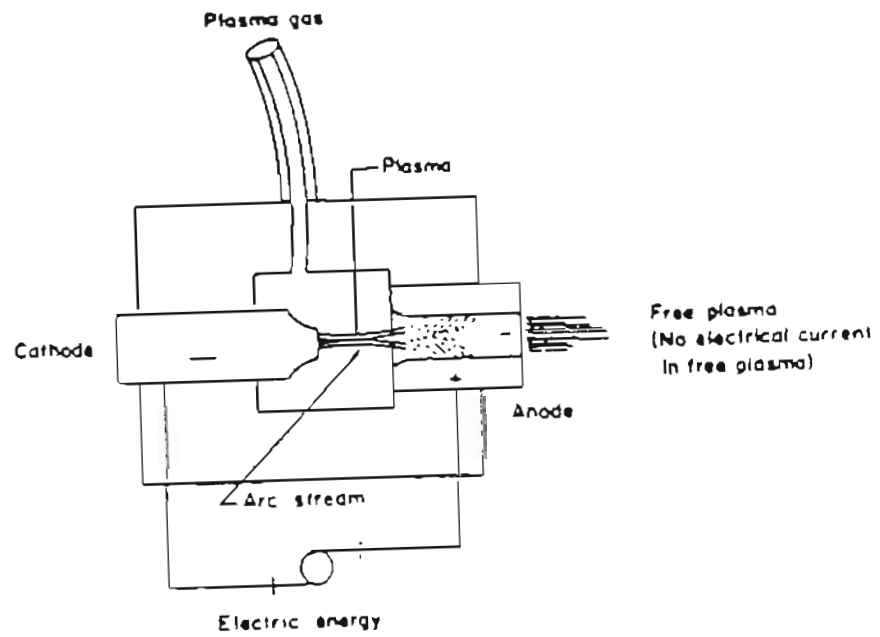


Figure 1.3. A basic plasma gun.

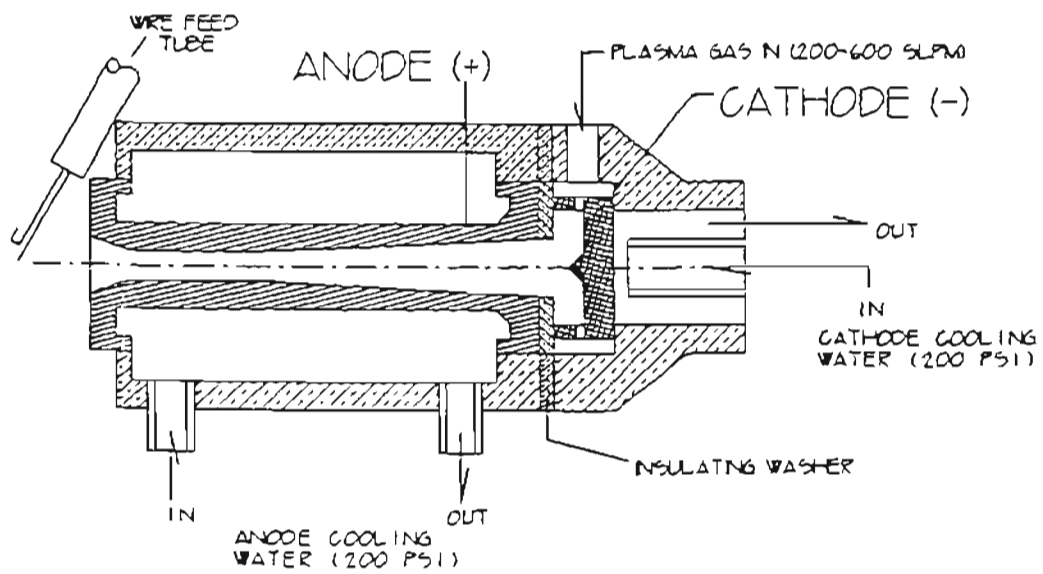


Figure 1.4. Modern plasma gun⁵¹.

1.4.3 The Arc.

The arc is the energy source for the system. It is not a solid body, but an electrically conductive region of gas⁵², whose function is to convert electrical energy to thermal energy⁵³. This is accomplished by establishing a neutral plasma state by electron collision processes within the electrical field. The arc consists of three major regions: the cathode sheath, the positive column, and the anode sheath. The positive column is an electrically neutral region that supplies energy for the thermal spray system to convert the gas into a plasma. It has charge equilibrium, the true plasma, while the cathode- and anode-sheath regions have a negative and a positive charge respectively, with high potential gradients⁵⁴. Approximate thermal equilibrium is achieved in the positive column region, with arc temperatures reaching to 30,000 K, in pure inert gas arcs depending upon the current intensity involved⁵⁵. The anode and cathode sheaths strongly control the stability of the arc. See figure 1.5 for a schematic of the arc regions⁵⁴.

1.4.4 Arc Stability.

Arc stability is achieved when the arc is aligned between the cathode and the anode without fluctuation⁵⁶. The arc is anchored at the cathode and the anode. The length of the arc is dependent on the input power, reaching 3-4 inches in the OGI system. Arc length is a function of the applied voltage. Stabilization can be achieved by the way the gas is introduced into the arc chamber, or nozzle. A swirl gas flow is created by injecting the gas in tangentially, causing a swirl around

the periphery of the chamber²⁶, see figure 1.6. This causes the anodic arc root to strike into the nozzle. The chamber is water cooled, to prevent damage from the intense heat and to help further stabilize the arc. The outer layer of gas, in contact with the walls of the nozzle, or anode, is cooler than the core, thus further constricting and stabilizing, the arc⁵⁷. This is called a "thermal pinch", which constricts the current to the core of the arc, greatly increasing the arc core temperature. There are other ways to aid in arc stabilization, such as water and magnetic stabilization⁴⁹, but the vortex gas method is the most commonly used in a plasma spray system.

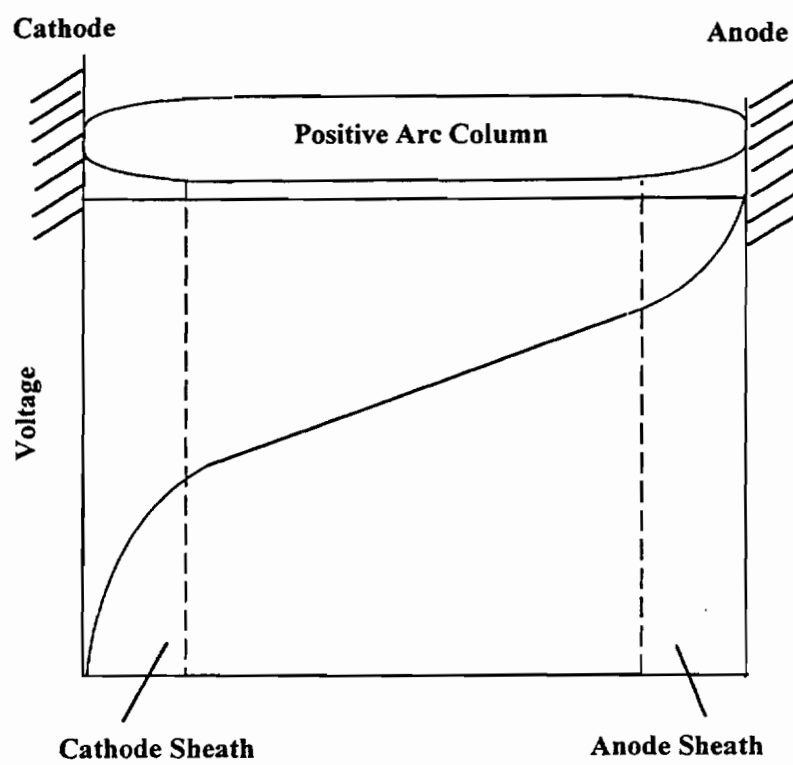


Figure 1.5. Arc schematic showing basic arc regions⁵⁴.

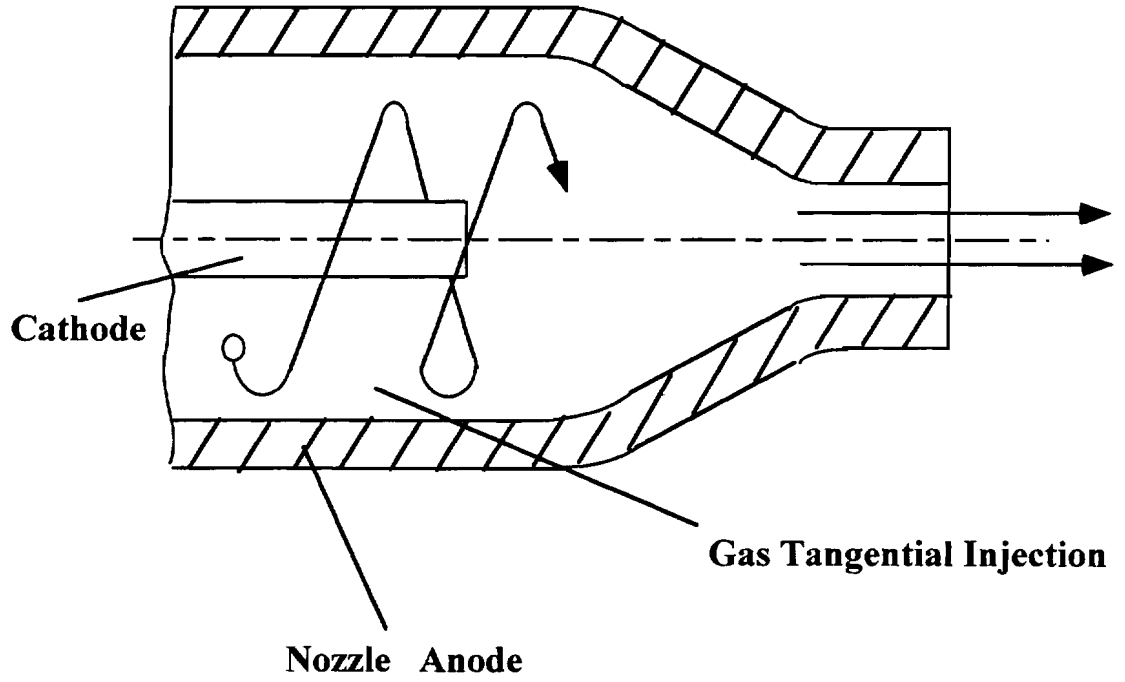


Figure 1.6. Swirl gas flow for arc stability²⁶.

1.5 Plasma Characteristics.

1.5.1 The Plasma.

A plasma is ionized matter in a gaseous state⁵⁰. A plasma occurs when the energy present in a gaseous system is greater than the ionization potential for the gas particles. The ionization potential of an atom is the energy required to overcome the bonding energy of an outer valence electron to the atom⁵⁸. There are three components to a plasma, electrically neutral gas molecules; charged particles (positive ions, negative ions and electrons); and electromagnetic radiation (photons) permeating the plasma-filled space⁵⁰. When a gas is highly ionized, intense particle motion throughout the plasma, which varies in magnitude and direction, produces strong localized electrical fields⁵⁰. A basic property of a plasma is its tendency toward electrical neutrality⁵⁹, even though containing both positive and negative particles within the system.

The atoms can be either excited or in the ground state, determining the degree of ionization. Examples of a cold plasma, a weak plasma where the mean energy is much lower than the ionization potential for the gas particles, are a neon lamp or sign, sodium or mercury vapor lamps, and the aurora sometimes visible in earth's atmosphere. A thermal plasma is defined as the mean energy being much higher than the ionization potential for the gas, and the electron temperatures equal the ion temperatures⁶⁰, an extreme example of which is a thermonuclear plasma.

The harnessing of the plasma has been successfully accomplished in plasma spray technology, a seemingly significant accomplishment when viewed from a cosmic perspective, where more than 95 percent of all matter in the universe is thought to occur in the form of a plasma⁶¹. From a more practical point of view, required is a steady, or continuous, plasma with the plasma jet directed in a controlled manner, see figure 1.1. An arc is struck between graphite or watercooled metal electrodes, providing an energy source wherein electrical energy is converted into thermal energy. A gas is forced under pressure through the arc, rapidly heating the gas, creating an ionized condition. As the gas is heated, rapid expansion occurs. This effect, plus the input pressure of the gas as it is introduced into the arc chamber, causes the hot plasma to be forced out of the nozzle at high velocity. The plasma jet will remain continuous as long as the gas supply is adequate and the arc remains intact. With plasma temperatures ranging from 12,000 to 20,000K⁶², and the high exit speeds, any material can be melted and propelled with this system⁴⁵.

1.5.2 Plasma Gas.

Nitrogen and argon are frequently used as primary plasma gases because of their stable natures. Neither tend to react with the powders or wire being sprayed, however in those conditions where nitriding may be a problem, Ar is normally used. Nitrogen is diatomic, N_2 , with a higher heat content than the monatomic argon, Ar. Energy is not only released through ionization, but molecular recombination as well⁵⁴. An example of the ionization process is partially shown in figure 1.7. The process for nitrogen is: $N_2 \rightarrow N + N \rightarrow N^+ + e$.

Dissociation of N_2 begins at about $3,000^\circ\text{C}$ and ionization at about $8,000^\circ\text{C}$, and Ar ionization begins at about $10,000^\circ\text{C}$. Ar plasma must be heated to about $16,000^\circ$ to achieve the same enthalpy as N_2 plasma⁵⁴. Good particle heating can be expected from Ar because of this very high temperature, along with very high plasma speeds. The higher the temperatures involved, the more rapid the gas volume expansion, and it is this rapid expansion that governs the plasma jet speed. N_2 plasma temperatures are roughly half that of Ar plasma, so the nitrogen plasma velocity should be about half that of the Ar plasma, given the same nozzle parameters⁶³. Because particle acceleration is a function of momentum transfer from the plasma to the particles, the higher molecular weight of the Ar contributes to higher particle speeds than what is achieved in a N_2 plasma jet.

Hydrogen is often used when a secondary gas is required or desirable⁶⁴. H_2 is used with N_2 or Ar in amounts of 5 to 35 percent to raise the arc voltage. Helium is sometimes used with Ar when hydrogen embrittlement, particularly on titanium substrates, is a consideration. A secondary gas is also used to narrow the spray core, resulting in higher plasma velocity and an increased thermal efficiency in the plasma plume, yielding among other benefits an increased deposition efficiency on small parts⁶³. These gases can be readily ionized and the speed and density of the resulting plasma is high enough to propel melted spray particles. These gases are also inexpensive, although Ar and He are higher priced than N_2 and H_2 , and are readily available.

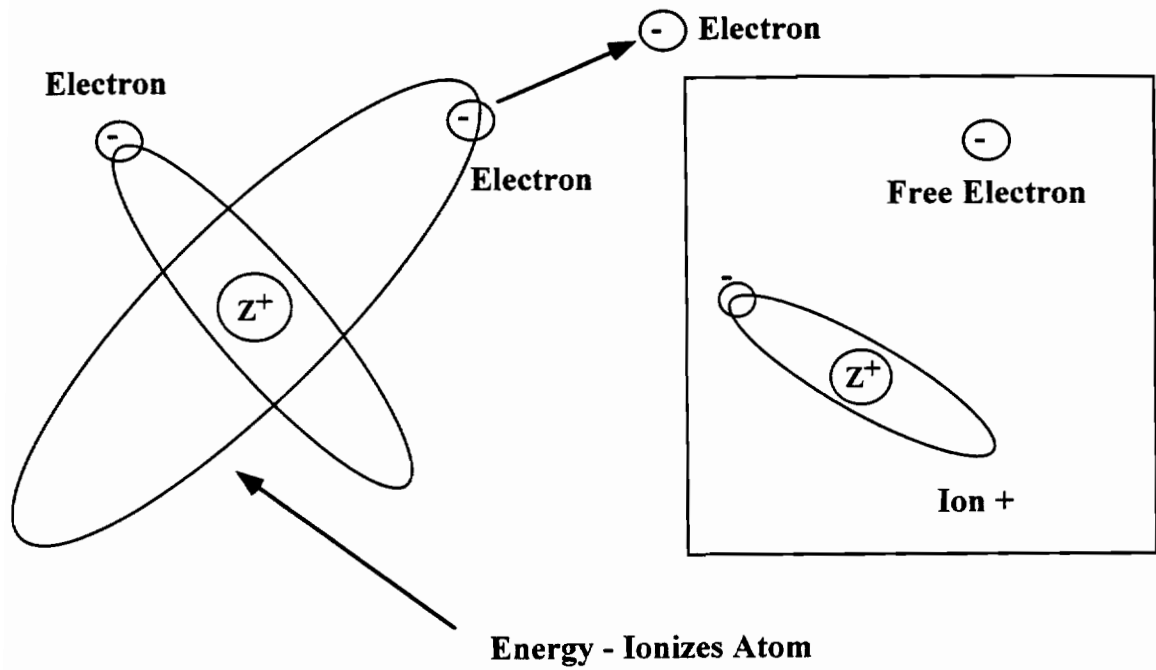


Figure 1.7. A neutral atom ionized, a component of a plasma⁵³.

1.5.3 Plasma Thermal and Velocity Profiles.

The temperature, or heat content, and the velocity of the plasma jet depend on the nozzle geometry and operating conditions of the plasma gun⁴⁹. Assuming a constant nozzle geometry, a reasonable assumption given that it is the most difficult parameter to change, the variables most responsible for plasma characteristics are 1) power input, amperage and voltage; 2) primary gas flow rate; and 3) secondary gas flow rate. For a given material there is an optimum parameter set that maximizes deposition efficiencies. An examination of the effects of changes in these parameters can be made if, when considering an individual parameter, the assumption is made that other relevant parameters are held constant.

Determining the effects of increased electrical input, or power, into the plasma torch requires an analysis of both amperage and voltage. Raising the amperage input increases the temperature of the arc. Because plasma velocity is a function of gas expansion when heated, the result is both an increase in plasma temperature, due to the higher heat content of the arc, and of plasma velocity, resulting from more rapid expansion of the gas. The arc length is a function of voltage, so that increasing amperage, while raising arc temperature by increasing arc diameter, does not change the arc length. An increase in voltage results in a longer arc, which provides a greater time period for the gas to be in contact with the arc. This also has the effect of increased plasma temperature and velocity. By controlling the power to the system, a large measure of control of the plasma is gained. Most commercial plasma spray systems are of a high amperage, low voltage

configuration, 40 to 100kW⁶⁵. The plasma gun anode and cathode are subjected to extremely high current densities, and frequent replacement of parts is required. A great advantage is gained if a lower amperage input can be achieved. A high voltage, low amperage system has much less heat resident in the gun, allowing significantly longer component life⁶⁵.

The primary gas flow rate is the second parameter relative to heat content and velocity of the plasma. As the flow rate increases, there is more gas passing through the arc, more gas to heat means a cooler plasma. When the flow rate becomes too high, the layer of gas in contact with the water cooled nozzle wall becomes cooler resulting in a higher plasma core temperature, but with a smaller arc radius, because of increased thermal-pinch effects⁶⁶. A reduced flow rate presents a lower gas volume to the arc, and with a constant thermal energy present in the arc, the gas is heated faster, yielding a higher plasma temperature. The higher temperature plasma is less dense, however, and while the particles in the plasma plume are heated to a higher temperature, the resulting particle speeds are lower. To achieve high particle speeds, both high plasma speeds and a high plasma density are required. Powder size will also play a part in final particle speed, and must be considered when determining primary gas flow parameters. Powder size effects are discussed in detail in a later section. If the flow rate is too low, the arc becomes less stable because the beneficial effects of the thermal pinch is lost, resulting in reduced core temperature because of the larger diameter of the arc. With the loss of core temperature, plasma speeds are reduced.

Secondary gas serves to increase the voltage input in the arc, with a resulting increase in the length of the arc. Increased arc length means longer exposure of the gas to the arc, increasing plasma temperature, and in turn increasing plasma speed. The addition of a secondary gas also increases plasma density, further increasing momentum and heat transfer to the particles.

Mapping of a plasma plume is difficult at best. There are steep thermal gradients in most areas of the plume, especially close to the plasma core. Core temperatures reach in excess of 12 000 K at the nozzle exit, cooling rapidly as the distance from the nozzle increases. It is useful, however, to draw isotherms to give a general picture of the shapes of the thermal regions between the nozzle and the target. The same procedure is used to draw velocity lines. Figure 1.8 shows velocity and thermal profiles of a N_2-H_2 plasma jet⁶⁷. It should be remembered that it is the shape of the profiles that are important here, actual distances vary with any change in spray parameters.

A significant consideration influencing thermal and velocity conditions is the atmospheric status at the time of spraying. When spraying in air, the plasma-atmosphere interface becomes compromised at the nozzle exit. Air becomes entrained in the plasma, making this boundary region ever wider until the target is reached. For this reason the plasma center region is the area of real interest. Particles should be introduced to the plume center to obtain proper melting and maximum speeds, regardless of the atmospheric conditions during spraying. Low pressure plasma spray (LPPS) and vacuum plasma spray (VPS) are alternative atmospheric spraying

conditions developed to reduce or eliminate the air entrainment problems.

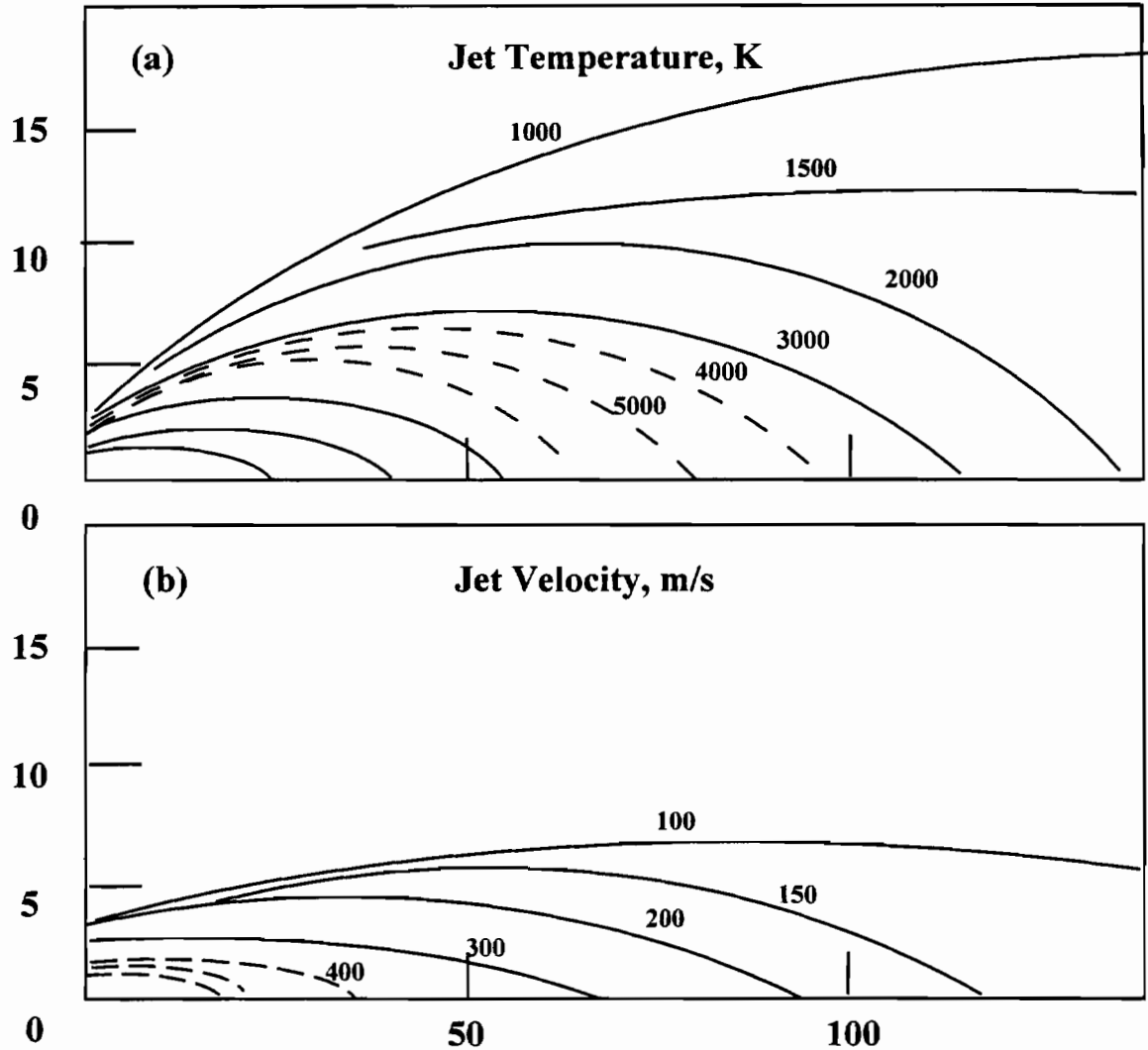


Figure 1.8. a) Temperature profile. b) Velocity profile⁶⁷. Temperature and velocity variation within dc N_2-H_2 plasma jet.

1.6 Behavior of Individual Particles.

As noted in a previous section, materials selection is an important factor when planning spray parameter optimization. The aspects of powder size or wire diameter, density, melting temperatures, and possible atmospheric reactions must all be considered.

Powder technology is such that most materials can be manufactured in powder form for thermal spraying. Ceramics to polymers, composites to metallics, many powders are readily available. Generally speaking, wires are limited to metallics. Powders and wires can be co-sprayed. In the development of a self lubricated coating, spraying graphite or other lubricating powder with a high carbon steel wire is one approach.

Wire should be of a hardness that will allow smooth wire feeding, of an appropriate diameter that will allow a consistent particle size to be melted and propelled by the plasma. Density of material and particle size are considerations of both powder and wire. For powders, sprayed particle size is determined by powder size, and density becomes even more critical. If the powder is light, it is more difficult to inject into the plume core. The particles cannot be fully melted and are propelled to the target in the outer, cooler, region of the plume. Proper adjustment of the carrier gas flow rate will in most cases overcome this, however there is a discrete range of powder sizes that a particular system can accommodate⁶⁸. Dense particles can be injected past the plume core, with the same result of being propelled in the cooler and slower outer plasma regions. If the particles are

too dense for the plume, usually because they are too large, they will fall below the plasma center line. This results in unmelted particles and/or missing the target altogether. If the powder particles are too small, especially if they are injected to the plasma core, they can vaporize and disappear from the system. This can also happen if the range of powder size is too large, because parameter optimization for one powder size may generate conditions that are too hot or too cold for other powder sizes. For this reason the powder size range must be narrow⁶⁹. The most appropriate size is dependent on the material and the thermal spray system employed.

Melting temperatures and atmospheric conditions must also be considered. Refractory materials, for example, require a hotter, longer arc than polymers, which require much cooler plasma conditions. Normally a desirable coating requires a fully melted particle impacting at high speeds, resulting in a dense, nonporous, coating. Sometimes, however, a porous coating is desired, requiring a partially melted particle at time of impact. Porosity enhances thermal shock resistance while decreasing thermal conductivity⁷⁰. Other factors such as the likelihood of a material reacting with atmospheric oxygen, or with a plasma gas, such as nitrogen or hydrogen, must also be considered.

1.7 Slide/Roll Ratio.

Pure rolling between two bodies occurs when the rotation of one exactly coincides with that of the other. When slippage happens, due to acceleration or braking of one component, creepage, or sliding/rolling, occurs. The slide/roll ratio is the difference of the surface velocities divided by the mean

of the two velocities.^{71,72,73} Equations for the mean surface velocity and the slide/roll ratio are:

$$V_m = (D_b N_b + D_t N_t) / 2$$

$$S/R = 2 (D_b N_b - D_t N_t) / (D_b N_b + D_t N_t)$$

D_b and D_t are the diameters of the bottom and top rollers and N_b and N_t are the bottom and top roller revolutions. Before slide/roll reaches saturation, a stick/slip regime is predominant, reaching incipient slip at saturation.

Severe slide roll ratios, up to 35%, occur in railroad operation and have been reproduced in laboratory tests using the Amsler Wear Test Machine.^{74,75,76,77} Specimen geometry, 5% and 35% slide/roll ratios, and contact pressure parameters for this work were selected to be consistent with previous work cited. No previous coating work had been performed, so this work concentrated on coating development and used evaluation protocols already established.

1.8 Wear.

Wear mechanisms in general were reviewed in the literature with respect to their application to coatings under rolling/sliding load conditions. Some wear mechanisms were identified as minor contributors in the research, and as such are commented on in this section. Erosion^{78,79}, chemical, oxidative^{80,81}, fretting^{82,83}, cavitation^{84,85}, and other wear

mechanisms that obviously played no part in this application are not commented upon here.

The wear regimes expected under rolling/sliding conditions have been detailed by Bolton and Clayton⁸⁶ as type I, mild wear, with the wear debris containing oxide particles; type II, a more severe wear, with the wear debris almost entirely metallic; and type III, a very severe wear condition that included roughening of the wear surface, with prominent score marks and gouging present. Before this work, much more loosely defined 'mild' and 'severe' were the wear mechanisms defined.⁸⁷ Work on coatings under rolling/sliding wear testing is noticeably absent from the literature. It was expected that the lamellar structure of a coating will have wear mechanisms not observed in uncoated steel.

Abrasion^{88,89}, wear by displacement of the material caused by hard particles, may be a factor in rolling/sliding conditions, especially if wear debris is loosened or broken. A hardness difference in abrading materials is normally present unless particles are actually loosened.^{90,91} An occasional three body abrasion effect was observed during wear testing of the coating.

Adhesion^{93,94} is also a factor in the stick/slip regime dominant during rolling/sliding before slide/roll saturation is achieved, especially during start-up when the surface area of asperities is increasing with the increasing load.⁹⁵ Sliding wear, with its attendant microstructural changes in the surface layer plays a significant role in the wear debris formation and in the conditioning of the substrate.^{96,97} Sliding tends to create a preferred orientation in the immediate

subsurface of the material.⁹⁸ Material transfer from the coated roller was observed during the first few hundred revolutions during wear testing. Material transfer⁹⁹ was a minor factor in wear of the coatings. Transfer from one component to another and back again is observed in many sliding conditions¹⁰⁰.

There are many factors controlling the frictional force generated by two surfaces in contact. The relative hardness¹⁰¹, asperity deformation, adhesion or the formation of wear debris¹⁰² and different phases in steels¹⁰³ are some that have been considered.

1.9 Rolling Contact Fatigue.

It is recognized that under the very high axle load conditions of modern railroad usage that rolling contact fatigue (RCF) is a significant factor in rail damage^{104,105,106,107}. Surface defects such as surface intrusions¹⁰⁸ and near surface inclusions¹⁰⁹ are RCF crack initiation sites. A crack may initiate without defects in the plastic flow region.^{110,111} Severe surface deformation layers have been observed in rail steels, especially under increased axle load, up to 5-10 times greater in curved track than in tangential track, which is consistent with increased RCF damage in curved track.¹¹² The plastic flow occurs from the accumulation of plastic deformation occurring over many RCF cycles.¹¹³ Steel coatings may display some of the work-hardening behavior associated with plastic deformation¹¹⁴, but this was not determined. Su¹¹⁵ has shown that RCF cracks can display severe branching behavior, something that would be significant in a lamellar structure such as a plasma sprayed coating. Lubrication serves to exacerbate the cracking, once

initiated, by exerting a powerful hydraulic opening force at the crack tip.

1.10 Lubrication.

Trackside lubricators, a mechanical pump which draws lubricant from a reservoir and delivers it to the track, are presently used in the railroad industry.¹¹⁶ Mechanical problems with these devices have shown them to be less than reliable.¹¹⁷ The latest versions of the lubricators show improved performance^{1180,119}, however further improvement in wheel/rail lubrication is very much desired. Lubricating grease is defined as 'a solid semi-fluid product of dispersion of a thickening agent in liquid lubricant. Other ingredients imparting special properties may be included.'¹²⁰ Greases are most often used where lubricant is required to maintain its initial position in a mechanism, especially where frequent relubrication is limited. Lubricant additives include viscosity index improvers, detergents, dispersants, oxidation inhibitors, emulsifiers, demulsifiers, and many others.¹²¹

Greases are available, including synthetics^{122,123}, with lubricant selection¹²⁴ made from a range of industrial classifications¹²⁵ that may provide the full film¹²⁶ lubrication desired in the evaluation of the lubricant reservoir quality of a 1080 steel plasma sprayed coating. Texaco 904 grease was chosen because of its successful use in previous work.¹²⁷ Further investigation into finding the best grease product for this application was not done because it was determined that the coating did not display lubricant reservoir qualities.

A solid lubricant is a thin film of solid superimposed between two rubbing surfaces to reduce friction and wear.¹²⁸ Lamellar solids have layers of crystal lattices with strong covalent bonds and relatively weak bonds between layers.¹²⁹ Molybdenum disulfide, MoS_2 , and graphite are solid lubricants with different qualities that may be considered in a coating. Graphite requires a thin film of contaminant such as oxygen or water to help weaken the bonds between lattice planes¹³⁰. Molybdenum disulfide has a lattice layer of sulphur between lattice planes¹³¹, and its efficiency is reduced in the presence of a contaminant. MoS_2 has wide lattice spacing between closed packed planes allowing easy slip. Graphite may not be a good choice to include with the coating because the plasma jet, while operating in air, is made up of nitrogen and hydrogen. At plume center, the desired area for coating particles to be propelled, there is little oxygen available. Plasma sprayed coatings have been used for self lubricating coatings^{132,133,134}, largely in the aerospace and automotive industries. The self lubrication possibility is one reason given as justification for this research.

CHAPTER TWO

2.0 SINGLE SPLAT ANALYSIS

2.1 Introduction.

This chapter is a synthesis of a literature survey, experimental work, and a concept. As a literature review, it is an extension of the previous chapter. As experimental work it is presented ahead of work done on coatings because it was a technique upon which much of the rest of the work rested. The concept came from a demonstration¹⁴³ of plasma spray equipment. Demonstrated was the collection of spray patterns onto glass slides to augment metallographic examination of a coating in the evaluation of the effect of working distance change. This demonstration illustrated various techniques used to help in spray parameter optimization.

The concept was to expand and improve on the spray pattern collection to the point of utilizing individual splats and splat distribution patterns to determine optimum spray parameters. Plasma sprayed coatings are made from individual

splat accumulation. A molten droplet becomes a splat upon impacting the substrate, flattening, and solidifying. If ideal splats could be achieved through a balance of the deposition parameters, then the conglomerate of splats, the coating, should be of high quality. Adjustable deposition parameters are power input, primary and secondary gas flow rates, wire feed rates, and working distance.

Observations from the laboratory microscopic examination is blended with the literature review to present a practical application of theory and experiment to produce a research technique that works.

2.2 Single Splat Analysis

A method to predict coating quality quickly and easily is very desirable when faced with the task of determining plasma spray parameters. Such a method should allow nondestructive analysis of specimens and promote quick evaluation even during the fine tuning of spray parameters. When appraising coating quality it is useful to examine the behavior of the most basic coating component, the individual splat. Such a technique is described here, and is called 'single splat analysis'.

When using the single splat analysis technique, it is necessary to connect what is noted in individual splat observation to spray parameters. The connection trail involves relating splat morphology to the incoming particle conditions of velocity, temperature and size. Particle conditions are directly related to the plume conditions of velocity and temperature. Plume conditions are a result of spray parameters. The adjustable spray parameters are primary and secondary gas flow rates, powder/wire feed rates, working distance, amperage and voltage.

A brief review of the effect of each of the spray parameters on the plume condition may be useful here. Increasing or decreasing the flow rate of the primary gas will lower or raise the plume temperature respectively. It will also increase or decrease the mass density of the plume, affecting the thermal and velocity transfer to the particles while in flight. The use of a secondary gas also affects the thermal and velocity transfer. In addition, the secondary gas serves to increase the system voltage, thus lengthening the arc, increasing the temperature and velocity of the plume.

Working distance controls the length of time the particle is in the plume. System amperage controls the temperature of the arc, and voltage the arc length.

Single splat analysis is a useful tool for predicting coating quality. During spray parameter development, individual splats are collected by rapidly passing a glass slide or metal coupon through the spray pattern at a specific working distance. Aluminum and steel coupons were used to determine whether the molten particle would spread in the same manner as on the glass slide. It is thought that the flattening and solidification behavior of the particle is very similar when collecting single splats as long as the material is polished smooth. A smooth specimen is required for single splat analysis because as soon as surface roughness is introduced the splat flattening behavior is changed by the nature of the roughness.

These samples are then examined under a stereo microscope. Identification of splat characteristics give clues as to which parameters should be adjusted. Poor splat morphologies such as bounce back, star patterns, empty splat centers, lack of small particles, and otherwise misshapen splats each give their own hint as to what is out of balance: particle size, speed and/or temperature. Adjustment to spray parameters can then be made to achieve better and better individual splats until optimum parameters are achieved. The most important adjustable parameters are primary and secondary plasma gas flow rates, the powder/wire feed rate, and the working distance. The single splat analysis technique works very well for thin coatings, however when thicker coatings are required, additional information is necessary for coating evaluation. As coating thickness increases, substrate

temperature increases. If this temperature increase is too great, the arriving particles impact a changing surface condition, different than that for which optimum parameters were developed. This can affect the mechanical properties, such as strength, ductility and hardness, of the resulting coating¹⁴⁴. Substrate cooling is required, and metallographic examination of the coating cross-section is recommended.

2.2.1 Stereomicroscopic Examination of Splats.

Some simple adjustments to the conditions of examination under the stereo microscope will be helpful in single splat analysis. The idea is to collect individual splats on the glass slide, so there will be areas of the glass that will be uncoated. When the slide is placed for viewing in the microscope, it is helpful to use different colored backgrounds. For steel, such as is used in this research, white, yellow, and orange are very good background colors. For example, if black is used, the splat surface can be seen very well, but if there is a center missing from the splat it often appears that there is a thin layer of material in the center. Looking at the same splat on white, yellow, or orange clearly shows the center missing, see Figures 2.1 & 2.2. Use of black allows too much opportunity for misleading information. White allows very clear views of outer surfaces, and, in conjunction with the other recommended colors, effective single splat analysis can be made without false impressions arising during microscopic observation. The slide can be conveniently passed over a specially prepared white/yellow/orange strip or placed on larger, individually colored backgrounds. Not using the multiple colored system may result in passing over subtle

information that can favorably influence the selection of optimum parameters.

Single splat analysis should concentrate on splats taken from plume center. Splats from the outer regions should be observed, but only to confirm analysis from plume center or to look for clues as to the cause for poor splat morphology present in the center region. As the glass slide is passed through the plume, normally in a vertical pass, a region on the slide can easily be determined as containing splats from plume center. This zone is much denser and has smaller splats, with the density decreasing with distance from the center region. Splat size can increase considerably in the area just outside this center region, especially when spray parameters are not in the optimum range. The closer to optimum spray parameters, the more apparent becomes the center region because of the increased numbers of very small splats.

The reason for a greatly increased amount of very small splats as optimum parameters are approached is that the plume is fine tuned to the correct temperature and velocity conditions to allow the very small particles to be melted, propelled, and impact their target in a molten or plastic state. Too much heat, either because the plume is too hot, vaporizing the particles, and/or too slow, with the particle in the plume too long resulting in overheating and vaporizing, will cause the very small particles to disappear from the system. Underheating, because the plume is too cold and/or too fast, will cause these particles to be unmelted at time of impact. If the plume is too slow relative to jet temperature the particles can solidify before impact. Unmelted particles bounce off rather than adhering. If there is a lack of these small particles in plume center region of the specimen, then

optimum parameters have not been achieved. This is especially significant when spraying wire, because of the wide range of particle sizes possible.

It is tempting to look at larger splats for idealized splat morphology and not consider the range of splat sizes present, but the first priority in parameter development is to maximize the quantity of these very small particles. Once this is achieved, optimum parameters are in the neighborhood. Figures 2.3 & 2.4 show how fine tuning the secondary gas parameters affect the splat pattern, especially the small splats. Attention is then shifted to larger splats, again concentrating on the plume center region. Clues for which parameters to adjust can be taken from the morphology of larger splats.

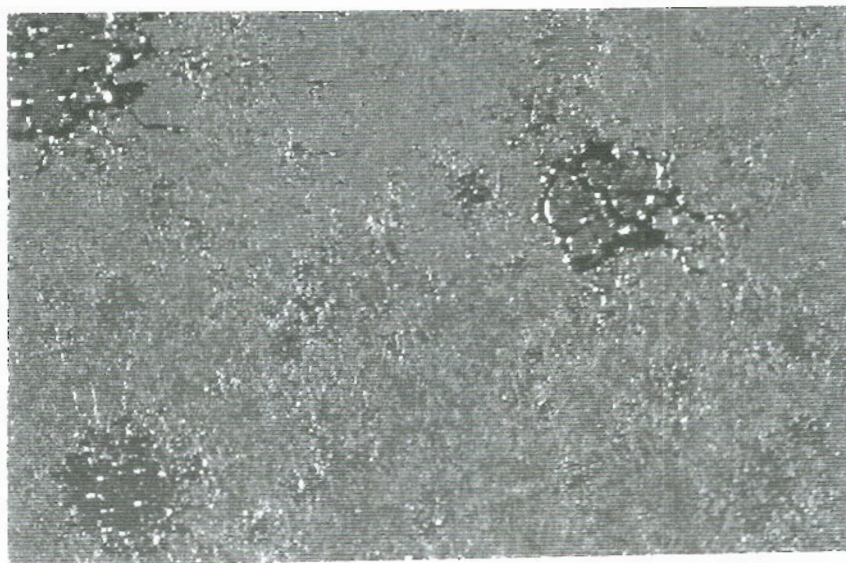


Figure 2.1. Splat field at plume center with black/white backgrounds. Especially note the centers of the larger splats.



Figure 2.2. Splat field with yellow (top)/orange (bottom) backgrounds.

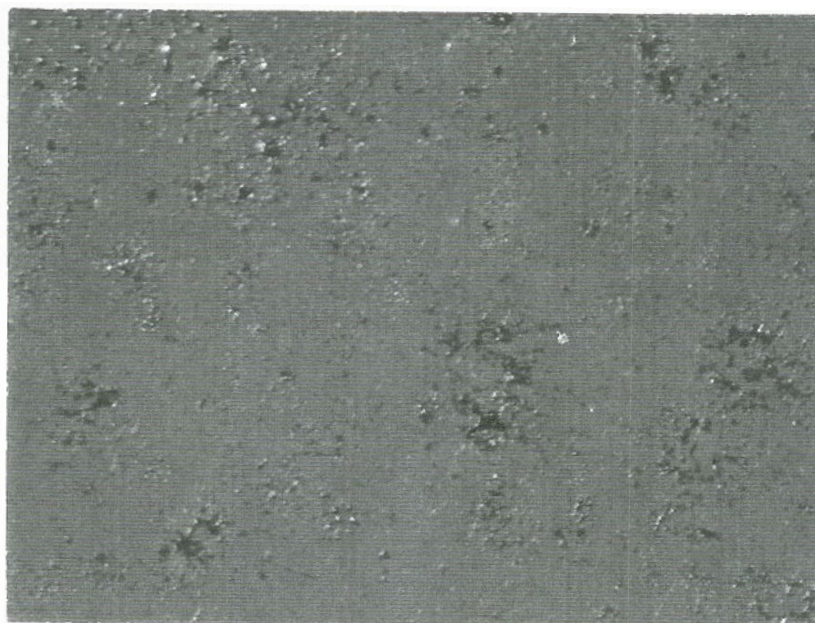


Figure 2.3. Primary gas (N_2): 235slm, secondary gas (H_2): 30slm, working distance: 225mm.



Figure 2.4. N_2 : 235slm, H_2 : 35slm, working distance: 225mm. Notice the increase in small splats with the small increase in secondary gas volume.

2.2.2 Splat Morphology.

Particles are mostly spherical during flight, and upon impact flatten, the material flows outward, and then solidifies into a final shape. Ideally this shape resembles a thin, flat pancake. see Figures 2.5 & 2.6. The splat cooling rate depends on splat thickness, material thermal properties, and contact area between the splat and the substrate¹⁴⁵. The flattening time is much faster than the freeze time, allowing the particle to completely flow and flatten before solidifying. Flattening time is on the order of 10^{-8} seconds and freeze time about 10^{-6} seconds¹⁴⁶. The degree of flattening is dependent largely upon particle temperature, impact velocity, viscosity, and surface tension of the droplet¹⁴⁷. Wetting between the coating material and the substrate is a factor, although normally a minor consideration.¹⁴⁸

If the material is not fully melted at impact, it will either be flattened and the unmelted portion becomes an inclusion, or the unmelted portion will bounce off, leaving a splat with no center. Some applications require a partially molten condition to produce desired coating properties, however, most coatings are of best quality when few or no inclusions are present. Porosity is nearly always found when inclusions exist because incoming particles cannot penetrate into the voids resulting from partially flattened particles.

Thermal conductivity of the spray material is important to the adherence of the splat¹⁴⁹. If the incoming particle is overheated, it will strike the substrate and flow too much before solidifying. This is the same effect of too high a velocity at impact. The particle shatters, leaving a center

with a star shaped outer region. If an overheated particle is too large, the bounce back effect occurs. Bounce back will also happen when incoming particles are larger than optimum size for the spray parameters and are fully melted upon impact. During powder or wire spraying, large particles can result from in-flight collisions occurring in the plasma jet regions away from the center line. When spraying wire, large particles can also result from either too fast or too slow wire feed rates.

Impact velocity also affects final splat morphology. If the velocity is too low, the splat cannot penetrate into all the surface cavities, resulting in porosity and poor adhesion at the substrate interface and poor cohesion within the coating thickness. The splats may be too thick, not flat, or the particle may bounce off upon impact. If the velocity is too high, the larger splats may shatter, yielding a malformed splat with poor adhesion. Generally speaking, high impact velocities and small particle sizes are required to achieve a low porosity, tightly adhering, small grained coating. High impact velocity assures maximum penetration into surface irregularities on the substrate. As the coating thickness builds, the same surface-filling benefits are present. This is why the spray parameters are optimized for the very small particle sizes.

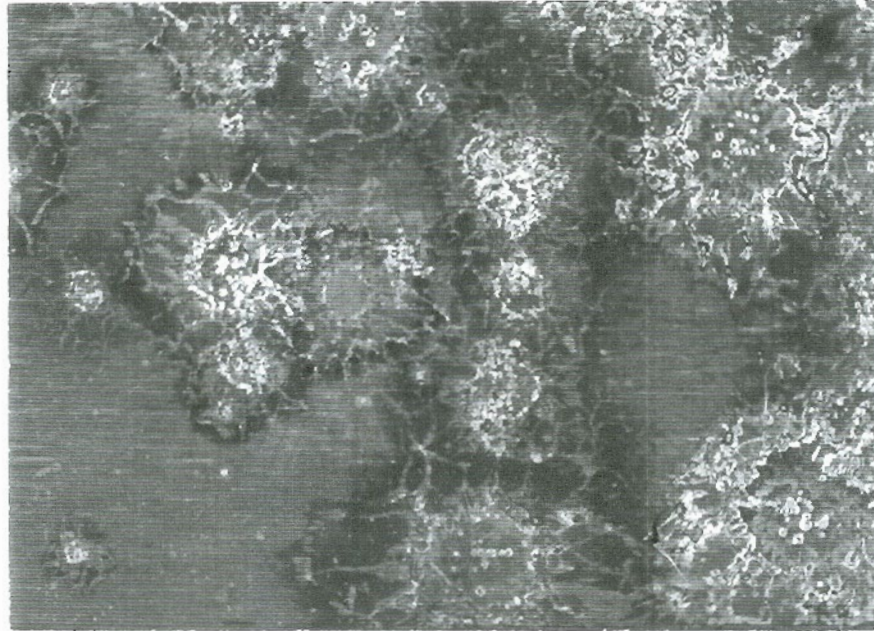


Figure 2.5. An idealized splat field. Steel sprayed on steel.



Figure 2.6. An idealized individual splat from the above field.

2.2.3 Working Distance Effects.

Time in flight is a critical parameter for achieving proper melting and impact speed for spray particles. The distance must be far enough to attain full melting and high speeds, yet close enough not to allow vaporization of small particles. Full melting and high particle speed, resulting from heat and momentum transfer from the plasma jet to the particles¹⁵⁰, is required to achieve dense, low porosity coatings. Too long a distance allows the particles, especially heavy particles, to fall too far below the plume center, resulting in falling out of the high temperature, high velocity region, possibly missing the target entirely. If this particle does hit the target it is too slow, not fully melted, or both. Unmelted particles bounce off. Partially melted particles impact, the melted outer surface adheres to the substrate, and the unmelted portion bounces off. In the latter case, a splat without a center can be observed when performing single splat analysis. Much of the same phenomena can be observed if the distance is too close, with unmelted particles bouncing off and partially melted particles acting as described above or being held as inclusions in the resulting coating. There may be in-flight impacting between particles when long working distances are utilized. This will result in some very large splats in an otherwise small splat field, especially noticeable in the regions away from plume center on the glass slide. Figures 2.7 & 2.8 show the effect of working distance when the other parameters are close to optimum.

As optimum gas parameters are approached, fine tuning of the resulting coating can be achieved by adjusting the working distance. If particles are fully melted and the plume is hot

enough to continue heating the particles during flight, overheating can occur. Overheating of small particles can result in vaporization, they disappear from the system. Only larger splats are visible on the substrate. Large particles, in the overheated condition, impact the substrate at high speeds. Ideally the particle impacts, spreads, flattens, and freezes. If a large particle is too hot upon impact, instead of flattening and freezing it will spread and the center portion, having significantly more mass than the outer region that is spreading and freezing, will bounce back away from the substrate, similar to the way a drop of water will bounce when striking a surface, and solidify in this position. All particles are subject to later-arriving particles impacting them as the coating thickness increases. The bounced back particles can then be broken off and captured as unmelted inclusions in the coating. As previously pointed out, at longer distances in-flight particles can strike each other, causing a much larger particle to be impacting the substrate. It is these large particles, especially if they are in a superheated condition, that are the most pronounced bounce-back splats. In general this occurs some distance away from the center of the plume, where there are more severe velocity and temperature variations than at plume center.

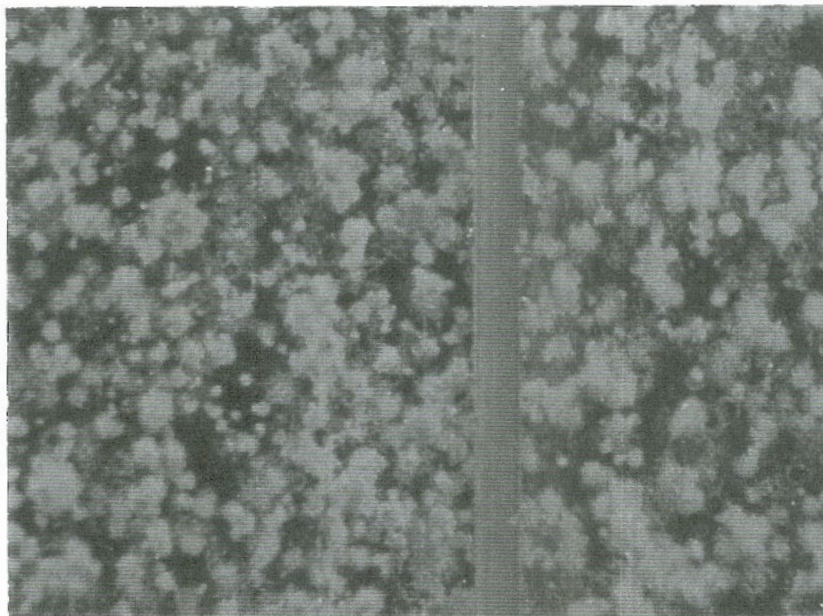


Figure 2.7. Working distance of 195mm (left) and 210mm. At 195mm there are unmelted particles and some empty centers.

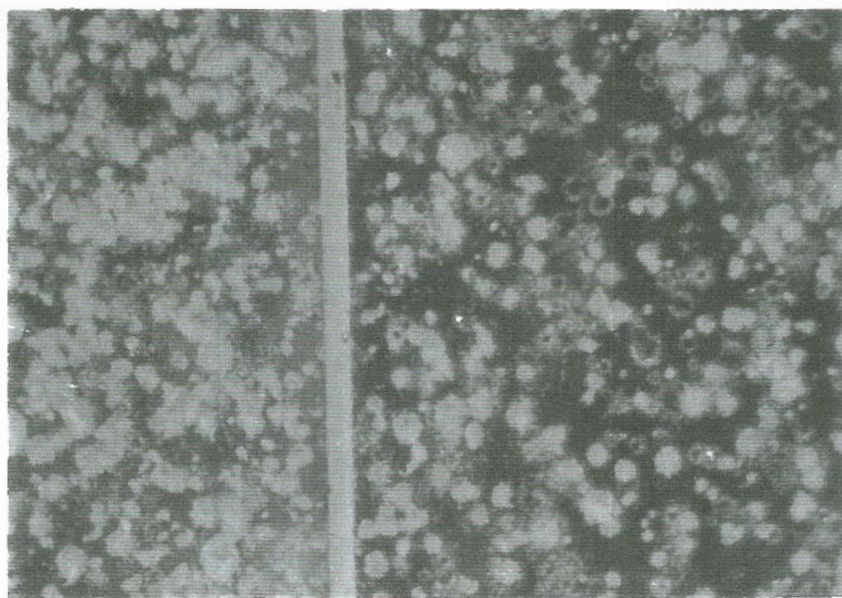


Figure 2.8. 210mm and 230mm. At 230mm there are empty centers and a lower particle density. Other spray parameters are the same. Zirconia on glass.

The following charts give an overview to the single splat analysis technique.

Table 2.1. SINGLE SPLAT ANALYSIS

| | |
|----------------------|-------------------------|
| PLUME CONDITIONS: | SPRAY PARAMETERS: |
| Velocity | Primary Gas Flow Rate |
| Temperature | Secondary Gas Flow Rate |
| | Working Distance |
| PARTICLE CONDITIONS: | Wire Feed Rate |
| Velocity | Amperage |
| Temperature | Voltage |
| Size | |

Table 2.2. PARTICLE CONDITIONS

| PARTICLE CONDITION | OBSERVATION |
|----------------------|--|
| Overheating: | Vaporization, lack of small splats. Bounceback. Too much outward flow, empty center region. |
| Underheating: | Particles bounce off, lack of small splats. Empty center region. Unmelted center may stick but be malformed. Unmelteds, partially melteds. |
| Velocity Too High: | Particle shatter, leaving a center with a star shaped outer region. Poor adhesion resulting from bounce. |
| Velocity Too Low: | Poor penetration into voids. Splats not flattened. Lack of small particles. |
| Particles Too Large: | Bounceback. Partially melteds. Too narrow a size range. |

Table 2.3. PARAMETER ADJUSTMENTS

| PARTICLE CONDITION | PARAMETERS |
|---|---|
| Overheating: | Decrease secondary gas flow. Increase primary gas flow. Decrease amperage, voltage. |
| Underheating: | Increase secondary gas flow. Decrease primary gas flow. Increase amperage, voltage. |
| Velocity Too High: | Decrease primary and/or secondary gas flow rates. |
| Velocity Too Low: | Increase gas flow rates. |
| Particles Too Large: (Lack of small particles) | Adjust wire feed rate. Other parameters not close to optimum. |

2.3 Practical Applications of Single Splat Analysis.

2.3.1 Process Changes.

As changes were made in the process, such as wire sizes, fixturing changes that allowed parameter changes, substrate cooling evaluation, changes in working distances, and exchanges of anode. Spray parameter optimization was confirmed through the use of single splat analysis.

2.3.2 Wire Selection.

Wire selection evolved through a series of materials. The first wire used was a 3/32" diameter, 1075 flux-cored steel. Several tests were made using this material, with mixed success. The basic problem turned out to be something perhaps unique to the thermal spray process. The behavior of the wire during melting appeared to be erratic. Single splat analysis showed that the splat morphology was not consistent. Fine tuning of the spray parameters did not improve this condition. It was determined that the coring materials reacted differently than the steel particles during the melting process in the plasma jet.

A 3/32" diameter music wire, 1080 plain steel, was next used. This produced a more consistent splat morphology, as determined by single splat analysis. The splat pattern was not optimal, however. Across the pattern many more large splats were present than were thought to be an ideal condition. Small splats delivered at high velocity produce the highest quality coatings. In an effort to attain a more consistent range of splat sizes, a 1/16" diameter wire was tried. This wire is the same high carbon steel wire as the larger diameter product,

only the wire diameter was different. It immediately was apparent that the smaller wire was melting in a more efficient way, with a greatly improved spray pattern. It was then possible to achieve large numbers of very small splats when optimum spray parameters were achieved. This wire, with all of its advantages, had a major drawback to the research. It was available only in one pound rolls. It was necessary to unwind the roll and coil it onto a reel for feeding into the spray system.

Spraysteel 80, a 1080 plain steel wire developed for a twin-wire arc system, 1/16" diameter, was the next wire used. This wire has all of the desirable features of the music wire plus availability in 30 pound coils ready for the wire feeder. 1080 plain steel, 1/16" diameter, was the wire used for the balance of the experimental work. Optimum parameters were worked out for this wire, through single splat analysis and metallographic examination, and used throughout most of the rest of the work.

Figure 2.9 is a photograph showing the microstructure typical for high wear resistant coatings. Its features include a dense microstructure, few large unmelted particles, and many very small particles. These small particles resulted from being molten when taken from the wire and are so small that they have solidified into a plastic state during flight and then are assimilated into the coating.



Figure 2.9. AMST27. Typical microstructure of high performance coating.

CHAPTER THREE

3.0 EXPERIMENTAL PROCEDURES

3.1 Introduction.

This section encompasses the experimental protocol required to produce specimens and conduct experiments to measure performance. It is necessary to include details regarding equipment, fixturing, and process control in order that experimental procedures may be understood.

At the onset of the experimental work, certain basic assumptions were made regarding the coating, its method of manufacture, desired performance characteristics, and experimental procedures to measure the performance.

The coating material was to be a high carbon plain steel, similar to the rail steel that would receive the coating, plasma sprayed onto Amsler rollers for wear testing under slide/roll conditions. Amsler rollers, made from rail steel, were to be of the same geometry as rollers used in previous work¹⁵¹, to be as consistent as possible for data comparison. Figure 3.1 shows an Amsler roller. All wear tests were to be performed in the as-sprayed condition, to simulate as closely as possible the conditions that would be encountered in field

operations. Amsler wear tests were planned for various slide/roll ratios, under various contact pressures, again for consistency in comparison with previous work. The contact pressure and slide/roll ratio test matrix was:

| Slide/roll | Contact pressure (MPa) | | | | |
|------------|------------------------|------|-----|-----|-----|
| 35% | 1220 | 1050 | 900 | 700 | 500 |
| 5% | 1220 | 1050 | 900 | 700 | |

These guidelines were observed throughout the research with only minimal revision. Those revisions were to test specific conditions and their relationship to coating performance. For example, coating thicknesses have ranged from 0.3mm to 2mm to determine the influence of coating thickness, if any, on wear performance and the incidence of debonding. Some post-spray processed rollers were tested, grinding the wear surface flat, in an attempt to minimize edge effects.

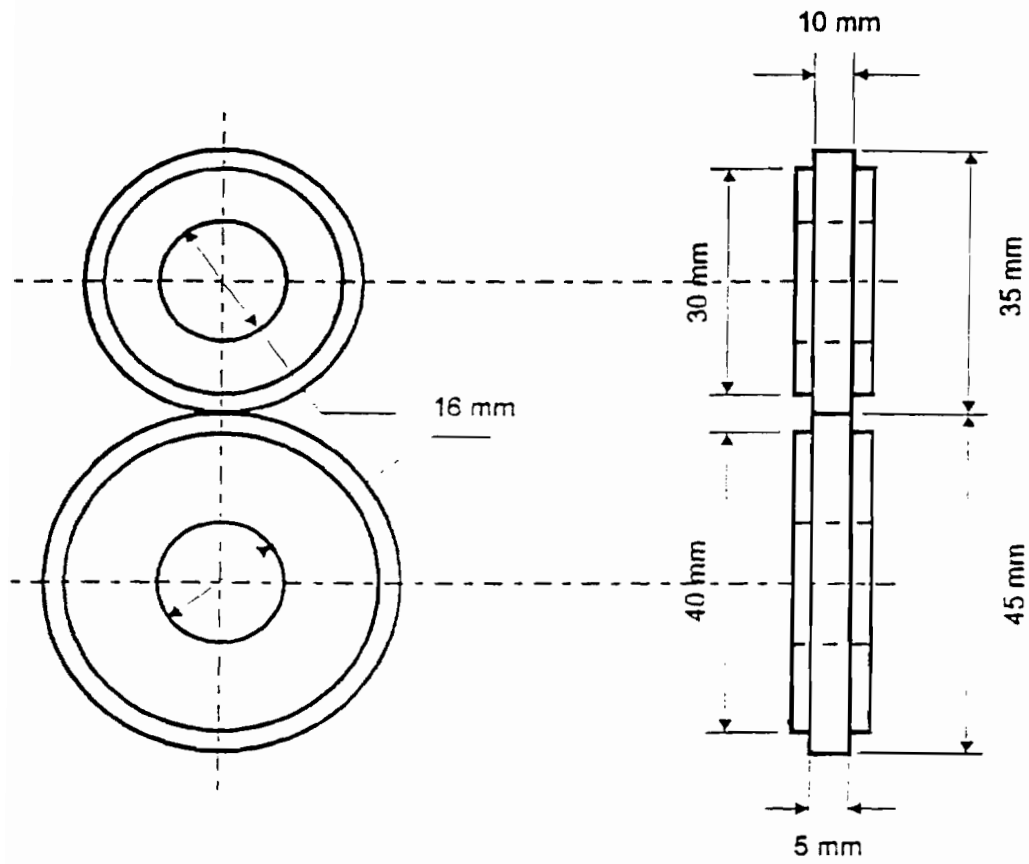


Figure 3.1. Amsler roller.

3.2 Plasma Spray Equipment.

The equipment used to make the coating is powered by two DC rectified constant current power supply devices. The plasma gun consists of a thoriated tungsten cathode and a copper anode in a water cooled brass housing. Plasma gases, power, and cooling water are routed through a control panel to the plasma gun. Figure 3.2 schematically shows the spray system. Cooling water flow rates are stepped up from about 2 gpm incoming to 5-7 gpm at 200 psi to achieve proper spray gun cooling. The wire feeder and the powder feeder are independent of the control panel and are adjusted directly on the individual device. Working distances are measured and set manually. Translation of the plasma jet is also performed manually. Further automation, even computer controlled operation, of the spray process could be implemented, however during the research phase it is impractical.

Surface preparation of the substrate before coating is an element of the research that required much experimental activity. Detailed protocol for substrate surface preparation in the laboratory is fully reported in the body of this work, and includes elements of both surface cleanliness and controlled roughening for improved mechanical bonding. Rail surface preparation in the field will call for using techniques developed in the laboratory on a very broad scale. Such technology is available in the corrosion field.^{135,136,137,138} Abrasives, in particular, are used in the laboratory and will be required in field operations. Proposed standards are available for high and low pressure wet abrasives that provide excellent guidelines¹³⁹ Wet abrasives applications¹⁴⁰, both high

and low pressure¹⁴¹ may be appropriate, with the precaution that the original profile not be compromised.¹⁴²

The first shot blast station is a sheet metal cabinet outside the spray booth. The grit can either be a chilled steel shot, alumina, or sand. In this cabinet grit can be easily changed according to surface preparation requirements. Secondary shot blasting was performed after clamping the substrate for spraying. A hand-held shot blasting gun was used, drawing grit from a portable container. Figure 3.3 shows secondary shotblasting.

Spraying was performed inside a sound-deadening spray booth. The sound level inside the booth is 100dB or more, with a sound attenuation of about 60dB through the booth walls. Appropriate ear and eye protection were standard procedure during all spraying operations. An exhaust fan removed residual heat and fumes from the booth. A water curtain was employed behind the spray target to capture overspray particles.

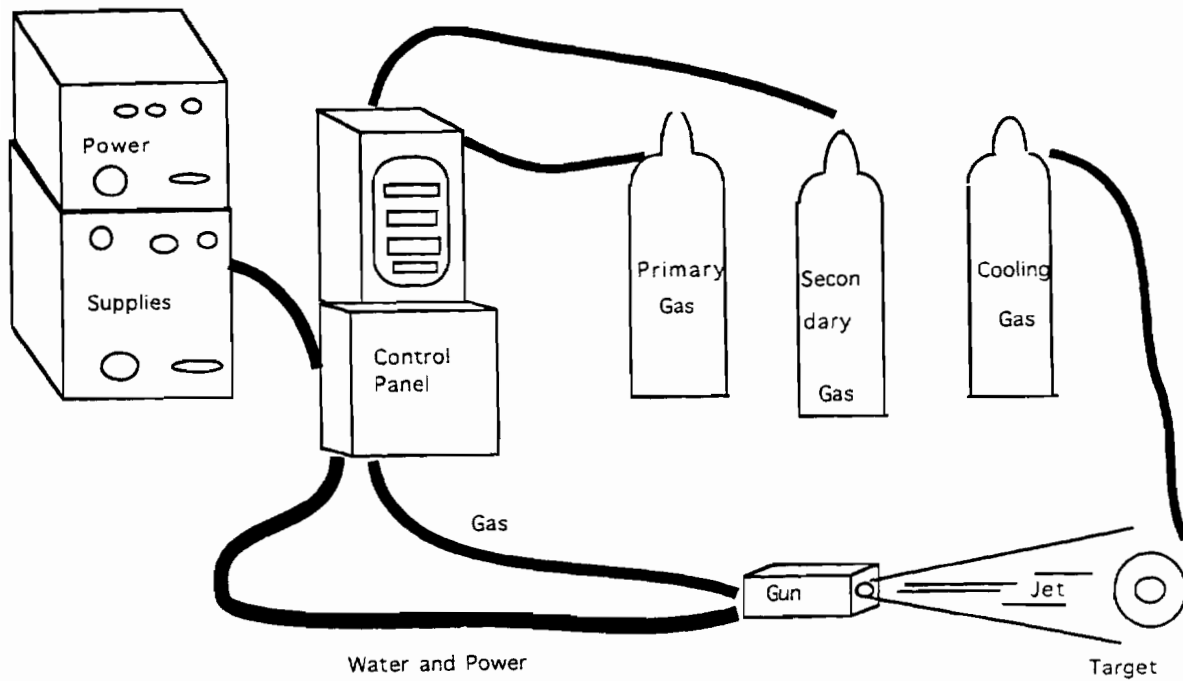


Figure 3.2. Plasma spray system schematic.

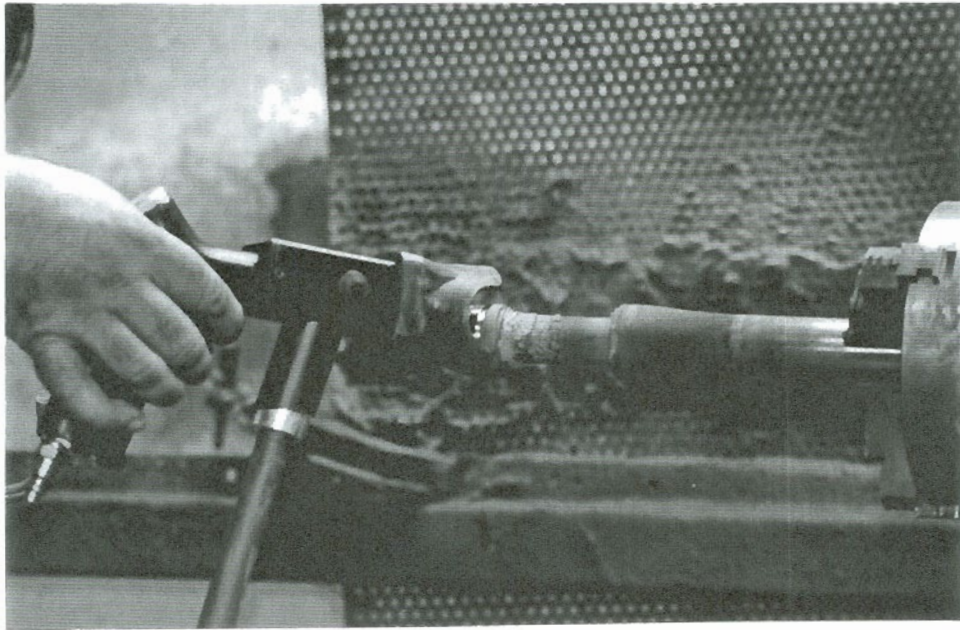


Figure 3.3. Secondary shotblast layout.

3.3 Plasma Spray Operation.

Power is set by selecting an operating amperage, voltage is a function of the amperage and gas parameters. Gas parameters and working distances are easy to duplicate, as they are metered or measured. The wire feed rate is also relatively easy to calibrate. The wire feeder has an infinite controller that can be set, moved, then reset with reasonable accuracy. Setting the wire feed rate by eye also yields a reasonable repeatability because of the fairly narrow optimal operating range. The spray pattern is highly visible during adjustment, and even very small variations in the feed speed is immediately noticeable in the spray pattern.

Establishing optimum feed rates for powder is more difficult because of the uneven manner which powder is introduced into the carrier gas stream. When observing powder feed into the atmosphere, it appears to be a repeated puffing pattern. Observing in air is a good start in setting powder feedrates, but final setting is done with the plasma jet operating. Direct observation of the powder feed can be made using a welding hood with a dark lens. The powder should be injected to the plume center, adjustments to the carrier gas flowrate are made to deliver the powder to this point. The powder volume is usually determined as the maximum amount that can be delivered to plume center and melted as it is propelled to the target. Single splat analysis can help in determining this, metallographic analysis of a full thickness coating can confirm the correct feedrate as well as other spray parameters.

3.3.1 Anode Calibration.

An improved anode was installed in the spray gun beginning with AMST23. This anode, and subsequent replacement anodes, were of a similar internal geometry. Anodes must be calibrated to optimum gas parameters when first put into service. This is accomplished by comparing gas parameters to the appearance of specific shock diamonds in the plasma jet and confirmed through single splat analysis.

Figure 3.4 schematically shows shock diamond formation. Visually the shock diamonds appear in the jet as little balls of light when viewed through a welders mask. The mask is required to eliminate the intense illumination present in the jet.

Often used parameters for the steel coatings in this research:

Power: 350 Amps
Primary gas: $N_2 = 235$ slm
Secondary gas: $H_2 = 30$ slm

At these parameters, voltage should be 390. The fourth shock diamond first appears about $H_2 = 24-25$ slm (standard liters per minute). If these values hold from old anode to new anode, the coating quality should be the same. If these values are even slightly different, parameters should be fine tuned to achieve optimization. To confirm that these observations will hold, the operator is required to perform this calibration at each anode change.

Spray parameters were nearly the same throughout the rest of the research except when purposely varied for parameter envelope testing. Spray parameter optimization was periodically confirmed with single splat analysis and metallographic examination. One reason was to make sure there was no drift in optimum parameters due to deterioration of the anode. Such deterioration can come about because of overheating, damage because of anchoring the arc, mechanical deformation from mishandling, and the like.

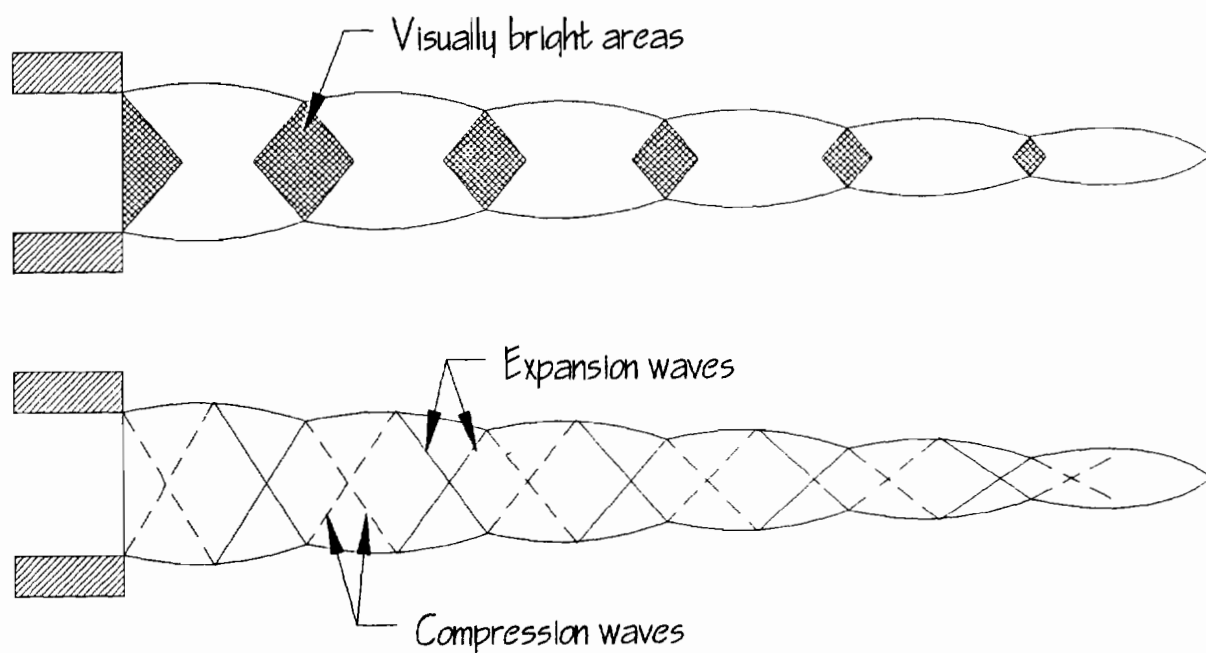


Figure 3.4. Calibration of anode to spray parameters is achieved by determining the gas parameter value of the appearance of the fourth shock diamond in the plasma jet.¹⁵²

3.3.2 Fixturing.

Successful coatings are in some manner dependent on the process used to generate the coating. Fixturing, how an object is held in position for coating, is an important aspect of the plasma spray process. Fixturing includes the clamping in place of Amsler rollers and rail sections, the spray targets, and the proper positioning of wire feeds, cooling gas and other elements of spray procedure. Because of the high temperatures present in the procedure, a continuous process of fixture development, replacement, and improvement was required.

A motorized chuck with a rotational speed of 200 rpm during spraying was used for all Amsler rollers. Because of the high heat present in the region within and adjacent to the plasma jet, the chuck required protection. It was determined that if 18 inches were allowed between the plasma jet and the chuck jaws there would be no damage to the chuck.

When two or more rollers were coated at the same time, it was very difficult to separate them after spraying. Fiberglass tape was used, but there was not enough distance between rollers on the fixture to allow easy separation in the region where overspray held them together, so graphite spacers in the shape of washers were used. The spacer can be easily broken when struck with a hammer, making roller separation fairly easy. Rollers were arranged with appropriate spacers and graphite washers for spraying. Up to ten rollers can be sprayed simultaneously using this device. Figure 3.5 shows a five roller array after spraying.

Glass slides were used in the single splat analysis technique. A simple fixture of a $1 \times 3 \times \frac{1}{4}$ steel bar 3 feet in

length with a spring clamp to hold the slide was used. The slide can then be quickly passed through the plasma jet to collect individual splats. Figure 3.6 shows single splat collection.

A bracket was made to hold the wire feed in different positions relative to the plasma spray nozzle. Injection angles of 45° and 90° can be used at different distances from the nozzle. It was determined that 90° and 45° injection angles as close to the nozzle as possible are the correct feed positions when spraying 1080 steel wire. Figure 3.7 shows the plasma gun with wire feed, powder feed, and cooling tubes.

A graphite rod with a one inch flat machined on one side was made to hold steel coupons. These coupons were used for microstructure specimens. The graphite rod works well because it acts as a heat sink during this process, and is relatively unaffected by the high temperatures of the plasma jet. Figure 3.8 shows a steel coupon being sprayed.

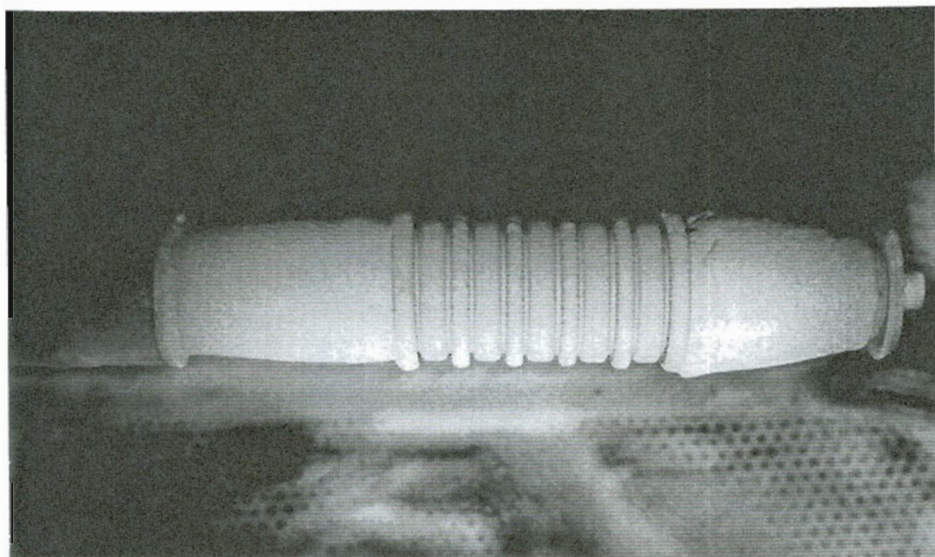


Figure 3.5. Five roller array, after spraying. Rollers are separated by graphite washers.

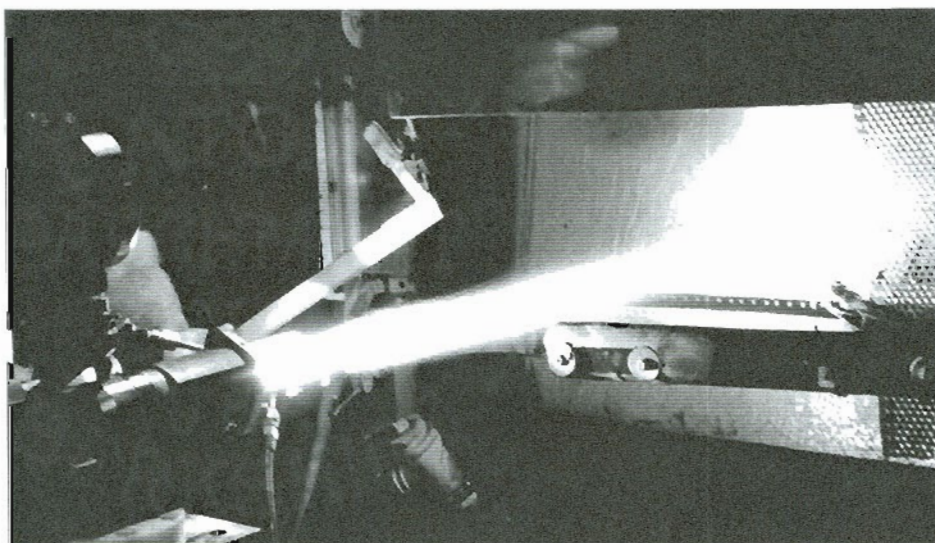


Figure 3.6. Single splats are collected by rapidly passing a glass slide through the plasma jet.

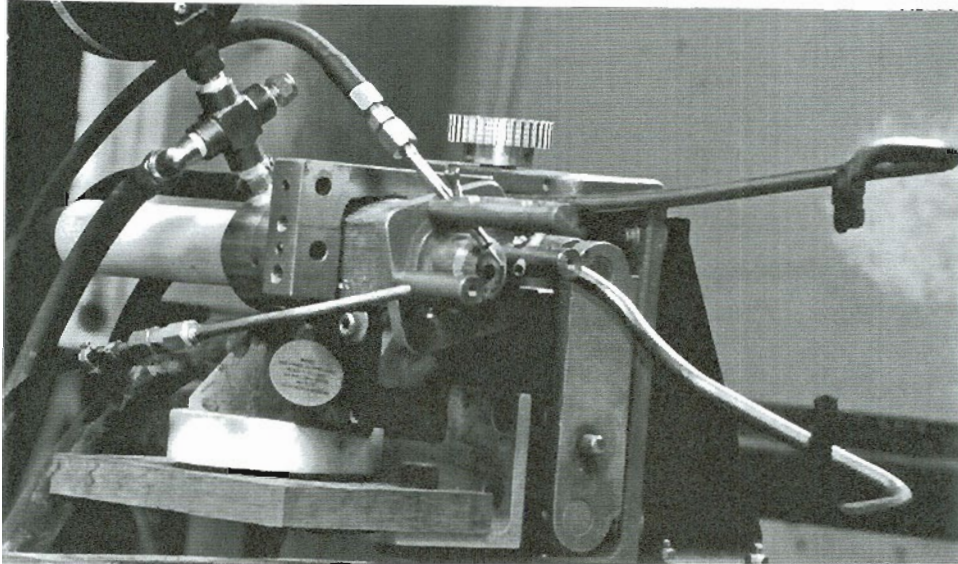


Figure 3.7. Plasma gun with wire and powder feed tubes. Backside cooling tubes extend some distance from nozzle.

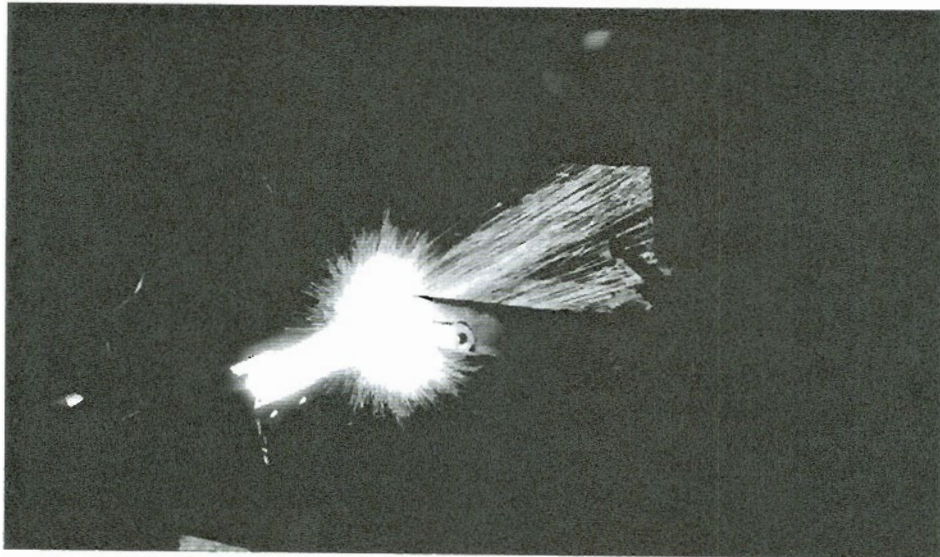


Figure 3.8. Steel coupon being spray coated for later use in metallographic examination.

3.3.3 Dwell and Traverse.

In the early stages of the research only one roller at a time was coated. The roller fit nicely into the center of the spray pattern at the desired working distance of 225mm. The dwell method was used, it was efficient because a shorter time was needed to achieve the desired coating thickness. Also only those splats from plume center, those that were optimized, were going onto the substrate. Difficulties arose when long dwell times, longer than 30 seconds, were required. Three minutes dwell was needed for a 1mm coating thickness.

Traversing involves moving the spray pattern across the target until it sees the boundaries of the pattern, much as one would if operating a paint sprayer. The jet can be briefly held off the target for additional cooling, or panned back immediately. Traversing did not appreciably lengthen the time on target beyond that of a dwell. Traversing is required when more than one roller is sprayed at the same time because they will not fit within the spray pattern center region and thus will coat unevenly. To spray thicker coatings, a substrate cooling had to be initiated.

3.3.4 Substrate Cooling.

Substrate cooling is required when spraying a thick coating. Enough heat must be removed from the accumulated coating to ensure that there will be no molten layer upon which the incoming particles could strike. The substrate cooling methods considered were:

Traversing, allowing brief cooling periods between passes.

Internal cooling of the substrate with liquid nitrogen.

A screen of cooling gas for the incoming particles to pass through just before reaching the target.

Back side cooling with a gas jet, such as N_2 or CO_2 .

Substrate cooling was accomplished by focusing jets of CO_2 gas onto the rollers during spraying. It is called backside cooling because the jets are directed onto the rollers just to the rear of vertical, at approximately the one and 5 o'clock positions, when oriented to a plasma jet flowing from left to right. See figure 3.9. The ends of the tubes were flattened out to give a wide pattern of gas onto the substrate. The cooling tubes were mounted on the plasma gun so that during the traversing operation the cooling jets follow the movement of the gun. Insulation of the tubes is not required because of the movement of the CO_2 , and the accumulation of a thin layer of coating, although clearing the overspray that tends to clog the tube ends is necessary during process set-up. A gauge pressure of 60 psi was required to maintain adequate flow for cooling.

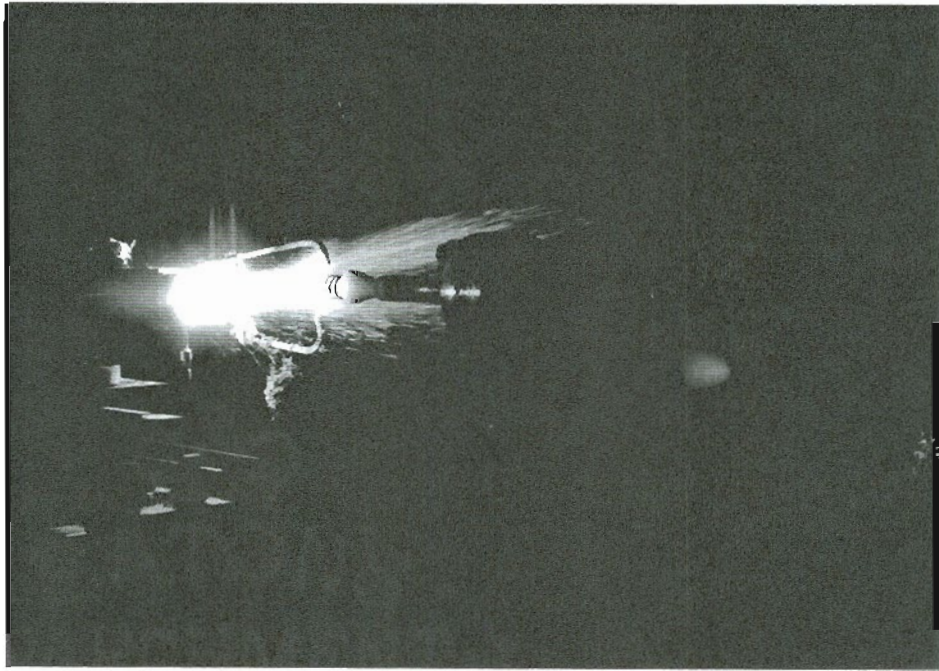


Figure 3.9. Backside cooling during spraying operation.

3.4 Materials.

The selection of a material of choice for the research involved experimentation with a variety of steel wires. Part of the original requirements of the research was that the sprayed coating be made from steel with approximately the same carbon content as that in rail steel.

The first wire was a 3/32" diameter 1075 flux-cored steel. AMST1-8 were performed with this wire. 35% slide/roll and contact pressures of 700-1220 MPa were used. A 3/32" diameter 1080 steel wire was then tried under 5% and 35% slide/roll and contact pressures from 500-1220 MPa, AMST7-15. A smaller diameter wire was thought to produce a better individual splat, so 1/16" diameter 1080 steel was tried, AMST16-22. This progression through a variety of similar wires lead to obtaining Spraysteel 80, a 1080 steel wire, 1/16" diameter, that was manufactured for twin-wire operations. This wire was used throughout the balance of the experimentation. All experiments beginning with AMST23 were performed on coatings made from this wire. During this selection process all wires tested were subjected to a wide range of slide/roll ratios and contact pressures. A complete history of wires used is discussed in detail in section 2.3.2

3.5 Substrate Preparation.

Surface preparation is vital in producing a coating that will not debond. A detailed protocol was worked out and meticulously followed. This surface preparation procedure was vital in reducing the incidence of type I debonding.

3.5.1 Surface Preparation Procedure.

The first step in surface preparation for Amsler rollers was washing with soap and water to eliminate as much as possible the oils present from machining. Just before spraying they were acetone rinsed, shot blasted, and rewashed with acetone. The substrate was roughened to improve the mechanical bonding between substrate and coating particles.

There is a necessary five plus minutes time lag between shotblasting and spraying, because of time requirements to chuck the roller and start the spray equipment. It was thought that surface oxides may accumulate during this time so a second shot blast operation was installed, such that there would be no time lag between shot blasting and spraying. One further bit of information was gathered when a handful of the chilled steel shot was placed in a beaker of acetone. Small particles of contaminant, dust and a discoloration in the acetone, became visible. To eliminate possible contamination of the substrate because of this contamination of the shot, a flood wash of acetone immediately after the secondary blasting was implemented. A flood wash consists of flooding the rollers while chucked and rotating and then removing the acetone with a strong air blast. An air blast is used as a way of mechanically removing any contaminant suspended in the acetone rather than allowing the acetone to evaporate. Evaporation tends to leave a possible contaminant residue concentrated in one location on the roller. Spraying should commence immediately upon completion of removal of the acetone flood.

3.5.2 Substrate Surface Appearance.

The surface finish after shot blasting is a function of the size of the blasting particles and the velocity at impact. After the surface has been blasted such that the entire original surface area has been altered, further blasting serves to remove surface material without additional change to the surface texture. Additional surface roughness can be achieved only through a larger particle size, increased particle velocity at impact, or softening of the surface. Figures 3.10 & 3.11 show the surface appearance of rollers blasted with silica and with steel shot.

Shot particle size change was accomplished by changing from silica to steel shot, the largest shot medium used. Amasteel LG25 cast steel grit was used. Increased velocity can be accomplished by moving the blast gun nozzle closer to the target, but this distance is already very small, and not much improvement can be expected.



Figure 3.10. Specimen surface appearance with silica as shot medium.



Figure 3.11. Specimen surface appearance with a steel shot medium.

3.5.3 Knurling.

Knurling, a surface roughening technique, was tried as a way to increase surface texture which, in turn, would increase the mechanical bonding of the coating to the substrate. Figure 3.12 shows a knurled roller.

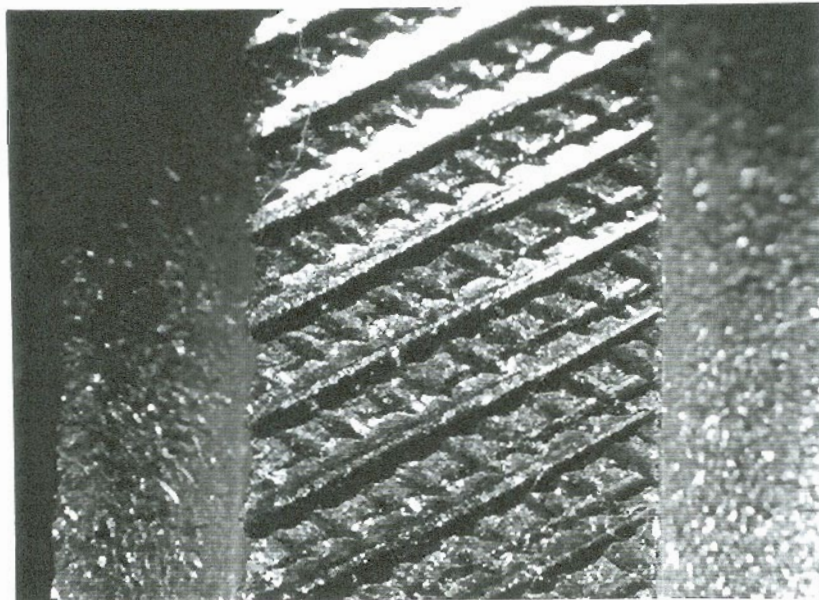


Figure 3.12. Very heavy knurling surface texture.

3.5.4 Substrate Preheating.

Substrate preheating was also tried as a way to make progress in the debonding problem. Substrate heating is accomplished by dwelling the plasma jet on the substrate to increase the surface temperature the incoming melted particles encounter upon impact. The effect is that the particles flow farther upon impact, and the surface area is greater as the splat thickness is reduced. Also residual stresses may be reduced in this condition. Preheating was accomplished by dwelling the plasma jet on the target for 30 seconds. The magnitude of substrate temperature increase was not determined, but the splats were shown to behave in their formation as that previously described. One experimental set, amst131-133, see Appendix 1, included preheating the substrate just before the second blasting. The idea was to more equalize particle and substrate temperatures to see if this might improve bonding.

3.5.5 NiCr Intermediate Layer.

It was thought that an intermediate layer of NiCr may absorb more of the shear forces at the interface without debonding. A 0.1mm layer and a 0.35mm NiCr layer were sprayed as intermediate layers between the substrate and 1080 steel coating. The gas parameters for spraying were the same for the NiCr powder as for the 1080 steel wire. The NiCr was sprayed for a specified time to achieve the desired thickness, then discontinued when the wire feeder for the steel was turned on. The NiCr was a discrete layer except for the very small thickness where the transition from NiCr to 1080 steel was made.

3.5.6 Coating Froth and Interrupted Spray.

A test matrix was formed to show that a coating could be sprayed on a roller with high confidence of expecting it to not debond during testing. Improved techniques were worked out on the experimental side. Zero time lag between shotblast and spray, flood washing of the blasted roller, and improved handling of the roller before spraying were featured. This was to include all of the substrate preparation improvements made up to this time. This is reported as AMST77-96, whose rollers were sprayed in blocks of five, with consistent spray conditions. The first block of five resulted in frothy coatings. "Froth" is the result of the coating substrate becoming overheated during the spraying operation. In this case the cooling gas, CO₂, for backside cooling, ran out without the operator noticing. The substrate heated enough that the incoming particles in the plasma jet impacted on a molten or partially molten surface. This results in the molten substrate splashing out, then solidifying in this splashed condition. The resulting coating is very porous and brittle, and coating failure occurs within a few revolutions.

AMST87-91 was a block that featured an interrupted spray. During spraying there was a wire feeder failure. Spraying was stopped to clear the feeder, which took long enough for the coating to cool much of the way to room temperature. Also edge effects were introduced during the grinding operation that flattened the rollers.

3.6 Wear Test Equipment.

All wear testing has been performed on the Amsler Wear Test Machine, see figure 3.13. Various slide/roll ratios are achieved by the combination of differing rotational speeds of the upper and lower shafts and by varying the diameters of the test rollers. The lower shaft rotates 1.104 times faster than the upper shaft. The upper roller diameter was fixed at 35mm and the lower roller diameter was determined by the desired slide/roll ratio.

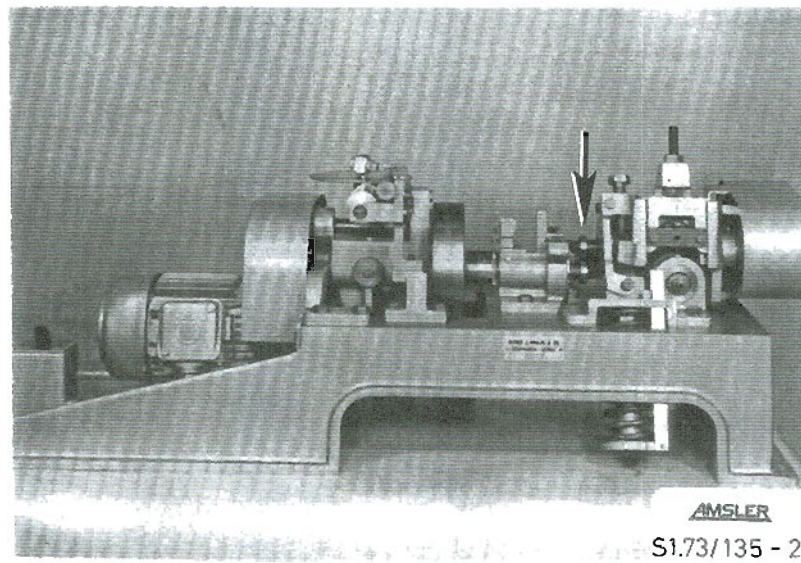


Figure 3.13. Amsler Wear Test Machine. Rollers mated, ready for testing.

3.7 Amsler Testing Equations.

Wear testing is accomplished by rotating mated rollers against each other under a load. Loading is accomplished by spring tension, loading reported in this research was 2,100 MPa or less. The load was calculated from the equation:

$$P_0 = 0.418 \left(\frac{LE}{R} \right)^{0.5}$$

where P_0 is the contact pressure, L is the load, E is the modulus, and $1/R = 1/R_1 + 1/R_2$. The elastic constants are not known for the coating material, but were approximated by that of plain steel. All contact pressures reported are based on calculations using this assumption.

The slide/roll ratio was calculated from the equation:

$$\gamma = \frac{2(1.104D_2 - D_1)}{1.104D_2 + D_1}$$

where D_1 and D_2 are the upper and lower roller diameters, respectively.

The coefficient of friction can be calculated from data gathered during Amsler testing. There is a pendulum attached to the lower roller with specified weights attached. A trace of pendulum deflection was made by a chart recorder during testing. Depending on the amount of deflection, the coefficient of friction at any point of the test can be calculated from the equation¹⁵³:

$$\mu = \frac{2.75d}{LR}$$

where d is the amount of deflection in Nm, read from the friction trace or from the scale on the machine, L is the load (Newtons), and R is the radius of the lower roller (meters). The constant¹⁵⁴, 2.75, was determined by weights added to the pendulum.

The Amsler machine has two rotational speeds, 400 and 200 rpm. All tests were performed at 200 rpm. The machine has capability to perform wear tests under several different conditions, however the mode of single plane, rotational testing was the only one used.

3.8 Dry Wear testing.

A "full" wear test, unlubricated, was defined as a coating tested under the specified contact pressure/creep conditions for 6000 revs. Normally this is with six 1000 rev iterations, although some were tested with no iterations, just running for either 6000 revs or to failure regardless of the number of revolutions. During the early work, Amsler testing was done at 100 revolution increments, at least for the first 1,000 revolutions. This was done to establish wear patterns during any break-in period. An example of running the wear test to the substrate is AMST133, which was run to a final coating thickness of 0.07mm, and then stopped because a large edge effect encroached upon the wear track, see figure 3.14. This is worn thin enough to consider it fully wearing out the coating.

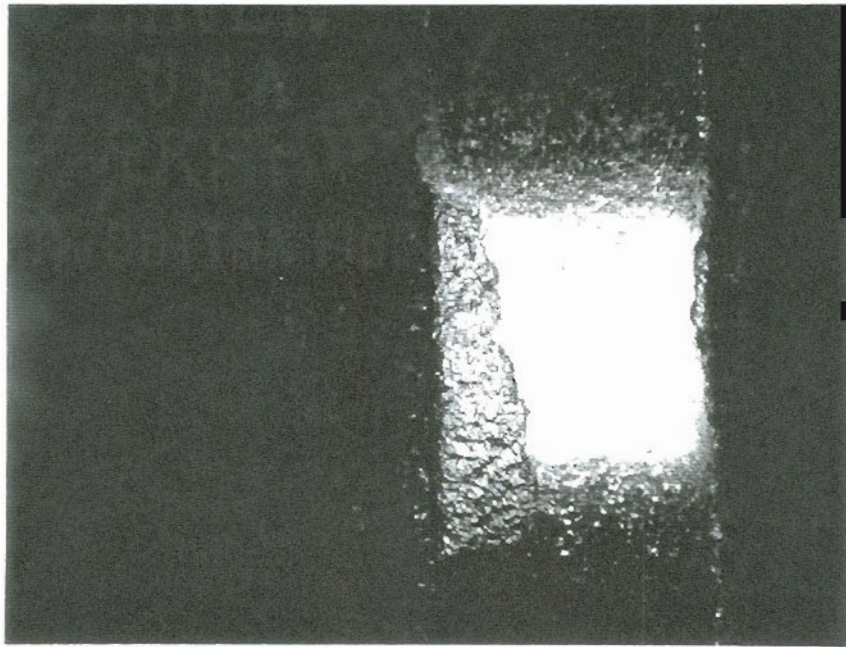


Figure 3.14. Appearance of a large edge effect on the wear track signalled the end of this test.

3.9 Lubricated Wear Testing.

Texaco 904 grease was used in all lubricated tests. All tests were performed in the as-sprayed condition. Rollers were cleaned in the normal manner by washing with acetone. The acetone was removed by blowing it off with an air blast or by evaporation with a heat gun. The rollers were mounted in the Amsler machine, a bead of lubricant was applied, and the rollers were rotated by hand for two revolutions, which served to spread the lubricant across the entire wear surface. Excess lubricant was removed from the sides of the roller with a spatula. The rollers were then removed from the Amsler machine and weighed to see how much lubricant was retained by the system of coated and uncoated rollers. These data are reported as "retained lubricant". The test was then begun, or continued, until the lubricant disappeared from the system, which was determined by the coefficient of friction increasing from a nominal 0.1 under full lubrication condition, to 0.4, representing the dry condition.

This cycle, application of lubricant, measuring the lubricant, and running until the lubricant disappeared, is termed an "interval" during the test. Each full test consisted of several intervals. Data reported are 1) retained lubricant (grams) per interval, 2) revolutions per interval, and 3) the wear rate ($\mu\text{g}/\text{m}/\text{mm}$). The wear rate for these lubricated tests is not useful as a statistic on its own, but it does allow one more point of comparison between similar tests.

3.10 Lubricated Test Procedures.

3.10.1 First Series: (AMST46-51)

Use roller "as sprayed" and 1220 MPa contact pressure.

1. Weigh the roller after cleaning.
2. Apply grease to roller with a syringe.
3. Put roller onto Amsler machine and rotate two times against the bottom roller.
4. Remove roller from Amsler, remove excess grease from roller sides and surface with a spatula.
5. Weigh lubricated roller.
6. Clean the bottom roller of all grease.
7. Run test until cut-off point of 6.5 N-m on deflection scale is reached.
8. Clean the roller, record data, repeat 1-6 until test is complete.

In this series, the coating thickness range was 0.6-1.0mm. Wire was Spraysteel 80, 1/16 diameter. The goal was to determine how much grease the coating could retain and the number of revolutions that could be achieved with this amount of grease. Figures 3.15 & 3.16 show application of grease with a syringe and excess grease removed with a spatula. It should be noted that as the test series progressed, greater skill was acquired in the excess grease removal (step 4 above). The bottom roller was cleaned of all grease before commencing each test, so that only the top roller was lubricated. After the first iteration the bottom roller became progressively roughened, and perhaps it should have been greased in the same

manner as the coated roller. In each case, the coating debonded before the completion of the test.

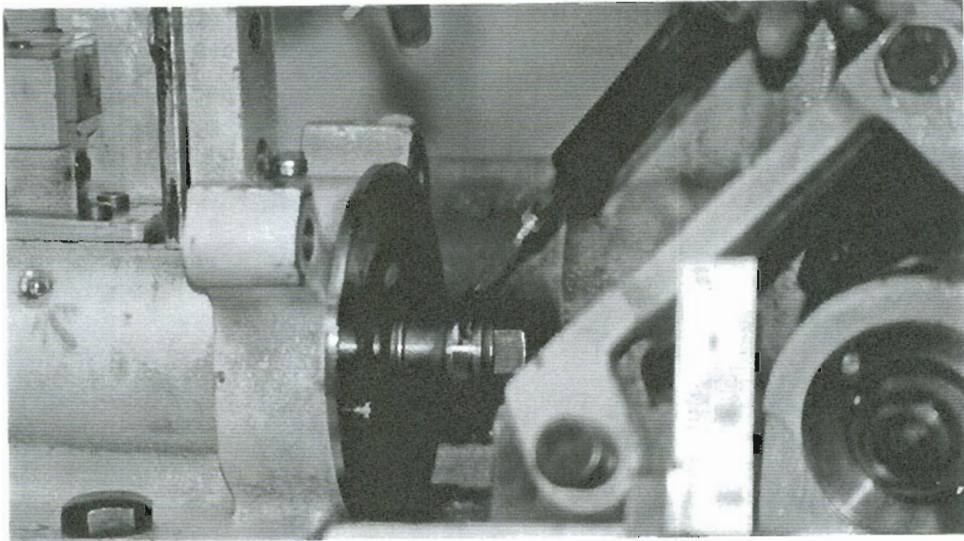


Figure 3.15 Application of grease with a syringe.

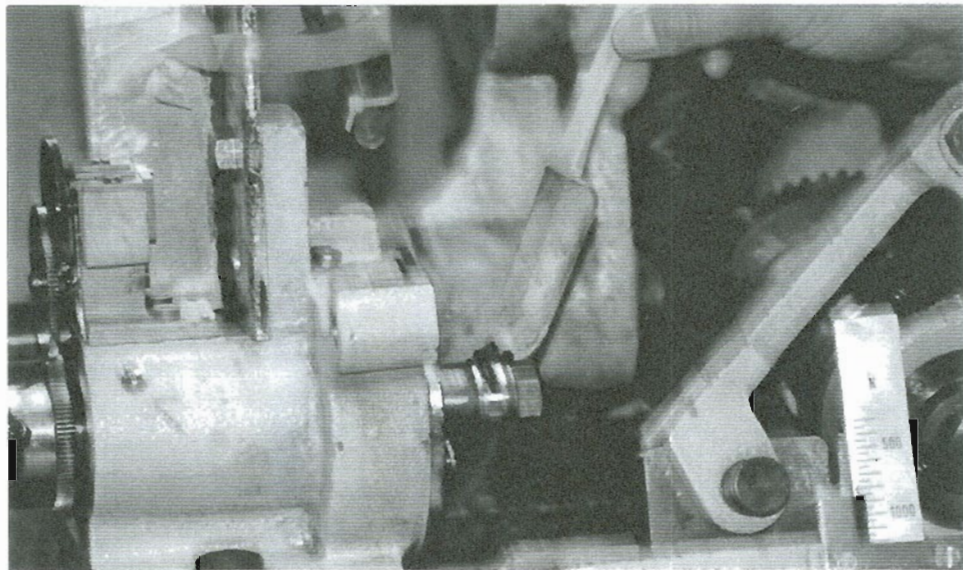


Figure 3.16. Removal of excess grease with a spatula.

3.10.2 Series Two: (AMST52-59).

Lubricant applied in these tests was applied by syringe to a clean bottom roller, laying a small bead of grease all the way around the perimeter. After weighing to record the exact amount of grease, the rollers were then mounted in the Amsler machine and turned by hand two revolutions. Excess grease was squeezed to the outside. This excess was not removed, the test was made with an excess amount of grease clinging to the outside of the rollers. An air blast was used to cool the rollers, with the air turned on at about 500 revolutions. This air blast blew off most of the excess grease, at least removing it from easy entry to the wear track. Waiting 500 revs to turn on the air allowed considerable heat to develop in the rollers, and they were warm to the touch when removing for cleaning and weighing.

Applying grease in this manner makes it difficult to mete out the exact amount each time, but by noting the volume exiting the syringe a reasonably consistent amount can be applied. For these tests, two rollers were knurled in various degrees to attempt to improve coating substrate bonding. In one case, AMST53, an increased coating thickness with normal substrate preparation, shot blasting only, no knurling, was prepared and tested to see whether coating thickness was a factor. Ten successful lubricated iterations were made before attempting dry tests. Dry tests were thought to be a way to accumulate data and reduce the coating thickness at the same time. The surface had roughened during lubricated tests, quite the opposite to what happens during dry testing, and debonding failure occurred during the first dry iteration. Coating

thickness was 1.65 mm, 12,900 revolutions over ten iterations were made. Average lubricant used was 0.0725 grams. A combination of knurling and coating thickness was attempted in an effort to produce better results. Knurling was later determined to not significantly improve bond quality and was discontinued as a substrate surface preparation technique.

3.10.3 Series Three (AMST175-183)

Debonding was such a problem during the lubrication testing it was decided to direct a major effort to understand debonding and to minimize its effects before further lubricated testing. The final tests were to be made using the techniques developed over the life of the research that were thought to minimize debonding incidence. Wear testing conditions were to be the same as earlier.

The matrix for this series included 5% and 35% slide/roll ratios at contact pressures of 700, 900, 1050, and 1220 MPa. The cut-off friction coefficient was 0.3, defining each interval during testing. The purpose of this series was two-fold. First, would debonding incidence be reduced from the earlier work, and second, evaluate the use of the coating for a lubrication reservoir.

To eliminate the possibility of some irregularity in the spray process influencing test results, one roller from the group of ten was tested dry. The rollers were sprayed in groups of five, the one selected for the dry test was chosen at random, without regard to position during spraying.

3.11 Water Lubrication.

It is very difficult to observe any defects in the coating during testing because of the grease on the roller. It was thought that closer observation could be made if water was used as a lubricant. This was tried, AMST174, with the idea that the failure mechanism under water lubricated conditions would be the same as that under greased conditions. Water was dripped onto the top roller at a rate that assured a continuous lubrication at the contact region.

3.12 Layered Coatings.

A layered coating is the coating of a roller, cooling to room temperature, then adding a second application of coating. The blank roller is shotblasted, knurled if desired, then shotblasted again. After the first coating, the roller is only shotblasted. Layers range from 1 to 3.5 minutes dwell time, 0.3 to 1+mm to over 1mm thick.

3.13 Parameter Envelope Study.

Much data had been accumulated from wear tests and metallographic examination of coatings that were made at what was thought to be optimum spray parameters. With the idea to determine how much of a range in these parameters, if any, would yield an acceptable wear performance, a series of tests, AMST61-76, was initiated to address this issue. This series included single splat analysis slides, metal coupons for metallographic specimens, and Amsler rollers of selected parameters for wear testing. All tests were made at 1220 MPa contact pressure and approximately 35% slide/roll ratio. The slide/roll varies somewhat according to coating thickness. The

rollers are machined to 33mm diameter and a 1mm coating thickness brings the roller to a target diameter of 35mm, which for the Amsler machine operating conditions and the lower roller diameter combination yields a 35% slide/roll ratio. It was expected that there would be a close range of wear rates until envelope limits are reached when there would be a sudden large jump in the wear rate and/or early coating failure. These tests were made using both W-8, HB260 a class U wheel steel, and W-3, HB301, a class C wheel steel. It was expected that there would be little if any difference in coating performance because of the different wheel steels, even though one was harder than the other.

3.14 Data Accumulation.

Before going into details on the experimental results, a general explanation of the reporting procedure and some of the common features of the graphs may be useful. Figure 3.17 shows a raw data sheet from a typical dry wear test. Calculations for load, slide/roll, and typical coefficient of friction is shown on this sheet. Central to the work is the weight loss data, from which wear rates are determined. Also recorded are revolutions and diameter changes. Contact width changes were recorded in uncoated specimen tests, largely during previous work, however because of overspray this is not possible for coated specimens.

The Amsler test identification numbers were assigned consecutively without regard to the type of test or wire used, AMST1 through to the end. It was thought that if the coating could stand up to the most extreme test conditions, 35% at 1220 MPa, that it would hold up to the rest of the matrix. Most of the testing was conducted under these conditions.

Contact width of the lower (uncoated wheel) roller was fixed at 5mm, see figure 3.1 for details of Amsler roller. Contact width of the coated roller was 5mm in most cases, however it ranged from 3mm to 5mm depending on the test. Rotation speed of the Amsler was a nominal 200rpm throughout the work. Coating thickness was targeted to be 1mm, however testing was performed over a range of 0.3 to 3.0mm.

High carbon, plain steel wire was used in all of the wear testing. The individual wire designation was noted for each test. The parameter set noted in the work sheet describes the primary gas, secondary gas, working distance and, in some cases, the injection angle of the wire into the plasma jet. The reference to steel type of top and bottom rollers refers to the rail (top roller) and the wheel (bottom roller) the from which the specimen was taken. Wheel steels were of both type U and type C wheels. The test conditions were DAS (dry, as sprayed), DGF (dry, ground flat), and lubed (lubricated with grease).

Each interval, usually a specified number of revolutions, in the test has weight loss, diameter change, and revolution count data recorded. This raw data was transferred to a spreadsheet and organized graphically as shown in figure 3.18.

| | |
|---------------------------------|------------------|
| Test Number: | AUST 117 |
| Contact Pressure (MPa): | 1220 |
| Slide/Roll (%): | 35 |
| Loading (N): | 2000 |
| Friction Coefficient (typical): | 0.16 |
| Contact Width (mm): | 7 |
| Motor Speed (RPM): | 200 |
| Coating Thickness (mm): | 0.96 |
| Wire: $\frac{1}{16}$ | 1020 |
| Parameter Set: | 2.30/30/2.25 90° |
| Steel Top: | x 95 |
| Steel Bottom: | w 9 |
| Test Conditions: | D45 (KURLED) |

AUST 117-121 sprayed as a block
 * 3 rollers knurled
 sand used for 2nd blasting. & time lag.
 Left-most roller
 KNURLED
 Note: In most cases, when machine is restarted after a data point, a slight roughening occurs, followed by going to a high friction state, then settling in to a steady state. Smoother rapidly follows.

| Interval No. | Rev (Bottom) | Work (Nm) | Weight Top | Weight Bottom | Dia Top (in) | Dia Bot (in) |
|--------------|--------------|-----------|------------|---------------|--------------|--------------|
| 0 | 56 990 | 788 | 49.9765 | 96.1571 | 1.288 | 1.777 |
| 1 | 57 990 | 832 | .7560 | .1233 | 1.275 | 1.776 |
| 2 | 58 990 | 877 | .4943 | .1138 | 1.369 | 1.776 |
| 3 | 59 990 | 923 | .1744 | .1083 | 1.362 | 1.7755 |
| 4 | 60 990 | 968 | 48.7404 | .1048 | 1.265 | 1.775 |
| 5 | 61 990 | 1014 | .3735 | .1017 | 1.349 | 1.775 |
| 6 | 62 990 | 1059 | .0527 | .0986 | 1.243 | 1.775 |
| 7 | | | | | | |
| 8 | | | | | | |
| 9 | | | | | | |
| 10 | | | | | | |

Note: Dia of roller is enlarged because of knurling.

Notes:

0. surface shows influence of knurling.
 1. some art. loss from use of wheel packer in removing roller from shaft.
 2. Edge effects started at edge of wear track. -
- PHOTOS TAKEN OF MOST SEVERE EDGE EFFECT REGION.
3. More edge effects, with more anticipated - could knurling have an effect? The wear track itself remains very smooth.
 4. Edge effects have become more severe. wear track affected slightly.
 5. Edge effects continued, but may be stabilized.

$$P_o = 0.418 \cdot 2 \cdot (LE/R)^{0.5} \quad \gamma = 2 \cdot (1.104 \cdot D_2 - D_1) / (1.104 \cdot D_2 + D_1) \quad u = (2.75 \cdot M) / (L \cdot R)$$

$$L = P_o \cdot 2 \cdot R / (0.418 \cdot 2 \cdot E) \quad \text{Stable } M = 7.5$$

$$P_o = 1220 \quad S/R \text{ ratio} = 35 \quad u = 0.457$$

$$E = 2.1 \times 10^5$$

$$1/R = 1/R_1 = 1/R_2$$

$$R = 9.86$$

$$L = 400$$

$$5L = 2000$$

34

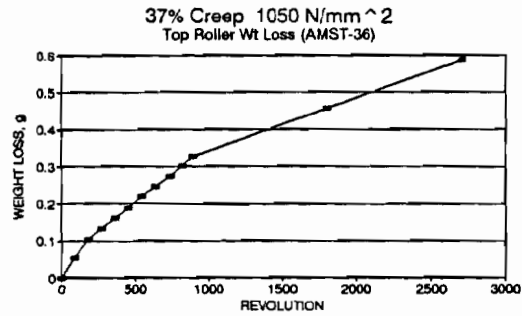
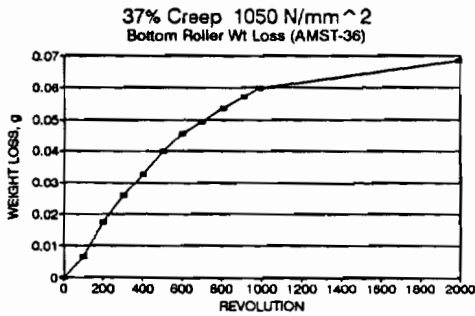
Step 1 - shot blast
 Step 2 - silica blast

Figure 3.17. Typical raw data sheet from a dry Amsler wear test.

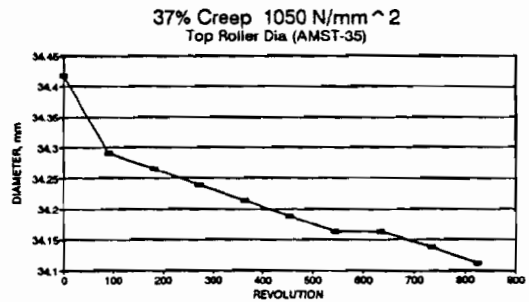
| | |
|--|-------------|
| AMSLER TEST NO.: | 38 |
| PLASMA SPRAY: Spray Steel 80 Wire | 1/16 dia |
| CONTACT PRESSURE (N/mm ²): | 1050 |
| CREEPAGE (%): | 37 |
| MOTOR SPEED (rpm): | 200 |
| COATING THICKNESS: (mm) | 0.7 |
| LOADING (N): | 1470 |
| Disk file: AMST-38 | Dry Air Str |

| | STEEL NO. | ROLLER DIMENSIONS | | WEAR RATE | Top | Bottom |
|--------|-----------|-------------------|--------------|-----------|----------|----------|
| | | WIDTH(mm) | DIAMETER(mm) | | g/rev. | 2.74E-05 |
| TOP | W-3 | 5 | 34.44 | µg/m | 1807.508 | 192.3723 |
| BOTTOM | W3 | 4.99 | 45.37 | µg/mm | 381.5016 | 38.47446 |

| INTERVAL No. | REVOLUTION READING (BOTTOM) | REVOLUTION | | WORK (N.m) | WEIGHT(g) | | WEIGHT LOSS(g) | | CONTACT WIDTH(mm) | | DIAMETER | | | | | | | |
|--------------|-----------------------------|------------|--------|------------|-----------|----------|----------------|--------|-------------------|--------|----------|--------|----------|--------|----------|------|--|-------|
| | | TOP | BOTTOM | | TOP | BOTTOM | TOP | BOTTOM | TOP | BOTTOM | TOP | BOTTOM | (INCHES) | (MM) | (INCHES) | (MM) | | |
| 0 | 3070 | 0 | 0 | | 45.9492 | 102.8284 | 0.0000 | 0.0000 | | | | | | | | | | |
| 1 | 3170 | 91 | 100 | | 45.8959 | 102.8218 | 0.0533 | 0.0068 | | | 4.99 | 1.355 | 34.42 | 1.7840 | | | | 44.81 |
| 2 | 3270 | 181 | 200 | | 45.8441 | 102.8109 | 0.1051 | 0.0175 | | | | 1.348 | 34.28 | | | | | |
| 3 | 3370 | 272 | 300 | | 45.8168 | 102.8025 | 0.1328 | 0.0259 | | | | 1.348 | 34.24 | | | | | |
| 4 | 3470 | 362 | 400 | | 45.7890 | 102.7957 | 0.1602 | 0.0327 | | | | 1.347 | 34.21 | | | | | |
| 5 | 3570 | 453 | 500 | | 45.7613 | 102.7883 | 0.1879 | 0.0401 | | | | 1.348 | 34.19 | | | | | |
| 6 | 3670 | 543 | 600 | | 45.7294 | 102.7827 | 0.2198 | 0.0457 | | | | 1.345 | 34.18 | | | | | |
| 7 | 3770 | 634 | 700 | | 45.7029 | 102.7791 | 0.2463 | 0.0493 | | | | 1.345 | 34.18 | | | | | |
| 8 | 3880 | 734 | 810 | | 45.6741 | 102.7748 | 0.2751 | 0.0538 | | | | 1.344 | 34.14 | | | | | |
| 9 | 3980 | 824 | 910 | | 45.6467 | 102.7712 | 0.3025 | 0.0572 | | | | 1.343 | 34.11 | | | | | |
| 10 | 4080 | 887 | 990 | | 45.6214 | 102.7685 | 0.3278 | 0.0599 | | | | 1.343 | 34.11 | | | | | |
| 11 | 5060 | 1803 | 1990 | | 45.4938 | 102.7599 | 0.4554 | 0.0685 | | | | 1.339 | 34.01 | | | | | |
| 12 | 6060 | 2708 | 2990 | | 45.3614 | | 0.5878 | | | | | 1.336 | 33.93 | | | | | |



Top Roller:
Regression Output:
Constant 0.09963
Std Err of Y Est 0.036739
R Squared 0.946398
No. of Observations 12
Degrees of Freedom 10
X Coefficient(s) 0.000198
Std Err of Coef. 1.47E-05



Bottom Roller:
Regression Output:
Constant 0.024748
Std Err of Y Est 0.008324
R Squared 0.780293
No. of Observations 10
Degrees of Freedom 8
X Coefficient(s) 2.74E-05
Std Err of Coef. 5.44E-06

Figure 3.18. Raw data organized into spreadsheet and graphs.

3.15 Wear Curve Guidelines.

To appropriately interpret results, certain principles relative to the spraying process must be clarified. Wear rate calculation, curve peculiarities, and basic relationships of the top and bottom rollers are presented here with this in mind.

The method of relating data gathered during wear testing to calculating wear rates can be illustrated by examining AMST27. This test was made with data collection at 100 revolution intervals for a total of 8500 revolutions, see figure 3.19. Note the correspondence between weight loss and diameter reduction in the top roller. This correspondence holds generally true throughout all the Amsler testing. The bottom roller generally can be said to add a small amount of weight very early in the test because of material transfer from the upper roller. This weight addition is small, and disappears within the first few hundred revolutions. In the case of AMST27, a weight gain of 0.0124 grams was recorded at 100 revolutions, and a net gain/loss of 0.000 grams at 200 revolutions. This temporary material transfer is thought to be insignificant, given that a successful coating must last much longer than 100 revolutions. The wear of the top roller is always greater than that of the bottom roller. The wear rate of the top roller is 350 ug/m/mm as opposed to the bottom roller wear rate of 16 ug/m/mm. The diameter reduction of the bottom roller is also minimal, as would be expected, given that the wear rate is so low. Total diameter reduction was 0.005mm, and that occurred during the first 25% of the test.

Wear rates are determined by the slope of the weight loss (g) vs revolutions curve. The units are weight loss per meter

rolled per millimeter of contact width, ($\mu\text{g}/\text{m}/\text{mm}$). When calculating wear rates, care must be taken to choose a section of the curve that is most linear, avoiding break-in zones and areas of sudden, localized weight-loss areas such as might come from edge effects or other artifacts of the test.

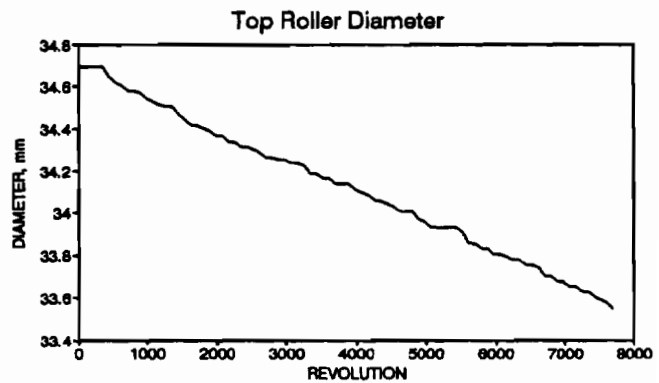
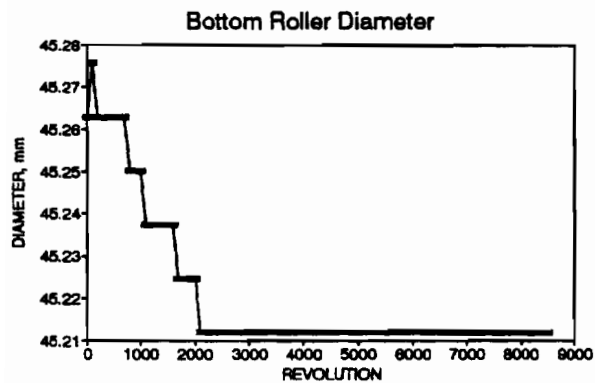
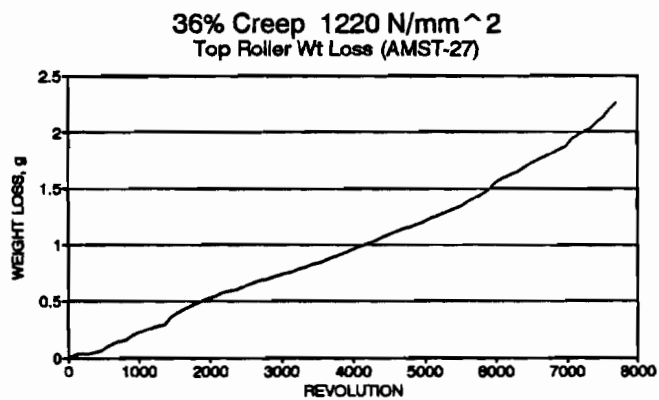
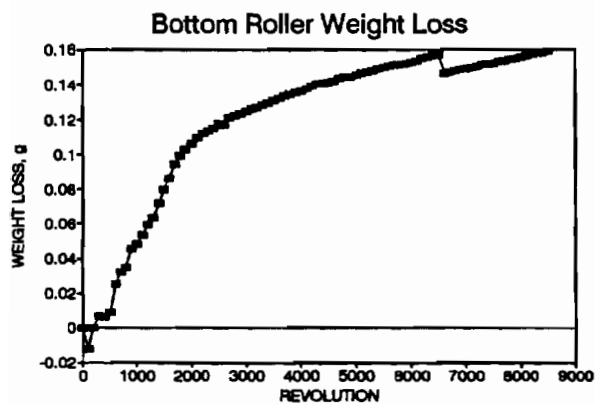


Figure 3.19. AMST27. Data collection interval is 100 revolutions.

CHAPTER FOUR

4.0 EXPERIMENTAL RESULTS

4.1 Introduction.

Wear rates of coated rollers compare very favorably with that of uncoated rollers. To set the tone for the results chapter a comparison of these results is presented here, see figure 4.1. The wear resistance of the coated rollers is much greater, by a factor of ten, than that of the uncoated rail steel wear tested in previous research.

Uncoated Rail Steels

1220 MPa 35% Slide/Roll

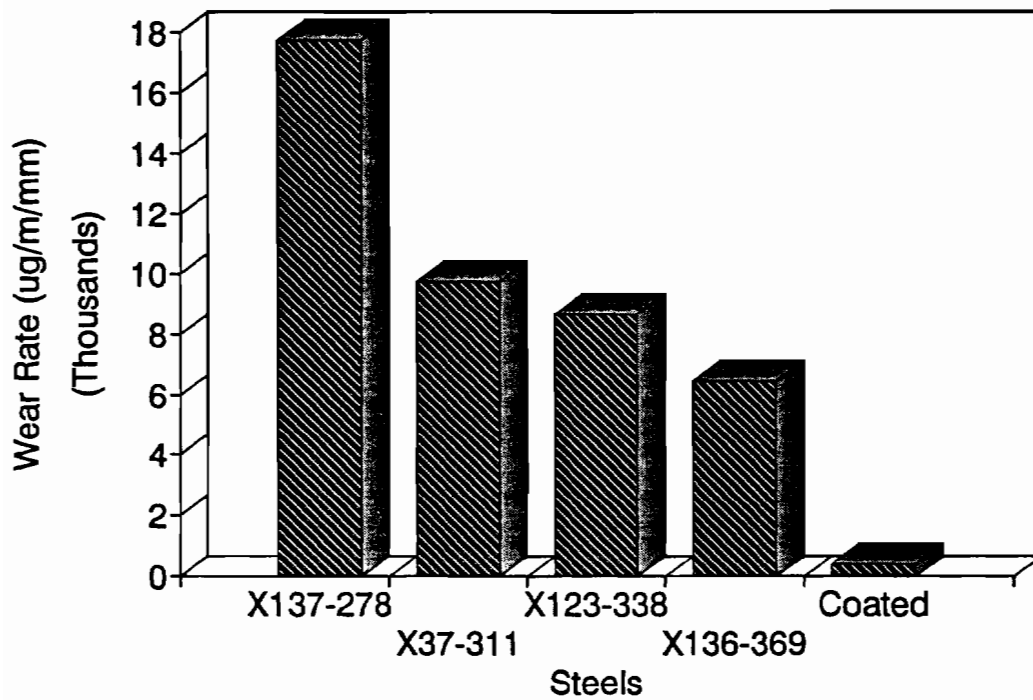


Figure 4.1. Wear rates of uncoated steels compared with coated steel.

4.2 Experimental Grouping.

There are details in each individual experiment that makes it unique, though in many cases the data from an individual experiment is applicable in more than one area of study. Wear data, for example, were collected during all testing, making debonding experiments and the spray parameter envelope trials compatible to the overall experimental scheme. For convenience of explanation it can be said that experimental work has fallen into five general groups. The categories are:

1. Early work.
2. Dry wear testing.
3. Lubricated wear testing.
4. Spray parameter envelope.
5. Debonding studies.

4.3 Early work.

4.3.1 Overview.

The category of 'early work' generally defines the experimental work from the onset of the research until the selection of 1/16 in. diameter Spraysteel 80 steel wire as the material of choice. For results and discussion purposes, the early work has been expanded to cover all work up to the lubricated coating test matrix.

In one case, the coating wore through after only 360 revolutions, and the longest lasting only 420 revs, and the other cases, failure occurred even earlier because of sections of coating breaking off, either from the edges or from

blistering of the coating. Figure 4.2 shows test results, AMST1-6. Wear rate information was calculated, however the test duration is too short for this to be reliable information.

AMST7-15 were testing a new wire, various substrate cooling methods, and layering. Figure 4.3 and 4.4 shows experimental results of this series of trials.

Because of a vastly improved spray pattern, 1/16" diameter wire was tested in AMST16-22. An immediate improvement in coating quality, measured in wear performance and durability, was noted. Spraysteel 80, a 1080 steel prepared for twin wire arc thermal spraying, was then used as a replacement. This wire had the advantage of being manufactured for use with a wire feeder, and was used on a continuing basis for most of the balance of the research. Figure 4.5 shows details of early work testing, AMST1-22.

AMST1-6 1075 Cored Wire

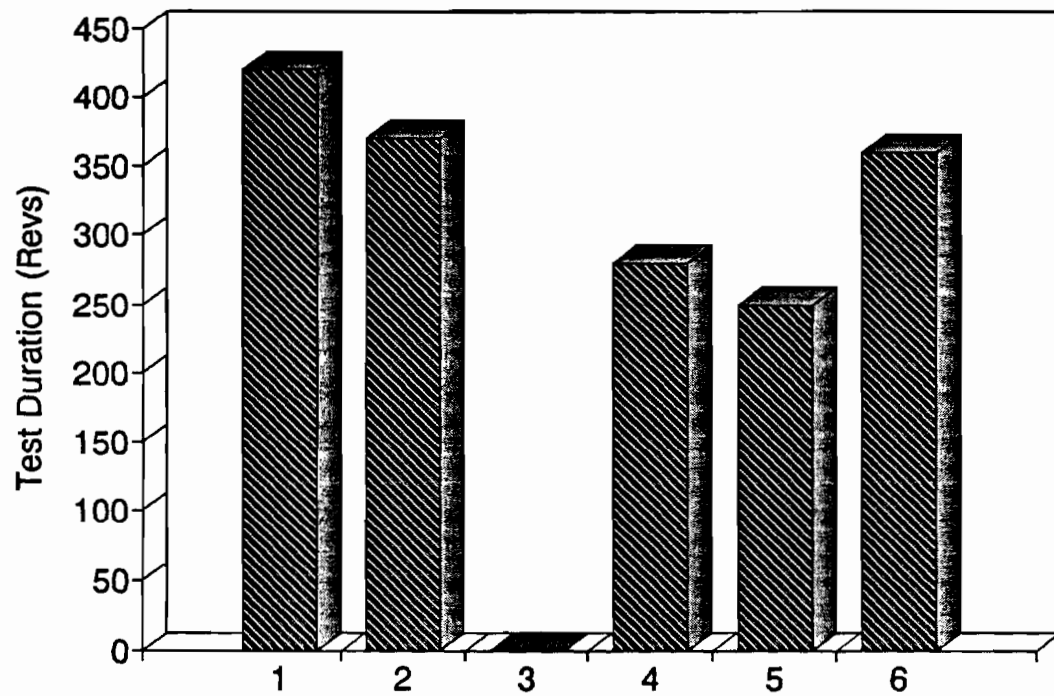


Figure 4.2. Early work. Test duration of coatings from 0.094 diameter 1075 Cored wire.

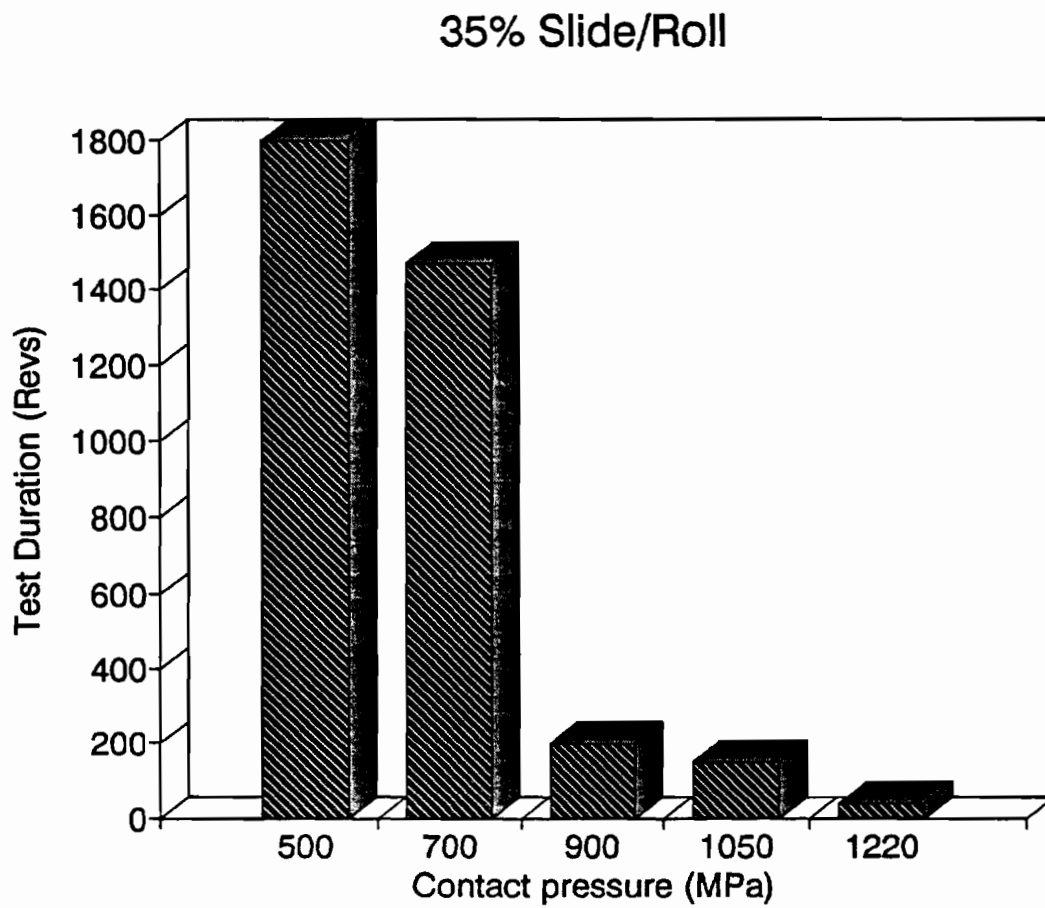


Figure 4.3 Early work. AMST7-11, 35% slide/roll.

5% Slide/Roll

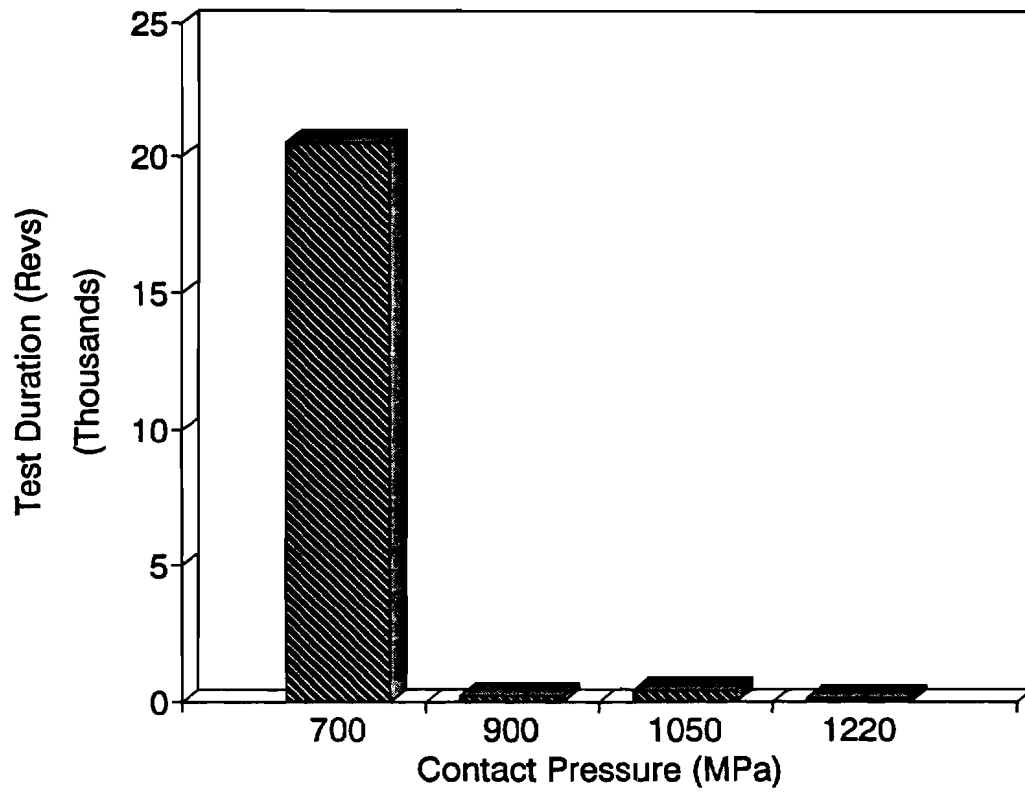


Figure 4.4. Early work. AMST12-15, 5% slide/roll.

Figure 4.5. Details of the early work testing.

| Test No. AMST | Wire | Contact Pressure | Creepage | Steel Bottom | Test Conditions | Coating Thickness | Parameter Set | Wear Rate Top | Bottom | Debond Type I | Debond Type II | Test Length |
|------------------|-----------------|---------------------|----------|-----------------|--------------------|----------------------|------------------|------------------|--------|------------------|-------------------|----------------|
| 1 | 1075 Cored 3/32 | 700 | 35 | W-3 | DAS | 0.30 | 180/0/180 | 1676 | 59 | | | 420 |
| 2 | 1075 Cored 3/32 | 1050 | 35 | W-3 | DAS | 0.30 | 180/0/180 | 1014 | 104 | | | 370 |
| 3 | 1075 Cored 3/32 | 1220 | 35 | W-3 | DAS | 1.00 | 180/0/180 | | | yes | | Immed |
| 4 | 1075 Cored 3/32 | 900 | 34 | W-3 | DAS | 1.00 | 180/0/180 | 2877 | | yes | | 280 |
| 5 | 1075 Cored 3/32 | 900 | 35 | W-3 | DAS | 0.30 | 180/0/180 | 3164 | | yes | | 250 |
| 6 | 1075 Cored 3/32 | 900 | 36 | W-3 | DAS | 0.50 | 180/0/180 | 7314 | 416 | | | 360 |
| 7 | .094 Music | 1220 | 35 | W-3 | DAS | 1.00 | 280/135/200 | | | yes | | 40 |
| 8 | .094 Music | 1050 | 35 | W-3 | DAS | 1.30 | 280/135/200 | | | yes | yes | 150 |
| 9 | .094 Music | 900 | 35 | W-3 | DAS | 1.00 | 280/135/200 | | | yes | yes | 200 |
| 10 | .094 Music | 700 | 35 | W-3 | DAS | 0.85 | 280/135/200 | 808 | 3 | | | 1470 |
| 11 | .094 Music | 500 | 35 | W-3 | DAS | 0.80 | 280/135/200 | 4050 | 91 | | | 1800 |
| 12 | .094 Music | 700 | 5 | W-3 | DAS | 0.84 | 280/135/200 | 15 | 0 | | | 20510 |
| 13 | .094 Music | 900 | 5 | W-3 | DAS | 0.88 | 280/135/200 | 11911 | 0 | yes | | 230 |
| 14 | .094 Music | 1050 | 5 | W-3 | DAS | 0.90 | 280/140/200 | 236 | 0 | yes | | 420 |
| 15 | .094 Music | 1220 | 5 | W-3 | DAS | 0.90 | 300/150/225 | | | yes | | 100 |
| 16 | 1/16 Music | 1220 | 35 | W-3 | DAS | 0.75 | 250/105/225 | | | yes | | 80 |
| 17 | 1/16 Music | 1220 | 35 | W-3 | Lubed | 0.75 | 250/80/225 | | | yes | | 70 |
| 18 | 1/16 Music | 1220 | 35 | W-3 | DAS | 0.10 | 250/105/225 | | | | | 200 |
| 19 | 1/16 Music | 1220 | 35 | W-3 | DAS | 0.75 | 250/105/225 | | | yes | | 90 |
| 20 | 1/16 Music | 1220 | 35 | W-3 | Lubed | 0.20 | 250/105/225 | 490 | 60 | | | 3200 |
| 21 | 1/16 Music | 1220 | 15 | W-3 | DAS | 0.25 | 250/105/225 | 2561 | | | | 760 |
| 22 | 1/16 Music | 1220 | 5 | W-3 | DAS | 0.25 | 250/80/220 | 1037 | | | | 1750 |

4.3.2 Wear Rates For Various Materials.

Figures 4.6, 4.7, and 4.8 show wear rates for each type of wire used during this period until the 1/16 diameter wire was proven, AMST1-22. No results are given in these figures for test lengths of less than 200 revolutions, and it should be kept in mind that these tests were performed under various contact pressure and slide/roll conditions. The wear rates of the lower, uncoated roller is much lower than that of the upper, coated roller. Lower roller wear rates can be read from the overall experimental chart in Appendix 1.

Significant individual test results from this period includes two tests made at 5% slide/roll ratio. AMST12, figure 4.9, shows a coating that did not wear out. The contact pressure was 700 MPa. This test was halted after 20,000 revolutions with little evidence of wear. Note that the wear rate is only 15 ug/m/mm. This test was run dry, as sprayed, with the diameter reduction of 0.11mm, which is only enough to flatten the surface roughness of the as sprayed condition.

AMST25 and AMST27 were tests of high performing coatings made at 1220 Mpa contact pressures. AMST27 has been fully reported earlier, Figure 3.18. AMST25 was tested at 5% slide/roll with 10,700 revolutions, see Figure 4.10. This roller was run until there was very little coating remaining. Note that the wear rate is 208 ug/m/mm, which fits into the lower region of that expected for 35% slide/roll. Throughout the wear testing, the wear rates of the 5% vs the 35% slide/roll conditions are very similar. Generally the 5% tests are slightly lower, however the envelope of wear rates for 35% would generally include the 5% results.

Early Work Wear Rates 1075 Cored Wire 3/32 in Dia.

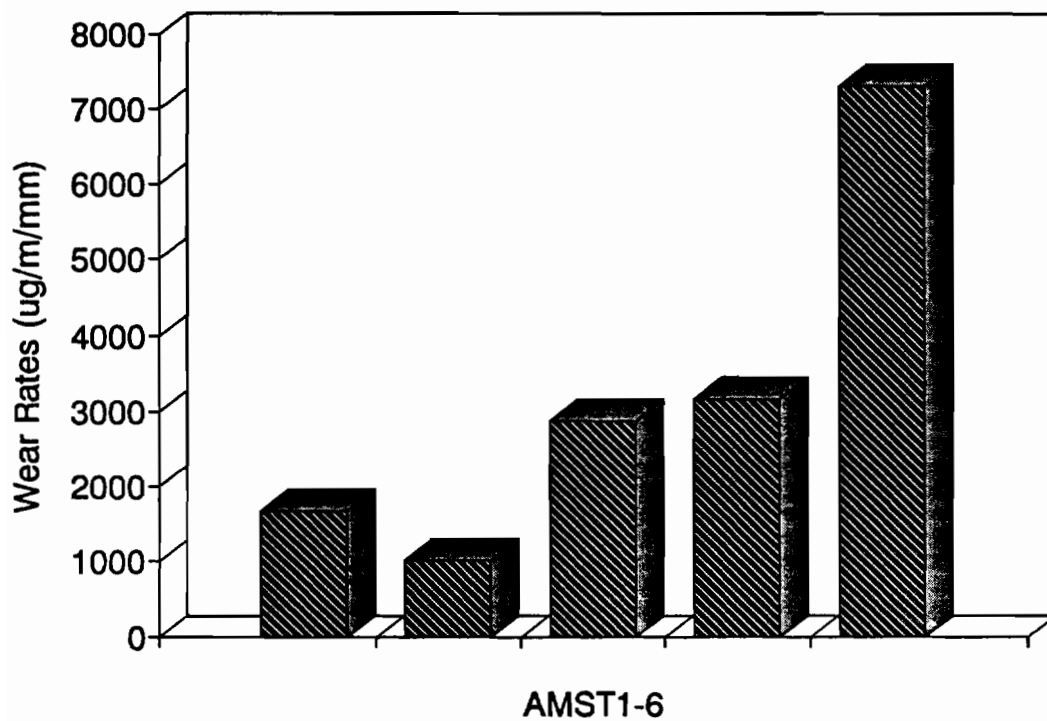


Figure 4.6. Early work wear rates. 0.094 diameter 1075 cored wire.

Early Work Wear Rates .094 Dia. Music Wire

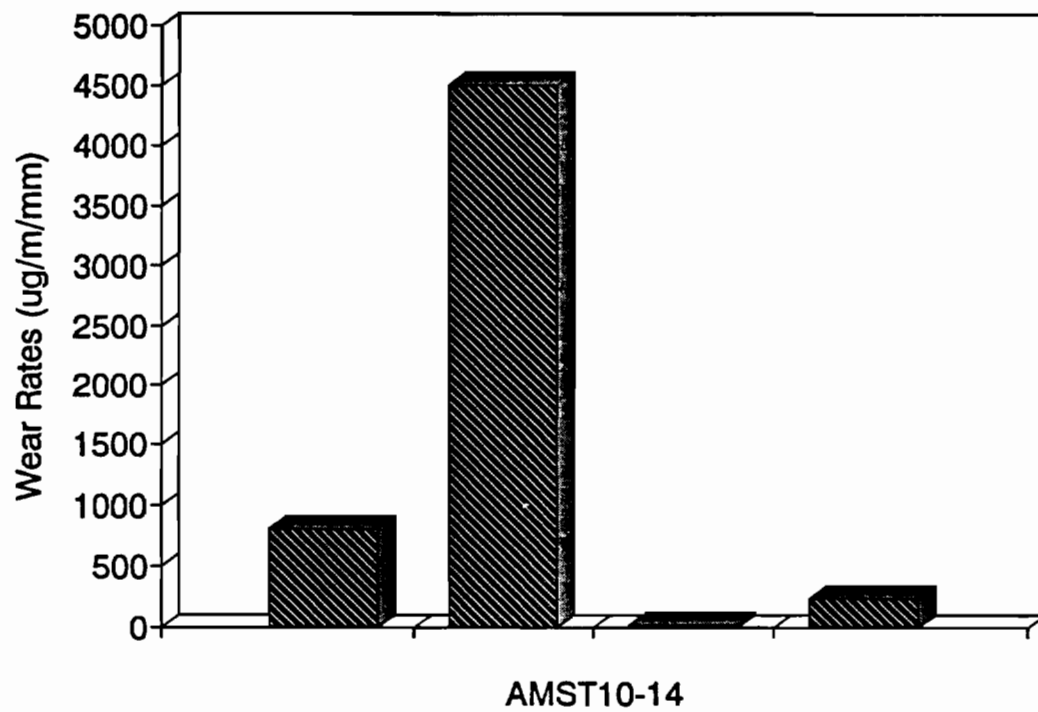


Figure 4.7. Early work wear rates. 0.094 diameter 1080 steel wire.

Early Work Wear Rates 0.625 Dia. Music Wire

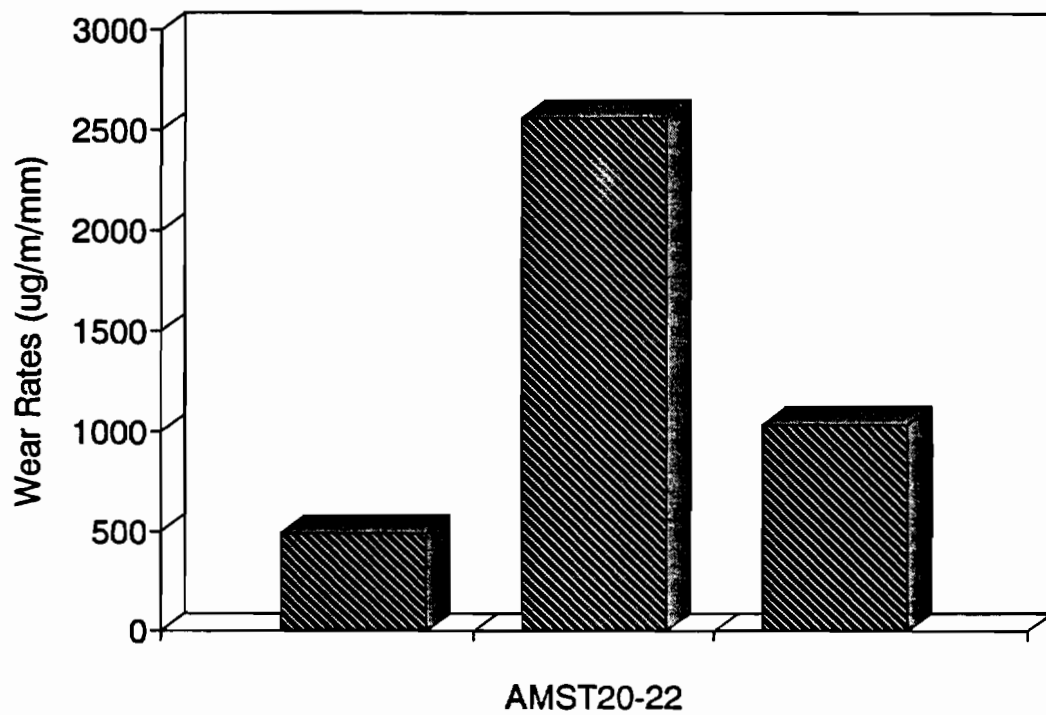


Figure 4.8. Early work wear rates. 0.0625 diameter 1080 steel wire.

| | |
|--|-------------|
| AMSLER TEST NO.: | 12 |
| PLASMA SPRAY: Music Wire 3/32 dia. | |
| CONTACT PRESSURE (N/mm ²): | 700 |
| CREEPAGE (%): | 5 |
| MOTOR SPEED (rpm): | 200 |
| COATING THICKNESS: (mm) | 0.84 |
| LOADING (N): | 571 |
| Test Condition: | DAS |
| Parameter Set: | 28Q/135/200 |
| Disk file: | AMST-12 |

| | STEEL NO. | ROLLER DIMENSIONS | | WEAR RATE | Top | Bottom |
|--------|-----------|-------------------|--------------|-----------|----------|----------|
| | | WIDTH(mm) | DIAMETER(mm) | | | |
| TOP | X-95 | | 35.15 | g/rev. | 7.69E-06 | -5.1E-08 |
| BOTTOM | W3 | 4.96 | 33.35 | µg/m | 13.92618 | -0.00967 |

Note: Wear Rate from 0-9520 revs.

| INTERVAL No. | REVOLUTION READING (BOTTOM) | REVOLUTION | | WORK (N.m) | WEIGHT(g) | | WEIGHT LOSS(g) | | CONTACT WIDTH(mm) | | DIAMETER | | | |
|--------------|-----------------------------|------------|--------|------------|-----------|---------|----------------|---------|-------------------|--------|----------|--------|-------|--------|
| | | TOP | BOTTOM | | TOP | BOTTOM | TOP | BOTTOM | TOP | BOTTOM | TOP | BOTTOM | TOP | BOTTOM |
| | | (INCHES) | (MM) | | (INCHES) | (MM) | (INCHES) | (MM) | | | | | | |
| 1 | 880480 | 0 | 0 | 289372 | 48.1221 | 41.0104 | 0.0000 | 0.0000 | | 4.96 | 1.384 | 35.15 | 1.313 | 33.35 |
| 2 | 880540 | 45 | 50 | 289372 | 48.1187 | 41.0103 | 0.0034 | 0.0001 | | 4.96 | 1.383 | 35.13 | 1.313 | 33.35 |
| 3 | 880600 | 100 | 110 | 289372 | 48.1190 | 41.0102 | 0.0031 | 0.0002 | | 4.96 | 1.382 | 35.10 | 1.313 | 33.35 |
| 4 | 880700 | 190 | 210 | 289373 | 48.1175 | 41.0103 | 0.0046 | 0.0001 | | 4.96 | 1.380 | 35.05 | 1.313 | 33.35 |
| 5 | 880800 | 281 | 310 | 289373 | 48.1187 | 41.0106 | 0.0054 | -0.0002 | | 4.96 | 1.379 | 35.03 | 1.313 | 33.35 |
| 6 | 880950 | 417 | 460 | 289374 | 48.1159 | 41.0103 | 0.0062 | 0.0001 | | 4.96 | 1.380 | 35.05 | 1.313 | 33.35 |
| 7 | 881100 | 553 | 610 | 289375 | 48.1142 | 41.0105 | 0.0079 | -0.0001 | | 4.96 | 1.380 | 35.05 | 1.313 | 33.35 |
| 8 | 881300 | 734 | 810 | 289377 | 48.1123 | 41.0105 | 0.0098 | -0.0001 | | 4.96 | 1.380 | 35.05 | 1.313 | 33.35 |
| 9 | 881500 | 915 | 1010 | 289378 | 48.1092 | 41.0109 | 0.0129 | -0.0002 | | 4.96 | 1.380 | 35.05 | 1.313 | 33.35 |
| 10 | 882000 | 1368 | 1510 | 289383 | 48.1013 | 41.0103 | 0.0208 | 0.0001 | | 4.96 | 1.380 | 35.05 | 1.313 | 33.35 |
| 11 | 882500 | 1821 | 2010 | 289387 | 48.0922 | 41.0109 | 0.0299 | -0.0005 | | 4.96 | 1.379 | 35.03 | 1.313 | 33.35 |
| 12 | 883000 | 2274 | 2510 | 289392 | 48.0861 | 41.0105 | 0.0360 | -0.0001 | | 4.96 | 1.378 | 35.00 | 1.313 | 33.35 |
| 13 | 884000 | 3179 | 3510 | 289400 | 48.0768 | 41.0108 | 0.0453 | -0.0002 | | 4.96 | 1.378 | 35.00 | 1.313 | 33.35 |
| 14 | 886000 | 4891 | 5510 | 289420 | 48.0672 | 41.0104 | 0.0549 | 0.0000 | | 4.96 | 1.378 | 35.00 | 1.313 | 33.35 |
| 15 | 891000 | 9520 | 10510 | 289468 | 48.0463 | 41.0104 | 0.0758 | 0.0000 | | 4.96 | 1.378 | 34.95 | 1.313 | 33.35 |
| 16 | 901000 | 18578 | 20510 | 289573 | | | | | | 4.96 | 1.375 | 34.93 | 1.313 | 33.35 |

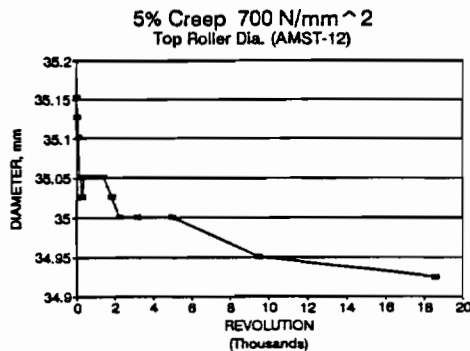
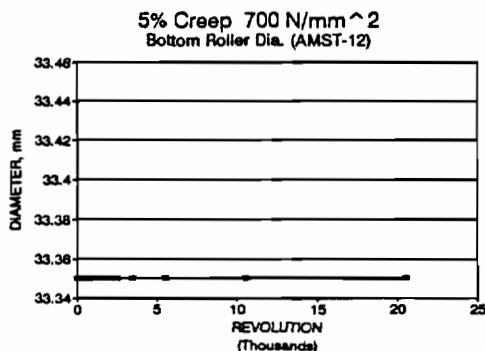
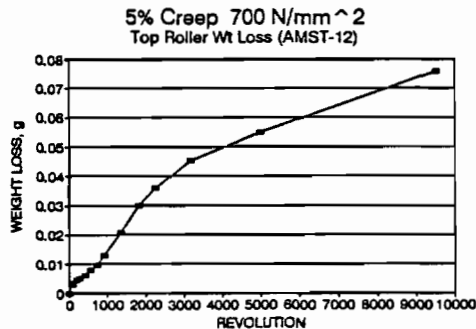
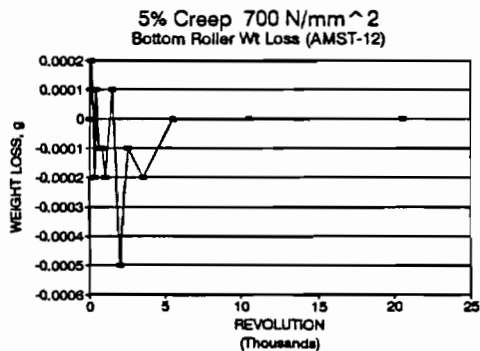


Figure 4.9. Early work. AMST12, a coating that did not wear out. 5% slide/roll, 700 MPa contact pressure.

AMSLER TEST NO.: AMST25
PLASMA SPRAY: Spray Steel 80 Wire 1/16 dia
CONTACT PRESSURE (N/mm²): 1220
CREEPAGE (%): 4.4
MOTOR SPEED (rpm): 200
COATING THICKNESS (mm): 0.94
LOADING (N): 1425
 Disk file: AMST-25

| | STEEL NO. | ROLLER DIMENSIONS | | WEAR RATE | Top | | Bottom | |
|--------|-----------|-------------------|--------------|-----------|----------|----------|--------|--|
| | | WIDTH(mm) | DIAMETER(mm) | | g/rev. | 0.000115 | 9E-08 | |
| TOP | W-3 | 4.1 | 35.25 | µg/m | 1040.387 | 85.82352 | | |
| BOTTOM | W3 | 4.99 | 33.38 | µg/mm | 208.0774 | 17.1847 | | |

Note: Wear rate on rollers calculated after run-in.

| INTERVAL No. | REVOLUTION READING (BOTTOM) | REVOLUTION | | WORK (N.m) | WEIGHT (g) | | WEIGHT LOSS (g) | | CONTACT WIDTH (mm) | | DIAMETER | | | |
|--------------|-----------------------------|------------|--------|------------|------------|---------|-----------------|---------|--------------------|--------|----------|--------|--------|--------|
| | | TOP | BOTTOM | | TOP | BOTTOM | TOP | BOTTOM | TOP | BOTTOM | TOP | BOTTOM | TOP | BOTTOM |
| | | (INCHES) | (MM) | | (INCHES) | (MM) | (INCHES) | (MM) | (INCHES) | (MM) | | | | |
| 1 | 42830 | 0 | 0 | 6381 | 48.1443 | 41.8402 | 0.0000 | 0.0000 | | | 1.388 | 35.25 | 1.3125 | 33.38 |
| 2 | 42890 | 91 | 100 | 6382 | 48.1443 | 41.8411 | 0.0000 | -0.0008 | | | 1.388 | 35.25 | 1.3125 | 33.38 |
| 3 | 42900 | 181 | 200 | 6382 | 48.1439 | 41.8415 | 0.0004 | -0.0013 | | | 1.388 | 35.25 | 1.3125 | 33.37 |
| 4 | 42910 | 272 | 300 | 6383 | 48.1441 | 41.8414 | 0.0002 | -0.0012 | | | 1.388 | 35.25 | 1.3125 | 33.37 |
| 5 | 42920 | 362 | 400 | 6385 | 48.1439 | 41.8415 | 0.0004 | -0.0013 | | | 1.388 | 35.25 | 1.3125 | 33.34 |
| 6 | 42930 | 453 | 500 | 6387 | 48.1437 | 41.8415 | 0.0008 | -0.0013 | | | 1.388 | 35.25 | 1.3125 | 33.34 |
| 7 | 42940 | 543 | 600 | 6389 | 48.1433 | 41.8417 | 0.0010 | -0.0015 | | | 1.388 | 35.25 | 1.3125 | 33.34 |
| 8 | 42950 | 634 | 700 | 6371 | 48.1429 | 41.8420 | 0.0014 | -0.0018 | | | 1.388 | 35.25 | 1.3125 | 33.34 |
| 9 | 42960 | 725 | 800 | 6373 | 48.1422 | 41.8420 | 0.0021 | -0.0018 | | | 1.388 | 35.25 | 1.3125 | 33.34 |
| 10 | 42980 | 908 | 1000 | 6377 | 48.1414 | 41.8423 | 0.0029 | -0.0021 | | | 1.388 | 35.25 | 1.3125 | 33.34 |
| 11 | 43010 | 1178 | 1300 | 6384 | 48.1405 | 41.8422 | 0.0038 | -0.0020 | | | 1.387 | 35.24 | 1.3125 | 33.34 |
| 12 | 43060 | 1630 | 1800 | 6395 | 48.1387 | 41.8431 | 0.0078 | -0.0029 | | | 1.387 | 35.24 | 1.3120 | 33.32 |
| 13 | 43110 | 2083 | 2300 | 6405 | 48.1181 | 41.8440 | 0.0282 | -0.0038 | | | 1.387 | 35.24 | 1.3120 | 33.32 |
| 14 | 43120 | 2174 | 2400 | 6407 | 48.1167 | 41.8420 | 0.0278 | -0.0018 | | | 1.387 | 35.23 | 1.3120 | 33.32 |
| 15 | 43130 | 2265 | 2500 | 6408 | 48.1148 | 41.8419 | 0.0295 | -0.0017 | | | 1.387 | 35.23 | 1.3120 | 33.32 |
| 16 | 43140 | 2355 | 2600 | 6409 | 48.1138 | 41.8412 | 0.0307 | -0.0010 | | | 1.387 | 35.23 | 1.3120 | 33.32 |
| 17 | 43150 | 2448 | 2700 | 6410 | 48.1132 | 41.8418 | 0.0311 | -0.0014 | | | 1.387 | 35.23 | 1.3120 | 33.32 |
| 18 | 43200 | 2898 | 3200 | 6421 | 48.0897 | 41.8420 | 0.0548 | -0.0018 | | | 1.387 | 35.23 | 1.3120 | 33.32 |
| 19 | 43250 | 3351 | 3700 | 6432 | 48.0558 | 41.8431 | 0.0887 | -0.0029 | | | 1.387 | 35.22 | 1.3120 | 33.32 |
| 20 | 43270 | 3533 | 3900 | 6435 | 48.0471 | 41.8428 | 0.0972 | -0.0024 | | | 1.388 | 35.21 | 1.3120 | 33.32 |
| 21 | 43290 | 3714 | 4100 | 6439 | 48.0369 | 41.8431 | 0.1074 | -0.0029 | | | 1.388 | 35.21 | 1.3120 | 33.32 |
| 22 | 43310 | 3895 | 4300 | 6443 | 48.0243 | 41.8429 | 0.1200 | -0.0027 | | | 1.385 | 35.19 | 1.3120 | 33.32 |
| 23 | 43330 | 4078 | 4500 | 6447 | 48.0093 | 41.8432 | 0.1350 | -0.0030 | | | 1.385 | 35.19 | 1.3120 | 33.32 |
| 24 | 43350 | 4257 | 4700 | 6450 | 48.9980 | 41.8424 | 0.1463 | -0.0022 | | | 1.385 | 35.19 | 1.3115 | 33.31 |
| 25 | 43450 | 5163 | 5700 | 6473 | 48.8652 | 41.8380 | 0.2791 | 0.0022 | | | 1.382 | 35.11 | 1.3110 | 33.30 |
| 26 | 43550 | 6069 | 6700 | 6497 | 48.7301 | 41.8311 | 0.4142 | 0.0091 | | | 1.378 | 35.01 | 1.3110 | 33.30 |
| 27 | 43650 | 6975 | 7700 | 6524 | 48.4980 | 41.8202 | 0.6463 | 0.0200 | | | 1.378 | 34.94 | 1.3110 | 33.30 |
| 28 | 43750 | 7880 | 8700 | 6548 | 48.1024 | 41.8063 | 1.0419 | 0.0339 | | | 1.372 | 34.85 | 1.3110 | 33.30 |
| 29 | 43850 | 8788 | 9700 | 6575 | 45.0431 | 41.5817 | 4.1012 | 0.0585 | | | 1.352 | 34.35 | 1.3110 | 33.30 |
| 30 | 43950 | 9692 | 10700 | 6603 | 45.0128 | 41.5627 | 4.1317 | 0.0775 | | | 1.313 | 33.35 | 1.3110 | 33.30 |

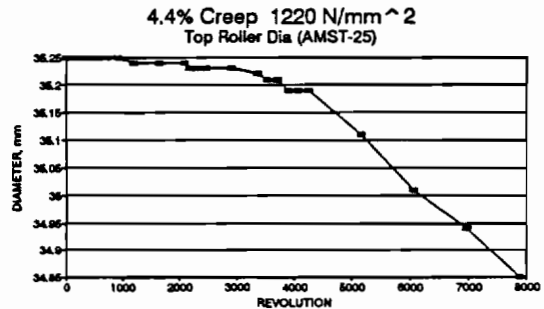
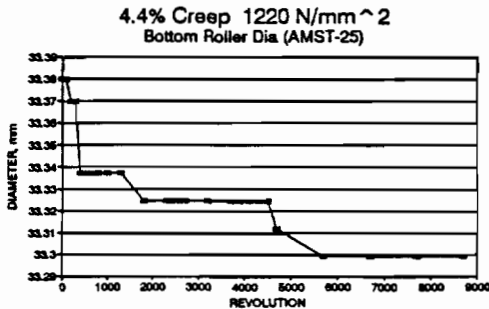
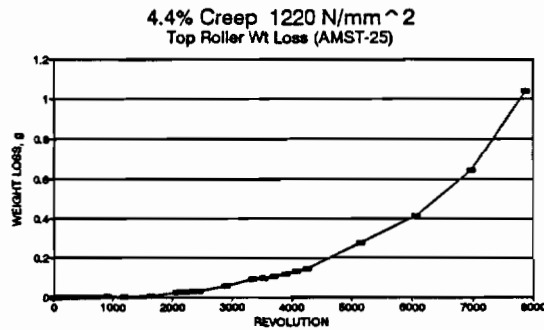
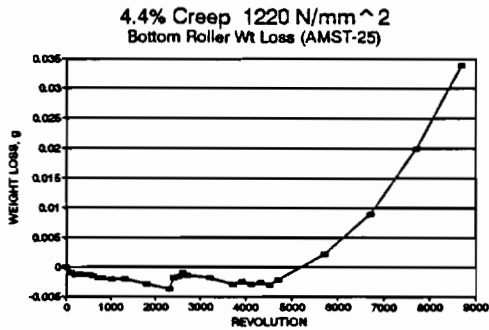


Figure 4.10. AMST25. 5% slide/roll, 1220 MPa contact pressure.

4.4 Dry Wear Testing.

Most of this testing was performed at 35% slide/roll ratio and at 1220 MPa contact pressure. Early experimentation showed that contact pressure did not influence wear rates much, so it was thought that repeated testing under the most rigorous conditions would furnish the most useful and telling results in developing a quality coating.

Most of the wear tests in this work were performed in the dry condition. While testing lubricated coatings was close to the heart of the research, it was necessary to work out the best quality coating upon which to perform lubricated tests. Problems such as parameter development, establishing the parameter envelope, and debonding issues were best addressed in the dry condition. Dry wear testing as a category encompasses all the others, even providing a basis for lubricated tests and was separated only for explanation and discussion purposes.

4.5 Lubrication Tests.

4.5.1 General Results.

Lubrication tests were performed to address the question as to whether coatings could act as an improved reservoir for lubricants under slide/roll loading conditions. In earlier research R. Devanathan performed Amsler tests using uncoated rollers to evaluate the performance of various lubricants¹⁵⁵. Data collected during his work was used for comparison with test results in this work. Of interest was the number of

revolutions per interval and the amount of retained lubricant per interval. An interval is described as one cycle of a test, where lubricant is applied, by syringe, and spread, the amount of lubricant recorded, the Amsler machine started and run until the lubricant disappeared from the system. The coefficient of friction was about 0.1 fully lubricated and about 0.45 if tested dry. The cycle, or interval, was considered complete when the friction coefficient reached 0.4. Several intervals were made for each test. In most cases the first interval, when the roller was the roughest, as it would be in the as-sprayed condition, retained the most grease. Also, not surprisingly, the most revolutions were achieved during the first interval.

The series AMST46-51, see Figures 4.11 & 4.12, consisted of rollers of approximately the same coating thickness and were tested under the same conditions.

An increase in revolutions per interval did not necessarily follow an increase in lubrication retained. The coatings in this series debonded before achieving what was considered a complete test. The longest performance was AMST46, lasting 3390 revolutions, 7 intervals. 4 of the 5 tests lasted only 3 or less intervals. AMST50 debonded during the first interval.

Coating failure due to debonding was a common occurrence during early lubrication testing. Debonding incidence was nearly 100% during this time, however some data were gathered before debonding. All of the rollers were sprayed under optimum spray parameters, which had been determined during earlier dry testing. Thicker coatings were made to test the idea that an increased coating thickness may improve the

debonding problem. Figure 4.13 shows little effect of coating thickness on test duration.

Wear rates were calculated for the lubrication tests, see figure 4.14. The results show that the wear rates fall into a fairly narrow band, showing the same basic trend as the dry tests. It should be noted that the wear rates are not a valid way to evaluate coating performance under lubricated conditions, and are used only as an additional data point to compare to other tests performed under the same or similar conditions.

Three additional tests, AMST53-55, were made under similar conditions, see figures 4.15 & 4.16. The main difference was the amount of lubricant applied before each interval. A larger amount of grease was applied, but the excess was not removed by spatula. It was allowed to remain for the test start, but then was quickly removed by the air blast employed for cooling during the test. One coating was thicker than usual, 1.65mm. Ten intervals were run, then this portion of the test was stopped. There had been a diameter reduction of 0.375mm, and the coating thickness was still greater than the 1.0mm of the other coatings. See figure 4.17 for coating thickness influence on the test duration. An attempt to run the coating under the same slide/roll ratio and contact pressure in the dry condition was made with the idea of reducing the diameter still more and obtain useful wear data at the same time. This coating failed by debonding soon after starting the first dry interval.

The 1mm coatings performed very much the same as the previous series AMST46-51. See figure 4.18 for wear rates.

Once again, wear rates are shown only as a point of similarity between lubricated coatings tested under the same conditions.

Revolutions Per Interval

1220 MPa 35% Slide/Roll

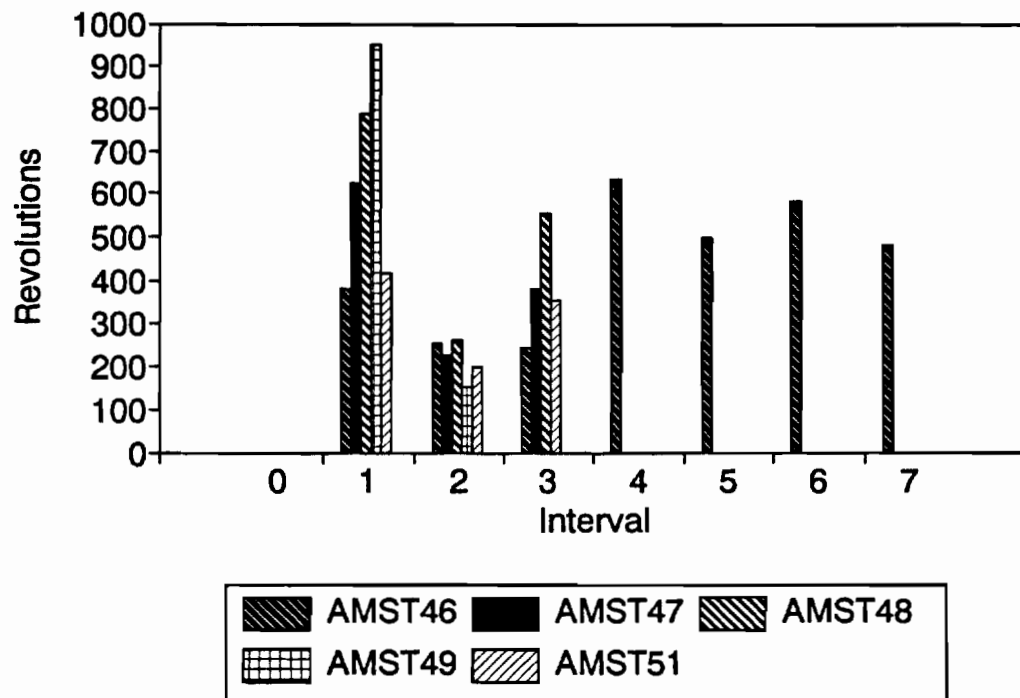


Figure 4.11. Lubrication tests. AMST4651, 35% slide/roll, 1220 MPa. Revolutions per interval.

Retained Lube Per Interval 1220 MPa

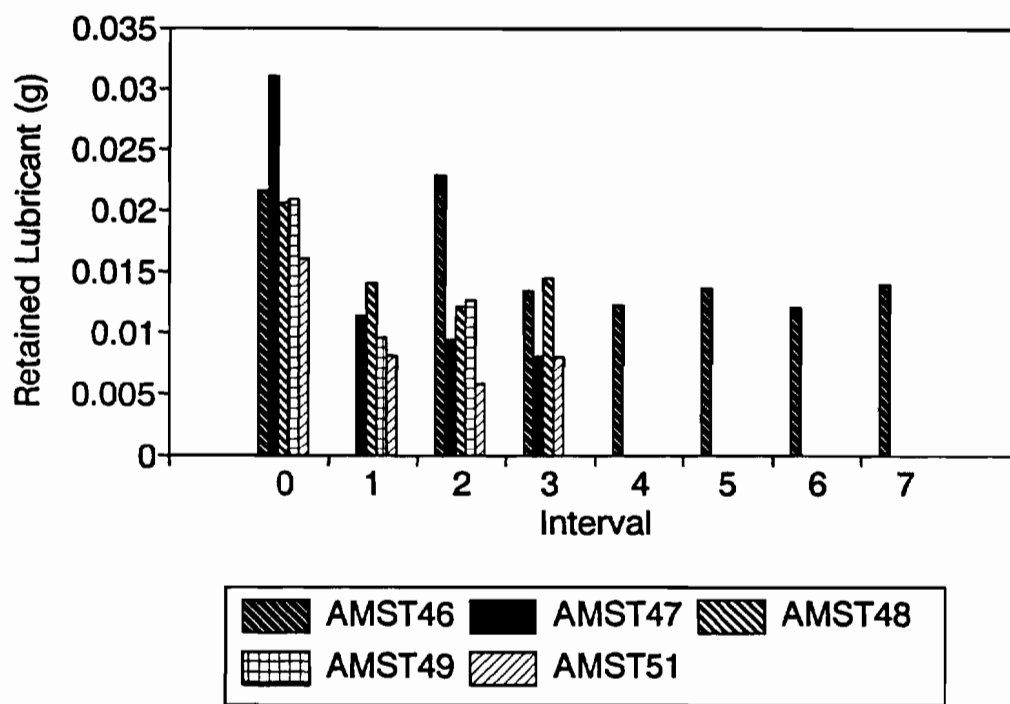


Figure 4.12. Lubrication tests. AMST4651. 35% slide/roll, 1220 MPa. Retained lubricant per interval.

Lube Tests

1220 MPA 35% Slide/Roll

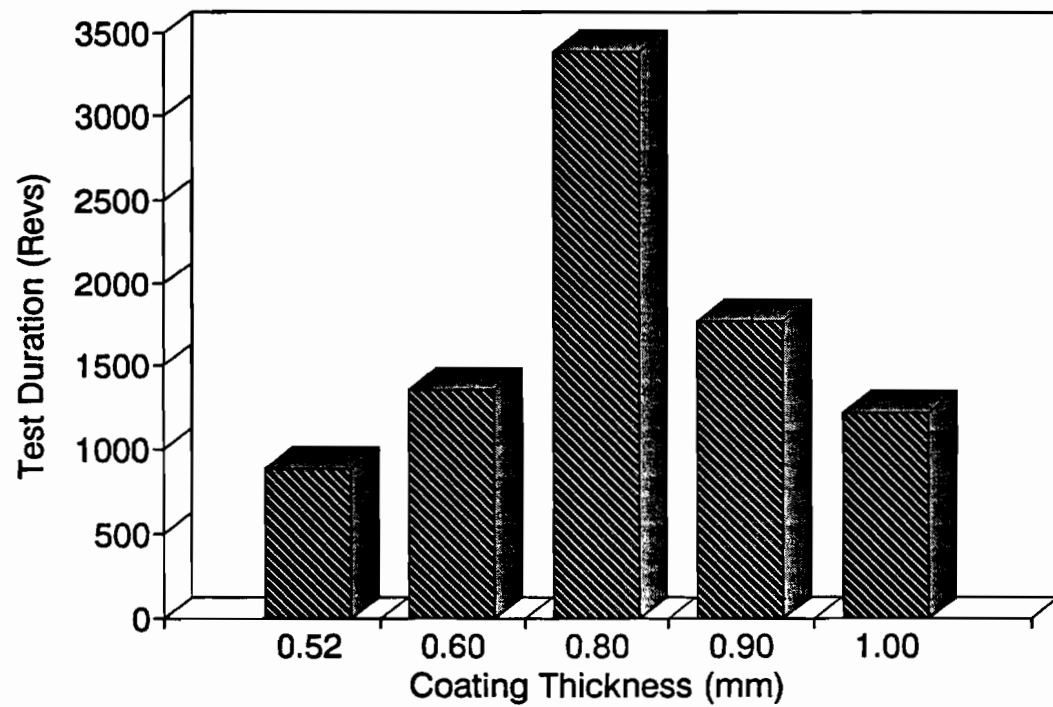


Figure 4.13. Lubrication tests. AMST4651. Little effect of coating thickness on test duration.

Lube Tests

1220 MPa 35% Slide/Roll

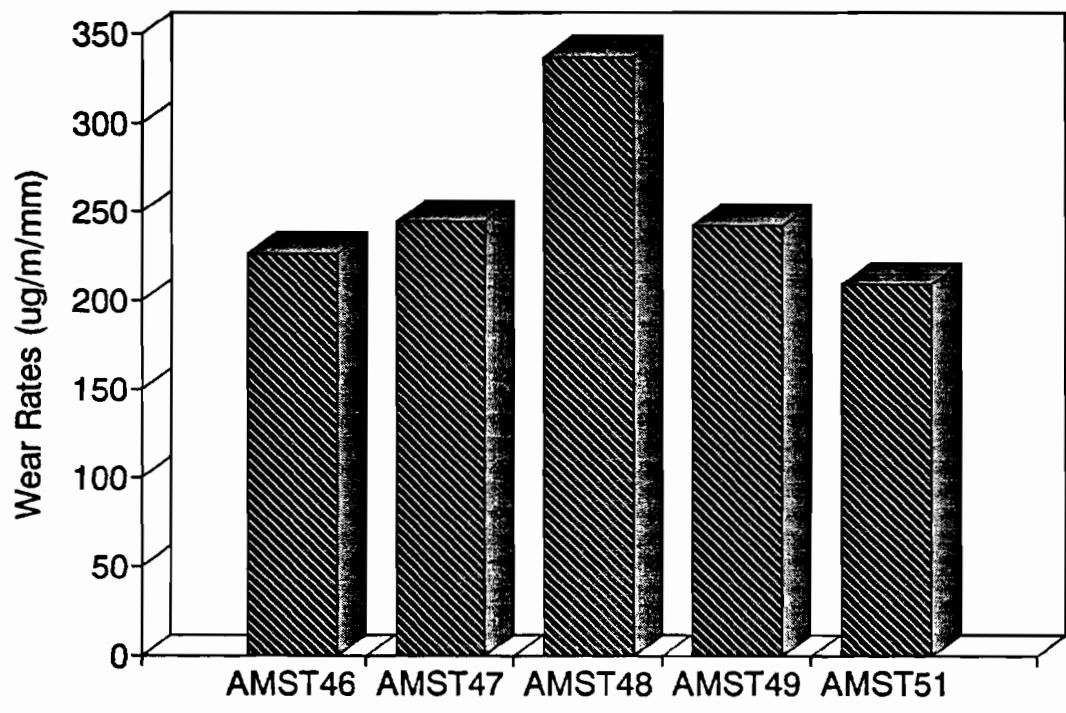


Figure 4.14. Lubrication tests. AMST4651 wear rates.

Lubricated Wear Tests

1220 MPa 35% Slide/Roll

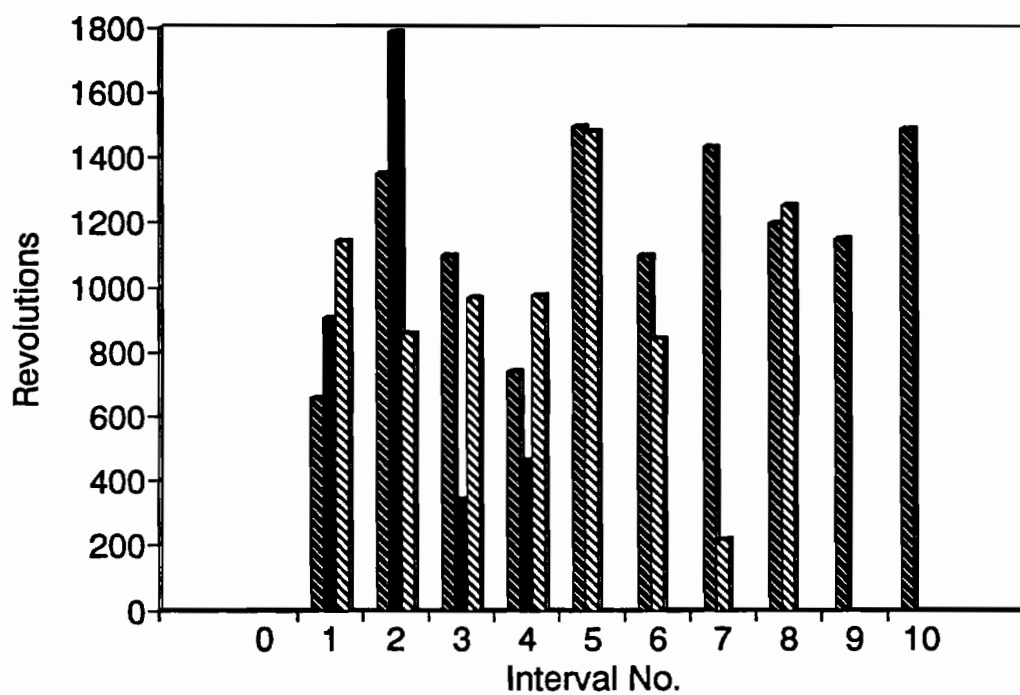


Figure 4.15. Lubrication tests. AMST5355. 35% slide/roll, 1220 MPa. Revolutions per interval.

Lubricated Wear Tests

1220 MPa 35% Slide/Roll

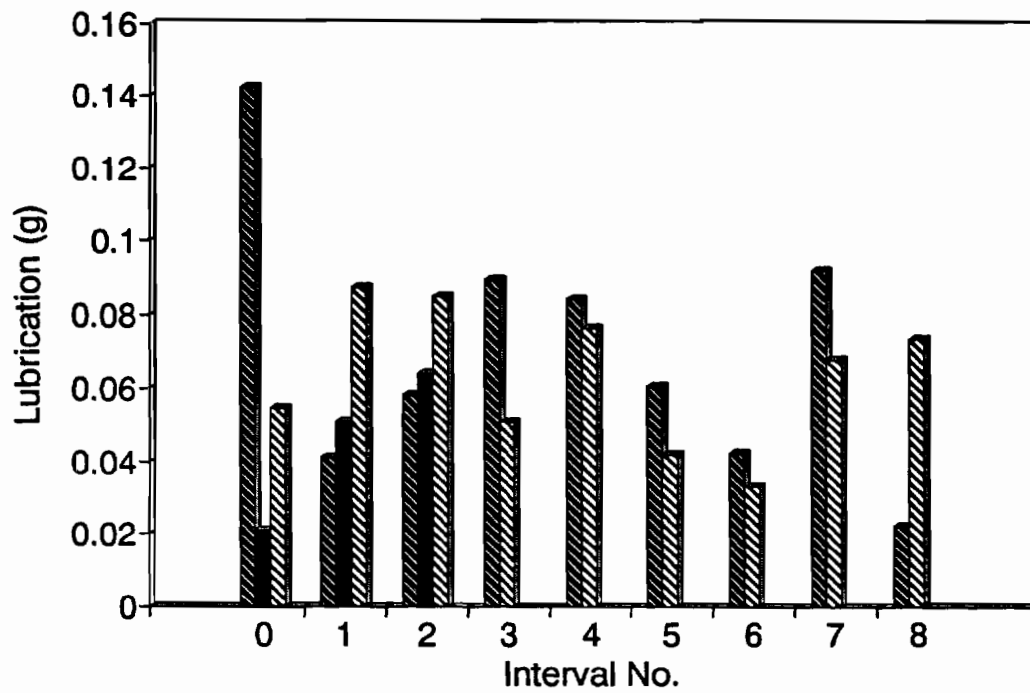


Figure 4.16. AMST5355. Retained lubricant per interval.

Lubricated Wear Tests

1220 MPa 35% Slide/Roll

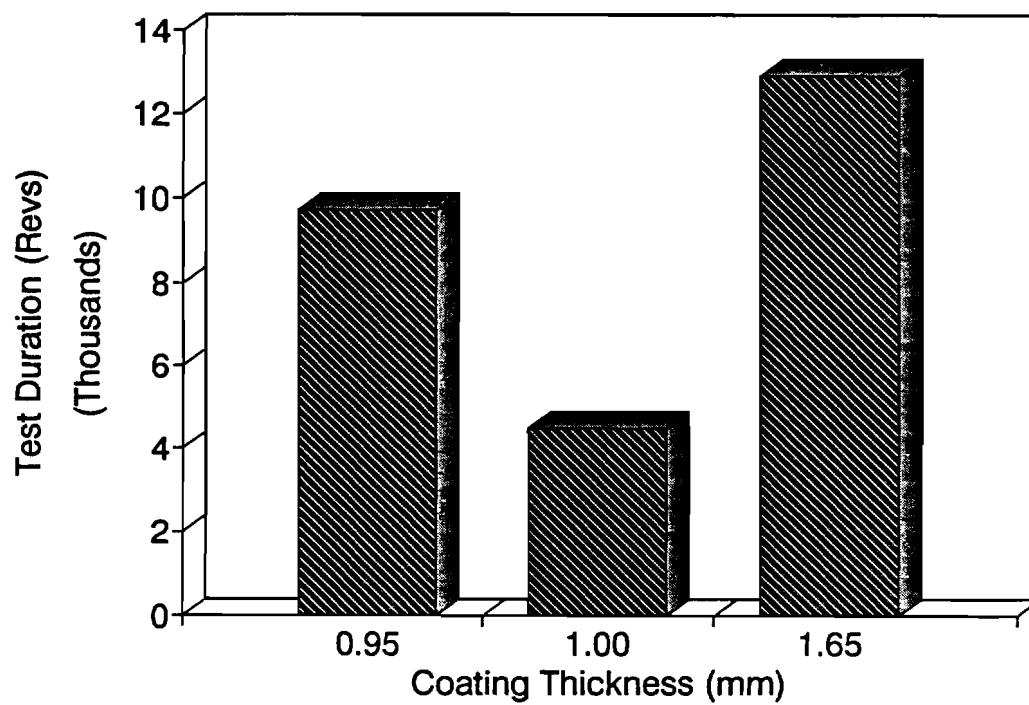


Figure 4.17. AMST5355. Influence of coating thickness on test duration.

Lubricated Wear Tests

1220 MPa 35% Creep

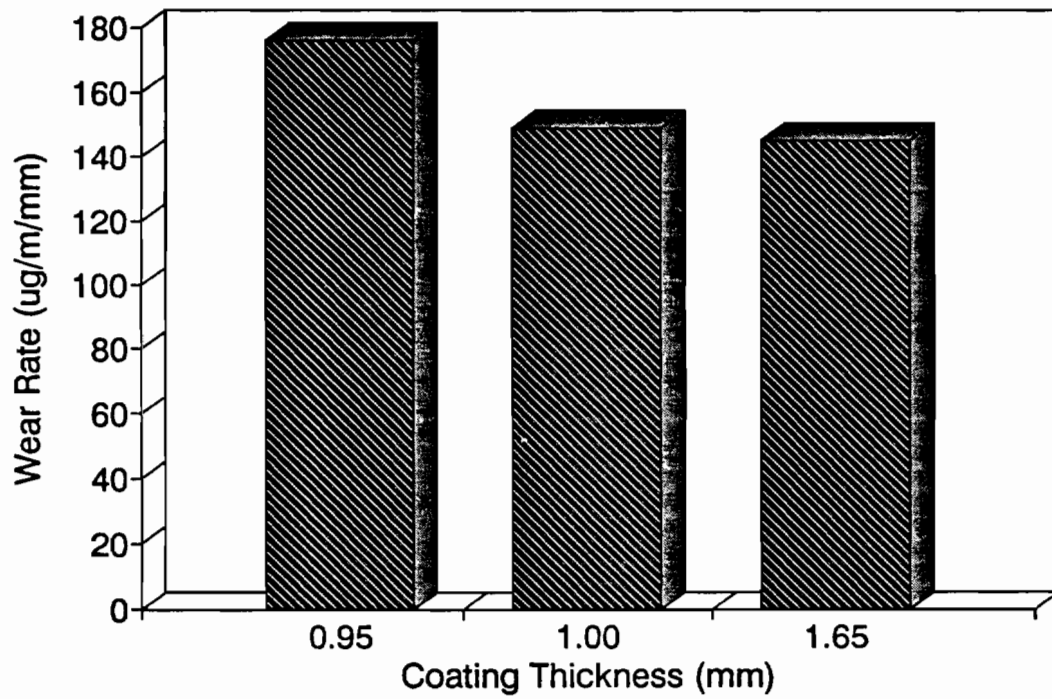


Figure 4.18. AMST5355. Little effect of coating thickness on wear rate.

4.5.2 Coated Vs Uncoated Lubrication Tests.

Tests were made with the idea of comparing lubrication test results of a coated roller with that of a lubricated uncoated roller, AMST56-57. Test conditions were the same. Reported are lubrication/interval, revolutions/interval, and wear rates. At least 10 intervals were made for each test. In these tests the trend was that the coated roller retained more lubricant per interval, but that the uncoated roller actually achieved more revolutions per interval. Wear rates are nearly the same. Figures 4.19-4.21 show these test results.

COATED VS UNCOATED

1220 MPa 35% Slide\Roll

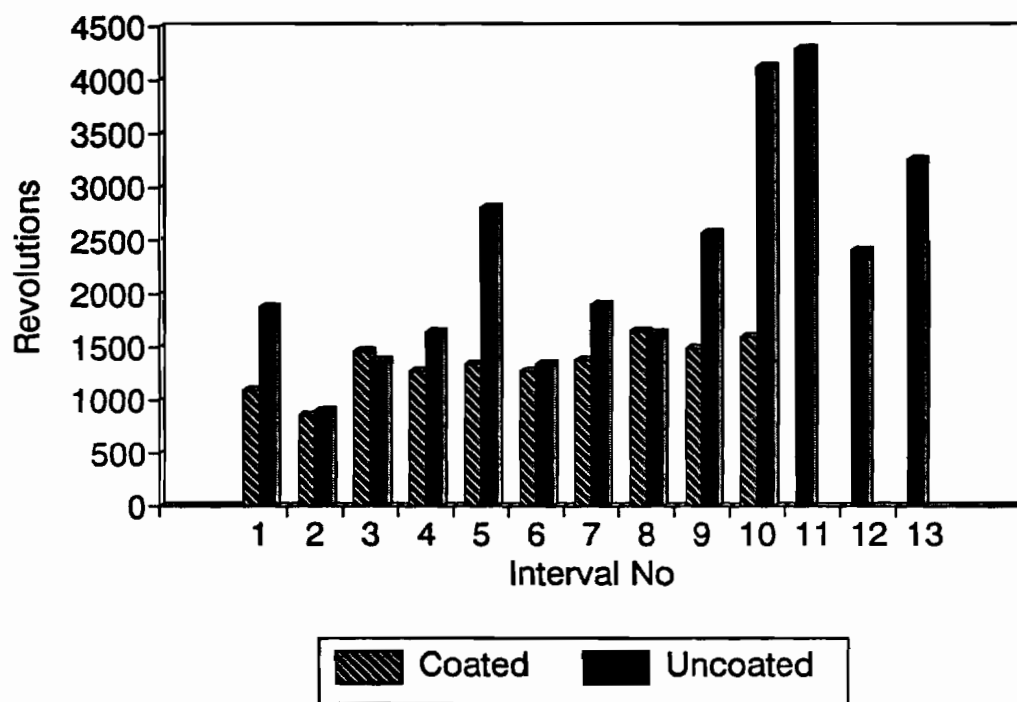


Figure 4.19. AMST5657. 35% slide/roll, 1220 MPa. Comparison of coated and uncoated rollers. Revolutions per interval.

COATED VS UNCOATED

1220 MPa 35% Slide\Roll

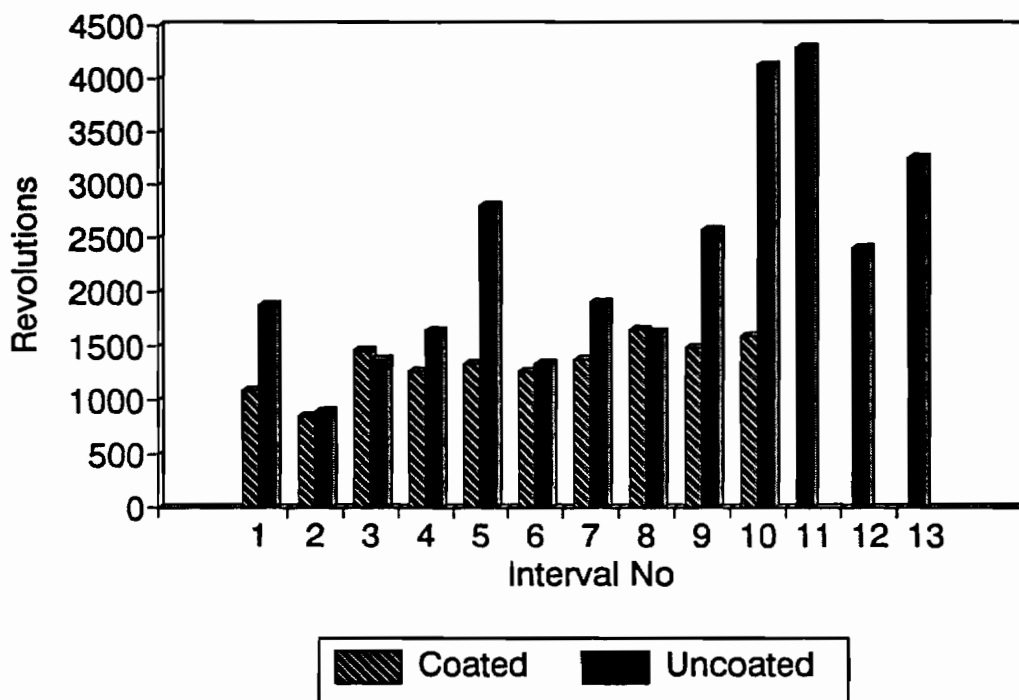


Figure 4.20. AMST5657. 35% slide/roll, 1220 MPa. Comparison of coated and uncoated rollers. Retained lubricant per interval.

COATED VS UNCOATED

1220 MPa 35% Slide/Roll

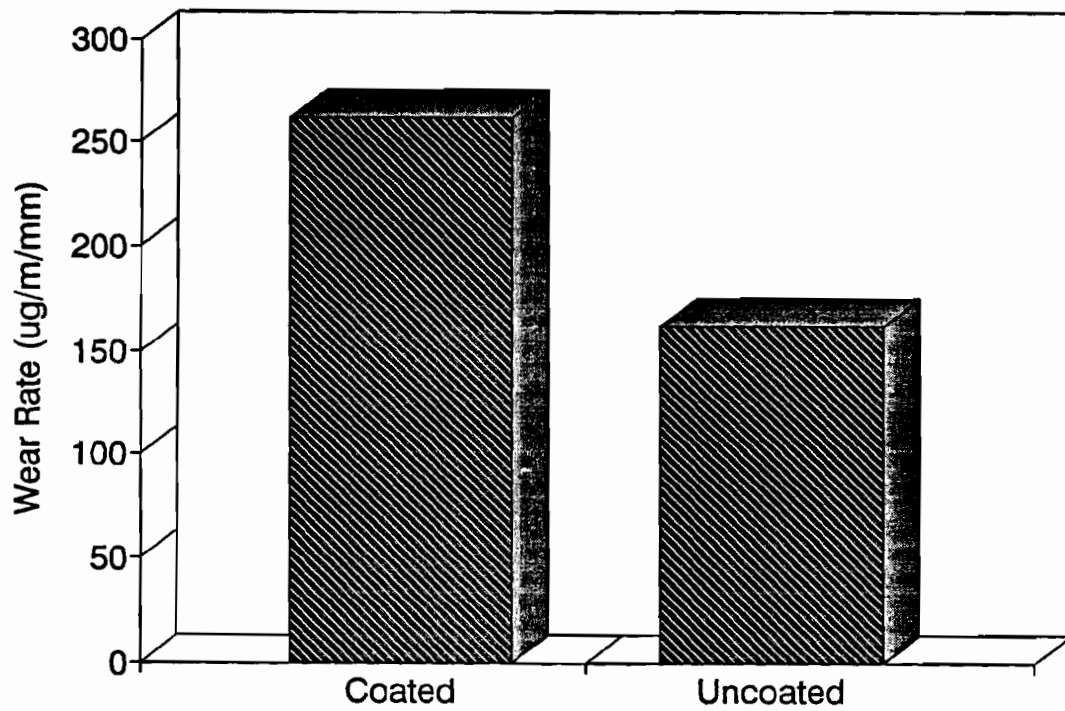


Figure 4.21. AMST5657. 35% slide/roll, 1220 MPa. Comparison of coated and uncoated roller wear rates.

4.5.3 Lubrication Test, Pure Rolling.

One test, AMST59, figure 4.21, was made with 0 slide/roll ratio. The first test interval was 10,000 revolutions, and the interval was increased until a final interval of 110,000 revolutions. There was virtually no wear detected on the coating. The friction coefficient did not change over the entire life of the test.

| | |
|-------------------------|------------------|
| Amsler Test No.: | 59 |
| Wire: | Music Wire 1/16 |
| Contact Pressure (MPa): | 1220 |
| Creepage (%): | 0 |
| Motor Speed (RPM) | 200 |
| Coating Thickness (mm): | 2.36 |
| Loading (N): | 2088 |
| Test Condition: | As Sprayed Lubed |
| Disk File: | AMST59 |

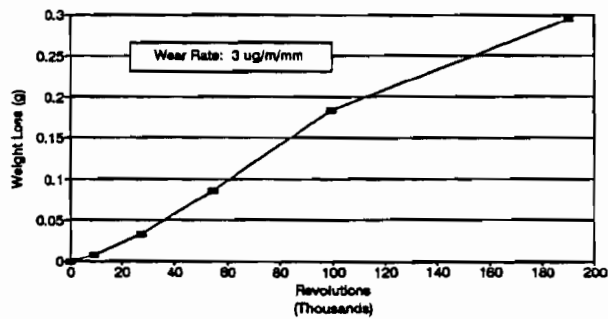
| | Steel No. | Roller Dimensions | | WEAR RA | Top |
|--------|-----------|-------------------|--------------|---------|-----------|
| | | Width(mm) | Diameter(mm) | | |
| Top | | 5 | 37.80 | ug/m | 13.617798 |
| Bottom | | 5 | 45.20 | ug/m/mm | 3 |

| Interval No. | Revolution Reading (Bottom) | Revolution | | Work (N/m) Net | Weight No Lube (g) | Lubed (g) | Net Lube Retained (g) | Weight Loss Top (g) | Diameter Top (inches) | (MM) | Rev Per Increment |
|--------------|-----------------------------|------------|--------|----------------|--------------------|-----------|-----------------------|---------------------|-----------------------|-------|-------------------|
| | | Top | Bottom | | | | | | | | |
| 0 | 169430 | 0 | 0 | 737 | 0 | 64.5974 | -64.5974 | 0 | 1.4860 | 37.74 | 0 |
| 1 | 179470 | 9094 | 10040 | 745 | 8 | 64.5895 | | 0.0079 | 1.4820 | 37.64 | 9094 |
| 2 | 199470 | 27210 | 30040 | 755 | 18 | 64.5636 | | 0.0338 | 1.4800 | 37.59 | 18116 |
| 3 | 229470 | 54384 | 60040 | 777 | 40 | 64.5109 | | 0.0865 | 1.4800 | 37.59 | 27174 |
| 4 | 279470 | 99674 | 110040 | 823 | 86 | 64.4137 | | 0.1837 | 1.48 | 37.59 | 45290 |
| 5 | 379470 | 190254 | 210040 | 920 | 183 | 64.3021 | | 0.2953 | 1.479 | 37.57 | 90580 |

Regression Output:

| | |
|---------------------|-----------|
| Constant | -0.001385 |
| Std Err of Y Est | 0.0141492 |
| R Squared | 0.9882558 |
| No. of Observations | 6 |
| Degrees of Freedom | 4 |
| X Coefficient(s) | 1.617E-06 |
| Std Err of Coef. | 8.814E-08 |

Lubrication Test: Weight Loss
1220 MPa No Creep (AMST59)



Retained Lubricant
1220 MPa No Creep (AMST59)

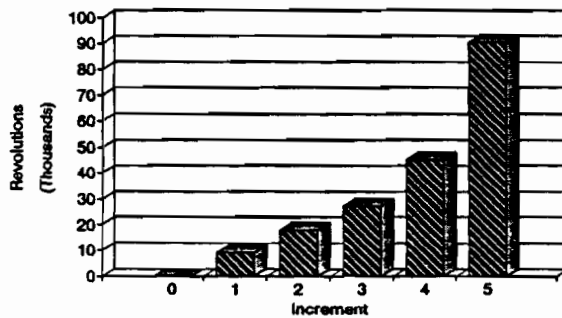


Figure 4.22. Lubrication test. Pure rolling.

4.5.4 Lubricated Testing of Layered Coatings.

Amsler tests, lubricated, were made with the layered coatings. In each case, debonding occurred after a short test duration. The break-in iteration was satisfactory, but the first or second iteration after break-in resulted in debonding at the coating/coating interface. One test, AMST58, see figure 4.23, was made with final coating thickness 1.65mm, with two layers of coating. Coating failure by debonding occurred at the interface for each layer. It appears that coating thickness under these conditions should be reported as the layer thickness and number of layers rather than the overall thickness of sprayed material. Figure 4.23 shows the appearance of the coating/coating interface.

Previous testing resulted in debonding when thin coatings, less than 1 mm, were used. The layered coatings would fit into this general category of thin coatings if each layer were defined as a coating.

| | |
|-------------------------|--------------------|
| Amsler Test No.: | AMST58 |
| Wire: | Spraysteel 80 1/16 |
| Contact Pressure (MPa): | 1220 |
| Creepage (%): | 32 |
| Motor Speed (RPM) | 200 |
| Coating Thickness (mm): | 1.65 |
| Loading (N): | 2040 |
| Test Condition: | Layered lubed |
| Parameter Set: | 230/30/225 |
| Disk File: | AMST58 |

| | Steel No. | Roller Dimensions | | WEAR RA | Top |
|--------|-----------|-------------------|--------------|---------|-----|
| | | Width(mm) | Diameter(mm) | g/rev | |
| Top | | | 36.30 | ug/m | 0 |
| Bottom | | 5 | 45.21 | ug/m/mm | 0 |

Layered Coating

1 min + 2 min + 2 min = 5 min dwell

| Interval No. | Revolution Reading (Bottom) | Revolution | | Work (N/m) Net | Weight No Lube (g) | Lube (g) | Net Lube Retained (g) | Weight Loss Top (g) | Diameter Top (inches) | (MM) | Rev Per Increment |
|--------------|-----------------------------|-------------|--------|----------------|--------------------|----------|-----------------------|---------------------|-----------------------|-------|-------------------|
| | | Top | Bottom | | | | | | | | |
| 0 | 920 | 0 | 0 | | 61.1675 | 61.2505 | 0.0830 | 0.0000 | 1.4290 | 36.30 | 0 |
| 1 | 2380 | 1322.463768 | 1460 | | 60.6810 | 60.7416 | 0.0606 | 0.4865 | 1.4100 | 35.81 | 1322 |
| 2 | 2440 | 1376.811594 | 1520 | | | | | | | | 54 |
| 3 | Debonded | | | | | | | | | | -1377 |
| 4 | Restart | | | | | | | | | | 0 |
| 5 | 2440 | 1376.811594 | 1520 | | 55.9187 | 55.9620 | 0.0433 | 5.2488 | 1.3800 | 35.05 | 1377 |
| 6 | 2870 | 1766.304348 | 1950 | | 55.6089 | 55.6629 | 0.0540 | 5.5586 | 1.7710 | 44.98 | 389 |
| 7 | 3030 | 1911.231884 | 2110 | | | | | | | | |
| 8 | Debonded | | | | | | | | | | |

Figure 4.23. Lubrication test. Layered coating.



Figure 4.24. Layered coating with the layer interfaces visible.

4.6 Parameter envelope.

4.6.1 General.

It had been determined that the parameter set 235/35/225 90° (primary gas, secondary gas in standard liters per min, working distance in mm, and 90° wire injection angle) provided optimum conditions for spraying. A substantial data base had been collected over the first 33 Amsler tests, and it was thought useful to see if there was a wider envelope of parameter sets available. AMST34-39 were made at various spray parameters to explore this idea, see figure 4.25. It was shown that there was a fairly wide envelope in which to work when evaluated by wear rates. Four of the five tests showed a range of 357 to 426 ug/m/mm. The fifth one shows a wear rate of 3893 ug/m/mm, clearly outside the envelope, and coating failure occurred quite early, about 700 revolutions. Only one other coating failed before 1000 revolutions, and one test even went more than 6000 revolutions.

It was also of interest to see the change in wear rate as the contact pressure was changed. AMST40-44 was a series to look at this. The nominal slide/roll ratio was 35%, and the contact pressures 1220, 900, 700, 500, and 1220 MPa, see figure 4.26. The wear rate range was 319 to 577 ug/m/mm, which is within the range of wear rates developed over time for 1220MPa. It seems that over this range of contact pressures the loading does not affect the wear rate of the coating.

After establishing techniques for parameter optimization through single splat analysis and metallography, it was of interest to determine the envelope of parameters that would

yield a quality coating, defined by wear rate. The block of tests, AMST61-76, to determine the spray parameter range that would yield coatings with acceptable wear performance showed many differing results. Figure 4.27 is an overview of this matrix. It attempts to show the effect of increasing, or decreasing, the amount of secondary gas in the plasma jet with a constant primary gas flow. It also shows the effect of maintaining a constant amount of secondary gas and increasing the volume of primary gas.

Wear rates show a non-distinctive pattern relative to the parameter changes, see figure 4.28. At higher secondary flow rates, the wear rate seems to increase, however it is likely that this is because of increased edge effects during wear testing. Wear rates for coatings that tested over the full 6,000 revolutions, definition of a full wear test as given in the experimental section, all tested within the expected range of 200 to 700 ug/m/mm. Generally, the very short duration tests had very high wear rates. In these cases, heavy edge effects occurred at the onset of the test. It can be also noted from looking at the comments column in Appendix 10 that edge effects were noted in nearly all of the tests. It is very difficult to determine the limits of the parameter envelope because of the debonding that occurs because of the formation of edge effects.

Photographs and image analysis show that as the gas volume is increased in the plasma generation, both primary and secondary gas, the amount of the oxide phase in the microstructure decreases. Figure 4.29 shows the change in microstructure as gas parameters were changed.

WEAR RATES

35% Creep Dry/As Sprayed

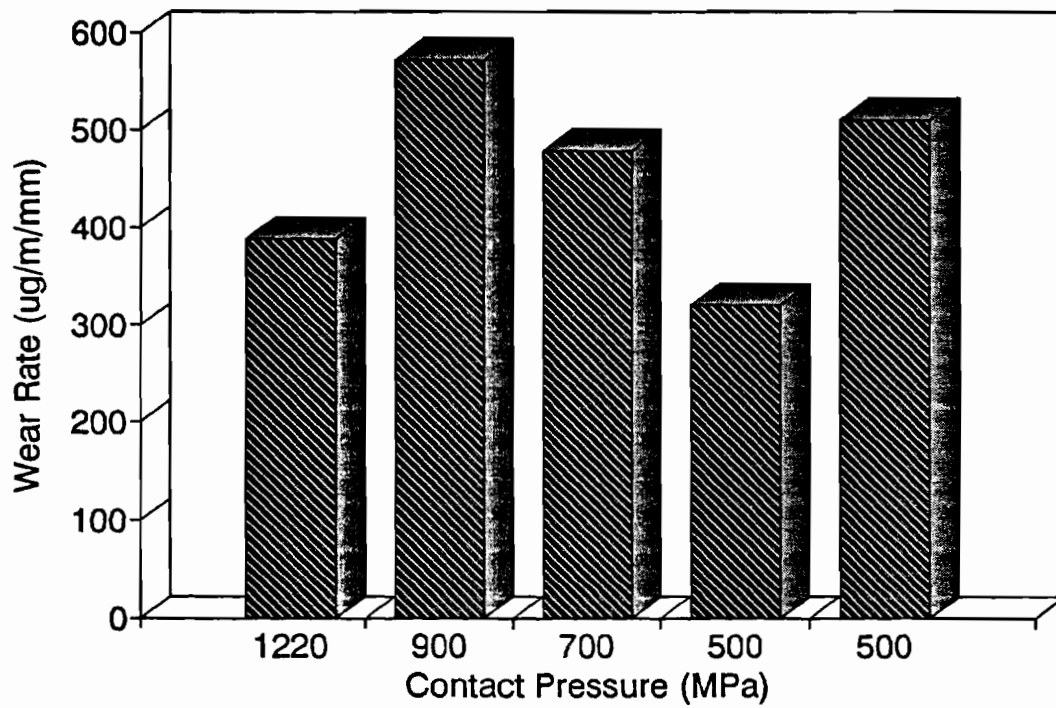


Figure 4.25. Wear rates are about the same regardless of contact pressures.

35% Creep 1050 MPa Wear Rates

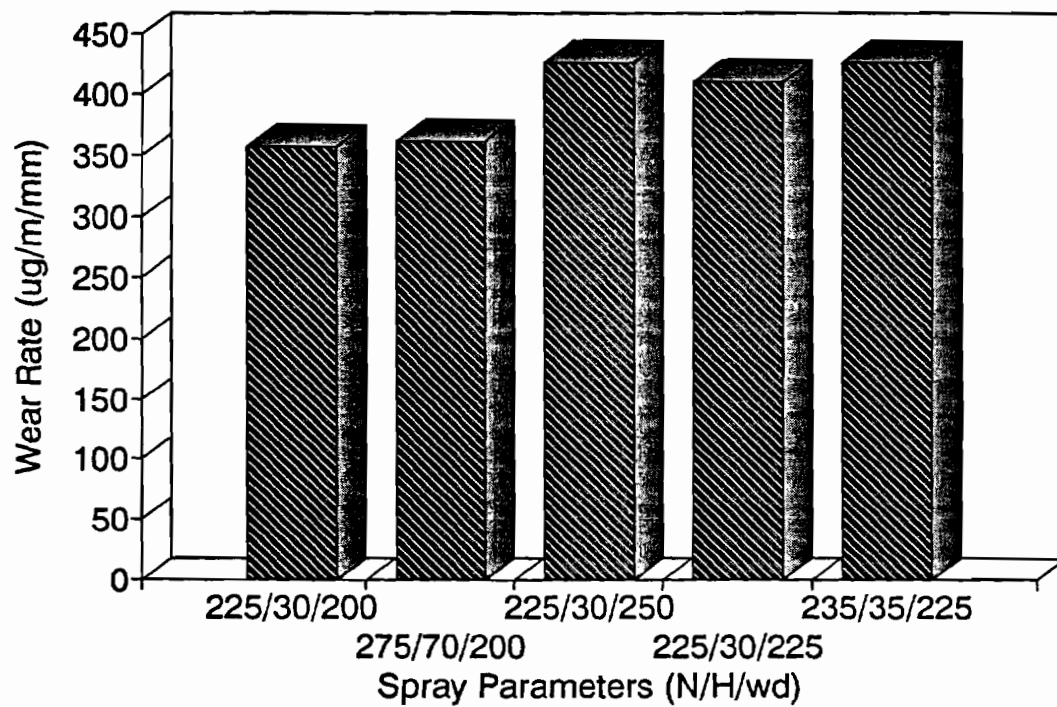


Figure 4.26. Wear rates about the same regardless of gas parameters.

| Test No. AMST | Wire | Contact Pressure | Creepage | Steel Bottom | Test Condition | Coating Thickness | Parameter Set | Wear Rate Top | Bottom | Debond Type I | Debond Type II | Test Length |
|------------------|-----------|---------------------|----------|-----------------|-------------------|----------------------|------------------|------------------|--------|------------------|-------------------|----------------|
| Test No. AMST | Wire | Contact Pressure | Creepage | Steel Bottom | Test Condition | Coating Thickness | Parameter Set | Wear Rate Top | Bottom | Debond Type I | Debond Type II | Test Length |
| 60 | 1/16 SS80 | 1220 | 36 | W-8 | DAS | 0.80 | 270/30/225 | | | X | | 180 |
| 61 | 1/16 SS80 | 1220 | 34 | W-8 | DAS | 1.25 | 210/30/225 | | | X | | 440 |
| 62 | 1/16 SS80 | 1220 | 34 | W-8 | DAS | 1.50 | 200/0/225 | 435 | | | | 6100 |
| 63 | 1/16 SS80 | 1220 | 35 | W-8 | DAS | 0.95 | 230/10/225 | 398 | | | X | 5520 |
| 64 | 1/16 SS80 | 1220 | 36 | W-8 | DAS | 0.82 | 230/50/225 | 1170 | | X | | 350 |
| 65 | 1/16 SS80 | 1220 | 33 | W-8 | DAS | 1.25 | 230/70/225 | 772 | | | X | 4020 |
| 66 | 1/16 SS80 | 1220 | 34 | W-8 | DAS | 1.17 | 250/30/225 | 2702 | | X | X | 360 |
| 67 | 1/16 SS80 | 1220 | 31 | W-8 | DAS | 1.75 | 210/30/225 | 689 | | | | 6100 |
| 68 | 1/16 SS80 | 1220 | 31 | W-8 | DAS | 1.58 | 250/30/225 | 442 | | | | 6000 |
| 69 | 1/16 SS80 | 1220 | 36 | W-8 | DAS | 0.88 | 250/15-7/225 | 322 | | | | 6000 |
| 70 | 1/16 SS80 | 1220 | 31 | W-8 | DAS | 1.67 | 250/50-25/22 | 5850 | | | X | 1710 |
| 71 | 1/16 SS80 | 1220 | 25 | W-3 | DAS | 1.56 | 230/70/225 | 15 | 2 | | X | 1470 |
| 72 | 1/16 SS80 | 1220 | 30 | W-3 | DAS | 1.50 | 230/50/225 | | | | X | 1470 |
| 73 | 1/16 SS80 | 1220 | 22 | W-3 | DAS | 2.11 | 200/0/225 | 293 | 12 | | X | 6000 |
| 74 | 1/16 SS80 | 1220 | 24 | W-3 | DAS | 1.63 | 230/50/225 | 2711 | 87 | | X | 2050 |
| 75 | 1/16 SS80 | 1220 | 24 | W-3 | DAS | 1.66 | 230/30/225 | 919 | 44 | | X | 7290 |

Figure 4.27. The parameter envelope test matrix.

Parameter Envelope Matrix

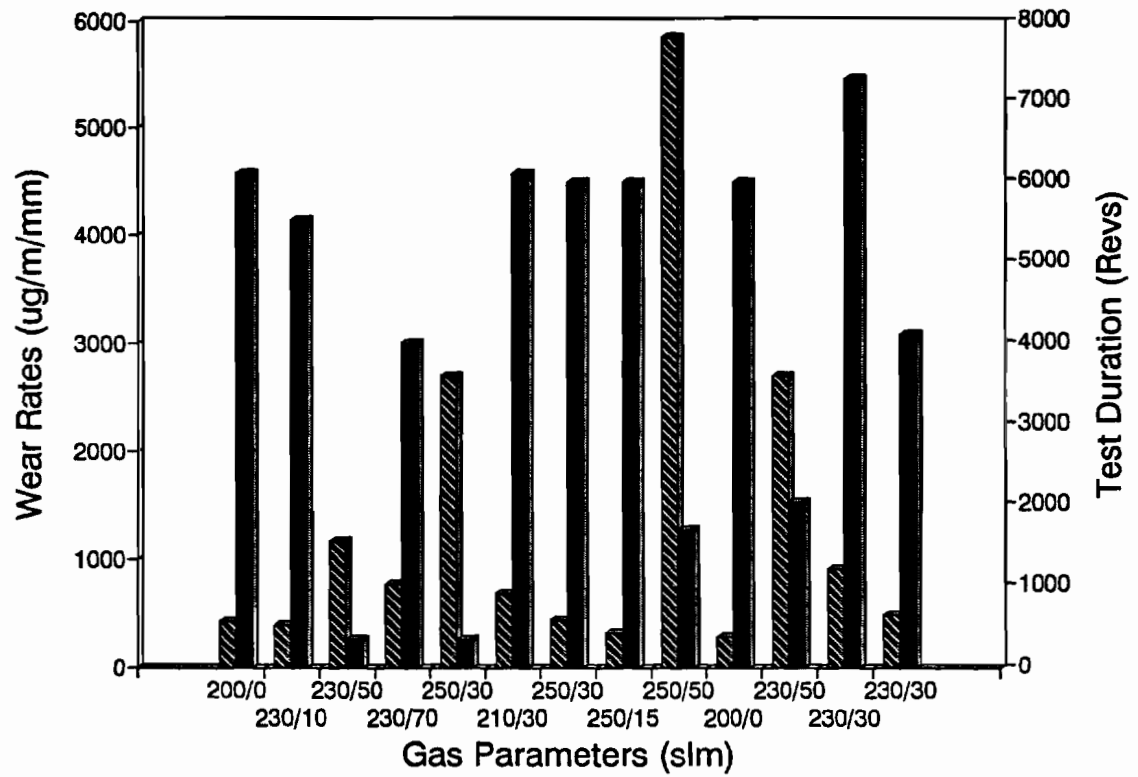
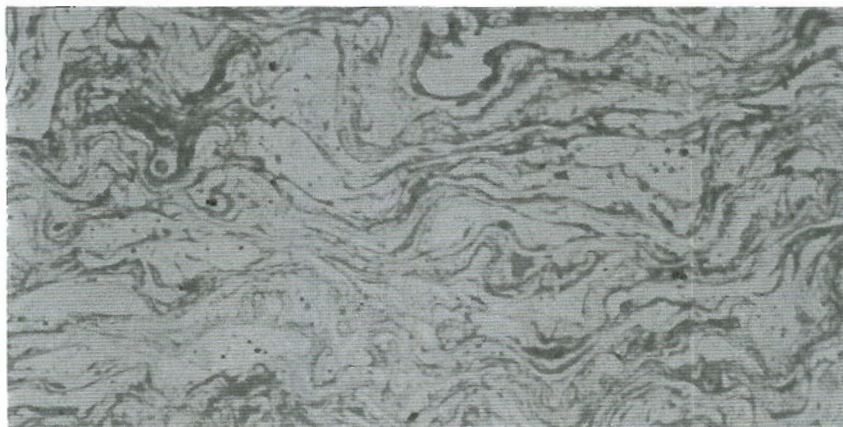
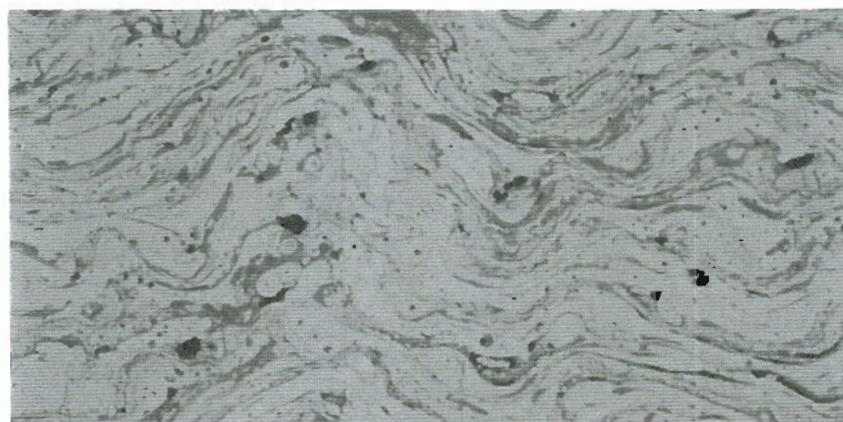


Figure 4.28. Parameter envelope. Wear rates and test durations for changing gas parameters.



a. 210/30.

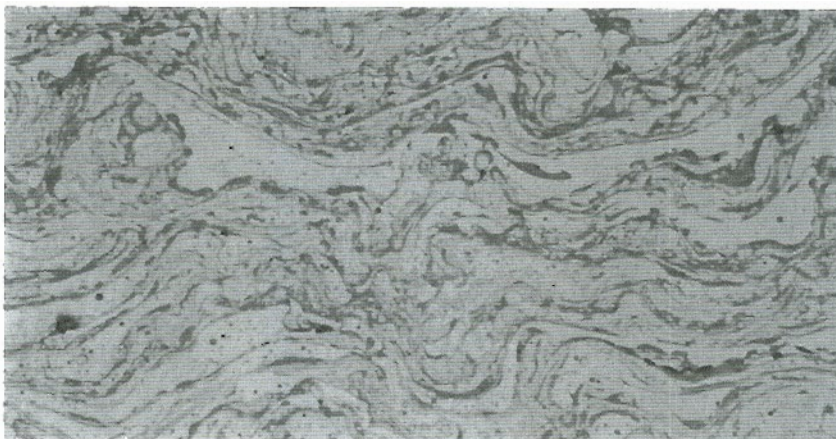


b. 240/30.

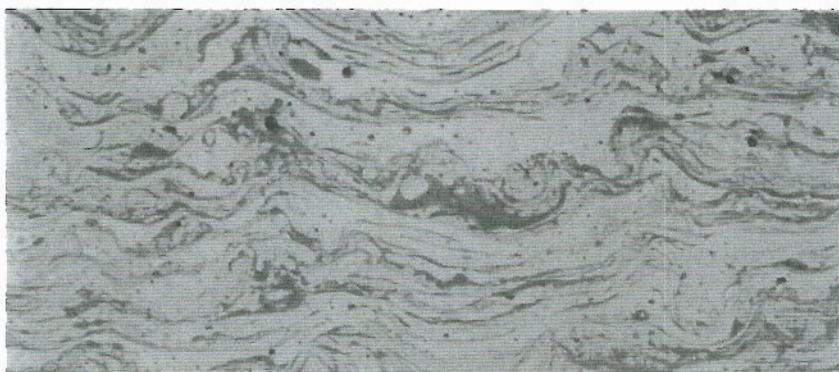


c. 270/30

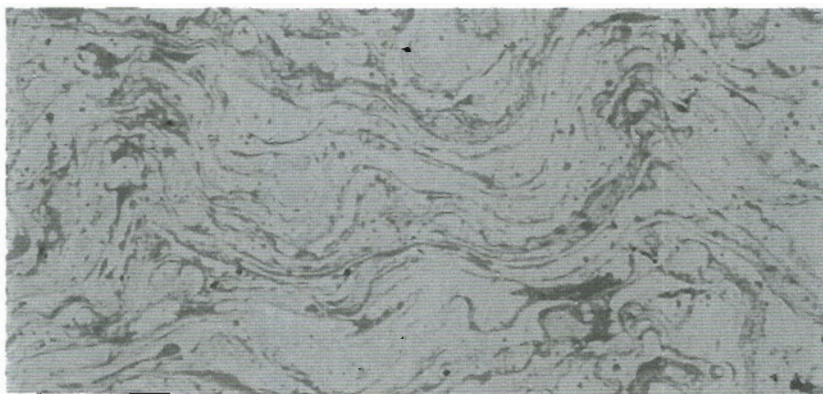
Figure 4.29. The change in microstructure as gas parameters are changed. 400x.



d. 230/10



e. 230/40



f. 230/70

Figure 3.41 cont'd. The change in microstructure as gas parameters are changed. 400x.



g. 250/10

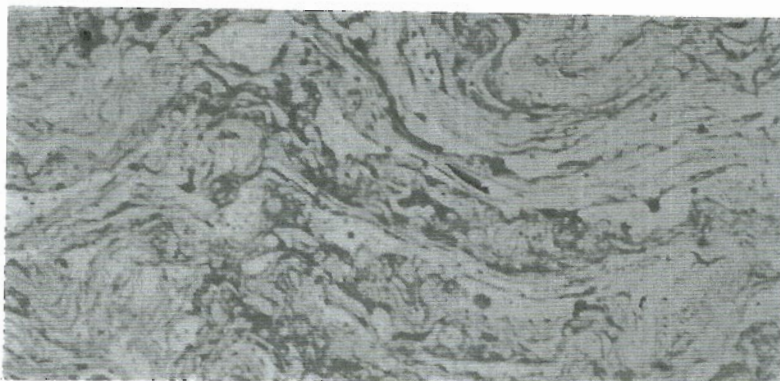


h. 250/50.



i. 250/70

Figure 41 cont'd. The change in microstructure as gas parameters are changed. 400x.



j. 210/0



k. 230/0



l. 250/0.

Figure 41 cont'd. The change in microstructure as gas parameters are changed. 400x

4.6.2 Microhardness.

Microhardness measurements were made to generate hardness profiles of these coatings. Figure 4.30 shows no clear pattern of hardness change relative to gas parameter change.

| Parameter Set | Average Hardness 500g/20sec X Layer | Sample Number |
|---------------|---|---------------|
| 230/0/225 | 322 | 1888 |
| 230/10/225 | 343 | 1889 |
| 230/20/225 | 289 | 1990 |
| 230/40/225 | 343 | 1991 |
| 230/50/225 | 344 | 1992 |
| 230/60/225 | 333 | 1993 |
| 230/70/225 | 335 | 1994 |
| 210/0/225 | 372 | 1996 |
| 240/30/225 | 331 | |
| 260/30/225 | 320 | 1886 |
| 250/0/225 | 373 | 1997 |
| 270/0/225 | 337 | 1998 |
| 250/10/225 | 303 | 1999 |
| 250/50/225 | 271 | 2000 |
| 250/70/225 | 294 | 2001 |
| 200/30/225 | 333 | 1876 |
| 220/30/225 | 331 | 1883 |
| 230/30/225 | 373 | 1875 |

Figure 4.30. Microhardness results of parameter envelope study.

4.7 Debonding Results, Dry.

During the early work, AMST1-44, debonding occurred 20 times, see figure 4.31. In several of the other tests debonding would have occurred had the test been carried further, but either testing was halted to retain a coating that was close to failure, or failure was thought to occur very soon. During this time the concept of a full wear test was not fully developed, tests were carried out until there was a compelling reason to halt. It can be seen that near the end of this period some progress had been made in reducing debonding. Figure 4.32 shows 8 consecutive tests that were carried out with no debonding. The wear rates of this group fits well with the other tests that are reported in the repeatability section.

Debonding incidence was also high during the parameter envelope matrix, AMST60-75. During this matrix it was discovered that wear performance was not much influenced as spray parameters were moved from optimum. What did happen was that as the volume of secondary gas was increased the formation of edge effects during testing was amplified. Coating failure occurred largely because of edge effects throughout this matrix. Parameter envelope limits were very difficult to determine because of this, and were not clearly identified. Figure 4.33 shows test durations, with 6,000 revolutions established as a full length wear test.

Figure 4.34 shows an overview of debonding test matrix AMST77-96. This matrix features coating froth, interrupted spray, and optimum spray conditions. Figure 4.35 shows 5 rollers from this matrix and 5 rollers that were sprayed at another time that had frothy coatings. Note the short test

duration. Coating failures of this type are not debonding failures, but are reported here because the end result of this failure is a bare substrate, with no coating adhering. A frothy coating disintegrates rapidly under loaded conditions.

AMST87-91 was a block that featured an interrupted spray. It was predicted that failure from edge effects would occur, and figure 4.36 shows the results of this block in terms of test duration.

Ten rollers, AMST82-86 and AMST92-96, were sprayed under what was thought to be optimum conditions. In the first block, no debonding occurred. In the second, 2 coatings failed under type II debonding, surface initiated edge effects, debonding. This matrix was 80% successful of all types of debonding, and no incidence of type I debonding. This shows that proper substrate preparation and strict control of the spray process will yield coatings that don't fail because of interfacial initiated type I debonding. Figure 4.37 shows the test results featuring wear rates and test duration. Within this group the wear rates fall into the expected range.

One test block, AMST117-121, featured knurling. One of five went the distance of 6,000 revolutions, see figure 4.38. AMST122-123 rollers were shot blasted with the steel shot. One roller was knurled and one not. The knurled roller did not debond, but the unknurled roller went 5090 revs, nearly a full test, see fig 4.39. It is now thought that knurling does not improve surface roughening for achieving a good mechanical bond at the substrate/coating interface. Silica, used in an attempt to roughen the knurled channels, is also thought not to be an effective blasting medium because of its small particle size.

During the test matrix from AMST97-154, see figure 4.40, note that only 2 of the coatings failed by type I debonding, AMST126 and AMST144. Experience shows that edge effects begin between 1,000 and 2,000 revolutions in the high quality coatings. Failure before 1,000 revs is nearly always type I if proper substrate and spraying procedures are observed, and optimum spray parameters are used. Failure between 1,000 and 2,000 revolutions may be of mixed mode, but debonding after 2,000 revolutions is nearly always type II in Amsler rollers. In the sense of type I debonding prevention, this matrix shows a 96% (51 of 53) success ratio. Total debonding was 49% (26 of 53), excluding the frothy coatings, AMST108-112.

Debonding: Early Work AMST1-44

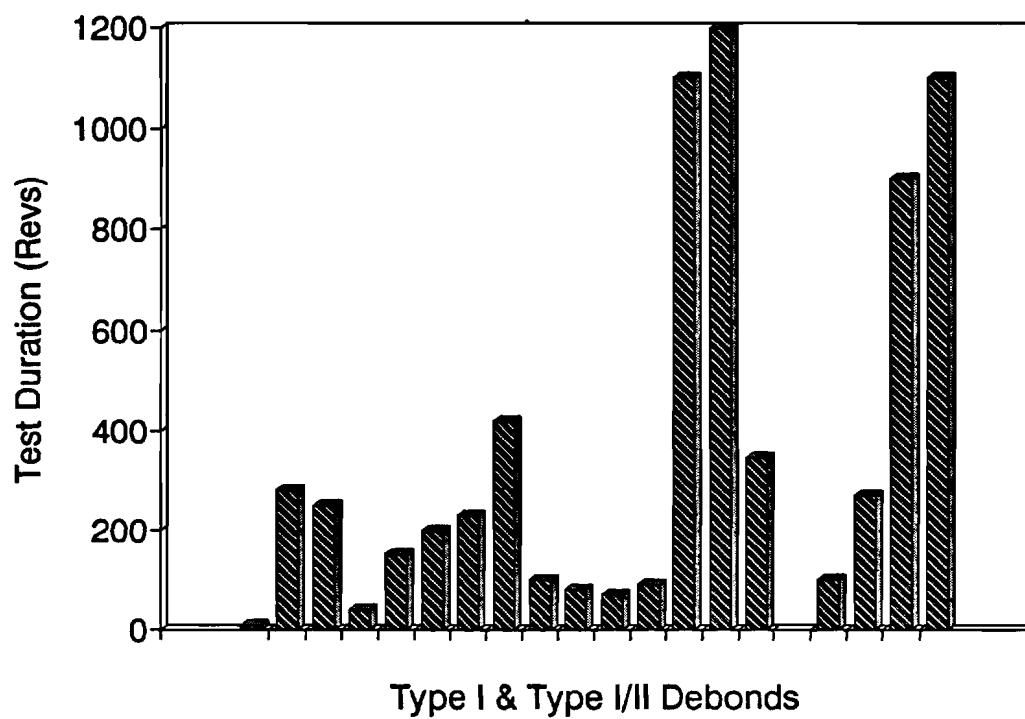


Figure 4.31. Early work. Test duration of debonded coatings.

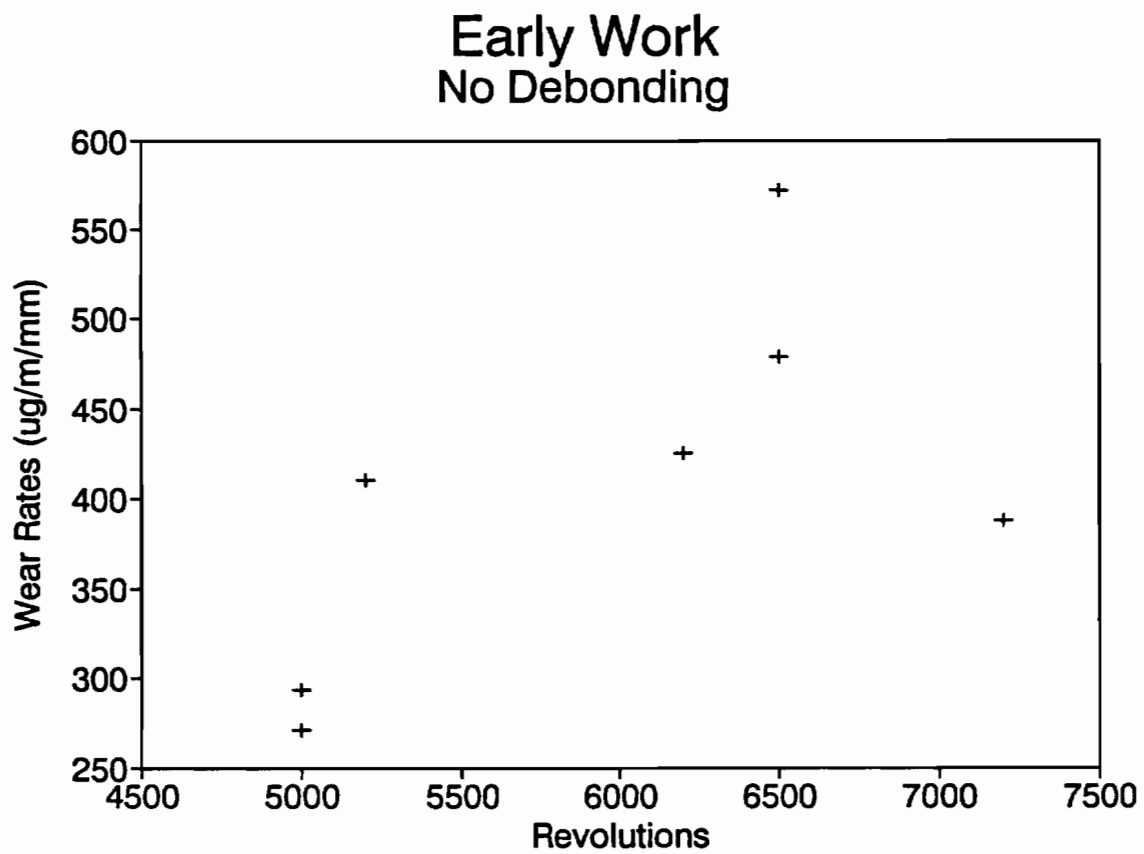


Figure 4.32. Early work. Wear rates and test durations of coatings without debonding.

Debonding: Parameter Envelope 1220 MPa 35% slide/roll (AMST60-76)

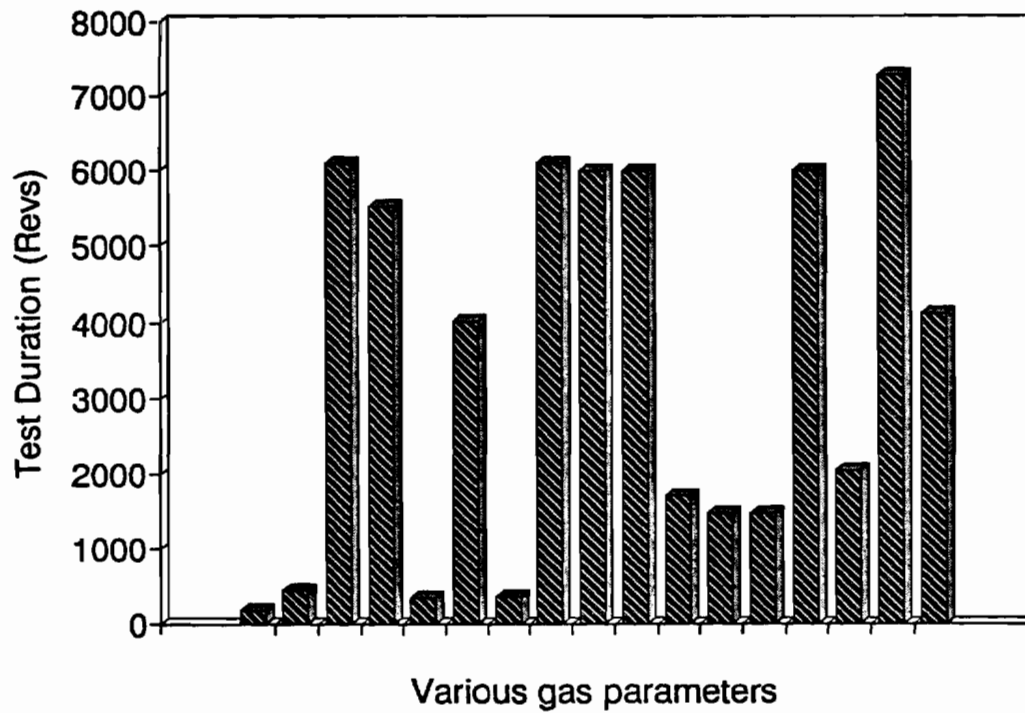


Figure 4.33. Debonding incidence during parameter envelope study.

| Test No. AMST | Wire | Contact Pressure | Creepage | Steel Bottom | Test Condition | Coating Thickness | Parameter Set | Wear Rate | | Debond Type I | Debond Type II | Test Length |
|------------------|-----------|---------------------|----------|-----------------|-------------------|----------------------|------------------|-----------|--------|------------------|-------------------|----------------|
| | | | | | | | | Top | Bottom | | | |
| 77 | 1/16 SS80 | 1220 | 38 | W-9 | DGF | 0.38 | 230/30/225 | | | Froth | | 260 |
| 78 | 1/16 SS80 | 1220 | 38 | W-9 | DGF | 0.41 | 230/30/225 | | | Froth | | 280 |
| 79 | 1/16 SS80 | 1220 | 38 | W-9 | DGF | 0.40 | 230/30/225 | | | Froth | | 220 |
| 80 | 1/16 SS80 | 1220 | 38 | W-9 | DGF | 0.44 | 230/30/225 | | | Froth | | 230 |
| 81 | 1/16 SS80 | 1220 | 38 | W-9 | DGF | 0.41 | 230/30/225 | | | Froth | | 230 |
| 82 | 1/16 SS80 | 1220 | 35 | W-9 | DGF | 0.78 | 230/30/225 | 262 | 7 | | | 6000 |
| 83 | 1/16 SS80 | 1220 | 35 | W-9 | DGF | 0.82 | 230/30/225 | 306 | 11 | | | 6000 |
| 84 | 1/16 SS80 | 1220 | 36 | W-9 | DGF | 0.72 | 230/30/225 | 208 | 7 | | | 6000 |
| 85 | 1/16 SS80 | 1220 | 35 | W-9 | DGF | 0.84 | 230/30/225 | 373 | 9 | | | 6000 |
| 86 | 1/16 SS80 | 1220 | 36 | W-9 | DGF | 0.75 | 230/30/225 | 301 | 8 | | | 6000 |
| 87 | 1/16 SS80 | 1220 | 38 | W-9 | DGF | 0.46 | 230/30/225 | | | | X | 1486 |
| 88 | 1/16 SS80 | 1220 | 38 | W-9 | DGF | 0.45 | 230/30/225 | | | | X | 1929 |
| 89 | 1/16 SS80 | 1220 | 38 | W-9 | DGF | 0.54 | 230/30/225 | | | | X | 2500 |
| 90 | 1/16 SS80 | 1220 | 38 | W-9 | DGF | 0.47 | 230/30/225 | | | | X | 1051 |
| 91 | 1/16 SS80 | 1220 | 38 | W-9 | DGF | 0.45 | 230/30/225 | | | | X | 2418 |
| 92 | 1/16 SS80 | 1220 | 34 | W-9 | DGF | 1.12 | 230/30/225 | 212 | 11 | | | 6000 |
| 93 | 1/16 SS80 | 1220 | 34 | W-9 | DGF | 1.12 | 230/30/225 | 407 | 25 | | X | 4360 |
| 94 | 1/16 SS80 | 1220 | 34 | W-9 | DGF | 1.11 | 230/30/225 | 197 | 12 | | | 6000 |
| 95 | 1/16 SS80 | 1220 | 34 | W-9 | DGF | 1.14 | 230/30/225 | 306 | 19 | | X | 5630 |
| 96 | 1/16 SS80 | 1220 | 34 | W-9 | DGF | 1.10 | 230/30/225 | 232 | 13 | | | 6000 |

Figure 4.34. Debonding study test block.

Debonding: Frothy Coatings

1220 MPA 35% slide/roll

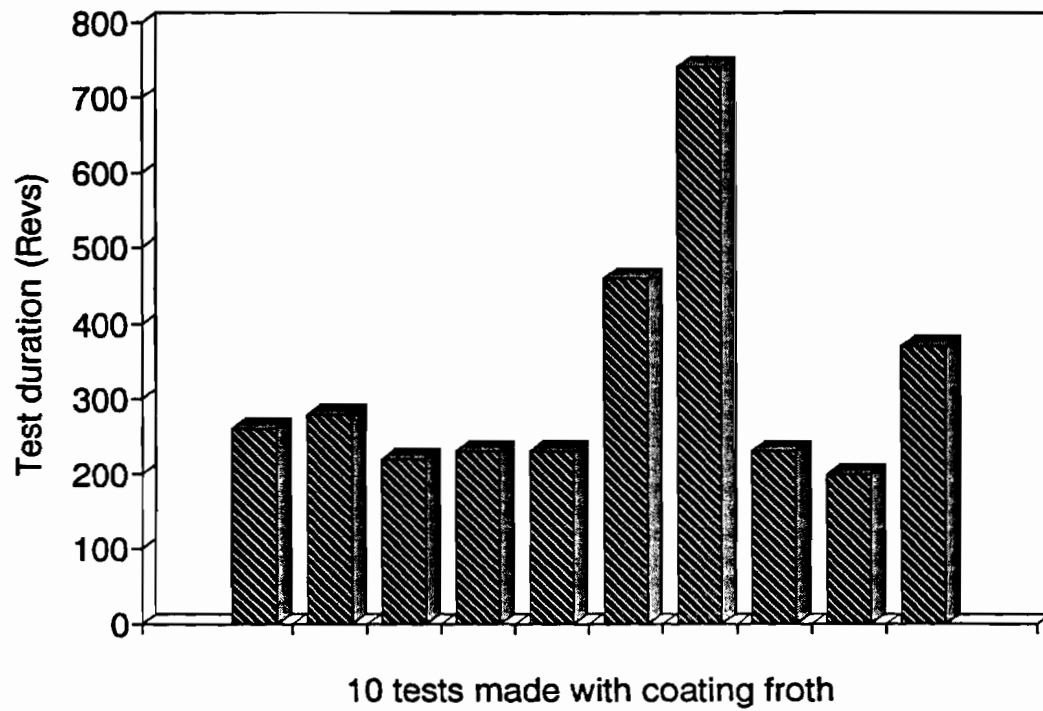


Figure 4.35. The effect of coating froth.

Debonding: Interrupted Spray 1220 MPA 38% Slide/Roll

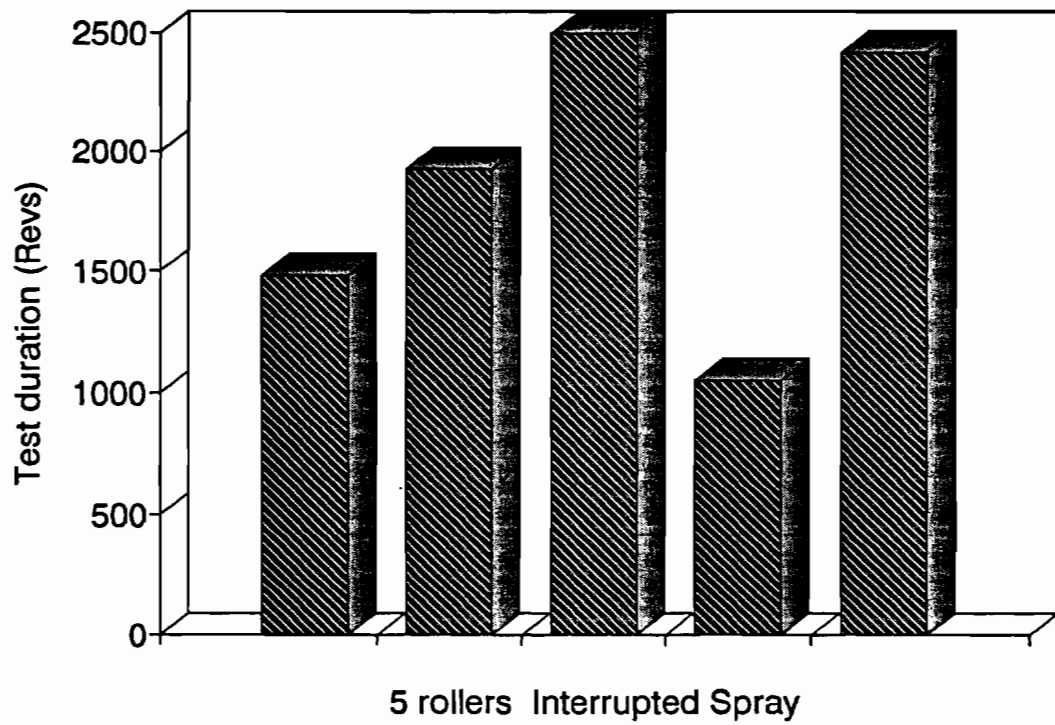


Figure 4.36. Interrupted spray test duration.

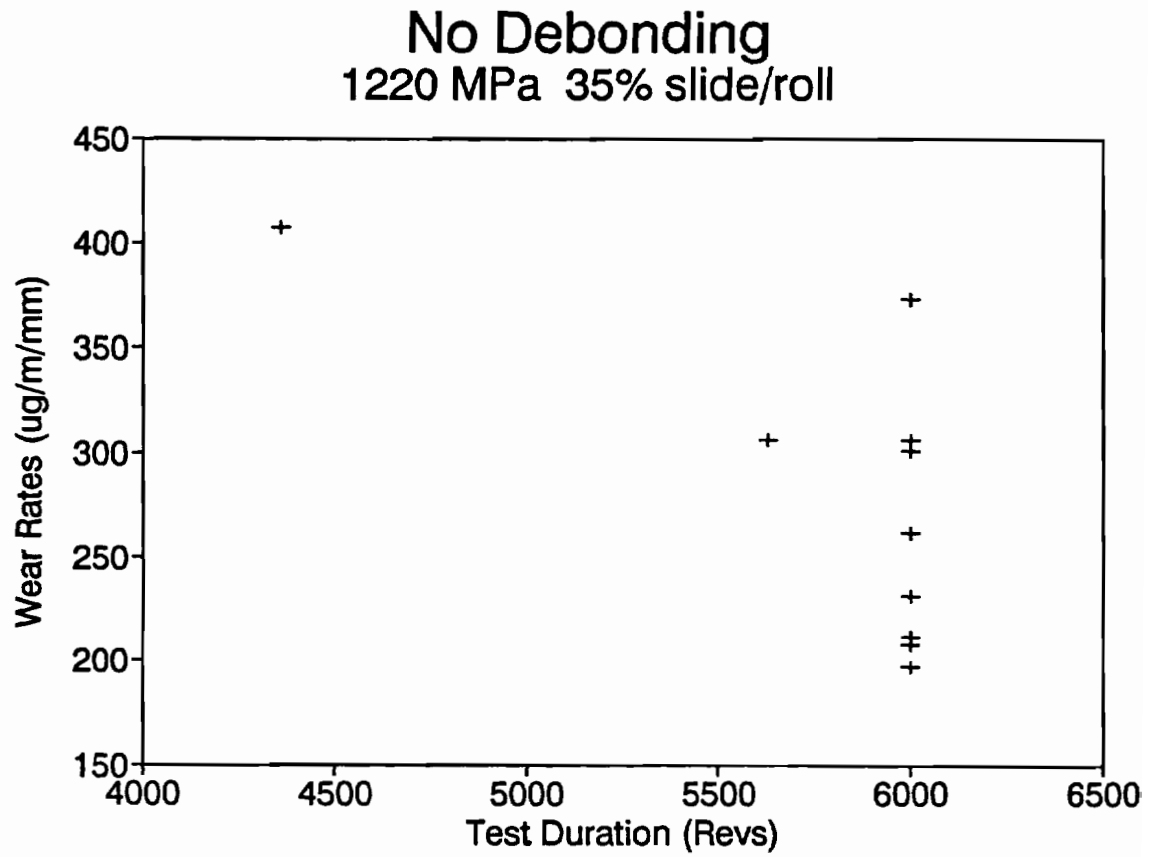


Figure 4.37. Ten roller block with no type I debonding, 2 events of type II debonding.

Debond: Knurling 1220 MPA 35% Slide/roll

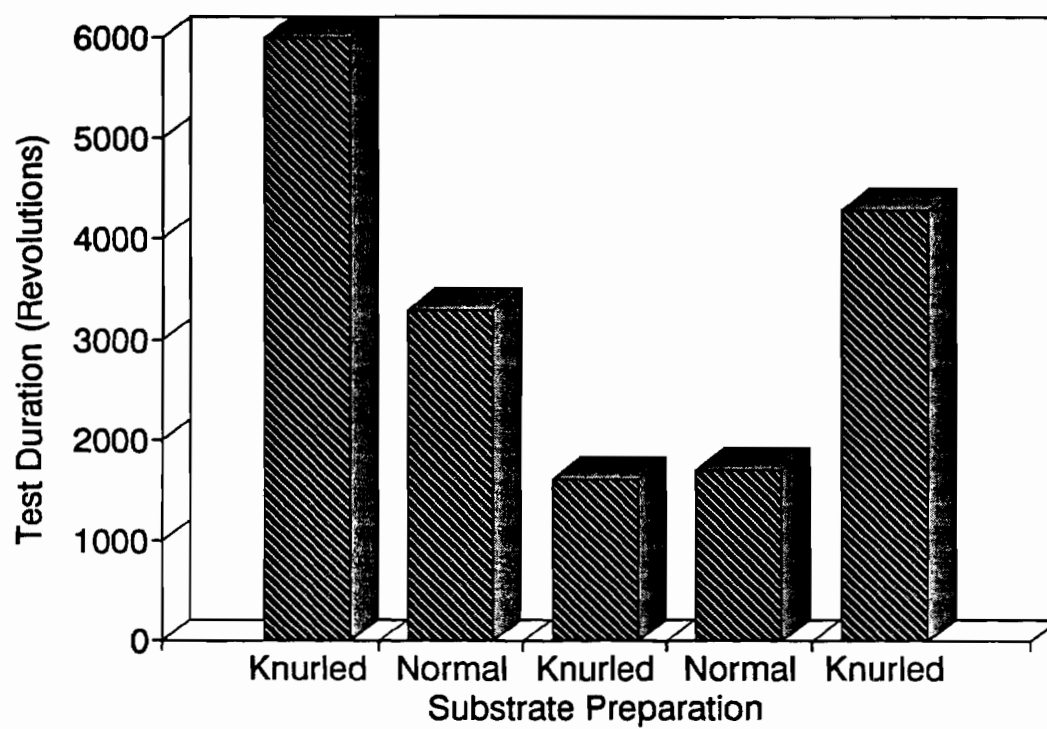


Figure 4.38. Knurled and normal substrate preparation effect on debonding.

Debond: Knurling
1220 MPa 35% Slide/Roll

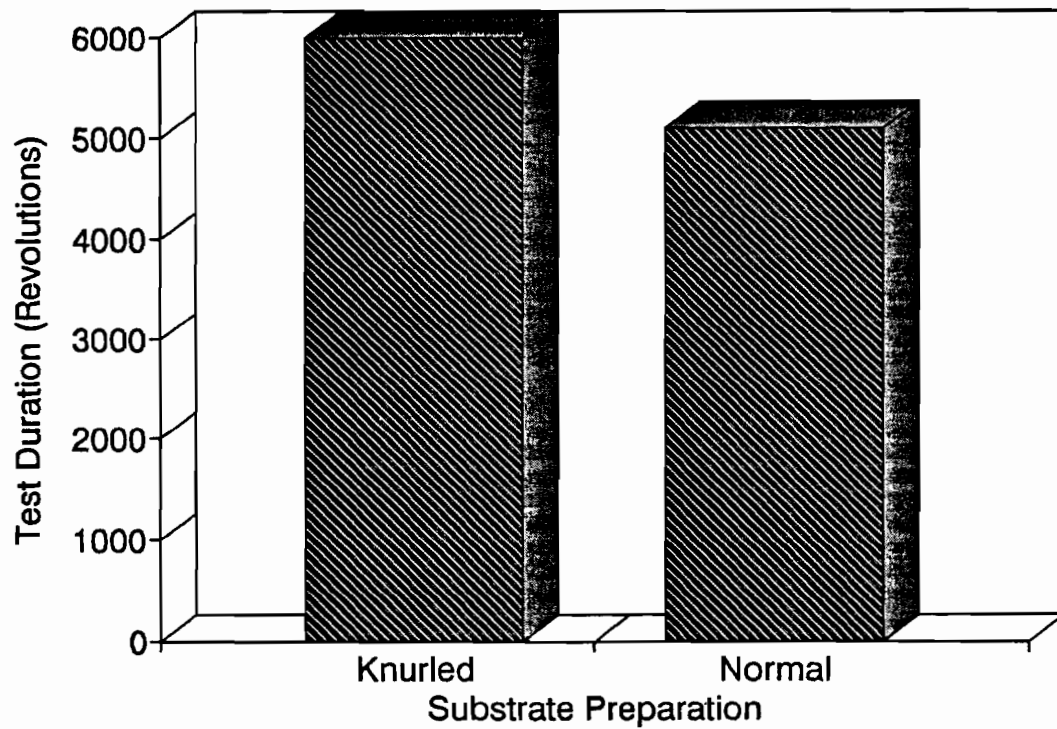


Figure 4.39. Knurling did not significantly improve the resistance to type I debonding.

| Test No. AMST | Wire | Contact Pressure | Creepage | Steel Bottom | Test Conditions | Coating Thickness | Parameter Set | Wear Rate Top | Bottom | Debond | Test Length |
|------------------|-----------|---------------------|----------|-----------------|--------------------|----------------------|------------------|------------------|--------|--------|----------------|
| 97 | 1080 1/16 | 1220 | 34 | W-9 | DGF | 0.35 | 230/30/225 | 386 | 8 | yes | 4770 |
| 98 | 1080 1/16 | 1220 | 33 | W-9 | DGF | 0.63 | 230/30/225 | 423 | 5 | yes | 2900 |
| 99 | 1080 1/16 | 1220 | 33 | W-9 | DGF | 0.56 | 230/30/225 | 392 | 6 | yes | 2220 |
| 100 | 1080 1/16 | 1220 | 33 | W-9 | DGF | 0.58 | 230/30/225 | 435 | | | 6000 |
| 101 | 1080 1/16 | 1220 | 33 | W-9 | DGF | 0.55 | 230/30/225 | 398 | | | 6000 |
| 102 | 1080 1/16 | 1220 | 32 | W-9 | DGF | 0.90 | 230/30/225 | 277 | 6 | | 6000 |
| 103 | 1080 1/16 | 1220 | 32 | W-9 | DGF | 0.88 | 230/30/225 | 480 | 4 | | 6000 |
| 104 | 1080 1/16 | 1220 | 32 | W-9 | DGF | 0.88 | 230/30/225 | 514 | 4 | yes | 3870 |
| 105 | 1080 1/16 | 1220 | 32 | W-9 | DGF | 0.91 | 230/30/225 | 589 | 5 | yes | 3050 |
| 106 | 1080 1/16 | 1220 | 31 | W-9 | DGF | 0.99 | 230/30/225 | 555 | | | 6000 |
| 107 | 1080 1/16 | 1220 | 33 | W-9 | DAS | 0.71 | 230/30/225 | | | yes | 460 |
| 108 | 1080 1/16 | 1220 | 33 | W-9 | DAS | 367.00 | 230/30/225 | | | yes | 740 |
| 109 | 1080 1/16 | 1220 | 33 | W-9 | DAS | 0.65 | 230/30/225 | | | yes | 230 |
| 110 | 1080 1/16 | 1220 | 33 | W-9 | DAS | 0.65 | 230/30/225 | | | yes | 200 |
| 111 | 1080 1/16 | 1220 | 33 | W-9 | DAS | 0.65 | 230/30/225 | | | yes | 370 |
| 112 | 1080 1/16 | 1220 | 35 | W-9 | DAS | 0.84 | 230/30/225 | | | yes | 1530 |
| 113 | 1080 1/16 | 1220 | 35 | W-9 | DAS | 0.83 | 230/30/225 | 312 | 7 | yes | 5010 |
| 114 | 1080 1/16 | 1220 | 35 | W-9 | DAS | 0.82 | 230/30/225 | 371 | 10 | yes | 3450 |
| 115 | 1080 1/16 | 1220 | 35 | W-9 | DAS | 0.83 | 230/30/225 | | | | 7740 |
| 116 | 1080 1/16 | 1220 | 35 | W-9 | DAS | 0.81 | 230/30/225 | | | yes | 4380 |
| 117 | 1080 1/16 | 1220 | 35 | W-9 | DAS | 0.96 | 230/30/225 | 663 | 11 | | 6000 |
| 118 | 1080 1/16 | 1220 | 35 | W-9 | DAS | 0.84 | 230/30/225 | 458 | 7 | yes | 3300 |
| 119 | 1080 1/16 | 1220 | 35 | W-9 | DAS | 0.89 | 230/30/225 | | | yes | 1620 |
| 120 | 1080 1/16 | 1220 | 35 | W-9 | DAS | 0.90 | 230/30/225 | | | yes | 1700 |
| 121 | 1080 1/16 | 1220 | 34 | W-9 | DAS | 1.05 | 230/30/225 | 770 | 7 | yes | 4290 |
| 122 | 1080 1/16 | 1220 | 32 | W-9 | DAS | 1.46 | 230/30/225 | 398 | 14 | | 6000 |
| 123 | 1080 1/16 | 1220 | 32 | W-9 | DAS | 1.42 | 230/30/225 | 508 | 7 | yes | 5090 |
| 124 | 1080 1/16 | 1220 | 33 | W-9 | DAS | 1.23 | 230/30/225 | 351 | 20 | yes | 5510 |
| 125 | 1080 1/16 | 1220 | 33 | W-9 | DAS | 1.30 | 230/30/225 | 408 | 16 | | 6000 |
| 126 | 1080 1/16 | 1220 | 36 | W-9 | DAS | 0.71 | 230/30/225 | | | yes | 1000 |
| 127 | 1080 1/16 | 1220 | 37 | W-9 | DAS | 0.70 | 230/30/225 | 519 | 7 | | 6000 |
| 128 | 1080 1/16 | 1220 | 37 | W-9 | DAS | 0.69 | 230/30/225 | 512 | 5 | yes | 4470 |
| 129 | 1080 1/16 | 1220 | 37 | W-9 | DAS | 0.67 | 230/30/225 | 354 | 26 | yes | 2000 |
| 130 | 1080 1/16 | 1220 | 37 | W-9 | DAS | 0.74 | 230/30/225 | | | | |
| 131 | 1080 1/16 | 1220 | 36 | W-9 | DAS | 0.75 | 230/30/225 | 320 | 13 | | 6100 |
| 132 | 1080 1/16 | 1220 | 35 | W-9 | DAS | 375.00 | 230/30/225 | 465 | 9 | | 2630 |
| 133 | 1080 1/16 | 1220 | 38 | W-9 | DAS | 0.34 | 230/30/225 | 535 | | | 4000 |
| 134 | 1080 1/16 | 1220 | 33 | W-9 | DAS | 1.31 | 230/30/225 | | | yes | 1050 |
| 135 | 1080 1/16 | 1220 | 33 | W-9 | DAS | 1.24 | 230/30/225 | | | yes | 4760 |
| 136 | 1080 1/16 | 1220 | 33 | W-9 | DAS | 1.25 | 230/30/225 | | | yes | 2150 |
| 137 | 1080 1/16 | 1220 | 33 | W-9 | DAS | 1.26 | 230/30/225 | 469 | | | 6000 |
| 138 | 1080 1/16 | 1220 | 33 | W-9 | DAS | 1.35 | 230/30/225 | | | yes | 1270 |
| 139 | 1080 1/16 | 1220 | 37 | W-9 | DAS | 0.61 | 230/30/225 | 492 | 10 | | 6000 |
| 140 | 1080 1/16 | 1220 | 37 | W-9 | DAS | 0.61 | 230/30/225 | 583 | 5 | | 6000 |
| 141 | 1080 1/16 | 1220 | 37 | W-9 | DAS | 0.61 | 230/30/225 | 611 | 4 | | 6000 |
| 142 | 1080 1/16 | 1220 | 37 | W-9 | DAS | 0.61 | 230/30/225 | 596 | 5 | | 6000 |
| 143 | 1080 1/16 | 1220 | 37 | W-9 | DAS | 0.65 | 230/30/225 | 486 | 5 | | 6000 |
| 144 | 1080 1/16 | 1220 | 35 | W-9 | DAS | 1.08 | 230/30/225 | | | yes | 30 |
| 145 | 1080 1/16 | 1220 | 34 | W-9 | DAS | 1.22 | 230/30/225 | 357 | | | 6000 |
| 146 | 1080 1/16 | 1220 | 34 | W-9 | DAS | 1.23 | 230/30/225 | 384 | 3 | | 6000 |
| 147 | 1080 1/16 | 1220 | 34 | W-9 | DAS | 1.09 | 230/30/225 | 613 | 4 | | 6000 |
| 148 | 1080 1/16 | 1220 | 34 | W-9 | DAS | 1.12 | 230/30/225 | | | | 5970 |
| 149 | 1080 1/16 | 1220 | 34 | W-9 | DAS | 1.20 | 230/30/225 | 459 | 61 | | 6000 |
| 150 | 1080 1/16 | 1220 | 34 | W-9 | DAS | 1.18 | 230/30/225 | 742 | 4 | | 6000 |
| 151 | 1080 1/16 | 1220 | 34 | W-9 | DAS | 1.18 | 230/30/225 | | | yes | 3400 |
| 152 | 1080 1/16 | 1220 | 34 | W-9 | DAS | 1.10 | 230/30/225 | | | yes | 5850 |
| 153 | 1080 1/16 | 1220 | 34 | W-9 | DAS | 1.19 | 230/30/225 | | | | 2440 |
| 154 | 1080 1/16 | 1220 | 35 | W-9 | DAS | 1.07 | 230/30/225 | 606 | 11 | | 6000 |

Figure 4.40. Overview of AMST97-154.

4.8 Debonding Results, Lubricated.

The lubrication test matrix, AMST45-59, showed a higher incidence of debonding. Of these 15 tests, 14 were of coated rollers. 11 of the 14 debonded, and the one of those that didn't debond was performed at zero creep. Figure 4.41 shows the lubricated test matrix of debonded coatings.

Debonding incidence was very high during early lubricated testing, however some data were gathered before the debonding. Some of the tests reported were from this group, as can be determined by the relatively short test duration, see Figure 4.42. These rollers were sprayed under optimum parameters to different coating thicknesses. Notice that the retained lubricant is somewhat greater for the first iteration. This is because the roller in the as sprayed condition is much rougher and will accept more lubricant. The revolutions per interval are not very linear, even with approximately the same amount of lubricant each interval.

The wear rates of all lubricated tests fall into a fairly narrow band, Figure 4.43, showing the same basic trend as the dry tests.

Further lubricated wear testing was done after the failure mechanisms were identified in the dry test conditions. Substrate preparation techniques were improved to the point that type I debonding was reduced to a very small percentage of occurrences. It was thought appropriate to run another test series of lubricated rollers using coatings sprayed under optimized substrate preparation and coating deposition.

The results of this test matrix did not differ significantly from that reported in the earlier round of testing. The lubricant used and the number of revolutions run from each test interval is approximately the same. In this series debonding occurred early in each test, with only one test going as long as 6 intervals, and this test was under a low contact pressure, 700 MPa. Figures 4.44 and 4.45 show the results of this series, AMST175-183. The series is divided into two groups, 5% and 35% slide/roll ratios. All of the 5% group debonded, the longest test debonding early into the 4th interval.

The roller selected for dry testing from this group tested without debonding for the full dry test length of 6,000 revs. Figure 4.46 shows that this roller fits in every way the pattern shown to be typical of a successful dry wear test. This shows that the process of specimen preparation was not faulty, but that the debonding is actually a function of the coating itself and the Amsler test conditions.

A water-lubricated roller was tested to try to observe edge effect occurrence. Failure occurred at 4890 revolutions. The Amsler machine was stopped before the coating was thrown off the substrate, however there was a short section of coating debonded, see figure 4.47. This photograph shows that the wear track of this coating had significant edge effects, especially at the crack site, and the diameter reduction 0.3 mm was enough for edge effects to occur. This diameter reduction is not nearly as much as a dry roller would have after this many revolutions, see figure 4.46, however it is more than grease lubricated rollers. This would be expected when comparing friction coefficients of the three conditions, 0.1 for grease lubrication (before the grease begins to

disappear), 0.26 for water lubrication, and 0.46 during dry testing.

Debonding: Lubricated Tests 1220 MPa 35% Slide Roll

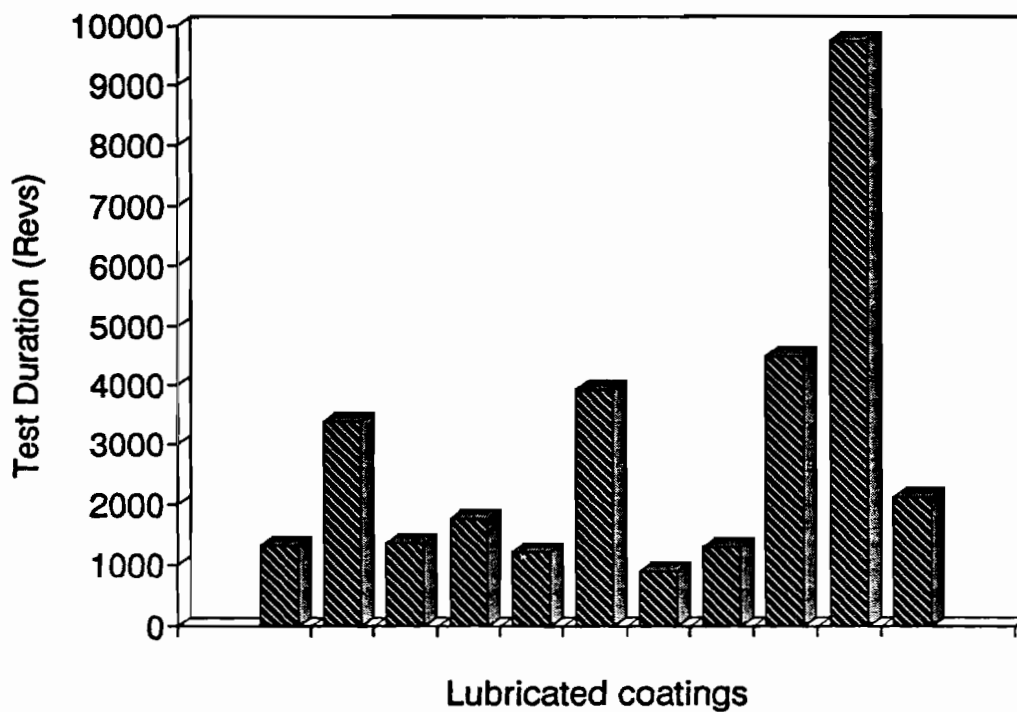


Figure 4.41. Very high debonding incidence of lubricated coatings. Wear rates and test duration.

Lube Tests

1220 MPa 35% Slide/Roll

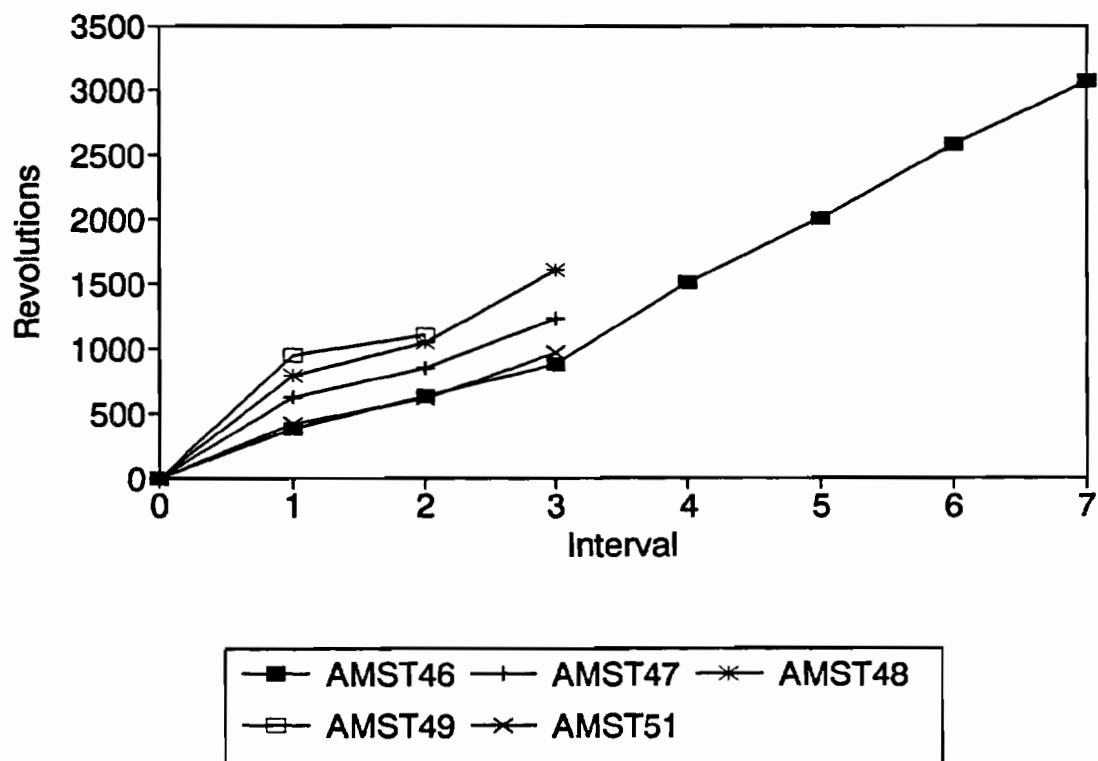


Figure 4.42. AMST4651. Most tests were of short duration.

Lube Tests

1220 MPa 35% Slide/Roll

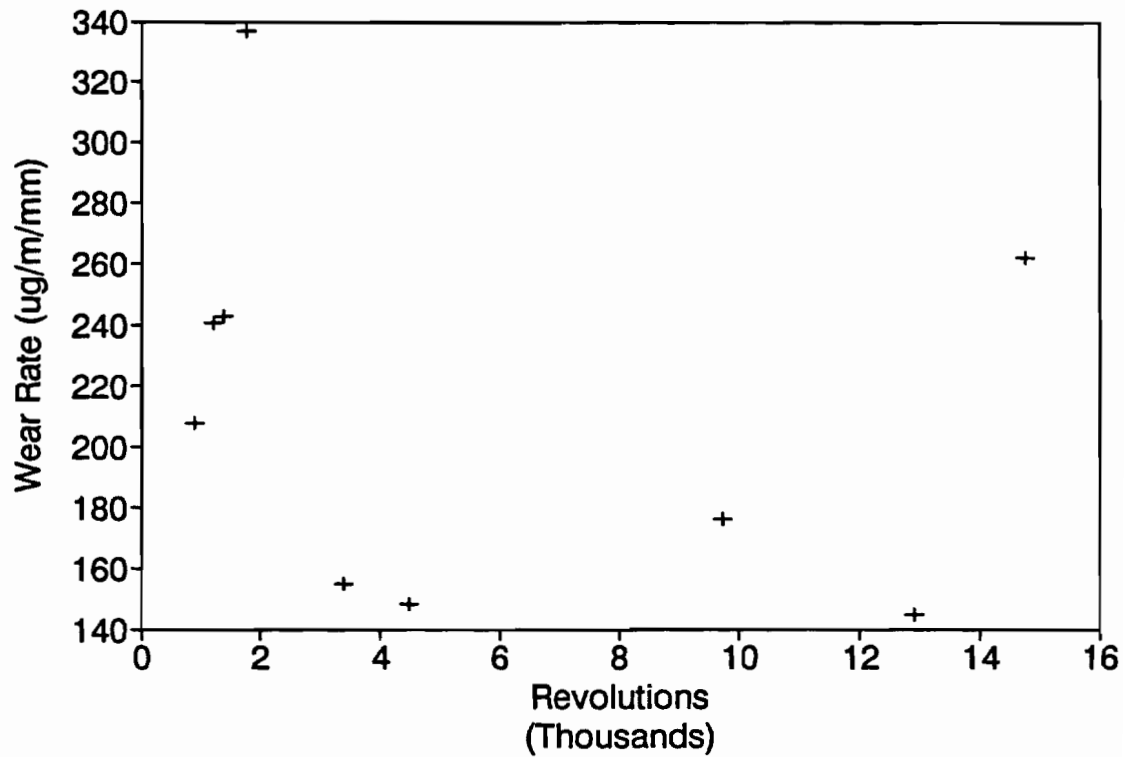
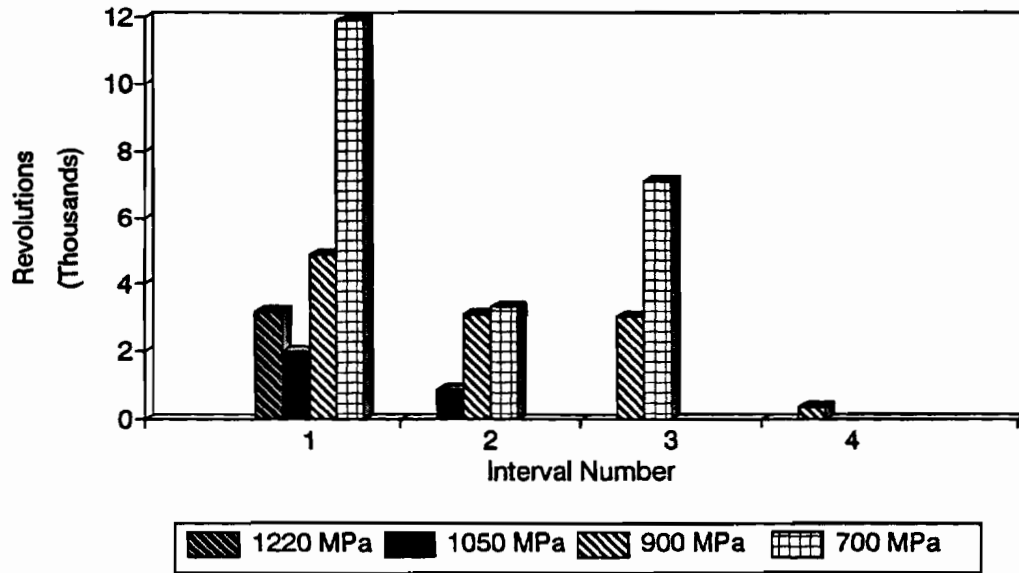


Figure 4.43. Wear rates of lubricated tests fall within an expected range.

Summary Lubricated Wear Tests: 5% Slide/Roll



Summary Lubricated Wear Tests: 5% Slide/Roll

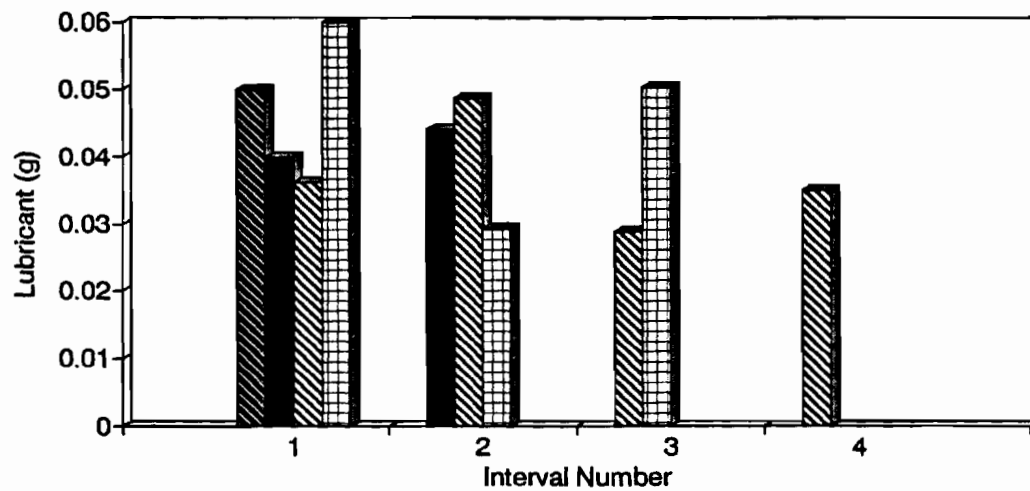
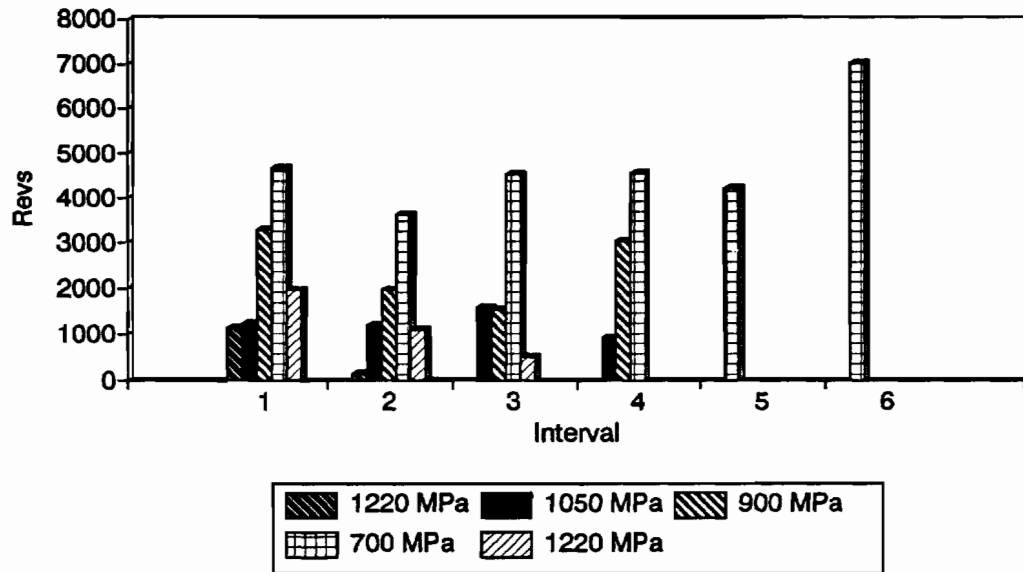


Figure 4.44. Lubrication tests. 5% slide/roll. a. revolutions per interval. b. Retained lubricant per interval.

Summary Lubricated Wear Tests: 35% Slide/Roll



Summary Lubricated Wear Tests: 35% Slide/Roll

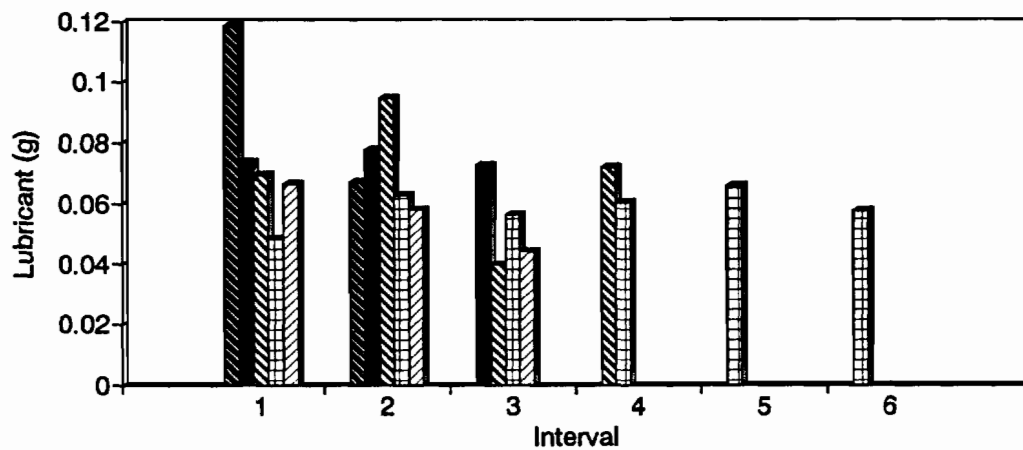


Figure 4.45. Lubrication tests. 35% slide/roll. a. revolutions per interval. b. Retained lubricant per interval.

| | |
|---------------------------------|---------------|
| Amsler Test No.: | AMST184 |
| Wire: | 1080 1/16 |
| Contact Pressure (MPa): | 1220 |
| Creepage (%): | 36 |
| Motor Speed (RPM) | 200 |
| Coating Thickness (mm): | 0.69 |
| Loading (N): | 1995 |
| Friction Coefficient (typical): | 0.46 |
| Test Condition: | DAS |
| Parameter Set: | Z30/30/225/90 |
| Disk File: | AMST184 |

| | Steel No. | Roller Dimensions | | WEAR RA g/rev | Top | Bottom |
|--------|-----------|-------------------|--------------|---------------|-----------|-----------|
| | | Width(mm) | Diameter(mm) | | 0.0002102 | 1.063E-05 |
| Top | X-95 | | 34.77 | ug/m | 1924 | 75 |
| Bottom | W-3 | 5 | 45.19 | ug/m/mm | 385 | 15 |

Test run without stopping for 6,000 revs.
 Roller was from same group as lubricated series.
 Edge effects on both sides at test end.
 One area of ee was broken out to substrate depth.

| Interval No. | Revoluon Reading (Bottom) | Revoluon | | Work (N/m) Net | Work (N/m) Net | Weight Top (g) | Weight Bottom (g) | Wt Loss Top (g) | Weight Loss Bottom (g) | Diameter Top (inches) | (MM) | Diameter Bottom (inches) | (MM) | Rev Per Increment |
|--------------|---------------------------|----------|--------|----------------|----------------|----------------|-------------------|-----------------|------------------------|-----------------------|-------|--------------------------|-------|-------------------|
| | | Top | Bottom | | | | | | | | | | | |
| 0 | 63510 | 0 | 0 | 499 | 0 | 48.0605 | 96.7270 | 0.0000 | 0.0000 | 1.3690 | 34.77 | 1.7790 | 45.19 | 0 |
| 1 | 69510 | 5435 | 6000 | 772 | 273 | 46.9183 | 96.6632 | 1.1422 | 0.0638 | 1.3410 | 34.06 | 1.7770 | 45.14 | 5435 |

Figure 4.46. AMST184. Dry wear test of a roller from the same group as the lubricated tests has been run to full dry wear test duration.

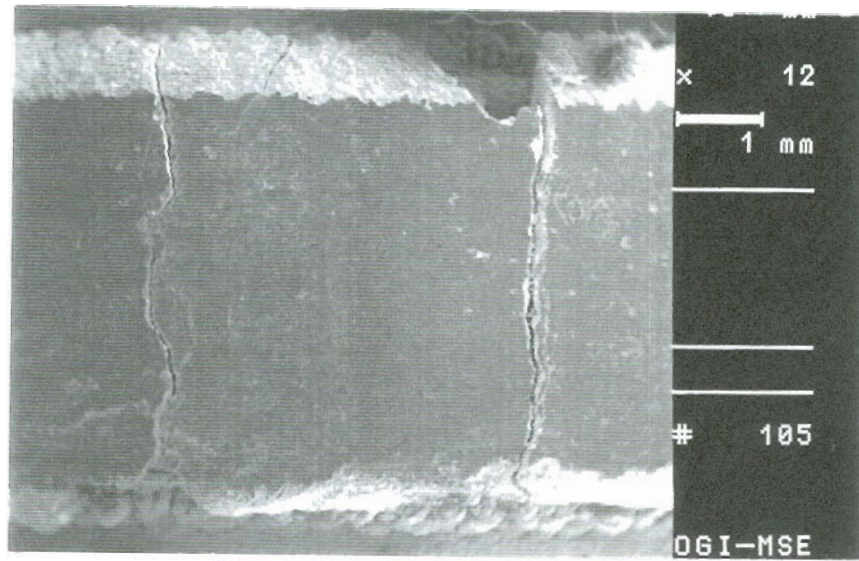


Figure 4.47. AMST174. Water lubricated coating failed after 4890 revolutions.

4.9 Intermediate Layers.

Some work was done to evaluate the effect of using an intermediate Nickel/Chromium layer between the steel coating and the substrate, AMST159-161 and AMST167-170. Figure 4.48 shows the durations of these tests. One roller, AMST160, was made with a Ni-Cr layer of 0.38mm thickness. This coating failed almost immediately and it was determined that the intermediate layer was too thick. The other rollers had a 0.1mm Ni-Cr layer. Two rollers, AMST159 and AMST161, ran to a full 6,000 revolution test, however the others failed because of type II debonding. Note that the wear rates of these two full tests fell into the expected range of 200 to 700 ug/m/mm. The use of an intermediate layer did not improve the debonding problem. Here again, as long as the thickness of the layer was not excessive, no type I debonding and substantial type II debonding can be expected.

Debonding Study 1220 MPA 35% Slide/Roll

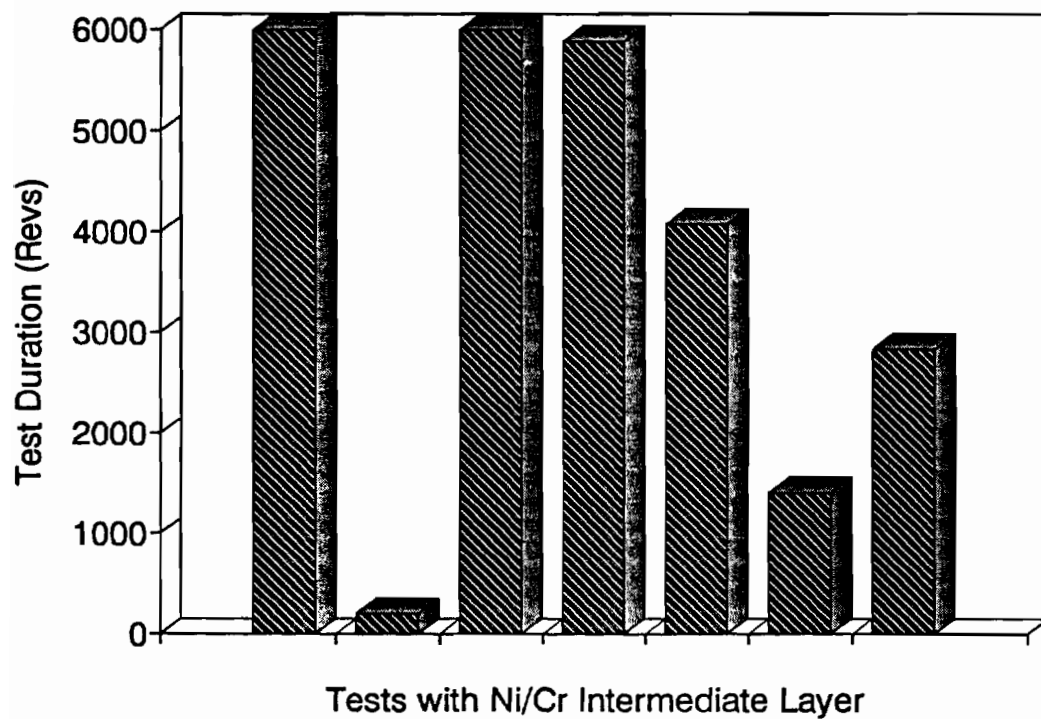


Figure 4.48. Test duration using a NiCr intermediate layer.

CHAPTER FIVE

5.0 DISCUSSION

5.1 Debonding

5.1.1 Bonding And Surface Preparation.

Debonding is a problem that has caused much discussion and experimentation in this research. The debonding in question occurs at the substrate/coating interface. It occurs most frequently under lubricated conditions, but is still a consideration for dry testing. Two effects are thought to be the main causes of this problem. One is the location of the zone of maximum shear in the depth of the coating. If this zone approaches the interface, this added shear force could influence the mechanical bond strength at the interface. Second is the quality of the mechanical bond. Surface preparation before spraying is the key to maximizing the mechanical bond. Surfaces were cleaned with soap and water, washed with acetone, grit blasted with steel shot, rewashed in acetone, placed in the

spraying fixture and sprayed. As short a time as possible is allowed between the grit blast and spraying to reduce the oxide formation on the substrate, usually about five minutes. This procedure evolved to include a second shotblasting and an acetone flood wash immediately before spraying. This eliminated the time lag between shotblasting and spraying, and the flood wash was removed with an air blast to eliminate the possibility of concentrated contaminants becoming deposited on the substrate during evaporation of the acetone.

The grit blasting roughens the surface allowing a strong mechanical bond when the spray particles are introduced to the substrate. A similar bond occurs between the particles as the coating thickness builds. Seldom does an interlamellar failure occur, most often the failure is at the substrate interface.

Knurling of the substrate has been tried with some success, although the roughening by this method might be considered a macro-roughening when compared with grit blasting. Testing showed that knurling did not achieve the desired result, in fact was more or less a non-factor in coating adhesion. Knurling is too coarse of a surface roughening to be effective. Also knurling is a surface deformation process rather than a material removal process. The force of the knives into the surface makes the surface finish of the indented areas very smooth, and it is very difficult to roughen these areas so that a good mechanical bond can occur. Silica, with its fine grit size, was tried as a blasting medium for this reason, but the surface finish that resulted was not rough enough over the rest of the surface for good bonding to occur. Even with this fine grit medium, the bottom of the knurl channel remains very smooth.

Figure 5.1 shows a tightly bonded coating/substrate interface. This specimen was etched to show this interface more clearly. Figure 5.2 shows an interface that has been knurled and shotblasted. Both of these photos show a tightly bonded interface region. Figure 5.3 shows a crack formed at the interface. This is from a coating that debonded almost immediately upon starting a dry wear test. The debonding was partial, retaining a small part of the coating on the substrate, which was sectioned and polished for this specimen.

Figure 5.4 shows porosity formation in a small region at the interface, making a potential debonding site. This coating, however, was successfully wear tested dry. Figure 5.5 shows extensive debonding damage near the interface. In this case the crack ran for a short distance interlamellarly, slightly above the coating/substrate interface. There also is a vertical crack to the surface, although it is not clear whether the crack originated at the interface or at the surface.

Figure 5.6 shows damage zones. In this extreme case there is a damage zone rather than a single crack. This is a section of coating that fully debonded. Some opening of the cracks occurred during specimen mounting.

It is possible for the debonding to occur at lamellar interfaces within the coating, a cohesive failure, this type of failure was not observed. When interlamellar separation has occurred it has nearly always been very near the coating/substrate interface, and then only for short distances, as was seen in the previous photos.

The bonding between coating and substrate, also between individual splats during coating formation, is largely

mechanical. Bond quality is determined by the degree of tooth between the splats and the substrate. It is necessary for the incoming particles to be molten or nearly molten upon impact to allow spreading, and the impact velocity to be high to achieve penetration. Surface roughening and cleanliness is required for mechanical bonding to occur.

Much progress was been made in this area, however the search for better techniques leading to improvement in substrate/coating bonding is a subject recommended future research.



Figure 5.1. Coating tightly bonded to substrate. Etched photo. 400x.

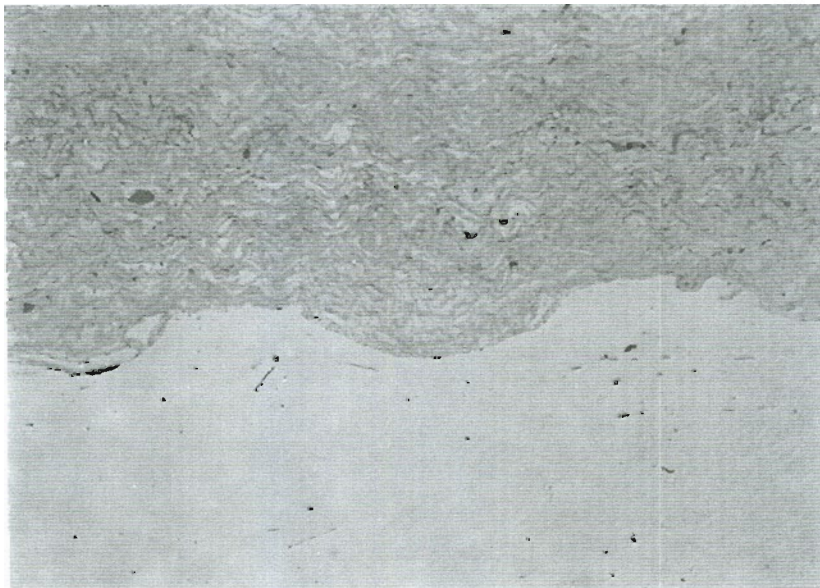


Figure 5.2. Knurled interface. 50x.

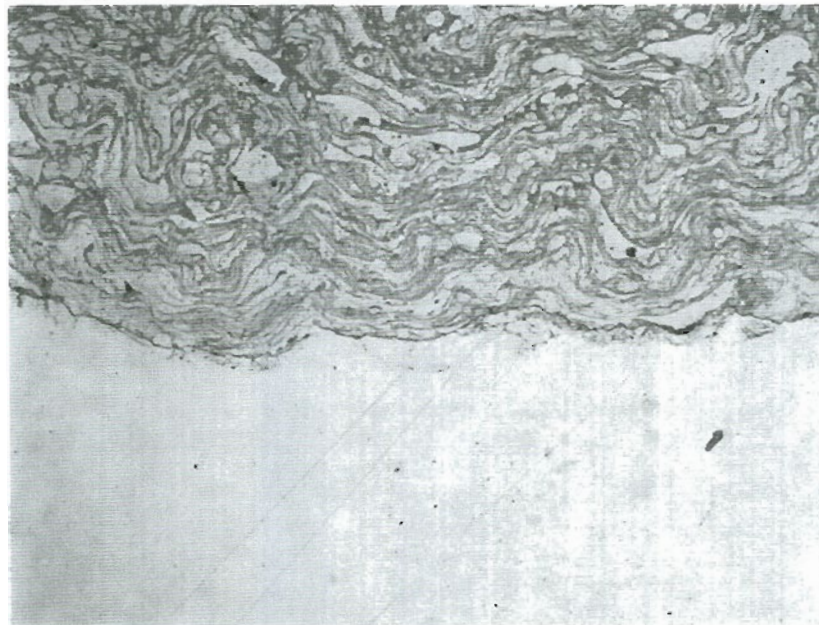


Figure 5.3. Crack formed at the coating/ substrate interface. 200x.

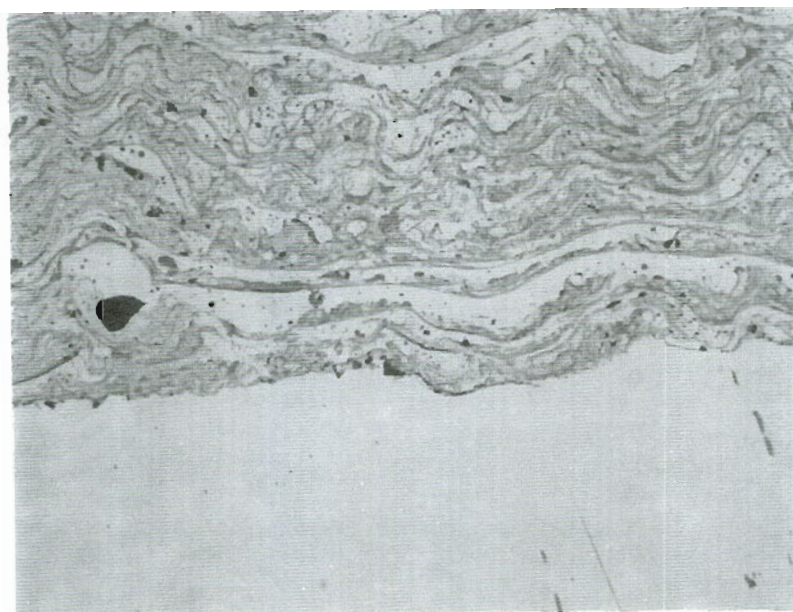


Figure 5.4. Porosity concentrated at the interface. 400x.

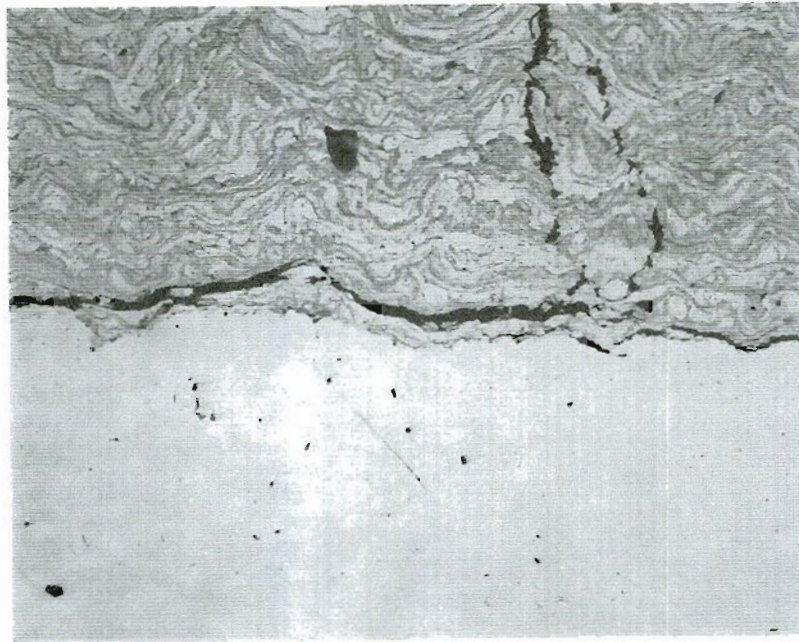


Figure 5.5. Extensive debonding damage at and near the interface. 200x.

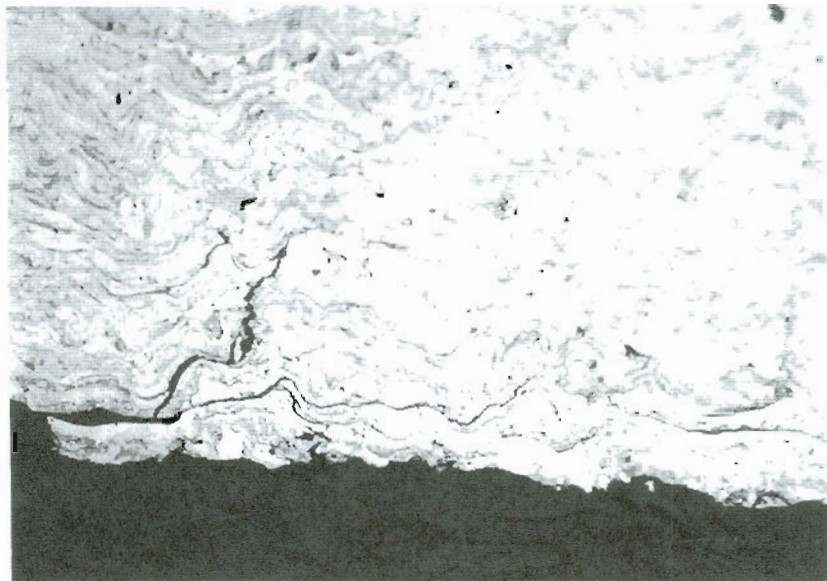


Figure 5.6. Damage zone in the debonded area. 200x.

5.1.2 Debonding Mechanisms.

It has been shown that debonding can occur by two distinct mechanisms. Type I is the separation of coating from the substrate by failure initiating at the coating/substrate interface. Type II is initiated by the loss of material at the surface, at the edge of the wear track. As the edge effects become more pronounced, loss of coating can occur within the wear track, compromising coating integrity in the wear track. A crack can occur, initiating in the edge effect, and extend to the substrate. Under load this crack can grow across the wear track and coating failure occurs. The end result of Type II failure looks very much like Type I failure, with sections of coating having lifted from the substrate, more or less intact.

It is very difficult to determine the active mechanism after failure occurs. Wear tests are run at high contact pressures, up to 1220 MPa, and slide/roll ratios, up to a nominal 35%. When failure occurs it is not possible to stop the Amsler machine instantaneously, at least one revolution will occur before stopping even under ideal conditions, and more likely three or four. After the initial failure occurs, additional damage happens before shutdown. More coating is removed, the substrate in the site of the initial debonding is damaged by rolling, the coating segment being removed can be broken into smaller pieces or damaged in other ways. Often the coating is straightened during this process instead of popping off with its natural curved shape, that following the shape of the roller.

If the wear test could be stopped immediately upon failure, one could expect to see some differences in the coatings relative to the failure mechanism. Type I debonding might show

longer segments of coating that have separated intact from the substrate. Few edge effects would be present, and those would be small, with coating loss occurring from the wear track edge extending away from the wear track and not very deep. Type II debonding would likely show short segments of coating removed. The edges of the wear track would appear to have lost material in such a way as to encroach upon the wear surface. This usually occurs in an irregular manner, so the entire edge may not be involved, but in the areas where it is the appearance is that of an erose edge.

Type I debonding usually occurs early during the wear test, usually within the first 1,000 revolutions. Type II debonding usually occurs after 2,000 revolutions. This statement is true only if all spraying conditions are optimum. Spray parameter adjustments or substrate preparation lapses will cause both types of failures, or other failures that result in the coating coming off the substrate. For example coating froth, caused by incoming particles impacting a molten surface, causes the coating to appear to be crushed during testing, with only very short segments of coating, if any, coming off intact.

5.2 Type I debonding

5.2.1 General Description

The appearance of a type I debond is shown in Figure 5.7. In this case the failure occurred while the roller was being turned by hand to check for edge effects. This coating had 1,000 revolutions at time of failure. The behavior of the coating is to want to lift straight up and peel off. Note that one side of the break is tightly bonded. Figure 5.8 is another case of type I debond. Note that there are no edge effects visible, but some

material loss on the vertical wall (respective to incidence of spray) of the roller. This roller also had approximately 1,000 revolutions before failure. Optical and SEM examination show that debonding does occur at the interface, with only very small regions failing at coating lamellae interfaces, see Figure 5.9.

Interfacial debonding is usually caused by improper or incomplete substrate preparation. The rollers after machining are finished to a smooth surface. This surface must be roughened because the primary bonding of coating to substrate is that of mechanical bonding. Smooth surfaces will not bond the coating, especially under loaded conditions, and the coating will fail very quickly. Surface oxides must also be removed before coating. Both roughening and oxide removal is accomplished by shot blasting the roller before spraying. The roller is thoroughly blasted in a special cabinet a few minutes before spraying. A secondary shotblasting is performed, followed by an acetone flood wash to remove contaminants, immediately before spraying. The secondary blasting serves to remove any late-forming oxides.

Appropriate measures in substrate preparation reduced the incidence of type I debonding. The failure where it is very difficult to tell if it is of type I or type II may well be a combination of the types. If a severe edge effect should coincide with an area on the interface that is imperfectly bonded, it would certainly accelerate failure. There are conditions where this is the likely cause of debonding. In failures occurring during the approximately 1,000 to 2,000 revolutions region, where edge effects are minor or at worst moderate, the failure frequently shows aspects of both type I and type II. Long sections are debonded and edge effects are present, but with little or no encroachment onto the wear track.

This does presume specimens prepared using optimum spray conditions.

Early in the research another type of coating failure was observed. In this case the geometry of the specimen was that of spraying onto a 10mm wide Amsler specimen without the top hat geometry. The wire sprayed was a 1075 flux cored wire. This was a thin coating, on the order of 0.3mm, wear tested against a normal wheel steel bottom roller with the top hat profile. Figure 5.10 shows delamination in the form of a blister, where the surrounding area remained tightly bonded. Figure 5.11 shows a blister and delamination of much of the surrounding area. Both of these rollers were not prepared in what later became the standard for substrate preparation. Machining grooves are visible in the second photo and only a very light texture is shown on the substrate in the other photo. These photographs graphically show the importance of proper substrate preparation.

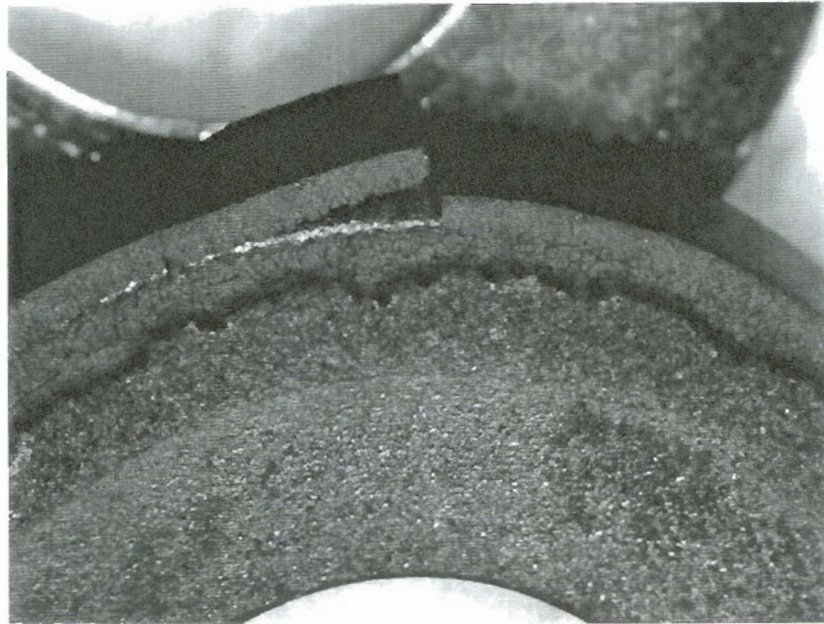


Figure 5.7. Type I debond. 5x.

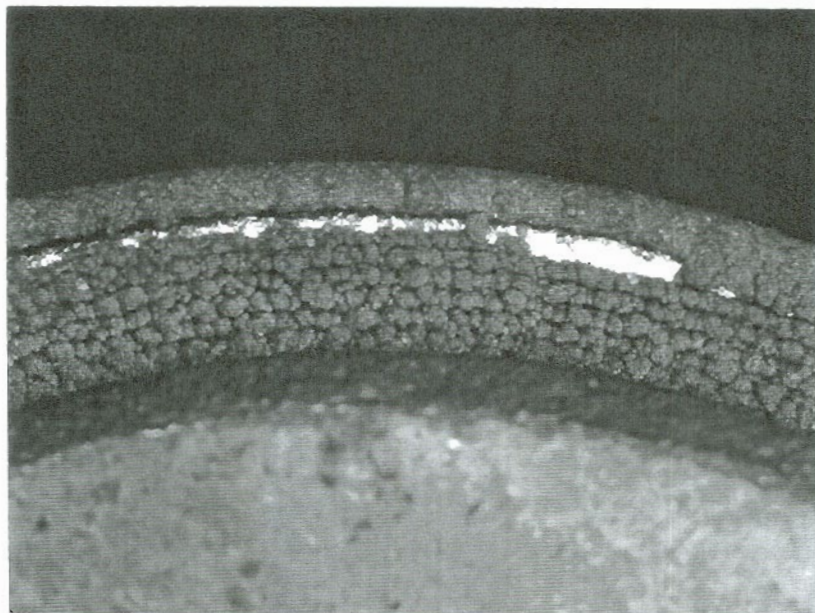


Figure 5.8. Type I debond. 10x.

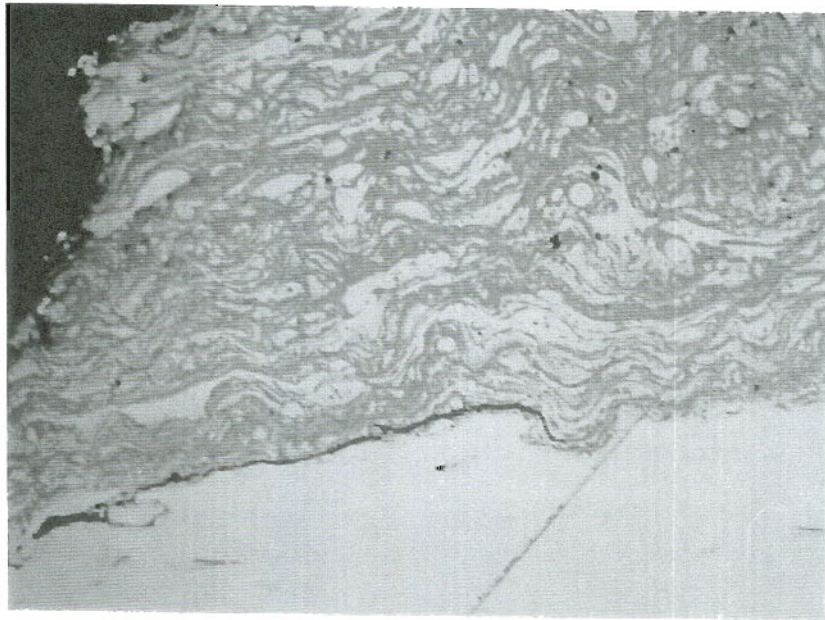


Figure 5.9. Delamination is at the coating/substrate interface with only short sections at lamellar interfaces. 300x.

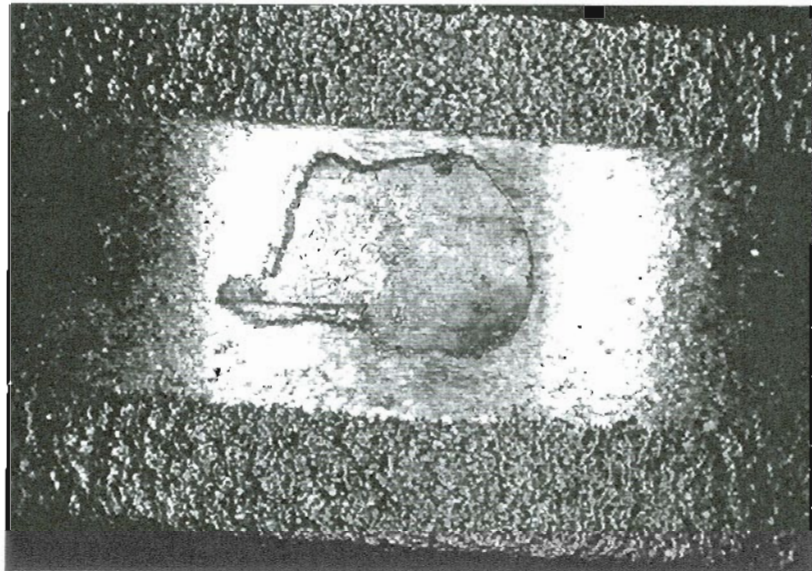


Figure 5.10. Delamination caused by a blister in wear track. 8x.

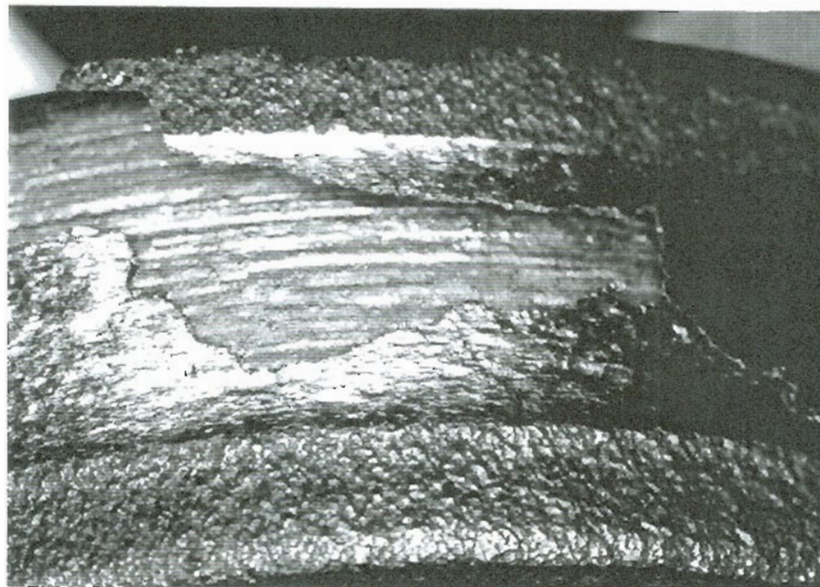


Figure 5.11. Blister and delamination of much of the surrounding area. 8x.

5.2.2 Type I Debonding Characteristics

When type I debonding occurs there is a tendency for long sections of coating to lift off the substrate. The coating seems to be strong in every other way, but it can be easily removed (after cracking) by lifting with a fingernail. This seems to imply that the mechanical bond is inadequate in the outward direction. Most of the forces under loading are compressive forces, and the coating bond handles very high compression well, shear forces less well, and tensile forces not well at all.

Debonding has been a major problem during the lubricated wear tests, more than in the dry condition. One possible influence is the change in location of the zone of maximum shear stress between these two types of tests. In the dry tests, the friction is much greater. The greater the coefficient of friction, the closer to the surface are the maximum shear forces. In the lubricated tests the friction coefficient is lower and the zone of maximum shear moves from the surface into the depth of coating. If this zone approaches the coating/substrate interface, this added shear force may influence the bonding strength at the coating/substrate interface.

Shear forces may be high enough to cause cracking at the interface, and once that happens it can be visualized how this can be quickly become a through-thickness crack. This is manifested on the surface as a transverse crack of full coating width. When the Amsler is stopped after cracking and before material loss to debonding, the material areas at the crack want to move outward, away from the substrate, see figure 5.12. This may indicate the presence of residual stresses within the

coating that are of a tensile nature. The effect of tensile residual stresses in the coating relative to the interface would be in a shear direction.

Residual stresses may accumulate during the splat solidification process. The temperature difference between the splat and the substrate causes rapid cooling of the splat. As the splat cools it applies a compressive force on the substrate. A tensile force is applied to the splat by the substrate, see Figure 5.13.

There also may be tensile forces generated in the zone just to the rear of the contact patch under rolling/sliding loading. If this is so, it may aggravate the residual stress condition within the roller. This force may be very small relative to the shear forces and the residual stresses and so be discounted, but it is acknowledged here for discussion purposes.

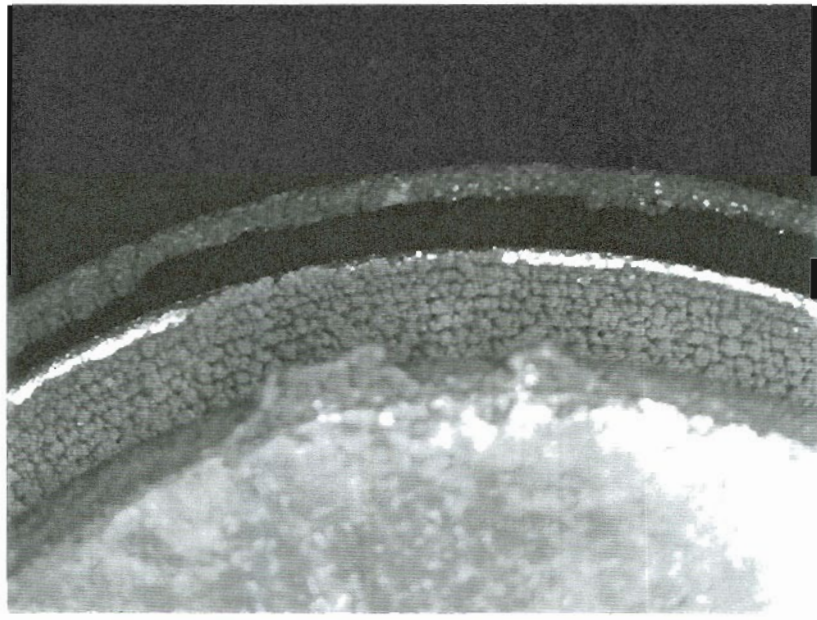


Figure 5.12. Type I debond. Coating wants to pull away from the substrate. 7.5x.

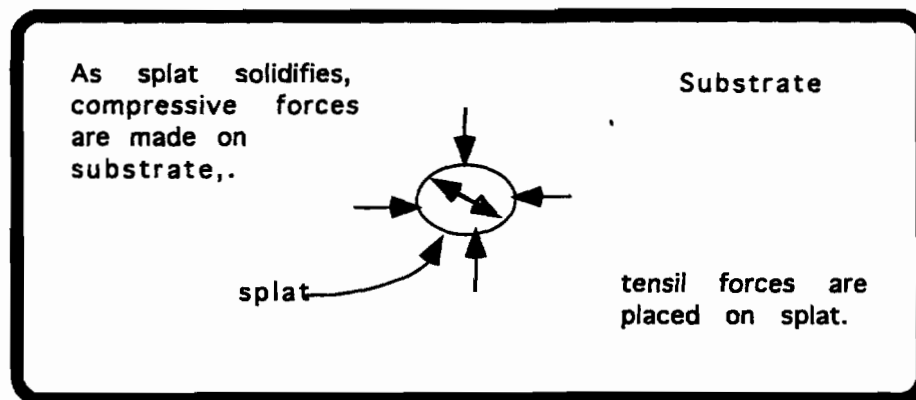


Figure 5.13. A tensile force is placed on the substrate as the splat cools.

5.3 Edge effects.

An edge effect is a piece of coating material lost during wear testing that came from an area other than the wear track and/or from a mechanism other than the wear process, see figures 5.14 & 5.15. Edge effects are the cause of several problems related to wear testing. In their most harmless state, relatively small particles removed from an area adjacent to, but not encroaching into, the wear track. Edge effects do, however, affect the data accumulated for calculating wear rates. Wear rates are determined in terms of weight loss per meter rolled per millimeter of contact width, ug/m/mm. This calculation is based on weight loss per revolution, thus any weight loss from other sources than the wear process will skew the wear rate results. Figure 5.16 shows how edge effect weight loss appears on what is otherwise a fairly linear wear rate curve. Edge effects usually become more pronounced as the test goes on because the wear track deepens into the coating. Figure 5.17 shows how the wear track deepens during the test progression, and the removal of material outside the wear track.

The upward trend at the end of the curve in figure 5.18 is a result of running this test for a long time, with the wear track depth sufficient to result in significant edge effects on a regular basis. In this test, the original coating thickness was 1mm and a final thickness of 0.25mm. When it was obvious that edge effects were distorting the true wear rate information, the test was stopped.

Edge effects are clearly visible during testing. The color of the exposed surface is lighter in appearance than the original surface. The Amsler machine operation speed is 200 rpm, too fast when operating to see anything by way of detail, but

close observation will show the appearance of edge effects early in their formation. The machine must be stopped for closer examination of the roller to determine whether the wear track has eroded, unless, of course, the wear track is grossly encroached upon, which would mean that failure is imminent. If the edge effects are very shallow, sometimes the wear track will self heal during operation. The coating wears down far enough to pass the defect without failing. This doesn't happen often, usually when some minor edge effects are introduced into the coating, more follow, and the longer the test, the more severe the edge effects. Another look at figure 5.17 will show how this is a likely scenario.

Specimen geometry is the main reason for the formation of edge effects. This research employs the standard 'top hat' Amsler roller profile in order to relate wear test results to those of uncoated rollers in earlier research⁶². This geometry poses some problems unique to spraying that have complicated the goal of achieving coatings that will perform under the slide/roll and contact pressure conditions required.

As the coating thickness increases during the spraying operation, the width of the surface sprayed also increases due to overspray. The coated surface, especially in a narrow specimen such as an Amsler roller, will have a slight crown after spraying. Both of these effects, increased width and crowning, are amplified as the coating thickness is increased, see Figure 5.19. The crown effect can be eliminated by grinding the coating flat over the wear surface, if desired. Most of the coatings have been tested in the as-sprayed condition because this is the likely condition for field use, in addition it was noted that coating performance was not improved by grinding the

surface. The crown effect was shown to have negligible influence on coating performance. The increased width is another matter.

Substrate preparation for coatings is focused on the 5mm section of the roller. However, during the spray operation there is overspray onto the shoulders of the roller. The wall of the shoulder is directly in line with the spray jet, making, in effect, a vertical surface for the incoming particles to attempt to impact upon and adhere. Probably the first ones that impact this wall are portions of larger particles that impact the very edge of the wear surface and overlap this edge, either right near the surface or will travel some distance down the vertical wall. What few particles do stick anywhere on this surface causes subsequent particles stick and bond to them rather than traveling all the way to the surface below. This causes a shadow effect in the coating, see Figures 5.20-5.22. This shadow effect causes porosity in this portion of the coating. Usually this porosity increases through the coating depth until the greatest amount is at or near the intersection of the shoulder and the vertical wall. In this condition the coating over the wear surface is very well bonded and fully supported. Porosity in this area of the coating is measured at one percent or less over a wide range of coatings. This is the area of coating that is wear tested and has been shown to successfully fulfill the requirements of this research. The overspray area is very weak, actually unsupported. This is where the edge effects are originated.

The nature of a sprayed coating is that the microstructure is lamellar its formation. If a microcrack is formed it will usually grow along the lamellar interface as long as it can, see Figure 5.23. The same is true for the occurrence of edge effects. As the wear track deepens there is a narrow ridge of

material formed outside the wear track on both sides. If the rotation of the rollers during the wear test were perfectly executed in a vertical plane, these ridges would probably be relatively undisturbed during the test operation. However under the conditions required for the test, 35% slide roll ratio, heavy accompanying contact pressures, up to 1220 MPa, and any built-in tolerance in the operation of the Amsler machine, this perfect plane cannot be achieved. Sideward pressures are placed on these ridges, causing them to chip off. This breakage is often not clean, it takes with it additional material below the ridge. The shape of the particles lost is influenced by the lamellar structure of the coating. Material is lost from the ridged area and the area under it. The coating under the ridge is poorly bonded to anything, and will not withstand much abuse. It is relatively easy for a crack to progress downward through the coating thickness at the edge of the wear track, often going to the substrate, see Figures 5.24 & 5.25. If material is lost only outside the wear track and not as deep as the interface, it is defined as a minor edge effect. Severe edge effects are those that have encroached upon the wear track or where a crack has progressed to the substrate.

Tapering of the edges before testing was tried as a way of reducing edge effects, but with negligible success. Various grinding and machining techniques were employed in an attempt to negate the geometry effect in wear test specimens with, at best, marginal results. Grinding and machining operations often introduced edge effect sites during specimen preparation, see Figure 5.26.

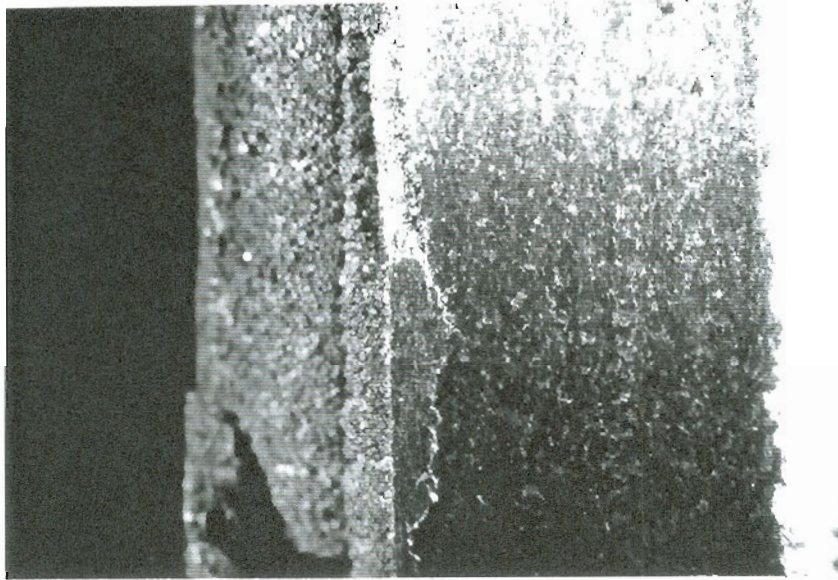


Figure 5.14. An edge effect at the edge of the wear track. 20x.

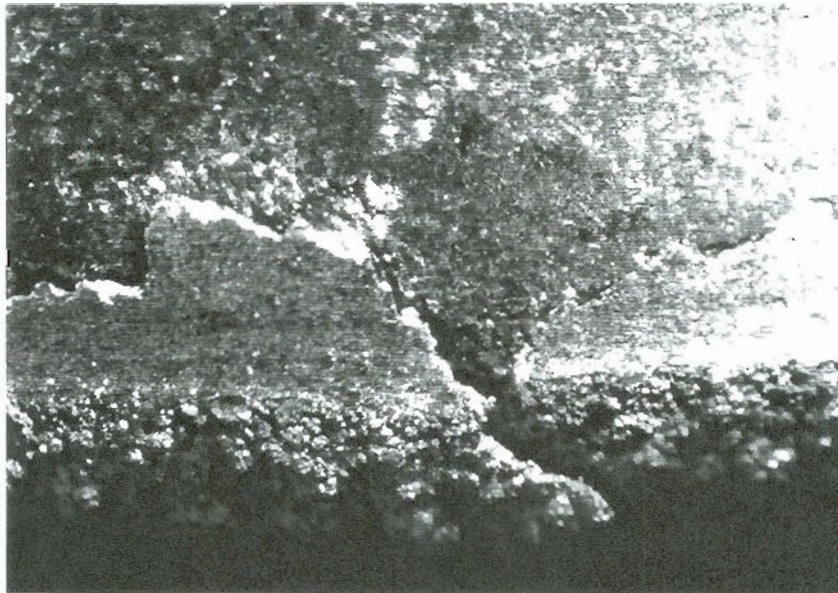


Figure 5.15. An edge effect that is ready to be thrown out of the wear track. 20x.

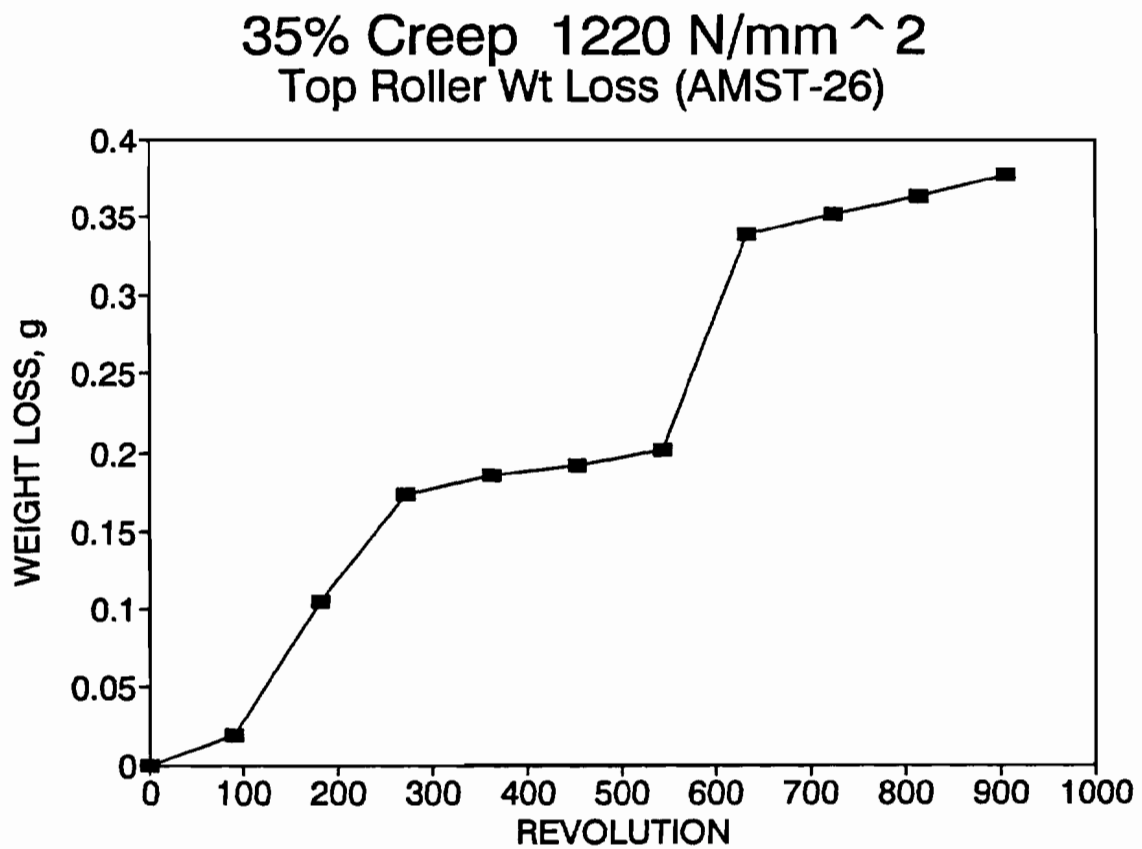


Figure 5.16. The appearance of an edge effect on the weight loss curve.

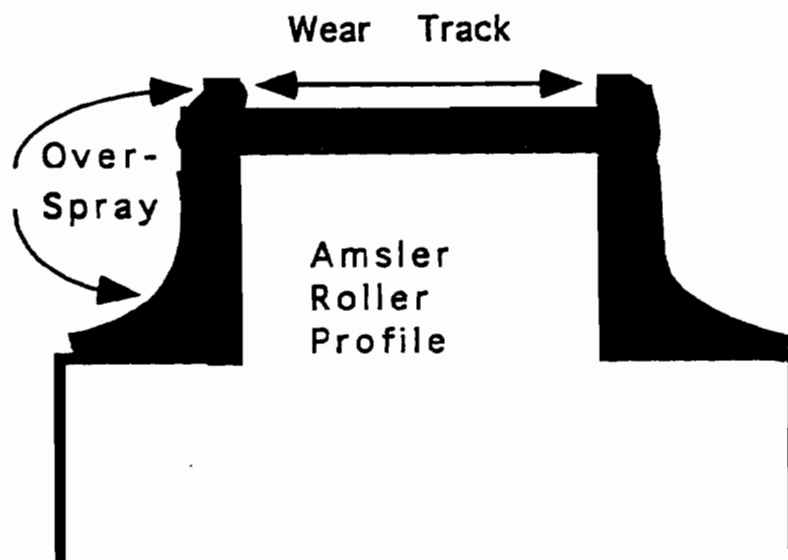
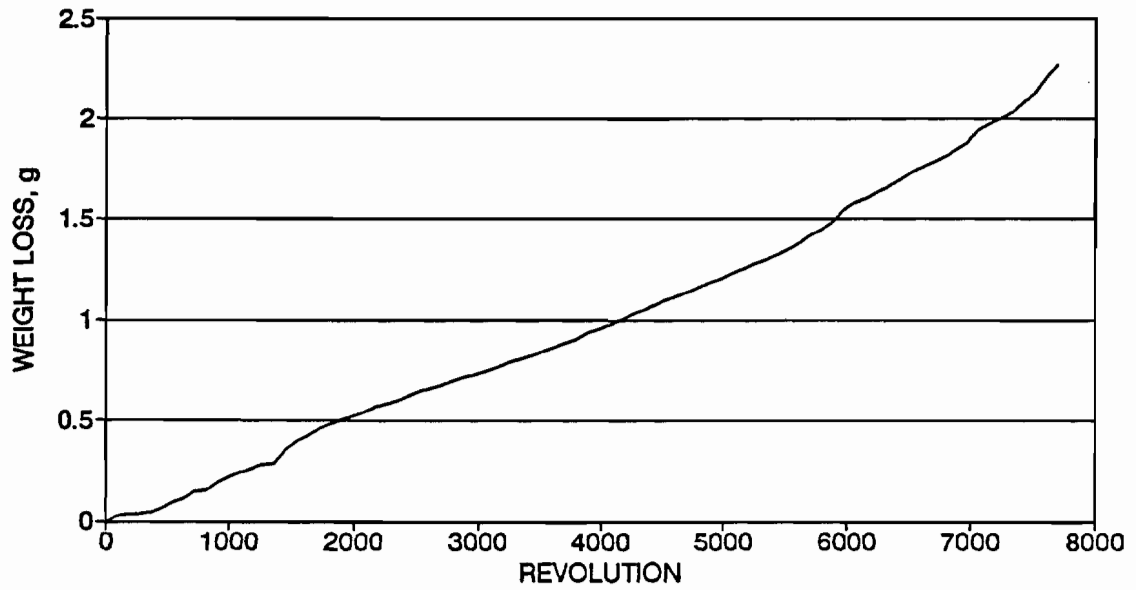


Figure 5.17. The wear track deepens as the test progresses.

36% Creep 1220 N/mm²
Top Roller Wt Loss (AMST-27)



36% Creep 1220 N/mm²
Top Roller Dia (AMST-27)

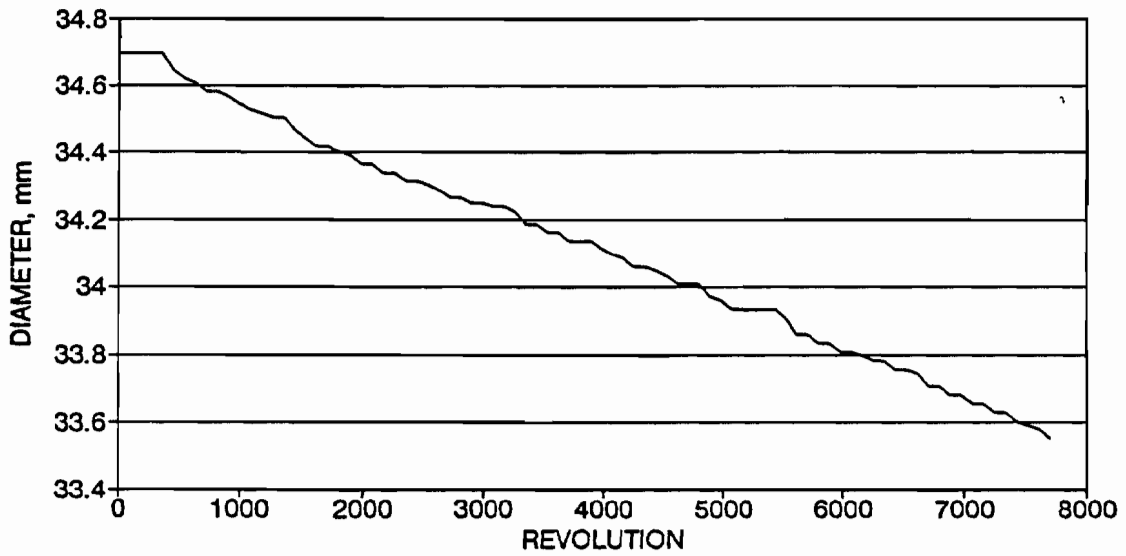


Figure 5.18. AMST27. Weight loss vs revolutions.

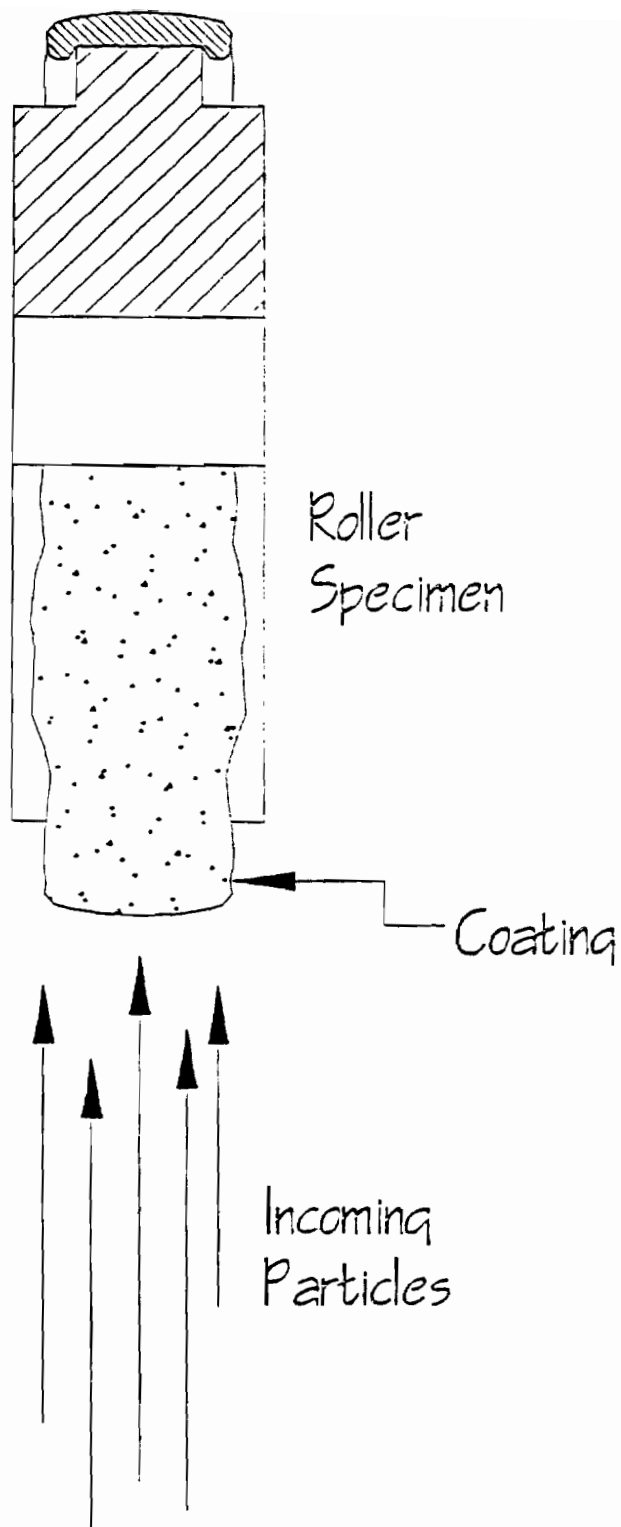


Figure 5.19. Crowning and increased width occur as coating thickness builds.

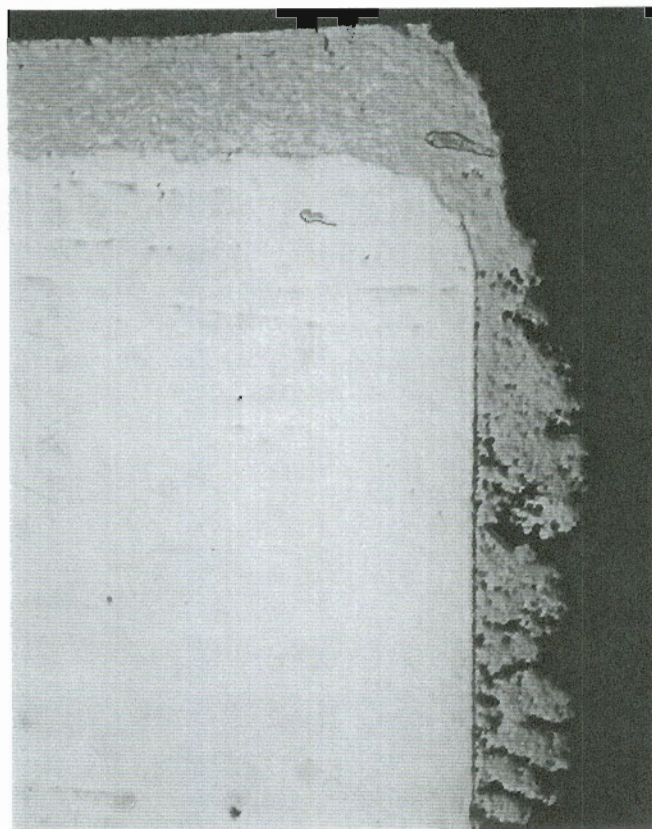


Figure 5.20. Shadow effect of coating onto a vertical surface.
50x.

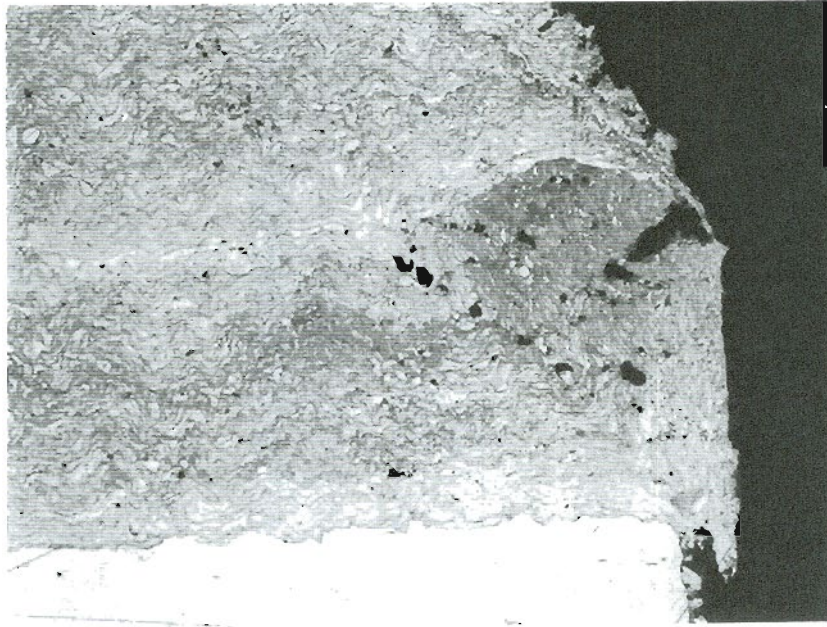


Figure 5.21. Shadow effect of spraying into a corner. 50x.



Figure 5.22. Higher magnification of the above photo. 100x.

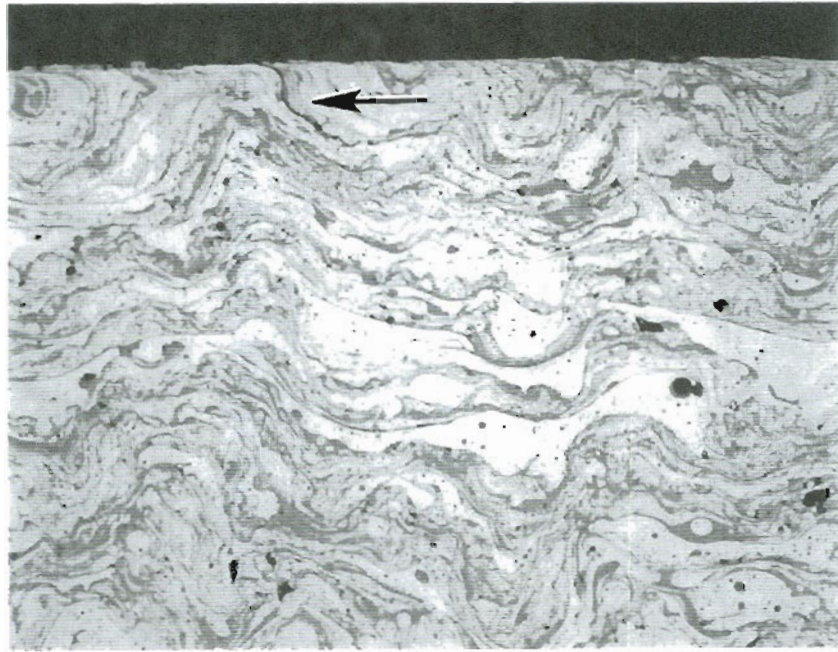


Figure 5.23. Crack growing along interlamellar interface near wear surface. 400x.



Figure 5.24. Crack from edge effect growing towards the substrate. 25x.



Figure 5.25. Crack from edge effect has grown to substrate. 45° view. 40x.

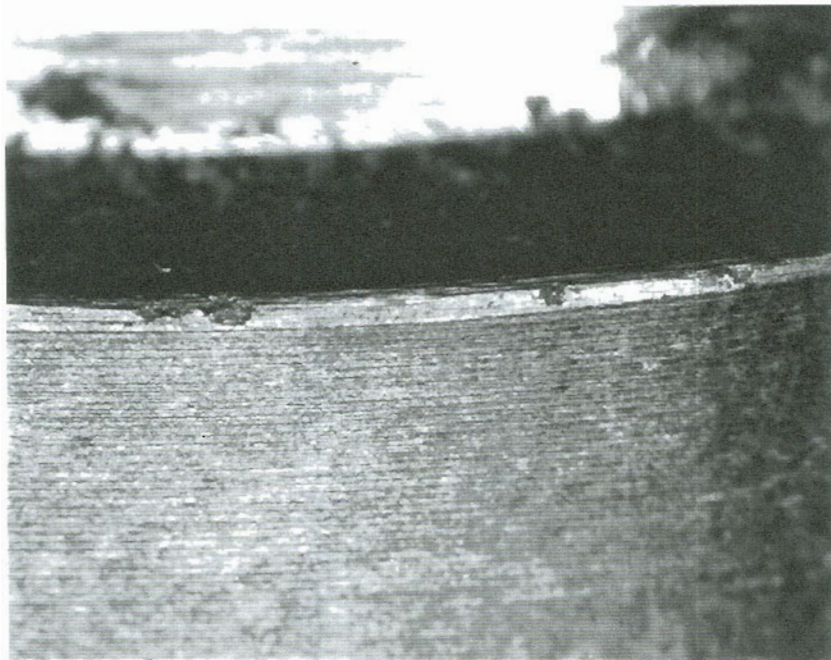


Figure 5.26. Edge effects induced during surface grinding before spraying. 15x.

5.4 Type II Debonding

During wear testing a larger piece of coating occasionally may be thrown out. Larger edge effects are great cause for concern because they can encroach upon the wear track, as shown earlier in figures 5.14 & 5.15. When this happens a crack often grows down through the thickness of the coating to the substrate, see figure 5.27. The forces exerted under loading can quickly cause the crack to spread across the coating, causing failure, see figure 5.28. This failure is classified in this research as Type II debonding, failure due to edge effects.

Edge effect cracks that go to the substrate will occasionally network in the region of the substrate edge, see figure 5.29. Figure 5.30 shows an edge effect particle at the coating/substrate interface ready to be thrown out, with a crack network beginning to form. When the edge effect encroaches upon the wear track the crack has more opportunity to extend across the coating instead of staying in the vicinity of the edges. When failure occurs, it appears as a debonding of the coating. It usually appears as a short section of coating lifting out, with the remainder of the coating intact. If the Amsler machine is allowed to rotate more than a very few revolutions after initial failure, more coating will be broken out. After failure, unless the debonded section has obvious edge effects it is very difficult to determine the cause, type I or type II debonding.

Minor edge effects in coatings produced under optimum, or close to optimum, conditions normally begin to occur between 1500 and 2000 revolutions. They first occur in the ridged area on the outside of the wear track, visible as different colored sites on the edge of the coating. Under close observation during Amsler operation, small particles can be seen flying out of the

system. An air blast is directed onto the rollers to reduce the effect of heat build-up during testing, and the particles quickly are blown away. Once edge effects are noted, close observation as the test progresses is required to detect wear track encroachment. If encroachment is suspected the test should be interrupted to take a closer look. Failure can be predicted based on this observation. It should be noted, however, that failure is not always imminent when encroachment is noticed. If the edge effect is deep, failure will occur more quickly than if relatively shallow. It has been occasionally noted that shallow edge effects will disappear as the wear process goes on and the wear depth overtakes the area of material loss.

Deep edge effects, those where the crack goes to the substrate, will occasionally expand into a crack network, as noted above. When the crack grows across the wear track, failure occurs. Figure 5.28, above, shows this type of failure. A crack grew across the coating width to the depth of the substrate. This crack originates from a small, deep edge effect. At the point of fracture more than one crack is sometimes noted when viewed from the coating/substrate interface, see figure 5.31. When debonded coating sections are looked at for microstructure, it can be seen that there is occasionally a damage zone in the area of fracture. The cracks seem to want to follow the lamellae interfaces as long as it can, crossing the lamellae only when the energy present can no longer be absorbed this way.

Type II debonding was the most common cause of coating failure in Amsler roller specimens. Specimen geometry is the main factor when discussing edge effects and subsequent coating failure. A geometry where there is a minimum of stress risers is the most desirable condition for coating performance if

debonding is the main failure criteria. Field application of the coatings will be under very different geometric conditions, rail sections being the substrate. In this sense, the laboratory test is a more difficult trial of the plasma spray technology than that of field conditions.

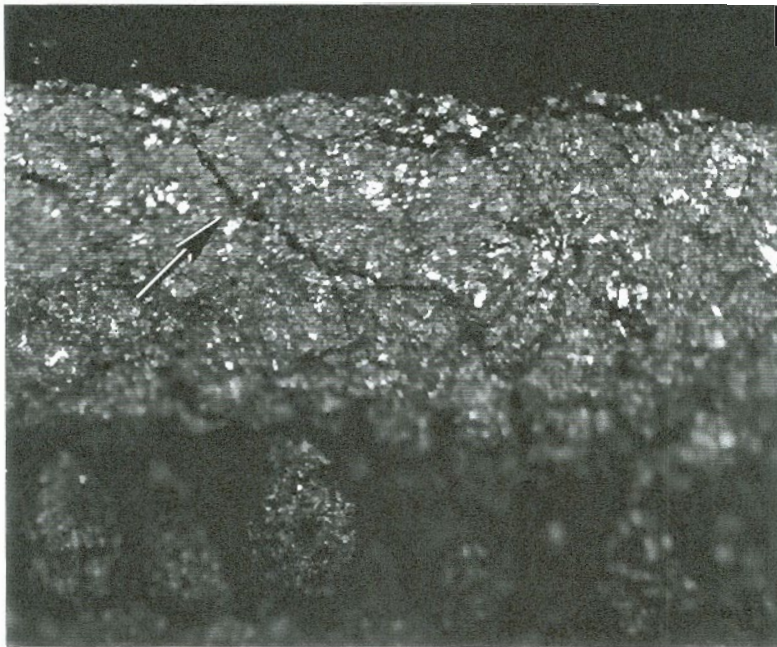


Figure 5.27. Crack from edge effect, leading to type II debonding. 40x.

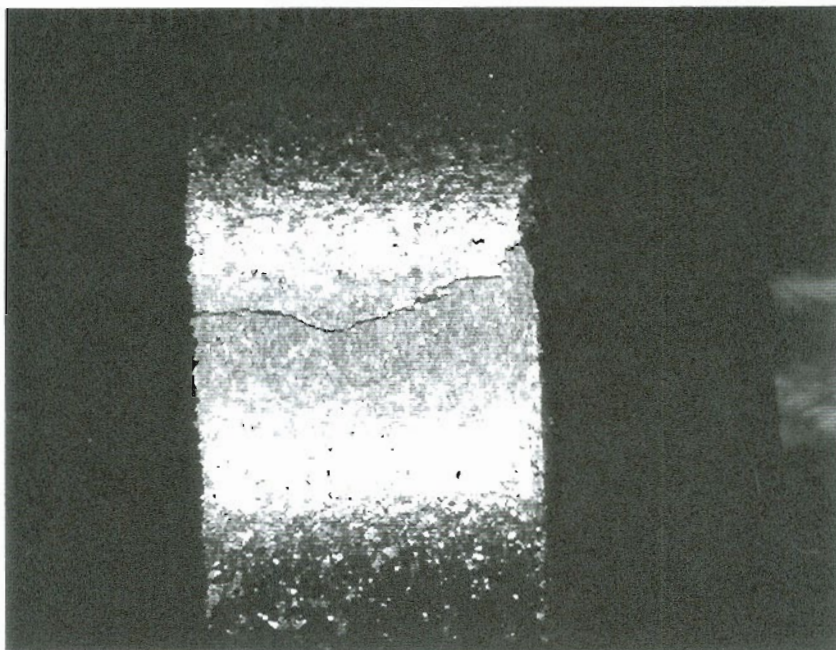


Figure 5.28 Type II debonding, crack across the wear surface.
10x.

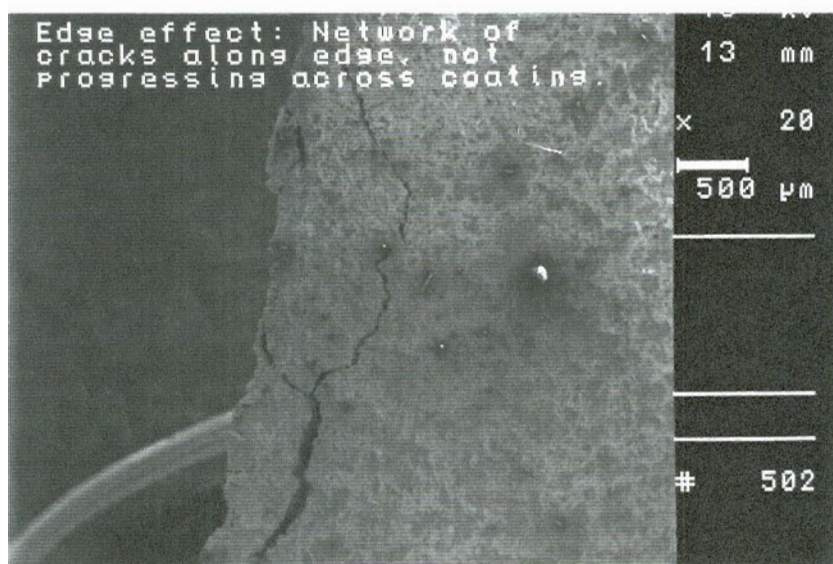


Figure 5.29. Fractured coating from the substrate interface side. Crack network along edge 20x.

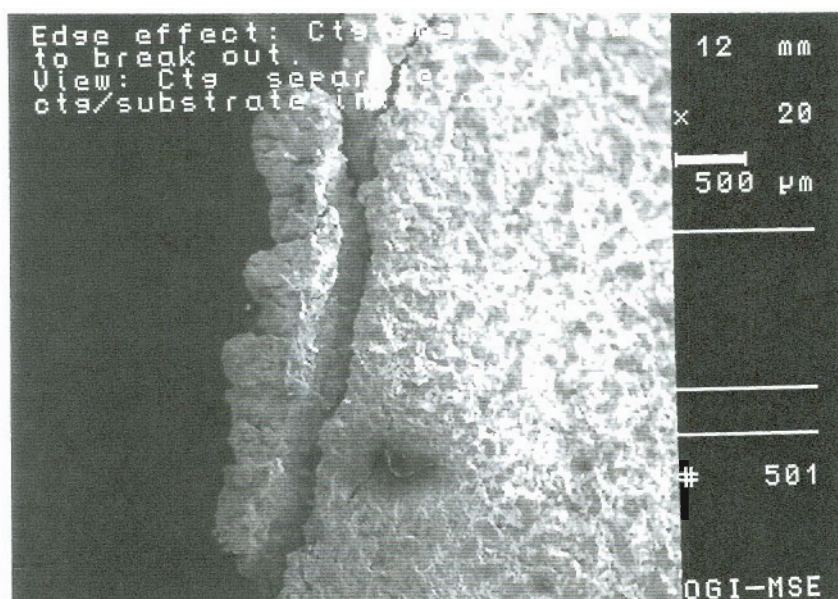


Figure 5.30. Edge effect particle loosened, view from coating/substrate interface. 20x

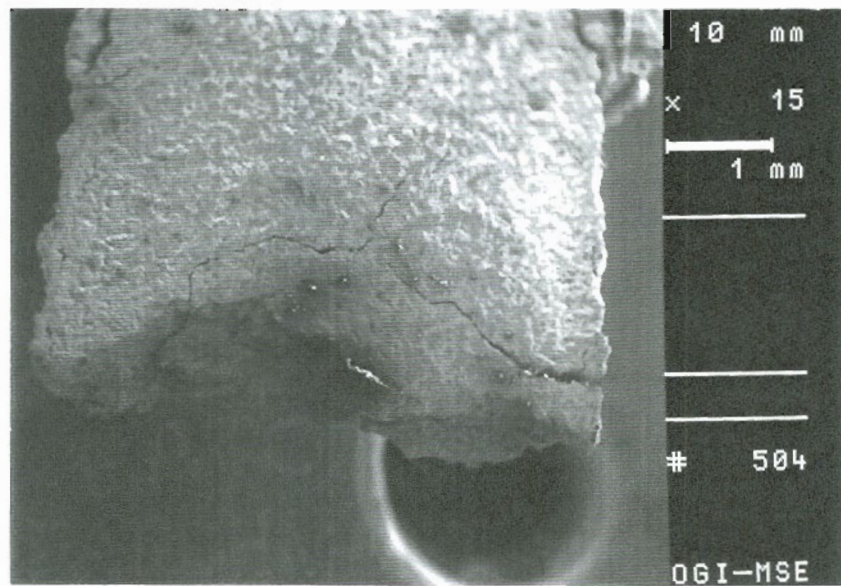


Figure 5.31. A damage zone is present in the fracture area. 15x.

5.5 Lamellar Structure And Formation Of Wear Particles.

5.5.1 Unlubricated.

The microstructure of a coating is lamellar in structure. The method of application is fully discussed elsewhere, but some important points in the coating process can be emphasized. The coating is an accumulation of individual particles built up during spraying. Ideally, the particles impact, flatten, and solidify with a sufficient time lapse between one particle impacting and the next one that hits the same spot. The rotation of the target, 200 rpm, with backside cooling further enhancing solidification, helps to assure a solidified surface for all incoming particles. These particles are of varying size, and impact the substrate with a more or less random size distribution. Also the individual particle that impacts a moving target will tend to form a splat that is elongated rather than the idealized flat, round pancake. Figure 5.32 schematically shows the influence of a rotating target relative to the incoming spray particles.

These factors combine to produce a layered microstructure with the individual components varying in size. This results in an uneven thickness in layers that are made from fully melted particles, with shorter, thicker components comprised of plasticized, partially melted particles, and some very small, partially melted particles. This mixture of individual splat shapes and sizes make up individual lamella with different thicknesses, and with size and shape variations within the layers. This results in a coating with undulations in the lamellar microstructure. The orientation of the lamellae is generally in a curvature that follows the surface shape of the substrate, however there are many localized variations,

occasionally there is even a nearly vertical orientation, see figure 5.33.

As the wear test progresses, wear particles are formed at the locations where the lamellae intersect the wear surface. As portions of the lamella wear very thin, some of the thin segments appear to lift, are broken, then removed, giving the appearance of tiny flakes. Figures 5.34 & 5.35 are photos of the overall microstructure of a successfully tested coating, with the second photo a higher magnification showing wear particles on the surface and a clear view of the previously described microstructural components.

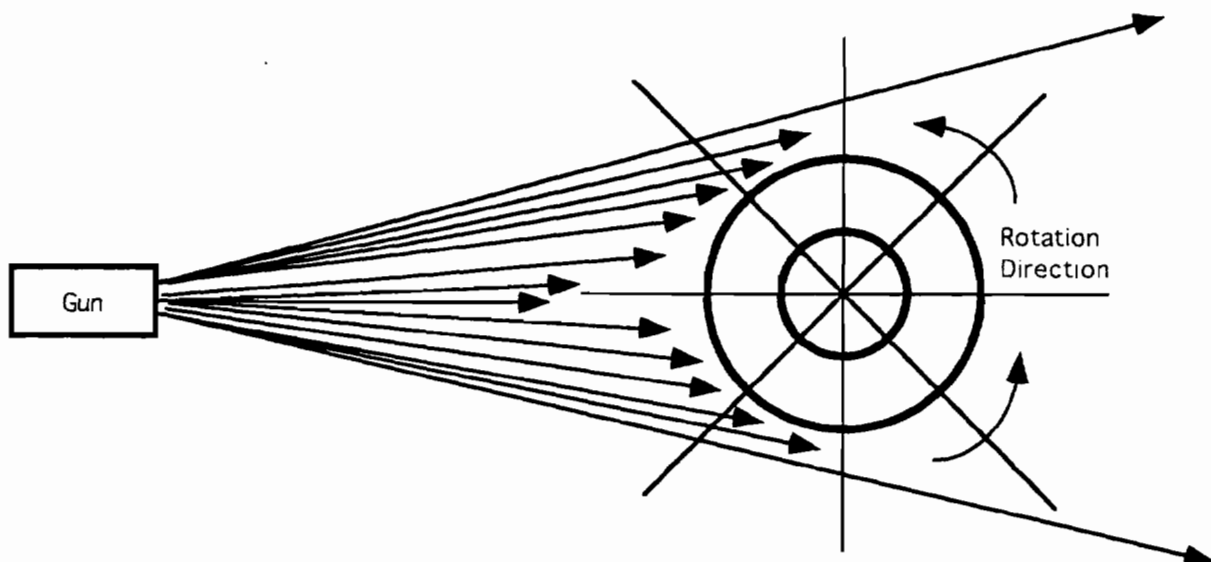


Figure 5.32. The angle of incidence between the incoming particles and the target differs according to the position of the particle within the plasma jet.

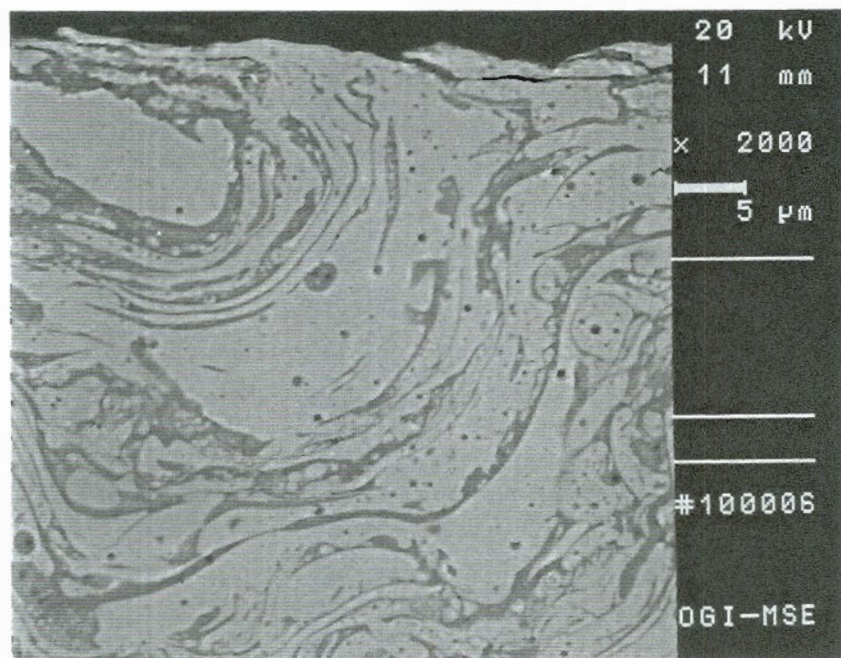


Figure 5.33. The undulation in coating microstructure occasionally occurs in a near vertical orientation of the lamellae. 2000x.

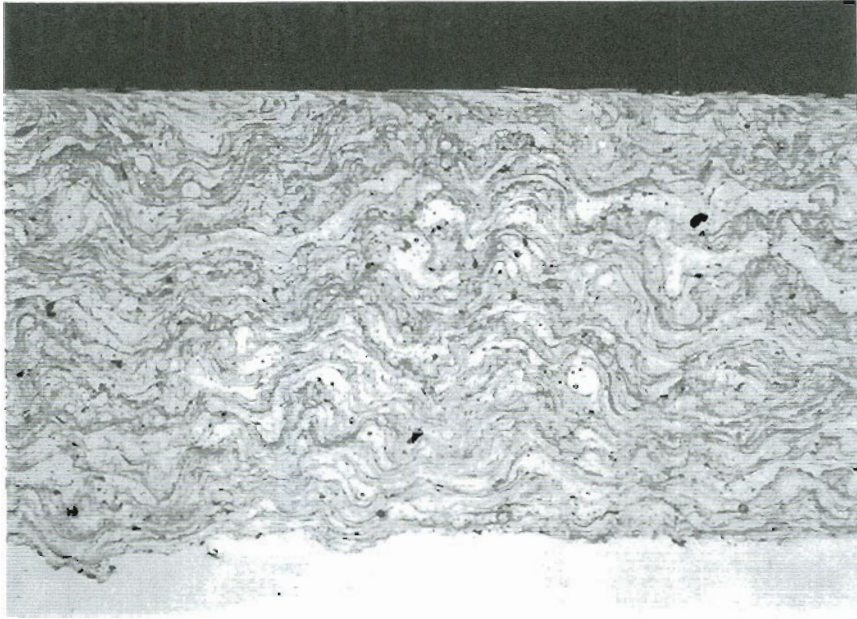


Figure 5.34. Microstructure of a successfully tested coating with wear particles visible. 200x.

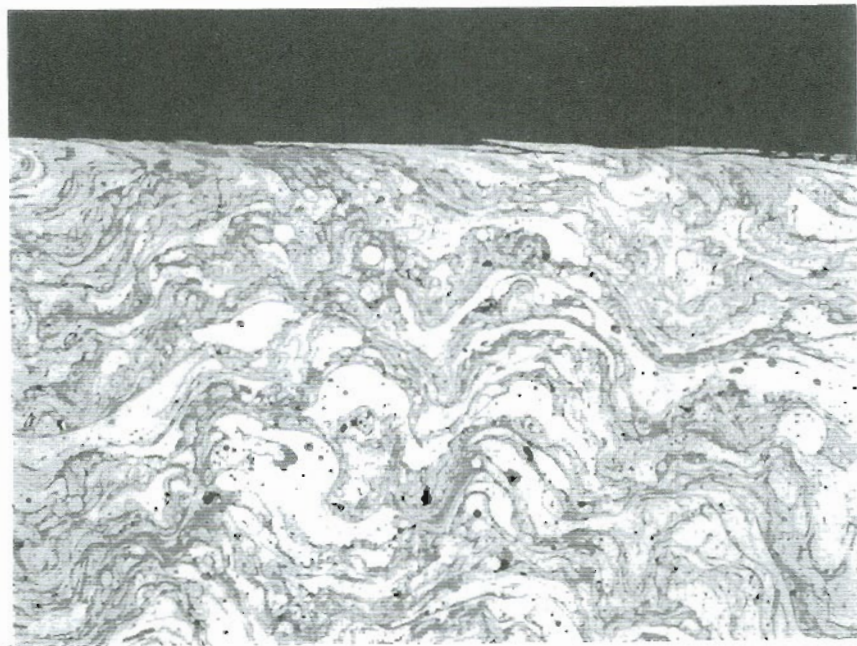


Figure 5.35. Higher magnification of the above photo. Note the wear particles. 400x.

5.5.2 Lubricated Rollers

There is a mechanism involved in the lubricated rollers that is similar to that in the dry condition, only more extreme. The undulations in the coating layers and the intersection of these layers with the surface again play the important role. Figure 5.36 shows the wear track of a roller that has been successfully tested in the lubricated condition. Notice here that the particle missing is much larger, huge in comparison, than that shown in figures 5.34 & 5.35 for the dry roller. There is a trail of evidence that helps to determine what is going on that contributes to this large particle removal. The first place to look is the wear surface, see figures 5.37 & 5.38. Notice that the wear surface of the dry tested roller is much smoother than that of the lubricated roller. The lubricated roller has a "hammered" appearance. This corresponds well with the cross section photo, figure 5.36. The next photos, figures 5.39 & 5.40, are higher magnifications of the same conditions.

Figures 5.41 & 5.42 are of the microstructures of rollers tested in the dry condition. They each show a crack extending along one of the lamellae interfaces, extending from the surface into the body of the coating. Notice that the orientation of the lamellae is almost vertical to the surface for a short distance in the region of the crack. These cracks do not affect the wear performance of the coating when tested dry. Both of these rollers were successfully tested for long periods before sectioning for microscopic study.

The idea put forth here is that this type of a crack can be propagated in lubrication tests. The coating is to act as a reservoir for lubricant during these tests, with the lubricant forced out into the contact area during loading and retreating

into the coating reservoir areas when unloaded. With a crack present, lubricant is forced into the crack during lubrication, then during loading the crack is hydraulically expanded because the interlamellar bond is not strong enough in that region to resist the applied force. The particles involved are broken out, and the particle size is much larger than that experienced in the dry condition. This mechanism is unique to coatings and not observed in uncoated rollers.

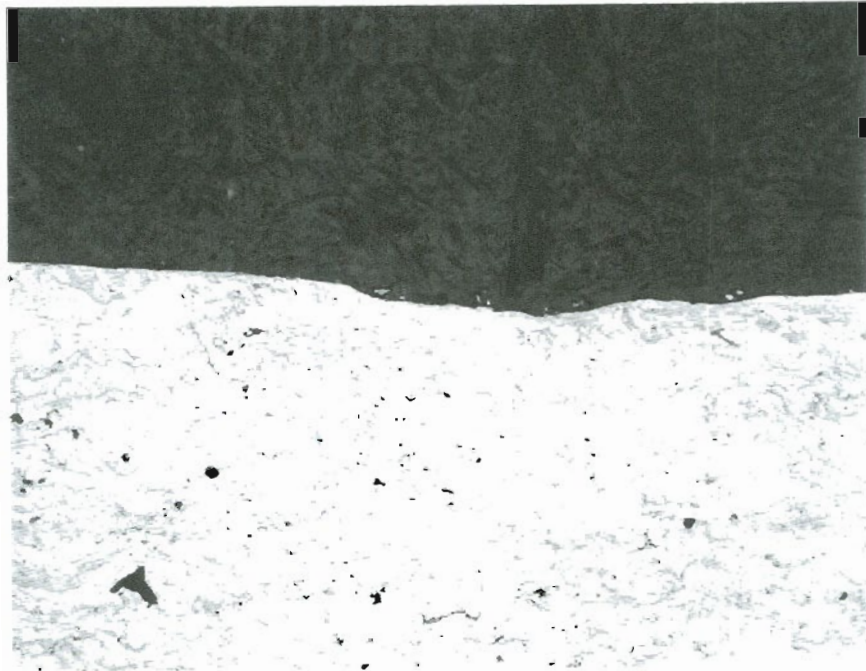


Figure 5.36. The wear track in cross-section showing a large wear crater. 100x

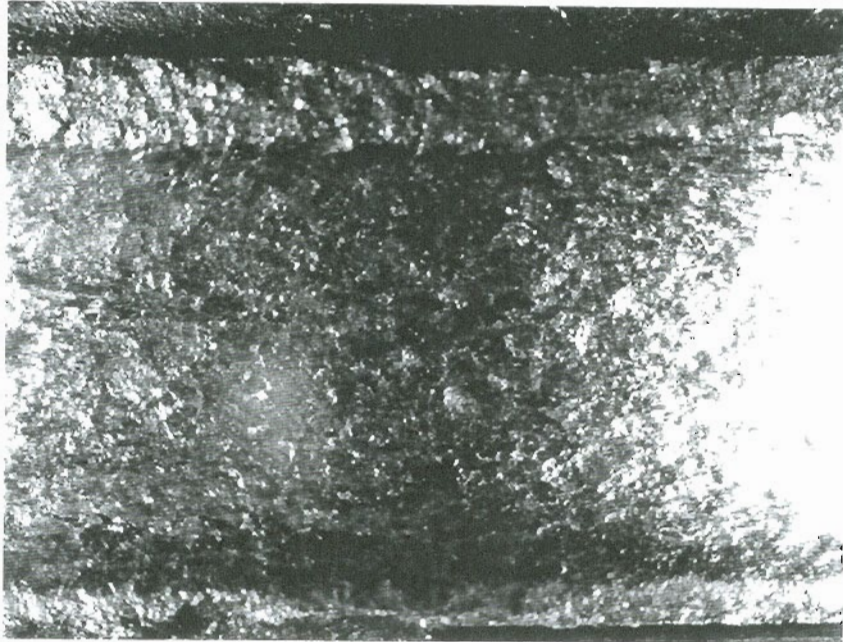


Figure 5.37. Wear surface of a lubricated roller. 10x.

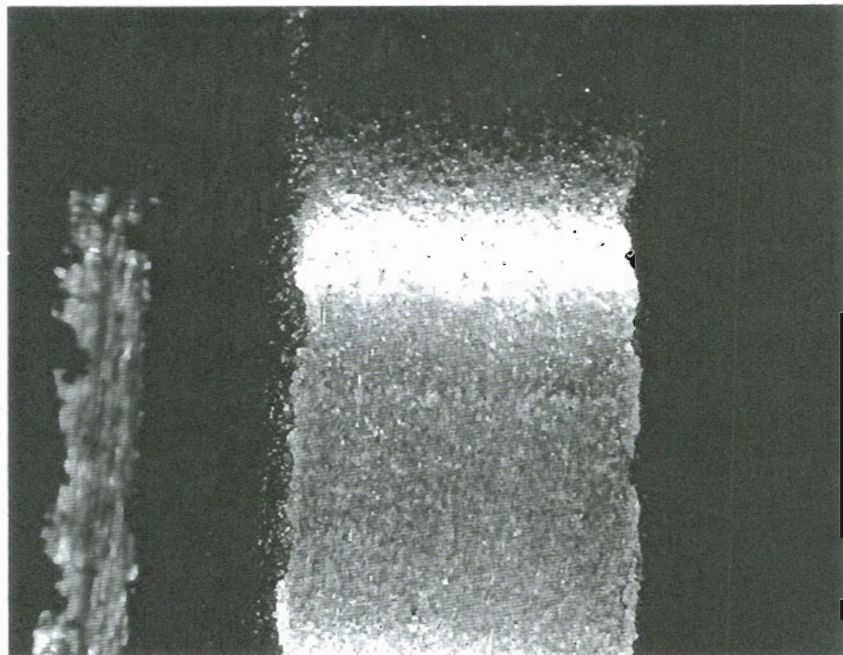


Figure 5.38. Wear surface of roller tested dry. 10x.

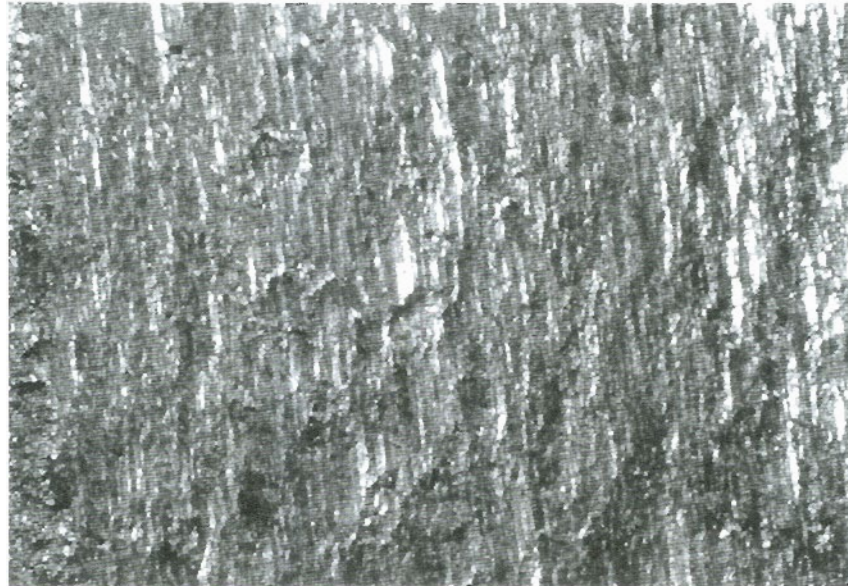


Figure 5.39. Higher magnification of lubricated wear track. 35x.

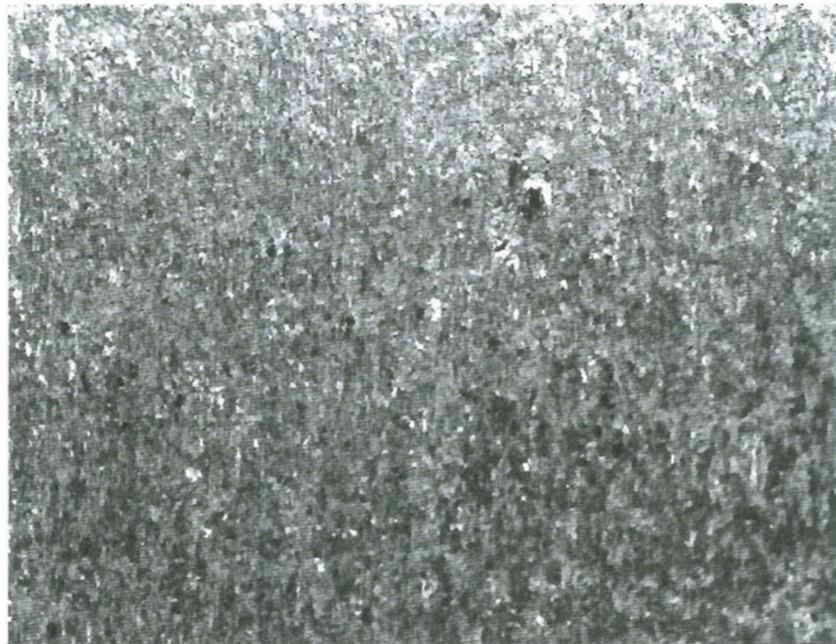


Figure 5.40. Higher magnification of coated tested dry. 35x.

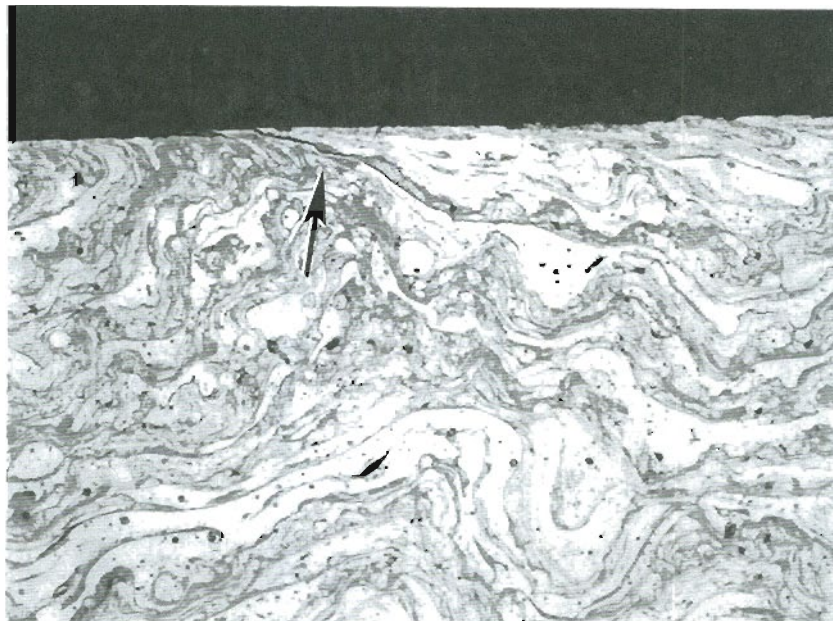


Figure 5.41. Cross-section of successfully dry tested coating. Note localized crack from wear surface into coating along lamellar interface. 400x

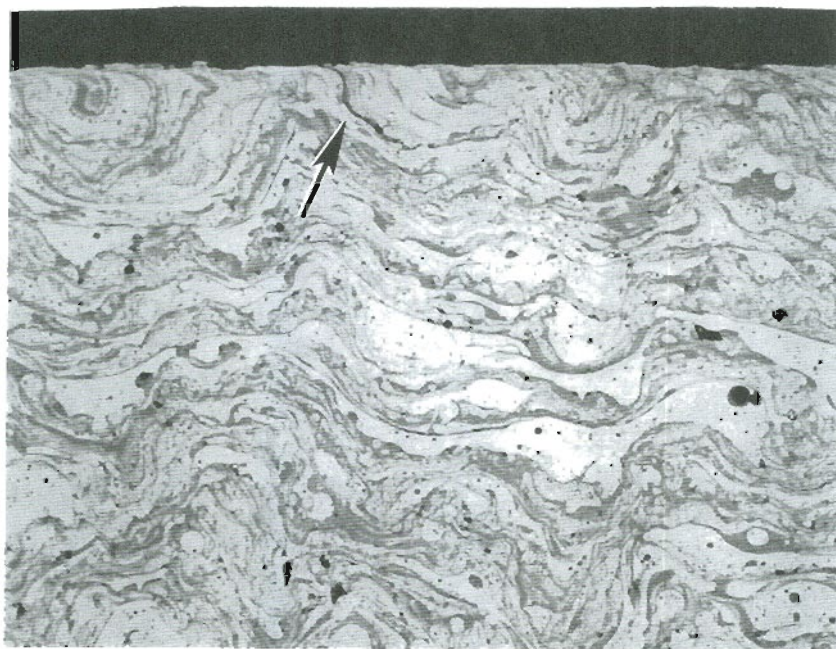


Figure 5.42. Another situation similar to that shown above. 400x

5.6 Lubrication Reservoir Effect.

The purpose of the lubricated tests was to determine any beneficial effect of the coating acting as a lubrication reservoir during sliding/rolling load conditions. In all of the tests performed, the early as well as the later groups of tests, the reservoir effect was not noted, probably because of the phenomena described in the previous section. Unless some additive, such as hollow spheres, were to be added to the coating during spraying, there is not an advantage in using the coating in place of plain steel for lubrication reservoir. Improved ways of providing porosity without loss of coating strength could be one subject of future work.

However, it should be noted that as long as the ultimate goal is the reduction in the friction coefficient between wheel and rail, the coated roller has a distinct beneficial effect. The friction coefficient for the coating has ranged from 0.44 to 0.46, unlubricated, over the slide/roll and contact pressure range tested in this research. This compares very favorably with the approximately 0.7 expected from the plain rail steels under similar conditions. It is thought that the reason for such a dramatic difference in performance is that the coated roller does not achieve the type III wear, as described by Bolton and Clayton⁸⁶ in their research, over the range of test conditions of this research.

5.7 Repeatability.

The question of obtaining wear test results within a certain expectation range is addressed by reviewing test results over a wide range of experiments. Wear data was recorded over

the entire range of testing, whether the tests were primarily for parameter envelope studies, debonding, or other research interests. For the purpose of this section, the wear test results are taken from AMST76 to AMST161. This range of testing occurred over an extended period of time and over a wide range of spraying conditions. A total of 50 tests were performed in such a manner as to have results for wear rate calculations, see figure 5.43. The other tests in this data base were either too short for wear rate calculations, or were run continuously until failure without recording intermediate weight loss data.

Most of the results reported here were from tests that ran 6,000 revolutions. 6,000 revolutions defined a full length test for this experimental group. The other data points are from tests with debonding failure, with enough data collected from which to calculate wear rates. The basic spray parameters of gas, working distance and power settings were constant. The conditions for each test can be seen in Appendix 1.

It can be seen from this data that the wear rates fall within a range of 200 to 700 ug/m/mm. In one respect it may seem that this is a wide range, it is more than 300% when comparing the lower rates to the higher ones, however even the highest wear rate is still very small when compared with previous research results of uncoated rollers, see figure 5.44. Wear rates on the upper side of the spectrum may be more influenced by edge effects, particles of material lost from areas other than the wear track. During wear testing, edge effects are nearly always present, however some rollers display more than others. The incidence of edge effects in varying degrees is presented as a reasonable explanation of the width of the expected wear rate band.

Spray parameter optimization and proper spray techniques must be employed to obtain quality coatings. When this condition is observed, at the contact pressure and slide/roll conditions necessary for this work, the coated rollers wear performance was predictable and repeatable, as seen by looking again at figure 5.44.

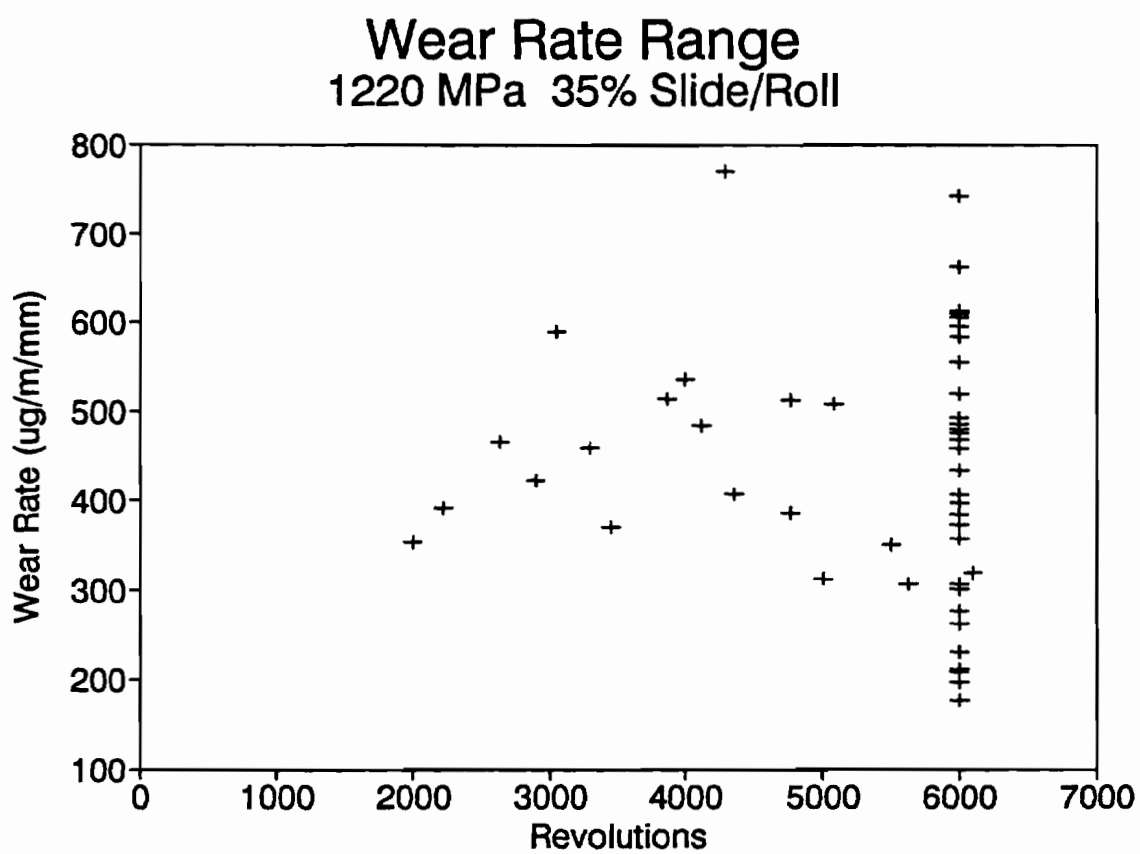


Figure 5.43. Wear rates range. 35% slide/roll, 1220 MPa. Tests were terminated at 6000 revolutions.

Uncoated Rail Steels

1220 MPa 35% Slide/Roll

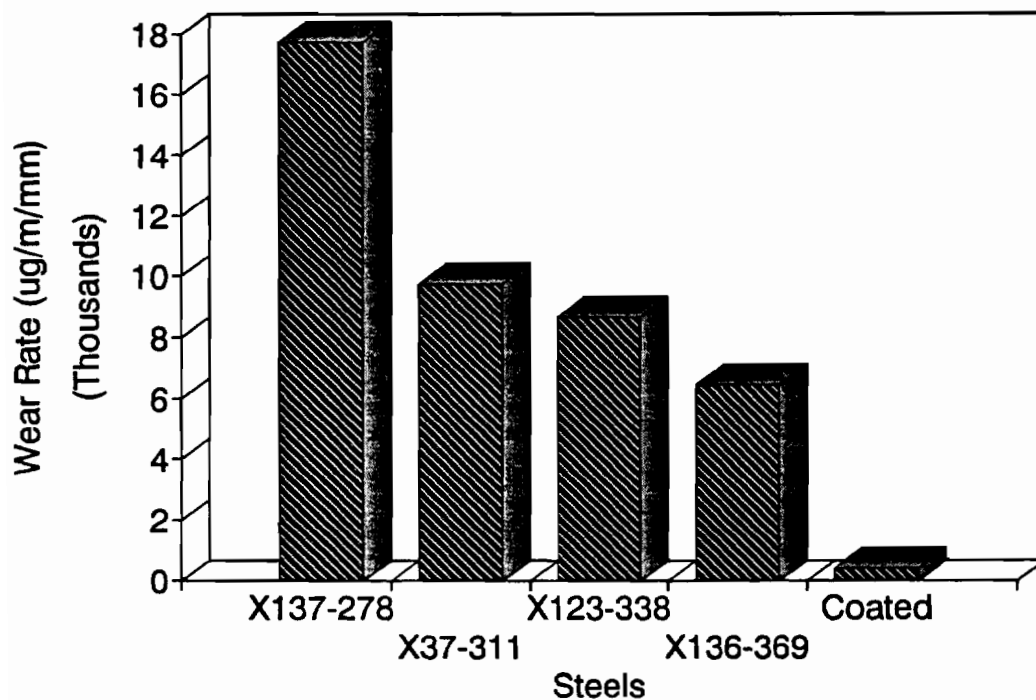


Figure 5.44. Wear rates of uncoated rail steel tested under the same Amsler test conditions as the coated rollers.

CHAPTER SIX

CONCLUSIONS

The considerations presented in these conclusions are such that are within the limits of the conditions of the test matrix presented in the body of this work.

1. Plasma sprayed 1080 steel coatings on Amsler rollers made from rail steel have a significantly lower wear rate than that of uncoated rail steel rollers.
2. The wear rates of the coatings are only minimally influenced by contact pressure or slide/roll ratios.
3. The spray parameter envelope to achieve quality coatings is wide enough to allow reproducibility under field conditions.
4. The limits of the spray parameter envelope are set by the likelihood of debonding rather than increasingly poor wear resistance.
5. The substrate preparation process has a significant effect on the coating/substrate bond durability.

- 6 The geometry of the substrate has a significant effect on the durability of the coating bond.
7. Two debonding failure mechanisms have been identified. Type I is an interfacially initiated delamination. Type II is surface initiated failure caused in large measure by the geometry of the substrate.
8. The plasma sprayed coating does not act as an effective lubrication reservoir under slide/roll loading conditions.
9. The coefficient of friction of the coated rollers is 0.46, a significant improvement over uncoated rail steel, which is approximately 0.7 for a 1220 MPa contact pressure and 35% slide/roll ratio.
10. Rail steel can be plasma spray coated with 1080 steel, using the techniques developed in this work, for in-track testing.

7.0 REFERENCES

1. ERRI Committee Report No. 1, *Review of Rolling Contact Fatigue in Rails*, Office for Research and Experiments of the International Union of Railways, April, 1990.
2. Knupp, G., L. Chidley, et al, *A Review of the Manufacture, Processing, and Use of Rail Steels in North America - a report of AISI technical subcommittee on rails and accessories*, ASTM STP, 1978, pp 7-20.
3. Sato, M., *Wear and RCF of Rail Steels*, Master's Thesis, Ohio State Univ, 1991.
4. Hanks, H. and J. Gussow, *Planning for Traffic Growth on Rail Lines*, Proc. Int. Conf. Heavy Haul Railways, USA, 1982, 82-HH-6.
5. O'Rourke, M., *Engineering Effects of Increasing Axle Load*, Proc. Int. Conf. Heavy Haul Railways, USA, 1982, 82-HH11.
6. Gaillyard, J., Manager of Engineering Methods & Research, Union Pacific Railroad, Personal Interview, 1996.
7. Devanathan, R, *AAR Lubrication Study, Report # 2*, Dept of Mat. Sci., Oregon Graduate Institute of Science & Technology, 1993.
8. Jiang, X., X. Fan, F, Gitzholder, et al, *Induction Plasma Spraying of Refractory Materials*, Thermal Spray: International Advances in Coatings Technology, Proceedings of the Int. Thermal Spray Conf., 1992, Ed. C. C. Berndt, ASM International, Materials Park, OH: 1992. pp 39-44.
9. Arvidsson, P., *Plasma and HVOF Sprayed Coatings of Alloy 625 and 718*, Thermal Spray Coatings: Properties, Processes and Applications, Proceedings of the 4th Nat. Thermal Spray Conf., 1990 Ed. Bernecki, T F, ASM International, Materials Park, OH: 1991. pp 357-362.
10. Sanoatg, S., Gumundsson, et al, *Plasma Spray Consolidation of Ni-Al Intermetallics*, Thermal Spray and Applications, Proceedings of the 4th Nat. Thermal Spray Conf., 1990, Ed.

Bernecki, T, ASM International, Materials Park, OH: 1992. pp 159-164.

11. Knight, R. and R. Smith, *HVOF Sprayed 80/20 Coatings - Process Influence Trends*, Thermal Spray: International Advances in Coatings Technology, Proceedings of the International Thermal Spray Conf., 1992. pp 159-164.

12. Gansert, D, E. Lugscheider, and U. Muller, *High Power Plasma Spraying of Oxide Ceramics*, Thermal Spray Research and Applications, Proceedings of the 3rd Nat. Thermal Spray Conf., 1990, Ed. Bernecki, T, ASM International, Materials Park, OH: 1991, pp 517-520.

13. Chuanxian, D. and T. Zhaohe, *Sliding Friction and Wear Behavior Mechanisms in Plasma Sprayed Ceramic Coatings*, Thermal Spray: International Advances in Coatings Technology, Proceedings of the International Thermal Spray Conf., 1992, Ed. C. C. Berndt, ASM International, Materials Park, OH: 1992. pp 673-678.

14. Shaoo, P. and R. Raghuraman, *Chromium Carbide Reinforced Composite Coatings for High Temperature Hard-Coat Applications*, Thermal Spray Coatings: Research, Design and Applications, Proceedings of the 5th Nat. Thermal Spray Conf., 1993, Ed. C. C. Berndt and T. Bernecki, ASM International, Materials Park, OH: 1993. pp 405-410.

15. Wang, Y and P. Kettunen, *The Optimization of Spraying Parameters for WC-Co Coatings by Plasma and Detonation Gun Spraying*, Thermal Spray: International Advances in Coatings Technology, Proceedings of the International Thermal Spray Conf., 1992. Ed. C. C. Berndt, ASM Internatioal, Materials Park, OH: 1992. pp 575-580.

16. Lane, C. and R. Sulit, *Extended Service Life with an Aluminum Composite Non-Skid Coating*, Thermal Spray Research and Applications, Proceedings of the 3rd Nat. Thermal Spray Conf., 1990, Ed. T. Bernecki, ASM International, Materials Park, OH: 1990. pp 105-108.

17. Bao, Y & D. Gawne, *Plasma Spraying of Glass-Polyamide Composite Coatings*, Thermal Spray Coatings: Research, Design and Applications, Proceedings of the 5th Nat. Thermal Spray Conf., 1993, Ed. C. C. Berndt and T. Bernecki, ASM International, Materials Park, OH: 1993. pp 417-420.

18. Tobe, S., S. Komada, H. Misawa, et al, *Rolling Fatigue Behavior of Plasma Sprayed Coatings on Aluminum Alloy*, Thermal

Skpray Research and Applications, Proceedings of the 3rd Nat. Thermal Spray Conf., 1990, Ed. T. Bernecki, ASM International, Materials Park, OH: 1990. pp 171-178.

19. Kamo, L., R. Kamo, and A. Iami, *Friction Characteristics of Ceramic Slurry and Plasma Sprayed Coatings*, Thermal Spray Coatings: Research Design and Applications, Proceedings of the 5th Nat. Thermal Spray Conf., 1993, Ed C. C. Berndt, and T. Bernecki, ASM International, Materials Park, OH: 1993. pp 463-468.

20. Krepiski, R., *Zinc-Silicate Composite Thermal Spray Coatings for the Corrosion Protection of Steel*, Thermal Spray Research and Applications, Proceedings of the 5th Nat. Thermal Spray Conf., 1993, Ed. C. C. Berndt and T. Bernecki, ASM International, Materials Park, OH: 1988. pp 291-296.

21. Ishikawa, K., M. Seki, and S. Tobe, *Application of Thermal Spray Coatings to Prevent Corrosion of Construction in Japan*, Thermal Spray Coatings: Research, Design and Applications, Proceedings of the 5th Nat. Thermal Spray Conf., 1993, Ed. C. C. Berndt and T. Bernecki, ASM International, Materials Park, OH: 1993. pp 679-684.

22. Hoel, R. and I. Kvernes, *The Microstructure of Thermal Barrier Coatings*, Thermal Spray: Advances in Coatings Technology, Proceedings of the Nat. Thermal spray Conf., 1987, Ed. D. Houck, ASM International, Materials Park, OH: 1988, pp 291-296.

23. Yonushonis, T, *Diesel Engine Evaluation of Thermal Barrier Coatings*, Thermal Spray Technology New Ideas and Processes, Proceedings of the Nat. Thermal Spray conf., 1988, Ed. D. Houck, ASM International, Materials Park, OH: 1989. pp 239-245.

24. *Welding Handbook*, 7th ed. American Welding Society, 1994.

25. Geibel, A., P. Verstreken, L. Delaey, et al, *Production of Free Standing Plasma Sprayed NiAl Components*, Thermal Spray: International Advances in Coatings Technology, Proceedings of the International Thermal spray Conf., 1992, Ed. C. C. Bernecki, ASM International, Materials Park, OH: 1991. pp 237-243.

26. Moreau, C., M. Lamontague, and P. Cielo, *Influence of Coating Thickness on the Cooling Rate of Plasma-Sprayed Particles Impinging on a Substrate*, Thermal Spray Coatings: Properties, Processes and Applications, Proceedings of the 4th

Nat. Thermal Spray Conf., 1991, Ed. T. Bernecki, ASM International, Materials Park, OH: 1991. pp 237-243.

27. Steffens, D., H. Drzeniek, and Z. Babiak, *Influence of Rare Earth Elements on Properties of Electric-Arc Sprayed Coatings Using Cored Wires*, Thermal Spray Technology New Ideas and Processes, Proceedings of the Nat. Thermal Spray Conf., 1988, Ed. D. Houck, ASM International, Materials Park, OH: 1989. pp 325-330.

28. Mei, L., P. Wei, C. Lin, et al, *Industrial Experiments on the Repair of 850mm Diameter Copper Rolling Mills Using Cored Wires*, Thermal Spray: International Advances in Coatings Technology, Proceedings of the International Thermal Spray Conf., 1992, Ed. C. C. Berndt, ASM International, Materials Park, OH: 1992. pp 643-646.

29. Glass, T. and J. DePay, *Protective Thermoplastic Powder Coating Specifically Designed Adhesive Polymers*, Thermal Spray Coatings: Properties, Processes and Applications, Proceedings of the 4th Nat. Thermal Spray Conf., 1991, Ed. T. Bernecki, ASM International, Materials Park, OH: 1991. pp 345-353.

30. Ligscheider, E., M. Loch, and H. Suk, *Powder Technology - State of the Art*, Thermal Spray: International Advances in Coatings Technology, Proceedings of the International Thermal Spray Conf., 1992, Ed. C. C. Berndt, ASM International, Materials Park, OH: 1992. pp 555-561.

31. Ingham, H. and A. Shepard, *Flame Spray Handbook, Vol 1*, 8th ed. METCO, Westbury, Long Island, New York, 1964.

32. Kreye, H., *Optimization and Control of the Spray Conditions in the Jet Kote Process*, Thermal Spray Technology New Ideas and Processes, Proceedings of the Nat. Thermal Spray Conf., 1988, Ed. D. Houck, ASM International, Materials Park, OH: 1989. pp 39-45.

33. *Perry's Chemical Engineers Handbook*, 6th ed. McGraw-Hill, 1984. pp 9-37.

34. Kaufold, R., A. Rotolico, J. Nerz, et al, *Deposition of Coatings Using a New High Velocity Combustion Spray Gun*, Thermal Spray Research and Applications, Proceedings of the 3rd Nat. Thermal Spray Conf., 1990, Ed. T. Bernecki, ASM International, Materials Park, OH: 1990. pp 561-574.

35. Cove, E. and R. Cole, *Hypervelocity Application of Tribological Coatings*, Thermal Spray Advances in Coatings Technology, Proceedings of the Nat. Thermal Spray Conf., 1987, Ed. D. Houck, ASM International, Materials Park, OH: 1988. pp 123-130.
36. Kreye, H. and U. Granz-Schnibbe, *High Velocity Flame Spraying of Chromium Oxide and Aluminum Oxide*, Thermal Spray Research and Applications, Proceedings of the 3rd Nat. Thermal Spray Conf., 1990, Ed. T. Berneki, ASM International, Materials Park, OH: 1990. pp 575-580.
37. Chuanxian, D. and T. Zhaohe, *Sliding Friction and Wear Behavior Mechanisms in Plasma Sprayed Ceramic Coatings*, Thermal Spray: International Advances in Coatings Technology, Proceedings of the International Thermal Spray conf., 1992, Ed. C. C. Berndt, ASM International, Materials Park, OH: 1992. pp 673-678.
38. Vuoristo, P., K. Niemi, and T. Mantyla, *On the Properties of Detonation Gun Sprayed and Plasma Sprayed Ceramic Coatings*, Thermal Spray: International Advances in Coatings Technology, Proceedings of the International Thermal Spray Conf., 1992, Ed. C. C. Berndt, ASM International, Materials Park, OH: 1992. pp 171-175.
39. Scholl, M. and P. Clayton, *Abrasive and Erosive Wear of Some Hypervelocity Air Plasma Sprayed Coatings*, Thermal Spray Coatings: Properties, Processes and Applications, Proceedings of the 4th Nat Thermal Spray Conf., 1991, Ed. T. Bernecki, ASM International, Materials Park, OH: 1991. pp 39-52.
40. Prichard, P., *Vacuum Plasma Spray of Cb and Ta Metal Matrix Composites, Metal & Ceramic Matrix Composites: Processing Modeling, & Mechanical Behavior*, The Minerals Society, 1990. pp 561-568.
41. Dsiam, J., *Effect of Spraying Parameters of the LPPS Method on the Structure of Ceramic Coatings*, Thermal Spray Coatings: Research, Design and Applications, Proceedings of the 5th Nat. Thermal Spray Conf., 1993, Ed. C. C. Berndt, and T. Bernecki, ASM International, Materials Park, OH: 1993. pp 487-492.
42. Jager, D., D. Stover, and W. Schlump, *High Pressure Plasma Spraying in Controlled Atmosphere Up To Two Bar*, Thermal Spray: International Advances in Coatings Technology, Proceedings of the International Thermal Spray Conf., 1992,

Ed. C. C. Berndt, ASM International, Materials Park, OH: 1992. pp 69-74.

43. Mallener, W. and D. Stover, *Plasma Spraying of Boron Carbide Using Pressures up to Two Bar*, Thermal Spray Coatings: Research, Design and Applications, Proceedings of the 5th Nat. Thermal Spray Conf., 1993, Ed. C. C. Berndt, and T. Bernecki, ASM International, Materials Park, OH: 1993. pp 291-295.

44. Lugscheider, E., U. Morkramer, and A. Ait-Mekideche, *Advances in PTA Surfacing*, Thermal Spray Coatings: Properties, Processes and Applications, Proceedings of the 4th Nat. Thermal Spray Conf., 1991, Ed. T. Bernecki, ASM International, Materials Park, OH: 1991. pp 529-536.

45. Pfender, E., *Fundamental Studies Associated with the Plasma Spray Process*, Thermal Spray Advances in Coatings Technology, Ed. D. Houck, ASM, Materials Park, OH: 1988. pp 1-10.

46. Jones, S., J. Auhl, and T. Meyer, *Particulate-Reinforced Aluminum-Based Composites Produced by Low Pressure RF Plasma Spraying*, Thermal Spray Coatings: Properties, Processes and Applications, Proceedings of the 4th Nat. Thermal Spray Conf., 1991, Ed. T. Bernecki, ASM International, Materials Park, OH: 1991. pp 329-335.

47. Wang, X., R. Kudesia, J. Lou, et al, *Deposition of Electronic Films by Atmospheric RF Plasma Aerosol Spray Technique*, Thermal Spray: International Advances in Coatings Technology, Proceedings of the International Thermal Spray Conf., 1992, Ed. C. C. Berndt, ASM International, Materials Park, OH: 1992. pp 567-574.

48. Zaat, J. *A Quarter of a Century of Plasma Spraying*, Annual Review of Material Science, Vol. 13 (1983) pp 9-42.

49. Apelian, D., M. Paliwal, R. Smith, et al. *Melting and Solidification in Plasma Spray Deposition --Phenomenological Review*, International Metals Reviews, Vol. 28 No. 5 (1983) pp 271-294.

50. von Engel, A. *Electric Plasmas: their nature and uses*, Taylor and Frances Ltd, London and New York, 1983. p 107.

51. Scholl, M. and Clayton, P., *Spray Forming By High Power High-Velocity Spraying*, Thermal Spray Coatings: Properties, Processes and Applications, Proceedings of the 4th Nat.

Thermal Spray Conf., 1991, Ed. T. Bernecki, ASM International, Materials Park, OH: 1991. pp 281-288.

52. Gu, B. and C. Wu, *The Gasdynamic and Electromagnetic Factors Affecting the Position of Arc Roots in a Tubular Heater*, *Acta Mechanica Sinica*, Vol. 7 No. 3 (1991) p 199.

53. *Physics of Welding, Welding Handbook, Vol 1*, Ed. L. Connor, 8th ed. American Welding Society, Miami, FL: 1987. pp 31-64.

54. *Welding Handbook, Vol 3*. 7th ed. American Welding Society,

55. *Physics of Welding, Welding Handbook, Vol 1*, Ed. C. Weisman, 7th ed. American Welding Society, Miami, FL: 1976. pp 52-59.

56. Fauachais, P., A. Coudert, M. Vardelle, et al, *State of the Art for the Understanding of the Physical Phenomena Involved in Plasma Spraying at Atmospheric Pressure*, *Thermal Spray Advances in Coatings Technology*, Ed. D. Houck, ASM International, Materials Park, OH: 1988. pp 11-19.

57. Cremers, C., H. Hsia, and J. Mahan. *Downstream Conditions in a Constricted Arc with Radial Injection*. *IEEE Transactions*, Vol. 1 No 3 (1973) pp 10-14.

58. Smirnov, B., *Plasma in Nature and in Laboratory Systems, Introduction to Plasma Physics*, MIR Publishers, Moscow: 1977. pp 9-17.

59. Spitzer, L. Jr. *Macroscopic Behaviour of a Plasma*, 2nd ed. Interscience Publishers John Wiley & Sons, New York, 1962. p 20.

60. Chang, C. and J. Szekely. *Plasma Applications in Metals Processing*, *Journal of Metals* Feb (1982) pp 57-64.

61. Van Kampen, N. and B. Felderhov. *Theoretical Methods in Plasma Physics*, North Holland Publishing Co., Amsterdam, 1967. p 1.

62. Ingham, H. and A. Shephard, *Flame Spray Handbook Vol III*, 8th ed. METCO, Westbury, Long Island, New York, 1964. pp 5-15.

63. Ingham, H. and A. Fabel, *Comparison of Plasma Flame Spray Gases*. *Welding Journal* Vol. 54 No. 2 (1975) pp 101-105.

64. Vollrath, J., A. Doolette, and S. Ramakrishnan, *The Electronic Plasma Gun*, Thermal Spray: International Advances in Coatings Technology, Proceedings of the International Thermal Spray Conf., 1992, Ed. C. C. Berndt, ASM International, Materials Park, OH: 1992. pp 117-121.

65. Kratochvil, W., G. Irons, and R. Czaplewski, *The Evolving Technology of High Energy Plasma Spraying*, Thermal Spray Coatings: Research, Design and Applications: Proceedings of the 5th Nat. Thermal Spray Conf., 1993, Ed. C. C. Berndt and T. Bernecki, ASM International, Materials Park, OH: 1993. pp 241-243.

66. Fauchais, P., J. Coudert, A. Vardelle, et al, *State of the Art for the Understanding of the Physical Phenomena Involved in Plasma Spraying at Atmospheric Pressure*, Thermal Spray, Advances in Coatings Technology, Ed. D. Houck, ASM International, Materials Park, OH: 1988. pp 11-19.

67. Vardelle, A., J. Baronnet, M. Vardelle, et al, *Measurements of the Plasma and Condensed Particles Parameters in a DC Plasma Jet*, IEEE Transactions on Plasma Science PS-8 Vol. 4 (1980) pp 417-424.

68. Kramarsic, R. and E. Muehlberger, *Methods to Improve Melting of Large Particles in a Plasma Stream*, Thermal Spray: International Advances in Coatings Technology, Proceedings of the International Thermal Spray Conf., 1992, Ed. C. C. Berndt, ASM International, Materials Park, OH: 1992. pp 63-68.

69. Swank, W., J. Fincke, and D. Haggard, *Plasma/Particle Interaction in Subsonic Argon/Helium Thermal Plasma Jets*, Thermal Spray Coatings: Research, Design and Applications, Proceedings of the 5th Nat. Thermal Spray Conf., 1993, Ed. C. C. Berndt, and T. Bernecki, ASM International, Materials Park, OH: 1993. pp 25-30.

70. Fincke, J. and W. Swank, *Air-Plasma Spraying of Zirconia: Spray Characteristics and Standoff Distance Effect on Deposition Efficiency and Porosity*, Thermal Spray: International Advances in Coatings Technology, Proceedings of the International Thermal Spray Conf., 1992, Ed. C. C. Berndt, ASM International, Materials Park, OH: 1992. pp 513-518.

71. Bower, A., and K. Johnson, *The Influence of Strain Hardening on Cumulative Plastic Deformation in Rolling/Sliding*

Line Contact, J. Mech. Physic. Solids, Vol. 37, No. 4, 1989, pp 471-493.

72. Clayton, P. and D. Hill, *Rolling Contact Fatigue of Rail Steel*, Wear, Vol. 117, 1987, pp 319-334.

73. Kalker, J., *Wheel-Rail rolling Contact Theory*, Wear, Vol. 144, 1991, pp 243-261.

74. Danks, D., *Wear and Microstructure of Eutectoid Steels*, PhD Thesis, Oregon Graduate Institute of Science & Technology, 1989.

75. Devanathan, R., *Wear Behavior of Bainitic Steels*, PhD Thesis, Oregon Graduate Institute of Science & Technology, 1991.

76. Dikshit, V., *Rolling Contact Fatigue Behavior of Pearlitic Steels*, PhD Thesis, Oregon Graduate Institute of Science & Technology, 1992.

77. Jin, N., *Mechanical Properties and Wear Performance of Bainitic Steels*, PhD Thesis, Oregon Graduate Institute of Science & Technology, 1995.

78. Finnie, I., *Erosion of Surface by solid Particles*, Wear, 3, 1960, pp 87-103.

79. Bitter, J., *A Study of Erosion Phenomena*, Wear, 6, 1, 1963, pp 5-21.

80. Rosenberg & Jordan, Trans. Am. Soc. Metals, 23, 1935, pp 577-582.

81. Archard, J., *Wear*, 2, 1958/1959. pp 438-455.

82. Mc Murchie, D, *Fretting Wear*, Unpublished Work, Dept. of Mat. Sci., Oregon Graduate Institute, 1993.

83. Hurricks, P. *The Fretting Wear of Mild Steel from 200 to 500°C*, Wear, 30, 1974, pp 189-212.

84. *Hydroabrasive Wear of Metals Under Cavitation*, Mashinostroekie, USSR, 1971.

85. Jia, Y., *Failure Analysis and Material Evaluation of TMP Refiner Plates*, PhD Thesis, Oregon Graduate Institute of Science & Technology, 1995.

86. Bolton, P. and P. Clayton, *Rolling-Sliding Wear Damage in Rail and Tyre Steels*, "Wear, Vol. 93, 1984, pp 145-165.
87. Archard, J. and W. Hirst, *The Wear of Metals Under Unlubricated Conditions*, Proc R. Soc. London, Ser A, 236 1956 p 397.
88. *Wear Control Handbook*, ed. M. Peterson and W. Winer, Am Soc Mech Eng, pp 1980.
89. Kragelski, I. and E. Marchenko, *Wear of Machine Components*, Journal of Lubrication Tech., Vol. 104, Jan 1982, pp 1-6.
90. Mulhearn, T. and L. Samuels, *The Abrasion of Metals: A Model of the Process*, Wear, Vol. 5, 1962, pp 478-498.
91. Richardson, R., *The Wear of Metals by Relatively Soft Abrasives*, Wear, Vol. 11, 1968, pp 245-275.
92. Tabor, D., *The Hardness of Solids*, Reviews Phys. Tech. 1970, 1, pp 145-179.
93. Eyre, T., *Wear Characteristics of Materials*, Tribology International, Vol. 9, No 5, 1976, pp 203-212.
94. Moore, D., *Principles & Applications of Tribology*, Permagon Press, 1975, p 272.
95. Uppal, Probert, and Thomas, Trans. Am. Soc. Metals, 23, 1935, pp 577-582.
96. Dupont, F. and I. Finnie, *The Simulation of Sliding Wear by Cyclic Deformation: Microstructural Aspects*, Wear, 140, 1990, pp 93-106.
97. Glardon, R., S. Chaves, and I. Finnie, *The Simulation of Sliding Wear by Cyclic Plastic Deformation Wear Under Combined Stresses*, J. Eng. Mat. Tech. Vol. 106, pp 248-252.
98. *Orientation Determination of Subsurface Cells Generated by Sliding*, Acta Metall. V 38, No 8, pp 1293-1305.
99. Feng, J., *Metal Transfer & Wear*, J. of Applied Physics, 23, 1952.
100. Heilman, P., J. Don, T. Sun, et al, *Sliding Wear and Transfer*, Int. Conf. on Wear of Materials, Reston, Va, 1983.

101. Bowden, F, and D. Taylor, *Theory of Plastic Deformation: Properties of Low Energy Dislocation Structures*, Mat. Sci. & Eng., A113, 1989, pp 1-41.
102. Dosloupoulos, Saka, and N. Suh, *Plowing Friction in Dry & Lubricated Metal Sliding*, J. of Tribology, 108, 1986, p 301.
103. Bowden, F. and D. Taylor, *The Friction & Lubrication of Solids*, Oxford Univ Press, Great Britain, 1986, p 9.
104. Steele, R., and D. Stone, AREA Proceedings, 87, 1986, 311.
105. Worth, J., P. Hornaday, P. Richards, *Prolonging Rail Life Through Rail Grinding*, Proc. 3rd Int. Conf. Heavy Haul Railways, 1986, IB-9-1.
106. Kalousek and Bethune, *Rail Wear Under Heavy Traffic Conditions*, ASTM STP 644, 1978, pp 63-69.
107. Clayton, P. and M. Allery, *Metallurgical Aspects of Surface Damage Problems in Rails*, Canadian Metallurgical Quarterly, 21, 5, 1982, pp 31-46.
108. Ghonem, H. and J. Kalousek, *Surface Crack Inintiation Due To Biaxial Compression/Shear Loading*, Proc. Int. Symposium Contact Mechanics and Wear in Wheel/Rail System, 1986, pp 339-360.
109. Suh, N., *The Delamination Theory of Wear*, Wear, 25, 1973, pp 111-124.
110. Clayton, P. and M. Allery, *Metallurgical Aspects of Surface Damage Problems in Rails*, Canadian Metallurgical Quarterly, 21, 5, 1982, pp 31-46.
111. A. Bower and K. Johnson, *Plastic Flow and Shakedown of the Rail Surface In Repeated Wheel-Rail Contact*, Wear, 144, 1991, pp 1-18.
112. Kumar, S., V. Aronov, B. Rajkumar, et al, *Experimental Investigation of Plastic Flow in Rails for a Laboratory Wheel Rail Simulation*, Canadian Metallurgical Quarterly, 21, 1, 1982, pp 59-66.
113. Hamilton, G., *Plastic Flow in Rollers Loaded Above the Yield Point*, Proc. Inst. of Mech. Eng. 177, 1963, p 667.

114. Kuhlman-Wilsdorf, D., *Theory of Plastic Deformation: Properties of Low Energy Dislocation Structures*, Mat. Sci. & Eng, A113, 1989, pp 1-41.
115. Su, X., *Surface Initiated Rolling/Sliding Contact Fatigue in Pearlitic and Low Carbon Bainitic Steels*, PhD Thesis, Oregon Graduate Institute of Science & Technology, 1996.
116. Frank, E., *Location of Lubricators*, Rail & Wheel Symp., AAR, 1982.
117. Clayton, P. and M. Allery, *Metallurgical Aspects of Surface Damage Problems in Rails*, Can. Metall. Q., 21, (1) 1982, pp 31-36.
118. Permar, R., *Current Rail/Flange Lubrication Practices on USA Transit Systems*, Rail & Wheel Lubrication Symp., 1987, AAR, III-4-1.
119. Loundsberry, S., *The Moore and Steel Approach to Wayside Rail Lubrication*, Rail & Wheel Lubrication Symp., AAR, 1987.
120. Wills, J., *Lubrication Fundamentals*, Marcel Decker Inc, N.Y., 1980, pp 59-68.
121. St. George, A. *Industrial Lubricant Additives*, Plant Engineering, Aug 14, 1986, pp 42-44.
122. Holzhauser, R., *Synthetic Lubricants*, Plant Engineering, Oct 7, 1991, pp 18-89.
123. Shelly, S., *Gearing Up For Synthetic Lubricants*, Chemical Engineering, July 1993, pp 67-69.
124. Marinello, L., *Interchangeable Lubricants*, Plant Engineering, June 9, 1983, pp 62-79.
125. Handler, L., *Sampling and Analysis of Industrial Lubricants*, Plant Engineering, Feb 13, 1986, pp 51-54.
126. Kramer, D., *How to Select the Proper Lubricant for Bearings*, Plant Engineering, Dec 26, 1985, pp 52-54.
127. Devanathan, R., *AAR Lubrication Study, Report # 2*, Unpublished Work, Dept. of Mat Sci., Oregon Graduate Institute of Science & Technology, 1993.
128. Campbell, W., *Solid Lubricants*, Standard Handbook of Lubrication Engineering, McGraw-Hill, USA, 1968, II-1.

129. Campbell, W. *Solid Lubricants*, Standard Handbook of Lubrication Engineering, McGraw-Hill, USA, 1968, II-4.
130. Johnson, V. and G. Vaughn, *Investigation of the Mechanism of Molybdenum Disulfide Lubrication in Vacuum*, J. of Appl. Physics, Vol. 27, No. 10, 1956, p 1173.
131. Peterson, M. and R. Johnson, *Factors Influencing Friction & Wear with Solid Lubricants*, Lubrication Engineering, VII, No. 5, 1955, p 325.
132. Sliney, H., *Solid Lubricants*, ASM Metals Handbook, V 18, 10th ed, 1993, p 119.
133. Solomir, J., *Wear Resistant Coatings & Self-Lubricating Plasma-Sprayed Coatings; Some of Their Properties & Performances*, Paper 37, Coatings Division, Nova-Werke AG, Switzerland, 1972.
134. Durge, W., et al, *Metal Encapsulated Solid Lubricant Coating System*, Patent # 5,302,450, Ford Motor Co, 1994.
135. Lichtensdtein, J., *Steel Surface Preparation for Protective Coatings*, Materials Performance, Jan 1980, pp 32-33.
136. Kelly, T., *Surface Preparation for In-Service Steel Materials Performance*, Materials Performance, 1982, pp 17-18.
137. Munger, C., *Surfaces, Adhesion, Coatings*, Corrosion 83, Paper No. 29, NACE International, April 1983.
138. Mc Crory, E., *Surface Preparation of Contaminated Steel Surfaces*, Corrosion 84, Paper No. 62, NACE International, April 1984.
139. Hatle, L. and J. Cook, *Achieving 'Zero-Detectable' Soluble Salt Contamination of Steel Substrates*, Corrosion 94, Paper No. 603, NACE International, 1994.
140. Appleman and Bruno, *Evaluation of Wet Blast Cleaning Units*, Proceedings of the SSPC 1985 Annual Symposium.
141. Nixon, J., *Surface Preparation Using High Pressure Water Blasting*, Corrosion 89, Paper No. 297, NACE International, Apr 1989.

142. Horne, A. *The Importance of Achieving Surface Profile In Railway Car Preparation*, Corrosion 88, Paper No. 446, NACE International, Mar 1988.

143. Scholl, M., *Plasma Equipment Operation*, Lecture and demonstration, Dept. of Mat. Sci., Oregon Graduate Institute Of Science and Technology, 1991.

144. Bolton, P., and P. Clayton, *Rolling-Sliding Wear Damage in Rail and TYre Steels*, Wear, 93, 1984, pp 144-165

145. Itoh, A., M. Hirata, and M. Ayagaki, *Effects of Substrate Temperature During Spraying on the Properties of Sprayed Coatings (1)*, Thermal Spray Coatings: Research, Design and Applications, Proceedings of the 5th Nat. Thermal Spray Conf., 1993, Ed. C. C. Berndt, and T. Berneki, ASM, Materials Park, OH: 1993. pp 593-600.

146. Fantassi, S., M. Vardelle, A. Vardelle, et al, *Influence of the Velocity of Plasma Sprayed Particles on the Splat Formation*, Thermal Spray Coatings: Research, Design and Applications, Proceedings of the 5th Nat. Thermal Spray Conf., 1993, Ed. C. C. Berndt and T. Bernecki ASM International, Materials Park, OH: 1993. pp 1-6.

147. Liu, H., E. Lavernia, R. Rangel, et al, *Deformation and Interaction Behavior of Molten Droplets Impinging on a Flat Substrate in Plasma Spray Process*, Thermal Spray Coatings: Research, Design and Applications, Proceedings of the 5th Nat. Thermal Spray Conf., 1993, Ed. C. C. Berndt and T. Bernecki, ASM International, Materials Park, OH: 1993. pp 457-462.

148. Jones, H., *Cooling, Freezing and Substrate Impact of Droplets Formed by Rotary Atomization*, Journal of Physics D: Applied Physics 4 (1971) pp 1657-1660.

149. Bergmann, C., *Influence of Thermal Conductivity of the Spray Powder on the Adherence of Plasma-Sprayed Ceramic Coatings*, Thermal Spray Coatings: Research, Design and Applications, Proceedings of the 5th Nat. Thermal Spray Conf., 1993, Ed. C. C. Berndt and T. Berneke ASM International, Materials Park, OH: 1993. pp 537-542.

150. Malmberg, S. and J. Heberlein, *Effect of Plasma Spray Operating Conditions on Plasma Jet Characteristics and Coating Properties*, Thermal Spray Coatings: Research, Design and Applications, Proceedings of the 5th Nat. Thermal Spray Conf., 1993, Ed. C. C. Berndt T. Bernecki ASM International, Materials Park, OH: 1993. pp 451-456.

151. Devanathan, R., *Lubrication Study*, Unpublished Work, Dept. of Mat. Sci., Oregon Graduate Institute of Science & Technology, 1991.
152. Scholl, M., Unpublished Work, Dept. of Mat. Sci., Oregon Graduate Institute of Science & Technology, 1995.
153. Operations Manual, Amsler Wear Test Machine.
154. Jin, N., Unpublished Work, Dept. of Mat. Sci., Oregon Institute of Science & Technology, 1994.
155. Devanathan, R., *Lubrication Study*, Report # 2, Dept. of Mat. Sci., Oregon Graduate Institute of Science & Technology, 1992.

APPENDIX

CHART OF EXPERIMENTS

Appendix 1 is an overall chart of experiments performed for this research. Most of the columns are self explanatory, however some abbreviations should be explained further. W-3, W-9, and W-10 wheels are standard class C wheels, W-8 is a class U wheel. Test conditions were either dry or lubed, DAS is dry, as sprayed; DGF is dry, ground flat. A parameter set is shown as Primary gas flow rate/ Secondary gas flow rate/Working distance. For example, AMST 1 parameter set was 180 slm (standard liters per minute) of nitrogen (N_2), 0 slm of hydrogen (H_2), and 180 mm working distance (180/0/180). The comments column contains only a word or short phrase explaining unusual observations or test conditions.

| Test No. AMST | Wire | Contact Pressure | Creepage | Steel Bottom | Test Conditions | Coating Thickness | Parameter Set | Wear Rate Top | Bottom | Debond Type I | Debond Type II | Test Length | Comments |
|------------------|-----------------|------------------|----------|--------------|-----------------|-------------------|---------------|---------------|--------|---------------|----------------|-------------|---|
| 1 | 1075 Cored 3/32 | 700 | 35 | W-3 | DAS | 0.30 | 180/0/180 | 1676 | 59 | | | 420 | Wore Through |
| 2 | 1075 Cored 3/32 | 1050 | 35 | W-3 | DAS | 0.30 | 180/0/180 | 1014 | 104 | | | 370 | Blistered |
| 3 | 1075 Cored 3/32 | 1220 | 35 | W-3 | DAS | 1.00 | 180/0/180 | | | yes | | Immed | |
| 4 | 1075 Cored 3/32 | 900 | 34 | W-3 | DAS | 1.00 | 180/0/180 | 2877 | | yes | | 280 | |
| 5 | 1075 Cored 3/32 | 900 | 35 | W-3 | DAS | 0.30 | 180/0/180 | 3164 | | yes | | 250 | Edge |
| 6 | 1075 Cored 3/32 | 900 | 38 | W-3 | DAS | 0.50 | 180/0/180 | 7314 | 416 | | | 360 | Wore Through |
| 7 | .094 Music | 1220 | 35 | W-3 | DAS | 1.00 | 280/135/200 | | | yes | | 40 | |
| 8 | .094 Music | 1050 | 35 | W-3 | DAS | 1.30 | 280/135/200 | | | yes | yes | 150 | Edge |
| 9 | .094 Music | 900 | 35 | W-3 | DAS | 1.00 | 280/135/200 | | | yes | yes | 200 | Edge |
| 10 | .094 Music | 700 | 35 | W-3 | DAS | 0.85 | 280/135/200 | 808 | 3 | | | 1470 | Blister |
| 11 | .094 Music | 500 | 35 | W-3 | DAS | 0.80 | 280/135/200 | 4050 | 91 | | | 1800 | Edge & Blister |
| 12 | .094 Music | 700 | 5 | W-3 | DAS | 0.84 | 280/135/200 | 15 | 0 | | | 20510 | |
| 13 | .094 Music | 900 | 5 | W-3 | DAS | 0.88 | 280/135/200 | 11911 | 0 | yes | | 230 | |
| 14 | .094 Music | 1050 | 5 | W-3 | DAS | 0.9 | 280/140/200 | 236 | 0 | yes | | 420 | |
| 15 | .094 Music | 1220 | 5 | W-3 | DAS | 0.9 | 300/150/225 | | | yes | | 100 | |
| 16 | 1/16 Music | 1220 | 35 | W-3 | DAS | 0.75 | 250/105/225 | | | yes | | 80 | |
| 17 | 1/16 Music | 1220 | 35 | W-3 | Lubed | 0.75 | 250/80/225 | | | yes | | 70 | |
| 18 | 1/16 Music | 1220 | 35 | W-3 | DAS | 0.10 | 250/105/225 | | | | | 200 | Wore Through |
| 19 | 1/16 Music | 1220 | 35 | W-3 | DAS | 0.75 | 250/105/225 | | | yes | | 90 | |
| 20 | 1/16 Music | 1220 | 35 | W-3 | Lubed | 0.20 | 250/105/225 | 490 | 60 | | | 3200 | Wore Through |
| 21 | 1/16 Music | 1220 | 15 | W-3 | DAS | 0.25 | 250/105/225 | 2561 | | | | 760 | Flaking, wore through |
| 22 | 1/16 Music | 1220 | 5 | W-3 | DAS | 0.25 | 250/80/220 | 1037 | | | | 1750 | Flaking, wore through |
| 23 | 1/16 SS80 | 1220 | 8.5 | W-3 | Lubed | 0.38 | 235/30/200 | | | | | 3370 | Wore through |
| 24 | 1/16 SS80 | 1220 | 8 | W-3 | DAS | 0.35 | 235/30/200 | 891 | | yes | yes | 1100 | Edge |
| 25 | 1/16 SS80 | 1220 | 4.4 | W-3 | DAS | 0.94 | 235/30/200 | 208 | 17 | | | 10700 | Edge |
| 26 | 1/16 SS80 | 1220 | 35 | W-3 | DAS | 1.00 | 235/30/200 | 250 | 104 | | yes | 1200 | Edge just before debond |
| 27 | 1/16 SS80 | 1220 | 36 | W-3 | DAS | 0.85 | 235/30/200 | 560 | 16 | | | 8500 | Edge 85 data points |
| 28 | 1/16 SS80 | 1220 | 36 | W-3 | DAS | 0.86 | 235/30/200 | | | yes | | 345 | |
| 29 | 1/16 SS80 | 1220 | 38 | W-3 | Lubed | 0.40 | 235/30/200 | 140 | 10 | | yes | 4050 | |
| 30 | 1/16 SS80 | 1050 | 35 | W-3 | DAS | 1.00 | 235/30/200 | 1160 | 27 | | | 800 | Edge |
| 31 | 1/16 SS80 | 1080 | 35 | W-3 | DAS | 1.00 | 240/40/225 | | | yes | | 100 | |
| 32 | 1/16 SS80 | 1050 | 36 | W-3 | DAS | 0.90 | 240/40/225 | | | | | 500 | Edge |
| 33 | 1/16 SS80 | 1050 | 38 | W-3 | DAS | 0.56 | 265/70/250 | | | yes | | 270 | |
| 34 | 1/16 SS80 | 1050 | 38 | W-3 | DAS | 0.65 | 265/70/250 | 3893 | 168 | yes | yes | 700 | Edge just before debond |
| 35 | 1/16 SS80 | 1050 | 37 | W-3 | DAS | 0.66 | 225/30/200 | 520 | 51 | | yes | 900 | Edge |
| 36 | 1/16 SS80 | 1050 | 37 | W-3 | DAS | 0.70 | 275/70/200 | 362 | 36 | | | 2990 | |
| 37 | 1/16 SS80 | 1050 | 38 | W-3 | DAS | 0.50 | 225/30/250 | 428 | | | yes | 1100 | Edge, crack on surface just before debond |
| 38 | 1/16 SS80 | 1050 | 37 | W-3 | DAS | 0.60 | 225/30/225 | 411 | | | | 5200 | |
| 39 | 1/16 SS80 | 1050 | 37 | W-3 | DAS | 0.70 | 235/35/225 | 428 | | | | 6200 | |
| 40 | 1/16 SS80 | 1220 | 35 | W-3 | DAS | 1.10 | 235/35/225 | 388 | | | | 7200 | Edge |

| Test No. AMST | Wire | Contact Pressure | Creepage | Steel Bottom | Test Conditions | Coating Thickness | Parameter Set | Wear Rate Top | Bottom | Debond Type I | Debond Type II | Test Length | Comments |
|------------------|------------|------------------|----------|--------------|-----------------|-------------------|---------------|---------------|--------|---------------|----------------|-------------|---------------------------|
| 41 | 1/16 SS80 | 900 | 35 | W-3 | DAS | 1.10 | 235/35/225 | 572 | | | | 6500 | |
| 42 | 1/16 SS80 | 700 | 35 | W-3 | DAS | 1.20 | 235/35/225 | 478 | | | | 6500 | |
| 43 | 1/16 SS80 | 500 | 35 | W-3 | DAS | 1.10 | 235/35/225 | 454 | | | | 6500 | |
| 43a | 1/16 SS80 | 1050 | 35 | W-3 | DAS | 1.10 | 235/35/225 | 294 | | | | 5000 | |
| 44 | 1/16 SS80 | 1220 | 35 | W-3 | DAS | 1.10 | 235/35/225 | 271 | | | | 5000 | |
| 45 | 1/16 SS80 | 1050 | 35 | W-8 | Lubed | 1.10 | 235/35/225 | | | | yes | 1310 | |
| 46 | 1/16 SS80 | 1220 | 35 | W-8 | Lubed | 0.80 | 235/35/225 | 155 | | | yes | 3390 | |
| 47 | 1/16 SS80 | 1220 | 37 | W-8 | Lubed | 0.80 | 235/35/225 | 243 | | | yes | 1360 | |
| 48 | 1/16 SS80 | 1220 | 36 | W-8 | Lubed | 0.90 | 230/30/225 | 337 | | | yes | 1770 | |
| 48 | 1/16 SS80 | 1220 | 35 | W-8 | Lubed | 1.00 | 230/30/225 | 241 | | | yes | 1220 | |
| 50 | 1/16 SS80 | 1050 | 36 | W-8 | Lubed | 1.10 | 230/30/225 | | | | yes | 3910 | |
| 51 | 1/16 SS80 | 1220 | 36 | W-8 | Lubed | 0.52 | 230/30/225 | 208 | | | yes | 890 | |
| 52 | 1/16 SS80 | 1220 | 37 | W-8 | Lubed | 0.50 | 230/30/225 | | | | yes | 1300 | |
| 53 | 1/16 SS80 | 1220 | 31 | W-8 | Lubed | 1.65 | 230/30/225 | 145 | | | | 12920 | |
| 54 | 1/16 SS80 | 1220 | 35 | W-8 | Lubed | 1.00 | 230/30/225 | 149 | | | yes | 4480 | Knurl |
| 55 | 1/16 Music | 1220 | 35 | W-8 | Lubed | 0.85 | 230/30/225 | 176 | | | yes | 8730 | Knurl |
| 56 | 1/16 Music | 1220 | 30 | W-8 | Lubed | 1.97 | 230/30/225 | 262 | | | | 14760 | Knurl, Ctg Surface ground |
| 57 | UNCOATED | 1220 | 35 | W-8 | Lubed | 0.00 | | 162 | | | | 33220 | |
| 58 | 1/16 Music | 1220 | 32 | W-8 | Lubed | 1.65 | 230/30/225 | | | | yes | 2110 | Knurl, Layered ctg |
| 59 | 1/16 Music | 1220 | 0 | W-8 | Lubed | 2.36 | 230/35/225 | 3 | | | | 210040 | 0% Creep |
| 60 | 1/16 SS80 | 1220 | 36 | W-8 | DAS | 0.80 | 270/30/225 | | | yes | | 180 | |
| 61 | 1/16 SS80 | 1220 | 34 | W-8 | DAS | 1.25 | 210/30/225 | | | yes | | 440 | |
| 62 | 1/16 SS80 | 1220 | 34 | W-8 | DAS | 1.50 | 200/0/225 | 435 | | | | 6100 | |
| 63 | 1/16 SS80 | 1220 | 35 | W-8 | DAS | 0.95 | 230/10/225 | 398 | | | yes | 5520 | |
| 64 | 1/16 SS80 | 1220 | 36 | W-8 | DAS | 0.82 | 230/50/225 | 1170 | | yes | | 350 | |
| 65 | 1/16 SS80 | 1220 | 33 | W-8 | DAS | 1.25 | 230/70/225 | 772 | | | yes | 4020 | Edge just before failure |
| 66 | 1/16 SS80 | 1220 | 34 | W-8 | DAS | 1.17 | 250/30/225 | 2702 | | yes | yes | 360 | Edge |
| 67 | 1/16 SS80 | 1220 | 31 | W-8 | DAS | 1.75 | 210/30/225 | 889 | | | | 8100 | |
| 68 | 1/16 SS80 | 1220 | 31 | W-8 | DAS | 1.58 | 250/30/225 | 442 | | | | 6000 | |
| 69 | 1/16 SS80 | 1220 | 36 | W-8 | DAS | 0.88 | 250/15-7/225 | 322 | | | | 6000 | |
| 70 | 1/16 SS80 | 1220 | 31 | W-8 | DAS | 1.67 | 250/50-25/225 | 5850 | | | yes | 1710 | Heavy Edge & flaking |
| 71 | 1/16 SS80 | 1220 | 25 | W-3 | DAS | 1.56 | 230/70/225 | 15 | 2 | | yes | 1470 | Debonded after break-in |
| 72 | 1/16 SS80 | 1220 | 30 | W-3 | DAS | 1.50 | 230/50/225 | | | | yes | 1470 | Frothy |
| 73 | 1/16 SS80 | 1220 | 22 | W-3 | DAS | 2.11 | 200/0/225 | 293 | 12 | | | 6000 | |
| 74 | 1/16 SS80 | 1220 | 24 | W-3 | DAS | 1.63 | 230/50/225 | 2711 | 87 | | yes | 2050 | Large flakes |
| 75 | 1/16 SS80 | 1220 | 24 | W-3 | DAS | 1.66 | 230/30/225 | 819 | 44 | | yes | 7290 | Flaking & edge |
| 76 | 1/16 SS80 | 1220 | 31 | W-3 | DAS | 1.30 | 230/30/225 | 484 | 22 | | yes | 4120 | |
| 77 | 1/16 SS80 | 1220 | 38 | W-9 | DGF | 0.38 | 230/30/225 | | | | yes | 260 | Frothy |
| 78 | 1/16 SS80 | 1220 | 38 | W-9 | DGF | 0.41 | 230/30/225 | | | | yes | 280 | Frothy |
| 79 | 1/16 SS80 | 1220 | 38 | W-9 | DGF | 0.40 | 230/30/225 | | | | yes | 220 | Frothy |
| 80 | 1/16 SS80 | 1220 | 38 | W-9 | DGF | 0.44 | 230/30/225 | | | | yes | 230 | Frothy |

| Test No. AMST | Wire | Contact Pressure | Creepage | Steel Bottom | Test Conditions | Coating Thickness | Parameter Set | Wear Rate Top | Bottom | Debond Type I | Debond Type II | Test Length | Comments |
|------------------|-----------|---------------------|----------|-----------------|--------------------|----------------------|------------------|------------------|--------|------------------|-------------------|----------------|---|
| 81 | 1/16 SS80 | 1220 | 38 | W-9 | DGF | 0.41 | 230/30/225 | | | | yes | 230 | Frothy |
| 82 | 1/16 SS80 | 1220 | 35 | W-9 | DGF | 0.78 | 230/30/225 | 262 | 7 | | | 6000 | Block of five |
| 83 | 1/16 SS80 | 1220 | 35 | W-9 | DGF | 0.82 | 230/30/225 | 308 | 11 | | | 6000 | with no debonding. |
| 84 | 1/16 SS80 | 1220 | 38 | W-9 | DGF | 0.72 | 230/30/225 | 208 | 7 | | | 6000 | |
| 85 | 1/16 SS80 | 1220 | 35 | W-9 | DGF | 0.84 | 230/30/225 | 373 | 9 | | | 6000 | |
| 88 | 1/16 SS80 | 1220 | 38 | W-9 | DGF | 0.75 | 230/30/225 | 301 | 8 | | | 6000 | |
| 87 | 1/16 SS80 | 1220 | 38 | W-9 | DGF | 0.48 | 230/30/225 | | | | yes | 1488 | Block of five: |
| 88 | 1/16 SS80 | 1220 | 38 | W-9 | DGF | 0.45 | 230/30/225 | | | | yes | 1929 | Interrupted spray. |
| 89 | 1/16 SS80 | 1220 | 38 | W-9 | DGF | 0.54 | 230/30/225 | | | | yes | 2500 | Poor sandblasting. |
| 90 | 1/16 SS80 | 1220 | 38 | W-9 | DGF | 0.47 | 230/30/225 | | | | yes | 1051 | EE from grinding. |
| 91 | 1/16 SS80 | 1220 | 38 | W-9 | DGF | 0.45 | 230/30/225 | | | | yes | 2418 | |
| 92 | 1/16 SS80 | 1220 | 34 | W-9 | DGF | 1.12 | 230/30/225 | 212 | 11 | | | 6000 | Block of five: |
| 93 | 1/16 SS80 | 1220 | 34 | W-9 | DGF | 1.12 | 230/30/225 | 407 | 25 | | yes | 4360 | EE in various degrees |
| 94 | 1/16 SS80 | 1220 | 34 | W-9 | DGF | 1.11 | 230/30/225 | 197 | 12 | | | 6000 | |
| 95 | 1/16 SS80 | 1220 | 34 | W-9 | DGF | 1.14 | 230/30/225 | 308 | 19 | | yes | 5830 | Debonding predicted here |
| 96 | 1/16 SS80 | 1220 | 34 | W-9 | DGF | 1.10 | 230/30/225 | 232 | 13 | | | 6000 | |
| 97 | 1080 1/16 | 1220 | 34 | W-9 | DGF | 0.35 | 230/30/225 | 388 | 8 | | yes | 4770 | Severe ee. |
| 98 | 1080 1/16 | 1220 | 33 | W-9 | DGF | 0.63 | 230/30/225 | 423 | 5 | | yes | 2900 | EE from grinding. |
| 99 | 1080 1/16 | 1220 | 33 | W-9 | DGF | 0.58 | 230/30/225 | 392 | 6 | | yes | 2220 | Debonding predicted from ee. |
| 100 | 1080 1/16 | 1220 | 33 | W-9 | DGF | 0.58 | 230/30/225 | 435 | | | | 6000 | Some ee. |
| 101 | 1080 1/16 | 1220 | 33 | W-9 | DGF | 0.55 | 230/30/225 | 398 | | | | 6000 | Some ee. |
| 102 | 1080 1/16 | 1220 | 32 | W-9 | DGF | 0.90 | 230/30/225 | 277 | 6 | | | 6000 | |
| 103 | 1080 1/16 | 1220 | 32 | W-9 | DGF | 0.88 | 230/30/225 | 480 | 4 | | | 6000 | |
| 104 | 1080 1/16 | 1220 | 32 | W-9 | DGF | 0.88 | 230/30/225 | 514 | 4 | | yes | 3870 | ee |
| 105 | 1080 1/16 | 1220 | 32 | W-9 | DGF | 0.91 | 230/30/225 | 569 | 5 | | yes | 3050 | ee |
| 106 | 1080 1/16 | 1220 | 31 | W-9 | DGF | 0.99 | 230/30/225 | 555 | | | | 6000 | |
| 107 | 1080 1/16 | 1220 | 33 | W-9 | DAS | 0.71 | 230/30/225 | | | | yes | 460 | Block of five: |
| 108 | 1080 1/16 | 1220 | 33 | W-9 | DAS | 387.00 | 230/30/225 | | | | yes | 740 | All frothy. |
| 109 | 1080 1/16 | 1220 | 33 | W-9 | DAS | 0.65 | 230/30/225 | | | | yes | 230 | |
| 110 | 1080 1/16 | 1220 | 33 | W-9 | DAS | 0.65 | 230/30/225 | | | | yes | 200 | |
| 111 | 1080 1/16 | 1220 | 33 | W-9 | DAS | 0.85 | 230/30/225 | | | | yes | 370 | |
| 112 | 1080 1/16 | 1220 | 35 | W-9 | DAS | 0.84 | 230/30/225 | | | | yes | 1530 | |
| 113 | 1080 1/16 | 1220 | 35 | W-9 | DAS | 0.83 | 230/30/225 | 312 | 7 | | yes | 5010 | Failed upon start-up after 5000 revs |
| 114 | 1080 1/16 | 1220 | 35 | W-9 | DAS | 0.82 | 230/30/225 | 371 | 10 | | yes | 3450 | |
| 115 | 1080 1/16 | 1220 | 35 | W-9 | DAS | 0.83 | 230/30/225 | | | | | 7740 | Ran until the coating failed, past 6000 revs. |
| 116 | 1080 1/16 | 1220 | 35 | W-9 | DAS | 0.81 | 230/30/225 | | | | yes | 4380 | |
| 117 | 1080 1/16 | 1220 | 35 | W-9 | DAS | 0.96 | 230/30/225 | 663 | 11 | | | 6000 | knurled. EE. |
| 118 | 1080 1/16 | 1220 | 35 | W-9 | DAS | 0.84 | 230/30/225 | 458 | 7 | | yes | 3300 | No visible ee. Not knurled. |
| 119 | 1080 1/16 | 1220 | 35 | W-9 | DAS | 0.89 | 230/30/225 | | | | yes | 1620 | Knurled. |
| 120 | 1080 1/16 | 1220 | 35 | W-9 | DAS | 0.90 | 230/30/225 | | | | yes | 1700 | Not knurled. |

| Test No. AMST | Wire | Contact Pressure | Creepage | Steel Bottom | Test Conditions | Coating Thickness | Parameter Set | Wear Rate Top | Bottom | Debond Type I | Debond Type II | Test Length | Comments |
|------------------|-----------|---------------------|----------|-----------------|--------------------|----------------------|------------------|------------------|--------|------------------|-------------------|----------------|---|
| 121 | 1080 1/16 | 1220 | 34 | W-9 | DAS | 1.05 | 230/30/225 | 770 | 7 | | yes | 4290 | Failure predicted, ee. |
| 122 | 1080 1/16 | 1220 | 32 | W-9 | DAS | 1.48 | 230/30/225 | 398 | 14 | | | 6000 | |
| 123 | 1080 1/16 | 1220 | 32 | W-9 | DAS | 1.42 | 230/30/225 | 508 | 7 | | yes | 5090 | EE. |
| 124 | 1080 1/16 | 1220 | 33 | W-9 | DAS | 1.23 | 230/30/225 | 351 | 20 | | yes | 5510 | No air blast on last interval. |
| 125 | 1080 1/16 | 1220 | 33 | W-9 | DAS | 1.30 | 230/30/225 | 408 | 16 | | | 6000 | Slight ee. |
| 126 | 1080 1/16 | 1220 | 36 | W-9 | DAS | 0.71 | 230/30/225 | | | yes | | 1000 | Crack appeared as machine turned off. |
| 127 | 1080 1/16 | 1220 | 37 | W-9 | DAS | 0.70 | 230/30/225 | 519 | 7 | | | 6000 | EE. |
| 128 | 1080 1/16 | 1220 | 37 | W-9 | DAS | 0.69 | 230/30/225 | 512 | 5 | | yes | 4470 | Air blast not on roller @ failure. |
| 129 | 1080 1/16 | 1220 | 37 | W-9 | DAS | 0.67 | 230/30/225 | 354 | 26 | | yes | 2000 | Failure @ start-up. |
| 130 | 1080 1/16 | 1220 | 37 | W-9 | DAS | 0.74 | 230/30/225 | | | | | | Ran to failure. |
| 131 | 1080 1/16 | 1220 | 36 | W-9 | DAS | 0.75 | 230/30/225 | 320 | 13 | | | 6100 | Minor ee. |
| 132 | 1080 1/16 | 1220 | 35 | W-9 | DAS | 375.00 | 230/30/225 | 465 | 9 | | | 2630 | |
| 133 | 1080 1/16 | 1220 | 38 | W-9 | DAS | 0.34 | 230/30/225 | 535 | | | | 4000 | EE. |
| 134 | 1080 1/16 | 1220 | 33 | W-9 | DAS | 1.31 | 230/30/225 | | | | yes | 1050 | Block of five. |
| 135 | 1080 1/16 | 1220 | 33 | W-9 | DAS | 1.24 | 230/30/225 | | | | yes | 4760 | |
| 136 | 1080 1/16 | 1220 | 33 | W-9 | DAS | 1.25 | 230/30/225 | | | | yes | 2150 | |
| 137 | 1080 1/16 | 1220 | 33 | W-9 | DAS | 1.28 | 230/30/225 | 469 | | | | 6000 | |
| 138 | 1080 1/16 | 1220 | 33 | W-9 | DAS | 1.35 | 230/30/225 | | | | yes | 1270 | |
| 139 | 1080 1/16 | 1220 | 37 | W-9 | DAS | 0.61 | 230/30/225 | 492 | 10 | | | 6000 | Block of five: |
| 140 | 1080 1/16 | 1220 | 37 | W-9 | DAS | 0.61 | 230/30/225 | 583 | 5 | | | 6000 | 30 sec pre-heat. |
| 141 | 1080 1/16 | 1220 | 37 | W-9 | DAS | 0.61 | 230/30/225 | 611 | 4 | | | 6000 | Ran nearly to interface. |
| 142 | 1080 1/16 | 1220 | 37 | W-9 | DAS | 0.61 | 230/30/225 | 596 | 5 | | | 6000 | |
| 143 | 1080 1/16 | 1220 | 37 | W-9 | DAS | 0.65 | 230/30/225 | 486 | 5 | | | 6000 | |
| 144 | 1080 1/16 | 1220 | 35 | W-9 | DAS | 1.08 | 230/30/225 | | | yes | | 30 | Debonded upon start-up. |
| 145 | 1080 1/16 | 1220 | 34 | W-9 | DAS | 1.22 | 230/30/225 | 357 | | | | 6000 | 144&145 post heat treated 600 for 30 min. |
| 146 | 1080 1/16 | 1220 | 34 | W-9 | DAS | 1.23 | 230/30/225 | 384 | 3 | | | 6000 | Tapered edge. |
| 147 | 1080 1/16 | 1220 | 34 | W-9 | DAS | 1.09 | 230/30/225 | 613 | 4 | | | 6000 | Sone ee. |
| 148 | 1080 1/16 | 1220 | 34 | W-9 | DAS | 1.12 | 230/30/225 | | | | | 5970 | |
| 149 | 1080 1/16 | 1220 | 34 | W-9 | DAS | 1.20 | 230/30/225 | 459 | 61 | | | 6000 | EE., |
| 150 | 1080 1/16 | 1220 | 34 | W-9 | DAS | 1.18 | 230/30/225 | 742 | 4 | | | 6000 | EE. |
| 151 | 1080 1/16 | 1220 | 34 | W-9 | DAS | 1.18 | 230/30/225 | | | | yes | 3400 | Severe ee. |
| 152 | 1080 1/16 | 1220 | 34 | W-9 | DAS | 1.10 | 230/30/225 | | | | yes | 5850 | Failure predicted because of ee. |
| 153 | 1080 1/16 | 1220 | 34 | W-9 | DAS | 1.19 | 230/30/225 | | | | | 2440 | EE. |
| 154 | 1080 1/16 | 1220 | 35 | W-9 | DAS | 1.07 | 230/30/225 | 606 | 11 | | | 6000 | Block of five: |
| 155 | 1080 1/16 | 1220 | 35 | W-9 | DAS | 1.00 | 230/30/225 | | | | yes | 0 | Pre-heat 30 sec, flood wash. |
| 156 | 1080 1/16 | 1220 | 35 | W-9 | DAS | 0.99 | 230/30/225 | | | | yes | 1030 | |
| 157 | 1080 1/16 | 1220 | 35 | W-9 | DAS | 0.98 | 230/30/225 | | | yes | | 310 | Nut not tight on lower shaft. |
| 158 | 1080 1/16 | 1220 | 35 | W-9 | DAS | 1.07 | 230/30/225 | | | yes | | 1040 | |
| 159 | 1080 1/16 | 1220 | 33 | W-9 | DAS | 1.27 | 230/30/225 | 177 | 17 | | | 6000 | Ni-Cr intermediate layer. |
| 160 | 1080 1/16 | 1220 | 34 | W-9 | DAS | 1.14 | 230/30/225 | | | yes | | 200 | Ni-Cr layer 0.36mm, too thick. |

| Test No. AMST | Wire | Contact Pressure | Creepage | Steel Bottom | Test Conditions | Coating Thickness | Parameter Set | Wear Rate Top | Bottom | Debond Type I | Debond Type II | Test Length | Comments |
|------------------|-----------|---------------------|----------|-----------------|--------------------|----------------------|------------------|------------------|--------|------------------|-------------------|----------------|---------------------|
| 161 | 1080 1/16 | 1220 | 37 | W-9 | DAS | 0.71 | 230/30/225 | 475 | 7 | | | 6000 | Ni-Cr layer 0.13mm. |
| 162 | | | | | | | | | | | | | |
| 163 | | | | | | | | | | | | | |
| 164 | | | | | | | | | | | | | |
| 165 | | | | | | | | | | | | | |
| 166 | | | | | | | | | | | | | |
| 167 | 1080 1/16 | 1220 | 34 | W-9 | DAS | 1.12 | 230/30/225 | | | | yes | 5580 | Ni-Cr layer |
| 168 | 1080 1/16 | 1220 | 34 | W-9 | DAS | 1.17 | 230/30/225 | | | | yes | 4070 | Ni-Cr layer |
| 169 | 1080 1/16 | 1220 | 34 | W-9 | DAS | 1.23 | 230/30/225 | | | | yes | 1400 | Ni-Cr layer |
| 170 | 1080 1/16 | 1220 | 33 | W-9 | DAS | 1.25 | 230/30/225 | | | | yes | 2830 | Ni-Cr layer |
| 171 | 1080 1/16 | 1220 | 36 | W-9 | DAS | 0.72 | 230/30/225 | | | yes | | 730 | Flat bottom roller. |
| 172 | 1080 1/16 | 1220 | 36 | W-9 | DAS | 0.67 | 230/30/225 | | | | yes | 1000 | Flat bottom roller. |
| 173 | 1080 1/16 | 1220 | 37 | W-9 | DAS | 0.67 | 230/30/225 | | | | yes | 3290 | Flat bottom roller. |
| 174 | 1080 1/16 | 1220 | 36 | W-9 | Water | 0.88 | 230/30/225 | 162 | | | yes | 4890 | Water Lubed. |
| 175 | 1080 1/16 | 1220 | 37 | W-9 | Lubed | 0.58 | 230/30/225 | | | | yes | 1440 | |
| 176 | 1080 1/16 | 1050 | 37 | W-9 | Lubed | 0.58 | 230/30/225 | 47 | | | yes | 5500 | |
| 177 | 1080 1/16 | 900 | 37 | W-9 | Lubed | 0.62 | 230/30/225 | 26 | | | yes | 11500 | |
| 178 | 1080 1/16 | 700 | 37 | W-9 | Lubed | 0.62 | 230/30/225 | 7 | | | yes | 31680 | |
| 179 | 1080 1/16 | 1220 | 38 | W-9 | Lubed | 0.50 | 230/30/225 | 26 | | | yes | 3970 | |
| 180 | 1080 1/16 | 1220 | 7 | W-9 | Lubed | 0.62 | 230/30/225 | | | | yes | 3500 | |
| 181 | 1080 1/16 | 1050 | 6 | W-9 | Lubed | 0.83 | 230/30/225 | 21 | | | yes | 3170 | |
| 182 | 1080 1/16 | 900 | 5 | W-9 | Lubed | 0.84 | 230/30/225 | 9 | | | yes | 12500 | |
| 183 | 1080 1/16 | 700 | 6 | W-9 | Lubed | 0.81 | 230/30/225 | 4 | | | yes | 24620 | |
| 184 | 1080 1/16 | 1220 | 36 | W-9 | DAS | 0.89 | 230/30/225 | 385 | | | | 6000 | |

BIOGRAPHICAL SKETCH

Born December 25, 1938, in Millville, Wisconsin, graduated from Ashland, Oregon, High School in 1956, served in the United States Marine Corps, and work as a craftsman in the building and machining trades highlight the early history of the author. Along the way Associate of Arts degrees in Social Sciences, Arts and Letters, and an Associate of Engineering in Manufacturing were earned. A B.S. in Manufacturing Engineering Technology, magna cum laude, was earned from the Oregon Institute of Technology in 1991. It was a matter of getting started and not wanting to quit, so graduate school was next. Oregon Graduate Institute of Science & Technology, Materials Science & Engineering department, offered a position as a graduate research assistant for the period of time required to pursue a PhD degree. Surface engineering and failure analysis are areas of special interest.